THE UNIVERSITY OF MICHIGAN

INDUSTRY PROGRAM OF THE COLLEGE OF ENGINEERING

DISSOCIATION-RECOMBINATION NON-EQUILIBRIUM IN THE LAMINAR HYPERSONIC BOUNDARY LAYER.

George R. Inger

A dissertation submitted in partial fulfillment
of the requirements for the degree of
Doctor of Philosophy in The
University of Michigan
1960

May, 1960

IP-433

FOREWORD

The author would like to express a sincere appreciation to the following faculty members for their assistance during his graduate studies at the University of Michigan: Dr. A. M. Kuethe, Dr. S. W. Churchill, Dr. W. W. Willmarth, Dr. R. C. F. Bartels, Dr. R. V. Churchill and Dr. J. E. Broadwell. A special note of gratitude is due Dr. T. C. Adamson, Jr., whose teaching, guidance and encouragement have all served as a welcome stimulus in the conception and execution of this thesis. Finally, the participation of Dr. J. L. York on the thesis committee is gratefully acknowledged.

TABLE OF CONTENTS

TABLE OF CONTENTS CONT'D

TABLE OF CONTENTS CONT'D

LIST OF ILLUSTRATIONS

LIST OF ILLUSTRATIONS CONT'D

LIST OF SYMBOLS

α_i	Mass fraction of i-th specie
α	Total atomic specie mass fraction ($\sum_{\text{ATOMS}} \alpha_i$)
β	Inviscid flow velocity gradient parameter $\left(\frac{du_e/dX}{u_e/X}\right)$
δ	Boundary layer or Couette flow channel thickness
ϵ	Boundary layer transformation parameter $\left(\frac{d\xi/dX}{\xi/X}\right)$
η	Similarity coordinate for transformed boundary layer equations
ζ	Boundary layer non-equilibrium parameter
ζ_c	Boundary layer surface catalysis parameter
γ_i	Catalytic efficiency with respect to i-th specie
$\bar{\gamma}$	Mean specific heat ratio for a real gas
λ	Mixture thermal conductivity
μ	Mixture coefficient of Viscosity
ω	Recombination rate temperature exponent
ψ	Boundary layer stream function
Φ	Viscous energy dissipation rate per unit volume
ρ_i	Mass density of i-th specie
ρ	Mixture density ($\rho = \Sigma\rho_i$)
ξ	Transformed X - coordinate of boundary layer
τ_W	Shear stress
θ	Non-dimensional boundary layer temperature variable (T/T_e)
$\not{\theta}$	Temperature perturbation from thermodynamic equilibrium

θ_A	Non-dimensional activation energy parameter (T_A/T_e)
χ	Non-dimensional atomic Nitrogen variable (α_4/α_{4e})
B	Inviscid flow velocity gradient (du_e/dX)
c_{p_i}	Constant pressure specific heat of i-th specie per unit mass
$\overline{c_p}$	"Frozen" mixture specific heat $(\sum_i \alpha_i c_{p_i})$
$\mathcal{C}_p$	Non-dimensional specific heat parameter $(\overline{c_p}/\overline{c_{p_e}})$
C	Chapman-Rubensin parameter $(\rho\mu/\rho_R\mu_R)$
d	Diameter
$\frac{D}{Dt}$	Total or substantial time derivative following a fluid particle
D_{ij}	Multicomponent diffusion coefficient
$\mathcal{D}_{ij}$	Binary diffusion coefficient
D_i^T	Thermal diffusion coefficient
$\mathcal{F}_g, \mathcal{F}_\chi, \mathcal{F}_w, \mathcal{F}_\theta$	Reaction rate derivatives evaluated at chemically frozen conditions
$\mathcal{E}_g, \mathcal{E}_\chi, \mathcal{E}_w, \mathcal{E}_\theta$	Reaction rate derivatives evaluated at thermodynamic equilibrium conditions
E_A	Activation energy
f	Boundary layer stream function variable
$\vec{F}_i$	Body force per unit mass acting on i-th specie
$\mathcal{F}_{1,2}$	Functions of the Equilibrium Reaction Rate Derivative
g	Non-dimensional stagnation enthalpy variable (h_s/h_{s_e})
$\mathcal{G}$	Non-dimensional reaction rate function
h_i	Enthalpy per unit mass of i-th specie
h	Enthalpy per unit mass of mixture

$h_{f_i}^{(o)}$	Heat of formation of i-th atomic specie at zero degrees absolute
h_s	Stagnation or total enthalpy ($h + u^2/2$)
I_z, I_θ	First order frozen perturbation analysis reaction rate integrals
$\mathcal{I}_z$, $\mathcal{I}_\theta$	Second order frozen perturbation analysis reaction rate integrals
k	Boltzmann constant
K_R'	Recombination rate constant
K_{c_i}	Surface catalysis rate parameter for i-th specie
K_N	Knudsen Number
k_R	Recombination rate parameter
k_F	Dissociation rate parameter
K_c	Equilibrium constant
$\overline{K}_i$	Net rate of i-th specie production by reaction per unit volume per unit mass
L	Characteristic length
L_e	Lewis number ($\rho\mathcal{D}_{12}\overline{c}_p/\lambda$)
m_i	Mass of i-th specie
M_∞	Flight Mach Number
M_i	Molecular weight of i-th specie
$\overline{M}$	Molecular weight of mixture
n_i	Number density of i-th specie
n	Number of density of mixture
N_i	Number of i-th specie moles
N	Number of moles of mixture
N_o	Avogadro's number
p_i	Partial pressure of i-th specie
p	Hydrostatic pressure

P_R	Prandtl number
$P_{\alpha\beta}$	Viscous stress tensor
$\dot{q}_W$	Heat flux rate accepted at interior of a solid boundary
$\dot{Q}_W$	Gaseous heat flux at wall
q	Non-dimensional dissociation energy parameter for the boundary layer theory
Q	Non-equilibrium parameter gradient factor for boundary layer $\left(\frac{d\zeta/dX}{\zeta/X}\right)$
$\vec{Q}$	Net heat flux rate in gas phase
r_o	Local body surface radius in a transverse plane
R	Local radius of curvature of body in meridian plane
R_i	I-th atomic specie reaction rate function; first order perturbation
$\mathcal{R}_i$	I-th atomic specie reaction rate function; second order perturbation
R_o	Universal gas constant
S_c	Schmidt number (P_R/L_e)
S_i	Net rate of i-th specie appearance per unit surface area
S_{i_c}	Net rate of catalytic production
t	Time
T	Absolute temperature
T_A	Characteristic activation temperature (E_A/R_o)
$\mathcal{T}$	Boundary layer total enthalpy perturbation
u,v	Velocity components along x,y respectively
$\vec{V}$	Mass average velocity of mixture
$\vec{\mathcal{V}}_i$	Diffusion velocity of i-th specie

w	Non-dimensional molecular Nitrogen variable (α_3/α_{3e})
W	Molecular Nitrogen perturbation from thermodynamic equilibrium
x,y	Orthogonal space coordinates along a body
z	Non-dimensional atomic Nitrogen variable (α_2/α_{2e})
Z	Atomic Oxygen perturbation from thermodynamic equilibrium
X	Atomic Nitrogen perturbation from thermodynamic equilibrium

Subscripts

A	Denotes atom
c	Complementary integral
CAT.	Catalytic wall value
e	Conditions at outer edge of boundary layer
EQ.	Denote thermodynamic equilibrium condition
F	Denotes chemically frozen condition
G	Gas
i	Denotes i-th chemical specie of the mixture
I, II, ...	First, second, etc. order perturbations from frozen flow
M	Denotes molecule
NON-CAT.	Non-catalytic wall value
p	Particular integral
R	Recombination or reference value
REF.	Reference condition
S	Stagnation conditions
W	Denotes wall condition

CHAPTER I

INTRODUCTION

The origin of real gas chemistry effects in aerodynamic problems, ignored in the chemically inert ideal gas model of air, lies in the possibility that the kinetic energy of flight, converted into the various internal energy modes, may be great enough to excite such phenomena as molecular vibration, dissociation and ionization. At hypersonic speeds, either shock wave compression or viscous deceleration may provide the appropriate conversion mechanism (the former dominates in the blunt-nose region near the stagnation point, while the latter may become important downstream on the longer hypersonic bodies). The actual energy distribution between the various internal energy modes is described by the governing conservation equations and boundary conditions for the flow; real gas effects not only modify existing terms in these equations but generally require the addition of new equations and data as well. The most important new physical features which must be accounted for are: (a) variable molecular weight, as reflected in the thermal equation of state, (b) the presence of a multicomponent gas mixture; this introduces the need for considering the individual behavior of the various component species by accounting for diffusion processes and the proper definition of thermodynamic variables as averages over the component specie properties, (c) chemical reactions between the various species, such as homogeneous dissociation and recombination, and between the gas and flow boundary surfaces (heterogeneous wall catalysis), and (d) molecular transport coefficients; not only must new coefficients be considered for the diffusion processes, but the usual expressions for viscosity and heat

conductivity are modified in the presence of a multicomponent mixture.

The relative importance of many of these real gas features to the calculation of the important aerodynamic quantities, such as heat transfer, skin friction, pressure distribution and thermodynamic state profiles in the flow, depends on the comparative rates at which the various physical processes occur. There arises, for this reason, the particular possibility of steady state chemical non-equilibrium in a dissociated gas flow, due to the "competition" between convection and diffusion and the local net volumetric reaction rates in the gas (a similar type of "competition" may exist between gaseous diffusion and heterogeneous surface reaction at a flow boundary). This paper is concerned with some aspects of such chemical non-equilibrium effects in the dissociated laminar hypersonic boundary layer.

The potential importance of the influence of real gas effects on certain problems in hypersonic aerodynamics, notably heat transfer rates, has spurred a considerable amount of theoretical and experimental work in recent years, some of which is reviewed in the survey articles by Rosner[1], Griffith[2], and Adams[3]. In particular, a number of important theoretical studies have been produced. Lees[4], in a notable paper, defined many of the main theoretical features attending the real gas boundary layer flow problem and explored many useful analytical approximations, such as the use of the "local" similarity boundary layer solutions and the direct neglect of pressure gradient and viscous dissipation effects, which grossly simplify the calculation of heat transfer on a highly cooled hypersonic vehicle surface. Further, approximate solutions for the two extremes of

thermodynamic equilibrium and chemically frozen flow heat transfer were given for a completely catalytic surface, assuming a Fick law for the diffusion processes. An experimental verification of the equilibrium heat transfer distribution calculations of Lees, particularly concerning the local similarity arguments, has been given by Kemp, Rose and Detra.[5] The work of Fay and Riddell[6] at Avco constitutes a more thorough treatment of the general case of dissociation-recombination non-equilibrium in the laminar boundary layer for either extreme of wall catalysis, under the conditions of an exact similarity solution possible at a symmetric body stagnation point. Assuming an effective binary mixture of air atoms and air molecules, using variable $\rho\mu$ and specific heat data and a particular form of the recombination rate law due to Davidson[23], the variation of the heat transfer was found as a function of an appropriate non-equilibrium parameter ζ, where ζ is defined as the ratio of a characteristic boundary layer convection time to a characteristic net reaction time. The results, which approximately confirm those of Lees[4] in the two extremes of thermodynamic equilibrium ($\zeta = \infty$) and chemically frozen flow ($\zeta = 0$), indicate that in the Lewis number range $.8 \leq L_e \leq 1.4$, the effect of non-equilibrium on heat transfer is very small for the catalytic wall case, but is quite noticeable for a non-catalytic surface when $10^{-5} \leq \zeta \leq 1$. Two reports by Adamson, Nicholls and Sherman[7,8] also consider some of the features of non-equilibrium in the laminar hypersonic boundary layer. In reference 7, the multicomponent behavior of a three specie mixture, as it affects the calculation of diffusion fluxes and net reaction rates, was discussed, and an approximate account of deviations from the binary

Fick diffusion law given. Further, the destruction of a similarity type of solution due to the non-equilibrium reaction rates, particularly for the flat plate boundary layer, was discussed. In reference 8, the significance of the characteristic non-equilibrium parameter ζ is discussed, and a method of analyzing the non-equilibrium deviations in the flat plate laminar boundary layer in terms of a series involving increasing powers of ζ was outlined. Using the recombination rate law proposed by Hirschfelder[9], some of the details of the zeroth, first and second order deviation equations were worked out, but no solutions given. A report by Scala[10] considers the solution of the chemically frozen stagnation point boundary layer equations for a binary mixture in the presence of an arbitrary degree of surface catalysis and thermal diffusion in the gas. The results indicate the effect of catalytic efficiency on heat transfer and thermodynamic state profiles, and show the effect of thermal diffusion on heat transfer to be very small for a cooled wall. A similar but more comprehensive analysis has been given by Goulard[11], excluding the thermal diffusion, using the highly cooled wall approximations suggested by Lees[4]. The role of the surface catalysis is very clearly displayed, entering the problem as it does through the specie boundary condition at the wall, in terms of an appropriate wall catalysis parameter ζ_c analogous to the non-equilibrium parameter ζ. The influence of surface material on catalytic efficiency is discussed, and the restriction on similarity type of solutions due to the presence of an arbitrary surface reaction rate is considered. Several articles by Rosner[12,13] have also dealt with gas flow over a catalytically reacting surface: in particular,

reference 13 stresses the physical significance of the parameter ζ_c as a ratio of characteristic diffusion and surface reaction times, and presents approximate local solutions for heat transfer in the presence of a general surface catalysis reaction rate. Finally, the subject of real gas boundary layer flow and heat transfer has been notably unified and extended in a recent and very comprehensive paper by Lees[14], which considers both laminar and turbulent reacting boundary layer flow in the presence of mass transfer at the wall. An impressive amount of ground is covered in this paper; concerning the laminar boundary layer problem, the important conclusions can be briefly summarized as follows. First, it was found that if one assumes a Fick law for the diffusion of each specie in a multi-component gas mixture, Lewis and Prandtl number equal to one, and a known gas composition at the surface, then the total enthalpy distribution, the heat transfer, and the distribution of each of the total chemical element mass fractions are explicitly independent of reaction in the gas, regardless of the viscosity law. The consequent similarity of the total enthalpy and various total chemical element profiles leads to a greatly simplified solution for the heat transfer in the presence of mass transfer at the wall.* The Fick law approximation is supported by the results of an investigation into multicomponent mixture diffusion by Knuth[15]. Second, the local similarity approximation for a reacting boundary layer was discussed; it was shown that non-equilibrium in the gas would restrict similarity solutions to the stagnation point whenever any of the conditions (a) Fick diffusion law, (b) $P_R = L_e = 1$, or (c) known surface composition, are

* Each total chemical element mass fraction must necessarily be independent of chemical reaction, either in the gas or on the surface.

noticeably violated. Third, a survey of various flat plate and stagnation point boundary layer solutions, in which detailed account of the variation of transport properties across the layer has been taken, leads to the conclusion that emperical correction of constant property approximate solutions on the basis of these particular results is a satisfactory procedure provided that species having physical properties radically different from those in the main flow are not injected or ablated into the boundary layer. Fourth, the usually neglected pressure diffusion mass flux and Von Karman diffusion stress component terms were subjected to a boundary layer order of magnitude computation, and shown to be negligable to the same order of approximation as the boundary layer equations themselves.

As a result of these and many other efforts, it appears that many of the major theoretical problems involving real gas effects in boundary layer flows have been solved to good approximation or otherwise shown to be unimportant. However, it is felt that a closer investigation of the dissociation-recombination non-equilibrium effects in the laminar hypersonic boundary layer, particularly in the presence of non-catalytic walls for which these effects appear quite pronounced, is warranted for the purpose of showing more clearly how deviations from equilibrium occur and how they are influenced by the various aerodynamic and chemical data relevant to the problem. Therefore, this thesis is addressed to a theoretical investigation of deviations from both the chemically frozen and thermodynamic equilibrium extremes, in the absence of surface mass transfer, to show the effect of dissociation-recombination on heat transfer and thermodynamic state profiles in the highly cooled boundary layer. The role of

activation energy, recombination rate temperature dependence, and variable freestream conditions causing local non-similarity effects due to the chemical reaction rate terms are considered. The dissociated boundary layer gas is represented as a four component mixture of two atomic and two molecular species, which is a good approximation to the real gas behavior of air when the presence of Nitric Oxide can be neglected.

CHAPTER II

THE BASIC GOVERNING RELATIONS FOR CHEMICALLY REACTING LAMINAR BOUNDARY LAYER FLOW

General Conservation Equations and Boundary Conditions

The basic governing relations represent the laws of mass, chemical specie, momentum and energy conservation in a flowing multicomponent reacting gas mixture. We will assume a radiation-free continuum flow in the following statements of these laws.

Specie Conservation

If we denote the difference between the total velocity of the i-th specie component and the mass average velocity of the whole mixture as the diffusion velocity $\vec{V}_i$, then the statement of conservation of i-th specie mass is

$$\rho \frac{\partial \alpha_i}{\partial t} + \nabla \cdot \rho \alpha_i \vec{V}_i = m_i \dot{K}_i , \tag{2.1}$$

accompanied by the subsidiary relations

$$\sum_i \alpha_i \vec{V}_i = 0 \tag{2.2}$$

$$\sum_i m_i \dot{K}_i = 0 \tag{2.3}$$

which express the fact that diffusion and net chemical reaction cannot alter the total mixture mass. Since

$$\sum_i \alpha_i \equiv \sum_i \rho_i / \rho = 1 , \tag{2.4}$$

one needs only N-1 of such specie conservation equations to completely describe an N component mixture.

According to Hirschfelder, et al[16], the i-th specie diffusion mass flux is given by

$$\rho\alpha_i\vec{V}_i = \frac{m_i m}{\rho}\sum_{j\neq i} m_j D_{ij}\left[\nabla\left(\frac{m_j}{m}\right)+\left(\frac{m_j}{m}-\alpha_j\right)\nabla\ln p - \frac{\rho\alpha_j}{p}\left(\frac{\vec{F}_j}{m_j}-\sum_L\frac{\alpha_L\vec{F}_L}{m_L}\right)\right] - D_i^T\nabla\ln T, \tag{2.5}$$

where the three terms under the summation represent ordinary mass, pressure and selective body force diffusion fluxes, respectively, and the last term is the thermal diffusion flux. D_{ij} is the multicomponent diffusion coefficient between species i, j in the presence of the other N-i-j species, and D_i^T is the thermal diffusion coefficient of the i-th specie. D_{ij} is not equal to the binary diffusion coefficient $\mathcal{D}_{ij}$ for a mixture of three or more components, since the presence of other species will alter the diffusion between any given two. The relationship between D_{ij} and the binary diffusion coefficients in general is given in Appendix A.

At any boundary between the gas and some other phase (such as a solid body surface), a specie boundary condition in the form of a conservation statement across the interface is required. Equating the net flux of i-th specie mass away from the surface due to diffusion and convection to the net rate of surface specie production per unit area, S_i, we have

$$\left[\rho\alpha_i(\vec{V}_i+\vec{V})\cdot\vec{N}\right]_w = S_i \tag{2.6}$$

where $\vec{N}$ is the interface unit normal (positive outward). In the absence of surface mass transfer, S_i would equal the net rate of catalytic reaction and $\sum_i S_i = 0$. (In the presence of a mass source at the interface, however, $\sum_i S_i$ would equal the net mass flow rate per unit area).

Overall Mass Conservation (Continuity)

A summation of Equation (2.1) over all component species, using Equations (2.2) and (2.3), produces the mass conservation equation for the entire mixture:

$$\frac{\partial \rho}{\partial t} + \nabla \cdot \rho \vec{V} = 0 . \tag{2.7}$$

The same procedure applied to the boundary condition (2.6) gives

$$(\rho \vec{V} \cdot \vec{N})_w = \sum_i S_i . \tag{2.8}$$

Momentum Conservation

If we denote by $\vec{F}_i$ the i-th specie body force per unit mass and by $P_{\beta\lambda}$ the symmetric viscous stress tensor acting in the λ direction a surface whose normal lies in the β direction, then the momentum conservation equation can be expressed in the form

$$\rho\left(\frac{\partial V_\lambda}{\partial t} + V_\beta \frac{\partial V_\lambda}{\partial X_\beta}\right) + \frac{\partial p}{\partial X_\lambda} = \frac{\partial P_{\beta\lambda}}{\partial X_\beta} + \rho \sum_i \alpha_i F_{i\lambda} . \tag{2.9}$$

The relationship between viscous stress and the rates of strain and dilitation of the flow for a continuum is

$$P_{\beta\lambda} = \mu\left(\frac{\partial V_\beta}{\partial X_\lambda} + \frac{\partial V_\lambda}{\partial X_\beta}\right) + \delta_{\beta\lambda} \Gamma \left(\frac{\partial V_\lambda}{\partial X_\lambda}\right) , \tag{2.10}$$

where μ is the coefficient of viscosity and $\Gamma = -2\mu/3$, assuming the average normal stress on a fluid element is the negative of the local hydrostatic pressure and independent of the rate of change of density in the flow. The viscosity coefficient in a gas mixture is a certain weighted average of the component viscosities (see Appendix A).

In a continuum flow, the mass average flow velocity and pressure in the gas adjacent to a boundary are equal to the corresponding values on the surface of the interface.

Energy Conservation

This statement of the first law of thermodynamics will be first given in terms of the mixture enthalpy h per unit mass, defined as the following mass average over the component enthalpies:

$$h = \sum_i \alpha_i h_i = \sum_i \alpha_i \left[h_{f_i}^{(o)} + \int_o^T c_{p_i} \, dT \right] , \qquad (2.11)$$

where $h_{f_i}^{(o)}$ is the heat of formation of the i-th specie at zero degrees absolute ($h_{f_i}^{(o)}$ will be taken positive for atomic species and zero for the molecular species). The energy conservation statement is then:

$$\rho \frac{\partial h}{\partial t} = \frac{\partial p}{\partial t} + \rho \sum_i \alpha_i \vec{v}_i \cdot \vec{F}_i + \Phi - \nabla \cdot \vec{Q} \qquad (2.12)$$

where

$$\Phi = P_{\alpha\beta} \frac{\partial V_\alpha}{\partial X_\beta} = \frac{1}{2} P_{\alpha\beta} \left(\frac{\partial V_\alpha}{\partial X_\beta} + \frac{\partial V_\beta}{\partial X_\alpha} \right) \qquad (2.13)$$

is the viscous energy dissipation rate per unit volume, and $\vec{Q}$ is the net heat flux per unit area through the gas. The effect of chemical reaction in the gas is implicit in Equation (2.12) by virtue of the above definition of h.

The heat flux vector is related to the state of the gas, according to Hirschfelder et al[16], as follows:

$$\vec{Q} = -\lambda \nabla T + \rho \sum_i h_i \alpha_i \vec{v}_i + \frac{kT}{n} \sum_i \sum_j \frac{m_i}{m_j} \frac{D_{ij}^T}{\mathcal{D}_{ij}} (\vec{v}_i - \vec{v}_j) . \qquad (2.14)$$

The three terms on the right side are the heat conduction, mass diffusion heat flux, and thermal diffusion heat flux, respectively.

The coefficient of thermal conductivity λ is an appropriately defined average of individual specie values in a multicomponent mixture; however, it is convenient to replace λ by the Prandtl Number *

$$P_R \equiv \mu \bar{c}_p / \lambda = \mu \sum_i \alpha_i c_{p_i} / \lambda \quad . \tag{2.15}$$

It has been shown[18] that the Prandtl Number is, for practical purposes, fairly constant over a wide range of temperatures for air; thus as long as we exclude mass injection of gases with radically different physical properties, we can express λ in terms of μ and $\bar{c}_p$ with known P_R.

At an interface between the gas and (say) a solid boundary, one must prescribe an energy balance including any possible heat of phase change (if this statement is in terms of the enthalpy, surface reaction effects will be implicit in that variable). Several recent articles have considered the formulation of this heat balance[14,19]; in general it reads

$$\dot{q}_W = \vec{Q}_W \cdot \vec{N} - \left(\rho \vec{V} \cdot \vec{N} h_G - \sum_j S_j h_j \right)_W \quad , \tag{2.16}$$

where $\dot{q}_W$ is the net rate of heat input per unit area into the boundary material depths, $\vec{Q}_W$ is the value of Equation (2.14) at the interface, S_j is the mass rate of disappearance of the j-th specie boundary phase constituent of enthalpy h_j, and h_G is the gas mixture enthalpy. The supposition of a continuum implies equality of gas and boundary temperatures at the interface. In conjunction with the use of Equation (2.16), one may

* $\bar{c}_p$ is the so-called "frozen" mixture specific heat.

pursue two courses: either prescribe the interface temperature and subsequently calculate $\dot{q}_W$ from the solutions to the governing equations, or prescribe $\dot{q}_W$ and calculate the surface temperature that the resulting flow solution assumes. The latter corresponds to the recovery temperature or thermometer problem when $\dot{q}_W$ is set equal to zero.

Several alternative forms of the energy Equation (2.12) prove useful in certain applications, namely the total enthalpy form and the "temperature" form in which the net gas phase reaction rates appear explicitly. Regarding the latter, the definition of h permits one to write

$$\frac{\partial h}{\partial t} = \sum_i h_i \frac{\partial \alpha_i}{\partial t} + \bar{c}_p \frac{\partial T}{\partial t} \,. \tag{2.17}$$

Further, $\partial \alpha_i / \partial t$ may be replaced by the diffusion and chemical reaction terms from the specie conservation equation to produce

$$\sum_i h_i \frac{\partial \alpha_i}{\partial t} = \sum_i h_i \left(\frac{m_i K_i}{\rho} \right) - \sum_i \frac{h_i}{\rho} \nabla \cdot \rho \alpha_i \vec{v}_i \,, \tag{2.18}$$

which, when inserted into Equation (2.17) and the result then used in the energy equation, eliminates the enthalpy in favor of the temperature and exhibits the reaction rates explicitly. Similarly, the use of the relation

$$\nabla h = \sum_i h_i \nabla \alpha_i + \bar{c}_p \nabla T \tag{2.19}$$

permits the gas heat flux to be rewritten in terms of the enthalpy as

$$\vec{Q} = -\frac{\mu}{P_R} \nabla h - \sum_i h_i \left(\frac{\rho \bar{c}_p}{\lambda} \alpha_i \vec{v}_i - \nabla \alpha_i \right) + \frac{kT}{n} \sum_i \sum_j \frac{n_i}{m_i} \frac{D_i^T}{\mathcal{D}_{ij}} \left(\vec{v}_i - \vec{v}_j \right) \,. \tag{2.20}$$

Thermal Equation of State

If we assume each component specie to behave as a perfect gas,*

$$p_i = k n_i T = R_o N_i T, \tag{2.21}$$

so application of Daltons Law gives

$$p = \sum_i p_i = R_o T \sum_i N_i = R_o N T. \tag{2.22}$$

Since

$$\rho_i = n_i m_i = N_i M_i ,$$

then

$$\begin{aligned} \rho &= \sum_i \rho_i = n \sum_i \frac{n_i}{n} m_i \\ &= N \sum_i \frac{N_i}{N} M_i = N \bar{M} \end{aligned} \tag{2.23}$$

where

$$\bar{M} = \sum_i \frac{N_i}{N} M_i \tag{2.24}$$

is the molecular weight of the mixture, defined as the appropriate molar average of the component molecular weights. Consequently, we have the thermal equation of state (2.22) as

$$p = \rho \left(\frac{R_o}{\bar{M}} \right) T . \tag{2.25}$$

The volumetric fraction is related to the mass fraction of a given specie as follows:

$$\frac{n_i}{n} = \frac{\alpha_i / m_i}{\sum_i \alpha_i / m_i} . \tag{2.26}$$

The inverse relation of the mass fraction to the mole fraction is

$$\alpha_i = (M_i / \bar{M})(n_i / n) . \tag{2.27}$$

* $n_i/N_i = R_o/k = N_o$ = Avogadros Number

Theoretical Representation of a Reacting Gas Mixture

Multicomponent Gas Diffusion

The mathematical description of multicomponent diffusion is generally quite complicated; accordingly, one must employ suitable approximations which adequately simplify the analysis without omitting the significant real gas effects. Several schemes have been suggested to meet this need: (1) The use of the binary Fick diffusion law for each specie in a multicomponent mixture of three or more species. This approximation possesses the two-fold advantage of the inherent simplicity of the binary form and an applicibility to any number of components for all temperatures. (2) The "quasi-two component" approximation scheme described by Adamson[7], which attempts to account for deviations from Fick's law in formulating the diffusion fluxes; originally developed for a three component mixture, this approach may readily be extended to four or more species.

Before taking up the four component case, consider first the multicomponent diffusion properties for a three component mixture of molecular oxygen and nitrogen and atomic oxygen (species 1, 3 and 2 respectively), for which we make the reasonable approximations $m_1 = m_3 = 2m_2$ and $M_1 = M_3 = 2M_2$. Using the relations between volume and mass fractions for this case,

$$\begin{aligned} \mathcal{M}_1/\mathcal{M} &= \alpha_1/(1+\alpha_2) \\ \mathcal{M}_2/\mathcal{M} &= 2\alpha_2/(1+\alpha_2) \\ \mathcal{M}_3/\mathcal{M} &= \alpha_3/(1+\alpha_2) \end{aligned} \quad ,$$

the general three component diffusion coefficient expression yields the following values:

$$D_{21}/\mathscr{D}_{12} = 1 + \frac{(\mathscr{D}_{23}/\mathscr{D}_{12} - 1)\alpha_3}{\mathscr{D}_{23}/\mathscr{D}_{12} + \alpha_3(1 - \mathscr{D}_{23}/\mathscr{D}_{12}) + \alpha_2\left(2\frac{\mathscr{D}_{13}}{\mathscr{D}_{12}} - \frac{\mathscr{D}_{23}}{\mathscr{D}_{12}}\right)} \tag{2.28}$$

$$D_{23}/\mathscr{D}_{23} = 1 + \frac{(\mathscr{D}_{23}/\mathscr{D}_{12} - 1)(1 - \alpha_2 - \alpha_3)}{\mathscr{D}_{23}/\mathscr{D}_{12} + \alpha_3(1 - \mathscr{D}_{23}/\mathscr{D}_{12}) + \alpha_2\left(2\frac{\mathscr{D}_{13}}{\mathscr{D}_{12}} - \frac{\mathscr{D}_{23}}{\mathscr{D}_{12}}\right)} \tag{2.29}$$

$$D_{31}/\mathscr{D}_{13} = 1 - \frac{(2\,\mathscr{D}_{13}/\mathscr{D}_{12} - \mathscr{D}_{23}/\mathscr{D}_{12})\alpha_2}{\mathscr{D}_{23}/\mathscr{D}_{12} + \alpha_3(1 - \mathscr{D}_{23}/\mathscr{D}_{12}) + \alpha_2\left(2\frac{\mathscr{D}_{13}}{\mathscr{D}_{12}} - \frac{\mathscr{D}_{23}}{\mathscr{D}_{12}}\right)} \tag{2.30}$$

$$D_{32}/\mathscr{D}_{23} = 1 - \frac{(2\,\mathscr{D}_{13}/\mathscr{D}_{12} - \mathscr{D}_{23}/\mathscr{D}_{12})(1 - \alpha_2 - \alpha_3)}{\mathscr{D}_{23}/\mathscr{D}_{12} + \alpha_3(1 - \mathscr{D}_{23}/\mathscr{D}_{12}) + \alpha_2\left(2\frac{\mathscr{D}_{13}}{\mathscr{D}_{12}} - \frac{\mathscr{D}_{23}}{\mathscr{D}_{12}}\right)} \tag{2.31}$$

The corresponding diffusion fluxes for the atomic and second molecular species (ignoring pressure, body force and thermal diffusion) are then obained from Equation (2.5) as follows:

$$\rho\alpha_2\vec{V}_2 = -\rho\mathscr{D}_{12}\left\{\frac{D_{21}}{\mathscr{D}_{12}}\nabla\alpha_2 + \left(\frac{D_{23} - D_{21}}{2\mathscr{D}_{12}}\right)\left[\alpha_3\nabla\alpha_2 - (1+\alpha_2)\nabla\alpha_3\right]\right\} \tag{2.32}$$

$$\rho\alpha_3\vec{V}_3 = -\rho\mathscr{D}_{12}\left\{\frac{(1+\alpha_2)D_{31}}{\mathscr{D}_{12}}\nabla\alpha_3 + \left[\frac{D_{31}}{\mathscr{D}_{12}}(2-\alpha_3) - \frac{D_{32}}{\mathscr{D}_{12}}\right]\nabla\alpha_2\right\}. \tag{2.33}$$

Now regardless of $\mathscr{D}_{13}$, the diffusion coefficients $\mathscr{D}_{12}$ are $\mathscr{D}_{23}$ should be equal when $m_1 = m_3$ and the collision cross-sections are the same, and this is verified by the diffusion coefficient estimates given in Appendix B. An immediate consequence of the single assumption $\mathscr{D}_{12} = \mathscr{D}_{23}$, from Equations (2.28), (2.29) and (2.32), is that

$$D_{23} = D_{21} = \mathscr{D}_{12}$$

and

$$\rho\alpha_2\vec{V}_2 = -\rho\mathscr{D}_{12}\nabla\alpha_2,$$

so that the atomic specie diffusion obeys Fick's law regardless of the

value for $\mathscr{D}_{13}/\mathscr{D}_{12}$. Further, the assumption $\mathscr{D}_{12}=\mathscr{D}_{23}$ simplifies Equations (2.30) and (2.31) to

$$D_{32}/\mathscr{D}_{12} = \frac{2\,\mathscr{D}_{13}/\mathscr{D}_{12} - (2\,\mathscr{D}_{13}/\mathscr{D}_{12}-1)\alpha_3}{1+\alpha_2(2\,\mathscr{D}_{13}/\mathscr{D}_{12}-1)} \tag{2.34}$$

$$D_{31}/\mathscr{D}_{12} = \frac{\mathscr{D}_{13}/\mathscr{D}_{12}}{1+\alpha_2(2\,\mathscr{D}_{13}/\mathscr{D}_{12}-1)}\,, \tag{2.35}$$

which in turn permits the third specie diffusion flux to be written as follows:

$$\rho\alpha_3\vec{V}_3 = -\rho\mathscr{D}_{12}\left\{\nabla\alpha_3 - \left(1-\frac{\mathscr{D}_{13}}{\mathscr{D}_{12}}\right)\left[\frac{\alpha_3\nabla\alpha_2+(1-\alpha_2)\nabla\alpha_3}{1+\alpha_2(2\,\mathscr{D}_{13}/\mathscr{D}_{12}-1)}\right]\right\}. \tag{2.36}$$

Equation (2.36) shows that the third specie diffusion will also obey Fick's law when either $\mathscr{D}_{13}=\mathscr{D}_{12}$ or when $\alpha_3/(1-\alpha_2)$ is a constant. However, the former condition, while giving a Fick diffusion flux, does <u>not</u> yield D_{32} or D_{23} equal to $\mathscr{D}_{12}$ (that is, the assumption $D_{ij}=\mathscr{D}_{ij}$ does not imply Fick diffusion for all the species present). On the other hand, the assumption $\mathscr{D}_{13}/\mathscr{D}_{12} = 1/2$, which appears to be nearer the actual value (Appendix B), gives $D_{32}=\mathscr{D}_{12}$ and $D_{31}=\mathscr{D}_{13}$ but does <u>not</u> give Fick diffusion for α_3. Regarding the second condition $\alpha_3/(1-\alpha_2)$ = constant, it can be shown that this relation is exact in the case of a completely non-catalytic wall in frozen flow. The combination of this fact with the fact that $1/2 \leq \mathscr{D}_{13}/\mathscr{D}_{12} \leq 1$ leads to the conclusion that the use of Ficks law for α_3, which implies neglect of the second term in brackets in Equation (2.36), may not introduce any significant error in an analysis of near frozen non-equilibrium behavior, particularly if α_3 itself has a weak effect on the calculations. Further discussion on this point is given later.

The quasi-two component scheme[7] for a three component mixture also employs the assumption $\mathscr{D}_{12} = \mathscr{D}_{23}$ and hence also yields Fick diffusion for α_2 regardless of $\mathscr{D}_{13}/\mathscr{D}_{12}$. However, this scheme differs from the foregoing in that it assumes $\mathscr{D}_{13} = 0$, which consequently gives $D_{31} = 0$,

$$D_{32}/\mathscr{D}_{12} = \alpha_3/(1-\alpha_2),$$

and

$$\rho\alpha_3\vec{V}_3 = \rho\mathscr{D}_{12}\left(\frac{\alpha_3}{1-\alpha_2}\right)\nabla\alpha_2 . \tag{2.37}$$

Now when the Fick law diffusion for α_3 is assumed ($\rho\alpha_3\vec{V}_3 = -\rho\mathscr{D}_{12}\nabla\alpha_3$), Equation (2.36) shows that the resulting α_3 diffusion flux error is

$$\rho\alpha_3\vec{V}_3 - (\rho\alpha_3\vec{V}_3)_{FICK} = \left(1-\frac{\mathscr{D}_{13}}{\mathscr{D}_{12}}\right)\left[\frac{\alpha_3\nabla\alpha_2 + (1-\alpha_2)\nabla\alpha_3}{1+\alpha_2(2\mathscr{D}_{13}/\mathscr{D}_{12}-1)}\right]\rho\mathscr{D}_{12}, \tag{2.38}$$

whereas the use of the quasi-two component diffusion approximation above gives an error of

$$\rho\alpha_3\vec{V}_3 - (\rho\alpha_3\vec{V}_3)_{QUASI\text{-}TWO} = -\frac{\mathscr{D}_{13}}{\mathscr{D}_{12}}\left(\frac{1+\alpha_2}{1-\alpha_2}\right)\left[\frac{\alpha_3\nabla\alpha_2 + (1-\alpha_2)\nabla\alpha_3}{1+\alpha_2(2\mathscr{D}_{13}/\mathscr{D}_{12}-1)}\right]\rho\mathscr{D}_{12}. \tag{2.39}$$

Hence the quasi-two component approximation is exact (and reduces to the Fick result) when $\alpha_3/(1-\alpha_2)$ = constant. Equations (2.38) and (2.39) show, assuming $\mathscr{D}_{13}/\mathscr{D}_{12} = 1/2$ for the sake of comparison, that the α_3 diffusion flux error for the quasi-two component approximation is always opposite in sign to and greater than (by a factor $1 + \alpha_2/1-\alpha_2$) the Fick law error. The Fick law therefore always has less absolute error, and the simpler mathematical consequences of using the Fick law would therefore definitely favor its use. The use of the quasi-two component scheme would be of interest, however, in that it represents the upper limit on the α_3 diffusion flux and so could be compared with the Fick

results (representing the lower limit), in order to "bracket" the actual value.

Regarding a mixture of four components, one would suspect on the basis of the foregoing discussion that each atomic specie diffusion flux obeys Fick's law, regardless of the individual molecular species behavior, as long as all the atomic specie diffusion coefficients are the same. Four component mixture calculations based on the general diffusion coefficient in Appendix A confirm this to be true. If all the specie diffusion coefficients are assumed equal, the Fick law is valid for every specie, as shown for any number of components by Knuth[15]. The Fick law approximation in conjunction with the four component mixture representation described in the next paragraph will be used in all the subsequent boundary layer theory given in this paper.

Four Component Mixture Relations

Consider a four component air mixture (neglecting NO), with α_1 for O_2, α_2 for O, α_3 for N_2 and α_4 for N. The relation between the volume and mass fractions is obtained from Equation (2.26) as follows:

$$\left.\begin{aligned} n_1/n &= \alpha_1/A = \left(m_3/m_1\right)\left(\alpha_1/\alpha_3\right) n_3/n \\ n_2/n &= \left(m_1/m_2\right)\alpha_2/A = \left(m_4/m_2\right)\left(\alpha_2/\alpha_4\right) n_4/n \end{aligned}\right\} \quad (2.40)$$

where

$$A = 1 + \alpha_2 + \alpha_4 + \left[\left(\frac{m_1}{m_2} - 2\right)\alpha_2 + \left(\frac{m_1}{m_4} - 2\right)\alpha_4 + \left(\frac{m_1}{m_3} - 1\right)\alpha_3\right]. \quad (2.41)$$

The reasonable approximations $m_1 \approx m_3 = 2m_2 = 2m_4$ are seen to greatly simplify these relations, since the entire bracketed term in Equation (2.41) vanishes. The mixture molecular weight, assuming $M_i/M_j = m_i/m_j$, becomes

$$\bar{M}/M_1 = (1 + \alpha_2 + \alpha_4)^{-1}. \qquad (2.42)$$

The assumption of Fick's law, $\rho \alpha_i \vec{V}_i = -\rho \mathcal{D}_{12} \nabla \alpha_i \quad (\mathcal{D}_{ij} = \mathcal{D}_{12})$, gives the diffusion heat flux term as

$$\rho \sum_i h_i \alpha_i \vec{V}_i = -\rho \mathcal{D}_{12} [(h_2 - h_1)\nabla\alpha_2 + (h_3 - h_1)\nabla\alpha_3 + (h_4 - h_1)\nabla\alpha_4] \qquad (2.43)$$

and the total heat flux becomes

$$-\lambda \nabla T + \rho \sum_i h_i \alpha_i \vec{V}_i = -\frac{\mu}{P_R}\left\{\bar{c}_p \nabla T + L_e[(h_2 - h_1)\nabla\alpha_2 + (h_3 - h_1)\nabla\alpha_3 + (h_4 - h_1)\nabla\alpha_4]\right\} \qquad (2.44)$$

$$= -\frac{\mu}{P_R}\left\{\nabla h + (L_e - 1)[(h_2 - h_1)\nabla\alpha_2 + (h_3 - h_1)\nabla\alpha_3 + (h_4 - h_1)\nabla\alpha_4]\right\} \qquad (2.45)$$

where $L_e \equiv \rho \bar{c}_p \mathcal{D}_{12}/\lambda$ is the Lewis number. As shown by Equation (2.45), the case $L_e = 1$ allows the heat flux to be expressed entirely by the enthalpy gradient. The additional approximations $c_{p_1} = c_{p_3}$ and $c_{p_2} = c_{p_4}$, with $h_{f_1}^{(o)} = h_{f_3}^{(o)} = 0$ and $h_{f_2}^{(o)} \neq h_{f_4}^{(o)} > 0$, give $h_3 = h_1$ (but $h_4 \neq h_2$) and therefore drop out the explicit contribution of α_3 in Equations (2.43) to (2.45).

Volumetric Dissociation-Recombination Rates

The general real gas flow conservation equations require a specification of the net chemical production rates of the various species per unit volume of gas; for the air mixture under consideration, this

introduces the dissociation-recombination chemistry. Consider the dissociation-recombination reaction

$$N_M + N_X \underset{K_R}{\overset{K_f}{\rightleftharpoons}} 2N_A + N_X \tag{2.46}$$

in the presence of an inert specie N_X, N_M and N_A being the molecular and atomic species, respectively; this reaction is of the form encountered for the present four specie air mixture. The net reaction rates are[20]:

$$\left.\begin{aligned} dN_A/dt &= K_f N_M N_X - K_R N_A^2 N_X \\ &= K_R N_X [(K_f/K_R) N_M - N_A^2] \\ dN_M/dt &= -\tfrac{1}{2}(dN_A/dt) \end{aligned}\right\} \tag{2.47}$$

where the mass rate of formation is found from the molar rate by

$$\mathcal{M}_A K_A = M_A \frac{dN_A}{dt} . \tag{2.48}$$

The equilibrium parameter $k_c \equiv k_f/k_R$ for this reaction is of the form (9):

$$K_c = \frac{N}{p} EXP\left(a - \frac{T_A}{T}\right) \tag{2.49}$$

where p is in atmospheres, a is a constant, and $T_A \equiv E_A/R_o$ is a characteristic activation energy temperature. Equations (2.47) show that while the inert third specie N_X does not affect the equilibrium composition of the gas ($\frac{dN_A}{dt} = \frac{dN_M}{dt} = 0$), it does play a role in any chemical non-equilibrium process. The value of the recombination rate parameter k_R is established by detailed theoretical analyses of the ternary collision processes (supported by extensive experimental study). It appears from current work with Oxygen and Nitrogen that k_R has the general form

$$K_R = K_R' T^{\omega} \tag{2.50}$$

with k_R' and ω of the order 10^{15} and -1, respectively, although widely differing values have been proposed by various investigators.[6,9,21]

Table I presents typical oxygen recombination rate data to illustrate the present day uncertainty. It is therefore very desirable to assess the sensitivity of the results of real gas analyses involving the reaction rates to the parameters k_R' and ω.

TABLE I

RECOMBINATION RATE DATA FOR OXYGEN

Source	k_R ($cm^6/mole^2$-sec.)	Value at 4000°K
Davidson[23]	$5 \times 10^{14}\ (T/300°K)^{-1.5}$	1.05×10^{13}
Logan[21]	$3 \times 10^{15}\ (T/300°K)^{.5}$	1.10×10^{16}
Hirschfelder[9]	$1.2 \times 10^{16}\ (T/300°K)^{2.5}$	7.80×10^{18}

The recombination-dissociation rates above, if applied to oxygen and nitrogen in air, would imply the assumption of no direct chemical interreaction between the two and constitutes a neglect of Nitric Oxide formation. It appears that the nitric oxide chemistry is not completely understood at present; an examination of current literature on the subject, however, indicates the following situation. (a) Several investigations into NO reactions[21,22,23] apparently produce favorable agreement with experiment when the chemical interreaction between the $O_2 \rightleftharpoons 2O$ and $N_2 \rightleftharpoons 2N$ processes is neglected. (b) Neglect of the coupling reactions due to NO, however, does not necessarily mean that NO alone, acting as a fifth specie, may not be as important as the oxygen and nitrogen dissociation-recombination rates in determining the non-equilibrium behavior. Some recent estimates by Logan[21] imply three main facts that suggest that NO may

play a very minor role in the present investigation. First, the concentration of NO in a high temperature air mixture at the edge of the boundary layer for low pressures (high altitudes) is very small and is noticeable only in a temperature range of approximately 3000-6000°K: for example, the maximum fractional concentration is about 4% at 5000°K for $p \simeq 100$ lb/ft^2. As long as the recombination constant and temperature dependence for NO are not very much greater than those for O and N, this would imply that the recombination rate of NO (which is proportional to the square of the concentration) is much less significant to a non-equilibrium analysis of the boundary layer than the O and N recombination rates. Second, the corresponding maximum amount of total internal energy possessed by the NO is 5%, which indicates that the neglect of NO would have a very small effect on the non-equilibrium heat transfer. Third, it was found that the low pressure production rate of nitric oxide is several orders of magnitude slower than the oxygen dissociation rate; this also suggests the NO chemistry plays a minor role in non-equilibrium air behavior in the boundary layer. The foregoing facts seem to indicate that it is reasonable to neglect the presence of nitric oxide in the present analysis, assuming the individual oxygen and nitrogen dissociation-recombination chemistry to be the important mechanisms.

We therefore take the four specie dissociated air mixture chemistry to be governed by the following two independent reactions:

$$\left.\begin{aligned} N_1 + N &\underset{K_{R2}}{\overset{K_{f_2}}{\rightleftharpoons}} 2N_2 + N \\ N_3 + N &\underset{K_{R4}}{\overset{K_{f_4}}{\rightleftharpoons}} 2N_4 + N \end{aligned}\right\} \qquad (2.51)$$

where the inert specie N (total number of particles) participates in both reactions indirectly as a third body collision partner. Since these two reactions are independent,

$$\mathcal{M}_1 K_1 + \mathcal{M}_2 K_2 = 0$$
$$\mathcal{M}_3 K_3 + \mathcal{M}_4 K_4 = 0 ,$$

which satisfies the $\sum_i m_i K_i = 0$ requirement. Since Equations (2.51) are of the form (2.46), the two net atomic specie reaction rates can be written, using Equations (2.47) to (2.49), as follows:

$$\mathcal{M}_2 K_2 = -\mathcal{M}_1 K_1 = K_{R_2} M_2 N^3 \left[\left(\frac{N_1}{N}\right) \frac{EXP(a_2 - T_{A_2}/T)}{p} - \left(\frac{N_2}{N}\right)^2 \right] \qquad (2.52)$$

$$\mathcal{M}_4 K_4 = -\mathcal{M}_3 K_3 = K_{R_4} M_4 N^3 \left[\left(\frac{N_3}{N}\right) \frac{EXP(a_4 - T_{A_4}/T)}{p} - \left(\frac{N_4}{N}\right)^2 \right] . \qquad (2.53)$$

Using the thermal equation of state, the volume-mass fraction relations and the molecular weight expression previously developed for this four specie mixture, these rate expressions can be written in terms of pressure, density, temperature and mass fractions as follows:

$$\mathcal{M}_2 K_2 = -2\rho K_{R_2} \left(\frac{p}{R_0 T}\right)^2 \left[\frac{\alpha_2^2}{1+\alpha_2+\alpha_4} - \left(\frac{1-\alpha_2-\alpha_4-\alpha_3}{4p}\right) EXP\left(a_2 - \frac{T_{A_2}}{T}\right) \right] \qquad (2.54)$$

$$\mathcal{M}_4 K_4 = -2\rho K_{R_4} \left(\frac{p}{R_0 T}\right)^2 \left[\frac{\alpha_4^2}{1+\alpha_2+\alpha_4} - \left(\frac{\alpha_3}{4p}\right) EXP\left(a_4 - \frac{T_{A_4}}{T}\right) \right] \qquad (2.55)$$

where

$$T_{A_{2,4}} = E_{A_{2,4}}/R_0 .$$

It is consistent with the assumed equality of physical properties between species 1 and 3, and species 2, 4 (except the heats of formation)

that we also assume $a_2 = a_4 = a$ and $k_{R_2} = k_{R_4} = k_R' T^{\omega}$. The last equality is not necessary but simplifies the non-equilibrium analysis ($\omega_2 = \omega_4$ and $k_{R_2}' = k_{R_4}'$ should be a good approximation, since the N and O recombination processes are independent of E_{A_2} and E_{A_4}). The reaction rates given by Equations (2.54) and (2.55) are especially convenient forms, since they show the net rate is essentially the product of a state function (proportional to density cubed) of the recombination chemistry and another function which vanishes in the classical thermodynamic equilibrium. The thermodynamic equilibrium composition is governed by the equations ($m_i K_i = 0$):

$$\frac{\alpha_{2_{EQ.}}^2}{1+\alpha_{2_{EQ.}}+\alpha_{4_{EQ.}}} = \left(\frac{1-\alpha_{2_{EQ.}}-\alpha_{4_{EQ.}}-\alpha_{3_{EQ.}}}{4p}\right) EXP\left(a - \frac{T_{A_2}}{T}\right) \qquad (2.56)$$

$$\frac{\alpha_{4_{EQ.}}^2}{1+\alpha_{2_{EQ.}}+\alpha_{4_{EQ.}}} = \left(\frac{\alpha_{3_{EQ.}}}{4p}\right) EXP\left(a - \frac{T_{A_4}}{T}\right) \qquad (2.57)$$

(The specie $\alpha_{3_{EQ.}}$, which is also required for the calculation of the equilibrium composition, is determined from an additional statement of the conservation of both total oxygen and nitrogen molecules in a closed system. See Appendix G).

The net production of total atomic specie mass by homogeneous chemical reaction, which is of interest when comparing the present formulation with that of other reacting boundary layer theories, is obtained by adding Equations (2.54) and (2.55):

$$-(m_2 K_2 + m_4 K_4) = 2\rho k_R' T^{\omega-2}\left(\frac{p}{R_0}\right)^2 \left\{\left[\frac{\alpha^2}{1+\alpha} - \left(\frac{1-\alpha}{4p}\right) EXP\left(a - \frac{T_{A_2}}{T}\right)\right] - \left[\frac{2\alpha_2\alpha_4}{1+\alpha} - \left(\frac{\alpha_3 EXP\, a}{4p}\right)\left(EXP\left(-\frac{T_{A_2}}{T}\right) - EXP\left(-\frac{T_{A_4}}{T}\right)\right)\right]\right\} \qquad (2.58)$$

where $\alpha \equiv \alpha_2 + \alpha_4$ is the total atomic specie. The first bracketed term in Equation (2.58) is a binary atomic reaction rate form based on α, such as used by Fay and Riddell[6]. The second term is an increment due to the importance of the individual second atomic and molecular specie behavior, not accounted for by α alone. This second bracket is composed of two parts: the first accounts for the reduction of the recombination rate from that based on α alone, while the second shows the effect of the molecular nitrogen due to the difference in activation energy between nitrogen and oxygen. When there is a significant atomic nitrogen population in the gas mixture, Equation (2.58) shows that the total atomic reaction rate can be seriously overestimated by the use of only the binary rate form based on the total atomic specie concentration α.

Heterogeneous Reaction Rates

The effect of possible chemical reaction between the flowing gas and the material of a boundary surface enters through the specie equation boundary conditions. Of particular interest is surface-catalyzed recombination of atomic oxygen and nitrogen in the gas, since the amount of diffusion heat flux into the surface depends on the degree of such catalytic activity. In an "open" system, in which diffusion and convection exist to "compete" with chemical reactions, surface catalysis can noticeably alter the composition of the gas near the surface (something it could not do in the steady state in a closed system). The catalytic production rate of any particular specie j in the gas can be written in the form

$$S_{j_c} = \rho_w K_{c_j} \left(\alpha_{j_{EQ.}} - \alpha_j\right)_w , \qquad (2.59)$$

where k_{c_j} is a characteristic surface reaction parameter, a function of surface temperature and material, and $\alpha_{j_{EQ}}$ is the equilibrium specie concentration at the surface temperature. (A more detailed discussion of surface catalysis is given in Appendix C.) Regardless of the detailed behavior, overall mass conservation requires the following relation between the individual catalysis rates:

$$\sum_j S_{j_c} = 0 .$$

For the previously chosen four specie model of a dissociated air mixture, the development in Appendix C shows that:

$$\left.\begin{aligned} S_{2_c} &= -\rho_w K_{c_2} (\alpha_2 - \alpha_{2_{EQ.}})_w \\ S_{4_c} &= -\rho_w K_{c_2} (\alpha_4 - \alpha_{4_{EQ.}})_w \\ S_{3_c} &= \rho_w K_{c_2} (\alpha_3 - \alpha_{3_{EQ.}})_w \end{aligned}\right\} \qquad (2.60)$$

which are generally required for the three specie conservation equation boundary conditions. It has been shown[10] that for cooled walls with temperatures below about 2000°K, the catalytic dissociation affect is negligable, i.e., that $\alpha_{2_{EQ_w}}$ and $\alpha_{4_{EQ_w}}$ can be set equal to zero and only catalytic recombination considered for the atomic species.

Chemically Reacting Boundary Layer Equations

The usual boundary layer order of magnitude analysis is assumed to be applicable to a reacting multicomponent gas mixture flow. In addition to the usual assumptions involved, the presence of diffusion and reaction rates in a real gas requires two other restrictions: first, the Schmidt number S_c must be of order one so that the composition boundary layer thickness is of the same order as the velocity and thermal layers; second, the streamwise variation of the reaction rates must be small

compared to variations in a direction normal to the body surface. Furthermore, boundary layer-inviscid flow interreaction phenomena such as induced pressure gradients, vorticity at the edge of the boundary layer, and any coupling between inviscid flow and boundary layer chemical reactions, will be neglected. The flow at the boundary layer edge is assumed a known inviscid solution for the given body.

Boundary Layer Equations

The boundary layer approximations applied to the general flow equations yield the following relations governing axi-symmetric or two dimensional real gas flow (body forces, radiation, thermal and pressure diffusion, and overall mass transfer at the body surface are omitted):

(1) Continuity*

$$\frac{\partial}{\partial x}(\rho u r_0^K) + r_0^K \frac{\partial}{\partial y}(\rho v) = 0 \quad . \tag{2.61}$$

(2) First Atomic Specie

$$\rho\left(u\frac{\partial \alpha_2}{\partial x} + v\frac{\partial \alpha_2}{\partial y}\right) = \frac{\partial}{\partial y}\left(\frac{\mu}{S_c}\frac{\partial \alpha_2}{\partial y}\right) - 2\rho K_R' T^{\omega-2}\left(\frac{p_e}{R_0}\right)^2 g_2 \tag{2.62}$$

where

$$g_2 \equiv \frac{\alpha_2^2}{1+\alpha} - (1-\alpha-\alpha_3)\frac{EXP(a - T_{A_2}/T)}{4 p_e} \tag{2.63}$$

$$g_4 \equiv \frac{\alpha_4^2}{1+\alpha} - \alpha_3 \frac{EXP(a - T_{A_4}/T)}{4 p_e} \quad . \tag{2.64}$$

(3) Second Atomic Specie

$$\rho\left(u\frac{\partial \alpha_4}{\partial x} + v\frac{\partial \alpha_4}{\partial y}\right) = \frac{\partial}{\partial y}\left(\frac{\mu}{S_c}\frac{\partial \alpha_4}{\partial y}\right) - 2\rho K_R' T^{\omega-2}\left(\frac{p_e}{R_0}\right)^2 g_4 . \tag{2.65}$$

* K = 0 for a two dimensional flow and K = 1 for an axially-symmetric flow.

(4) Second Molecular Specie

$$\rho\left(u\frac{d\alpha_3}{dx}+v\frac{d\alpha_3}{dy}\right)=\frac{d}{dy}\left(\frac{\mu}{Sc}\frac{d\alpha_3}{dy}\right)+2\rho K_R' T^{\omega-2}\left(\frac{p_e}{R_0}\right)^2 g_4 . \tag{2.66}$$

(5) Momentum

$$\rho\left(u\frac{du}{dx}+v\frac{du}{dy}\right)+\frac{dp_e}{dx}=\frac{d}{dy}\left(\mu\frac{du}{dy}\right). \tag{2.67}$$

(6) Energy Equations

In terms of the static enthalpy (with $c_{p_1}=c_{p_3}$ and $c_{p_2}=c_{p_4}$), given by

$$h=h_1+\alpha_2(h_2-h_1)+\alpha_4(h_4-h_1), \tag{2.68}$$

we have

$$\rho\left(u\frac{dh}{dx}+v\frac{dh}{dy}\right)=u\frac{dp_e}{dx}+\mu\left(\frac{du}{dy}\right)^2+\frac{d}{dy}\left\{\frac{\mu}{P_R}\left[\frac{dh}{dy}+(Le-1)\left[(h_2-h_1)\frac{d\alpha_2}{dy}+(h_4-h_1)\frac{d\alpha_4}{dy}\right]\right]\right\}. \tag{2.69}$$

The stagnation enthalpy form of this equation, on the other hand, reads

$$\rho\left(u\frac{dh_s}{dx}+v\frac{dh_s}{dy}\right)=\frac{d}{dy}\left\{\frac{\mu}{P_R}\left[\frac{dh_s}{dy}+(P_R-1)\frac{d(u^2/2)}{dy}+(Le-1)\left[(h_2-h_1)\frac{d\alpha_2}{dy}+(h_4-h_1)\frac{d\alpha_4}{dy}\right]\right]\right\} \tag{2.70}$$

where $h_s \equiv u^2/2 + h$.

Equation (2.69) can alternatively be written in a form involving the temperature, in which the reaction rates appear, by expressing the enthalpy derivatives in terms of temperature and concentration derivatives (see Equations (2.17) to (2.19)):

$$\begin{aligned}\rho\bar{c}_p\left(u\frac{dT}{dx}+v\frac{dT}{dy}\right)&=u\frac{dp_e}{dx}+\mu\left(\frac{du}{dy}\right)^2+\frac{\mu}{Sc}(c_{p_2}-c_{p_1})\frac{d\alpha}{dy}\frac{dT}{dy}\\&+\frac{d}{dy}\left(\frac{\mu\bar{c}_p}{P_R}\frac{dT}{dy}\right)+2\rho K_R' T^{\omega-2}\left(\frac{p_e}{R_0}\right)^2\left[(h_2-h_1)g_2+(h_4-h_1)g_4\right]\end{aligned} \tag{2.71}$$

where

$$c_p = c_{p_1}+\alpha(c_{p_2}-c_{p_1}). \tag{2.72}$$

(7) Thermal Equation of State

$$p=p_e(x)=\rho\left(\frac{R_0}{M_{11}}\right)(1+\alpha)T. \tag{2.73}$$

Boundary Conditions

At the outer edge of the boundary layer ($y \to \infty$), the solution must match the known inviscid flow: $u(X,\infty) = u_e(X)$, $T(X,\infty) = T_e(X)$, $\alpha_i(X,\infty) = \alpha_{ie}(X)$ and $h_s(X,\infty) = h_{s_e} = \text{constant}$. Further, when the viscous transport terms and interreaction phenomena are equated to zero at the edge of the layer, the foregoing equations give

$$\left.\begin{aligned} \rho_e u_e \frac{du_e}{dX} &= -\frac{dp_e}{dX} \\ \rho_e \frac{dh_e}{dX} &= \frac{dp_e}{dX} \\ u_e \frac{d\alpha_{2e}}{dX} &= -2K_R' T_e^{\omega-2}\left(\frac{p_e}{R_o}\right)^2 g_{2e} \\ u_e \frac{d\alpha_{4e}}{dX} &= -2K_R' T_e^{\omega-2}\left(\frac{p_e}{R_o}\right)^2 g_{4e} = -u_e \frac{d\alpha_{3e}}{dX}. \end{aligned}\right\} \quad (2.74)$$

The two specie relations show that the assumption of an equilibrium inviscid free-stream flow ($g_{2_e} = g_{4_e} = 0$) permits the neglect of the $d\alpha_{i_e}/dX$ terms in the boundary layer equations.

At the surface of the body, on the other hand, we have $u(X,0) = v(X,0) = 0$, $T(X,0) = T_w$, the specie diffusion-surface reaction rate balance (neglecting catalytic surface dissociation)

$$\left.\begin{aligned} \mathscr{D}_{12} \frac{d\alpha_2}{dY}(X,0) &= K_{c_2}\alpha_2(X,0) \\ \mathscr{D}_{12} \frac{d\alpha_4}{dY}(X,0) &= K_{c_2}\alpha_4(X,0) \\ \mathscr{D}_{12} \frac{d\alpha_3}{dY}(X,0) &= -K_{c_2}[\alpha_3(X,0) - \alpha_{3_{EQ.}}(X,0)] \end{aligned}\right\}, \quad (2.75)$$

and finally the heat flux of the gas into the surface,

$$-\dot{Q}_w = \frac{\mu}{P_R}(0)\left\{\bar{C}_p \frac{\partial T}{\partial Y} + L_e\left[(h_2 - h_1)\frac{\partial \alpha_2}{\partial Y} + (h_4 - h_1)\frac{\partial \alpha_4}{\partial Y}\right]\right\}_{Y=0} \tag{2.76}$$

$$= \frac{\mu}{P_R}(0)\left\{\frac{\partial h}{\partial Y} + (L_e - 1)\left[(h_2 - h_1)\frac{\partial \alpha_2}{\partial Y} + (h_4 - h_1)\frac{\partial \alpha_4}{\partial Y}\right]\right\}_{Y=0} . \tag{2.77}$$

Some Special Features of the Equations

Several special cases of the foregoing boundary layer equations warrant attention before taking up any detailed solutions.

(a) Inspection of the stagnation enthalpy form of the energy Equation (2.70) shows that when the surface enthalpy is known (known surface temperature and gas composition), and when $L_e = P_R = 1$, the use of the Fick law diffusion approximation causes h_s to be governed by a reaction-independent differential equation of the same form as for low speed, perfect gas flow:

$$\rho\left(u\frac{\partial h_s}{\partial X} + v\frac{\partial h_s}{\partial Y}\right) = \frac{\partial}{\partial Y}\left(\frac{\mu}{P_R}\frac{\partial h_s}{\partial Y}\right)$$

and the surface heat flux is given entirely in terms of the enthalpy gradient,

$$-\left[\dot{Q}_w\right]_{L_e=1} = \frac{\mu}{P_R}(0)\left(\frac{\partial h_s}{\partial Y}\right)_{Y=0} .$$

Therefore, when $L_e = 1$ and the gas composition at the surface is known, the sum of the conduction and diffusion heat fluxes (although each is individually sensitive to reaction) remains invariant to chemical reaction of any form in the gas. This special case has been thoroughly exploited by Lees.[4,14] Futhermore, if there is a negligable pressure gradient,

the h_s profile is completely similar to the velocity profile regardless of the viscosity law (as seen by a comparison of the enthalpy and the momentum equations) when h_W = constant:

$$h_s = C_1 + C_2 \cdot u .$$

All of these conclusions are for arbitrary gas phase reaction rates. However, when any one or all of the assumed conditions above are substantially untrue, then the h_s variable will not be a suitable one for the energy equation and heat transfer calculation.

(b) An interesting qualitative similarity between the effects of the reaction rates in the gas and the pressure gradient effect in the momentum equation may be shown. In the gas adjacent to the wall, the momentum equation gives

$$\left[\frac{\partial}{\partial Y}\left(\mu \frac{\partial u}{\partial Y}\right)\right]_{Y=0} = \frac{dp_e}{dX} \quad , \tag{2.78}$$

whereas from the atomic specie equations,

$$\left[\frac{\partial}{\partial Y}\left(\frac{\mu}{S_c} \frac{\partial \alpha_{2,4}}{\partial Y}\right)\right]_{Y=0} = 2\rho_W K_R' T_W^{\omega-2}\left(\frac{p_e}{R_0}\right)^2 g_{2,4}(0) . \tag{2.79}$$

Equation (2.78) indicates the well known fact that an unfavorable ($dp_e/dX > 0$) pressure gradient causes an inflection point at some $Y > 0$ in the velocity profile. Equation (2.79) illustrates a similar fact, namely that when $g_{2,4}$ are positive in the neighborhood of the wall (recombination dominating dissociation in the gas near the wall), a point of inflection will exist in each of the atomic specie profiles. The initial increase in slope near the surface will be most prominent in regions of high pressure and in cases for which the recombination

rate temperature dependence ω is the largest positive number. This reaction rate effect for near frozen flow is illustrated in Figure 1a for a highly cooled catalytic ($\alpha_{2W} = 0$) and non-catalytic ($\left(\frac{d\alpha_2}{dY}\right)_W = 0$) wall. A similar conclusion can be drawn regarding the temperature profile in the gas near the surface when the viscous dissipation is considered negligable; from Equation (2.71) (assuming $c_{p_2} = c_{p_1}$), one has

$$\left[\frac{\partial}{\partial Y}\left(\frac{\mu}{P_R}\bar{c}_p\frac{\partial T}{\partial Y}\right)\right]_{Y=0} = -2\rho_W T_W^{\omega-2}\left(\frac{p_e}{R_0}\right)^2\left[(h_2-h_1)g_2+(h_4-h_1)g_4\right]_{Y=0}. \quad (2.80)$$

Here, the predominance of recombination acts in the opposite sense to that in the specie profiles (i.e., like a favorable pressure gradient), and an inflection point in the T(Y) profile will occur only when dissociation is the dominant reaction in the gas near the wall. This behavior is illustrated in Figure 1b for a cooled wall.

(c) Several combinations of the specie mass fractions are governed by equations that are independent of the detailed gas reaction rates, and therefore show a general similarity to the enthalpy and velocity profile under certain conditions. Addition of Equations (2.65) and (2.66) gives

$$\rho\left[u\frac{\partial(\alpha_3+\alpha_4)}{\partial X}+v\frac{\partial(\alpha_3+\alpha_4)}{\partial Y}\right] = \frac{\partial}{\partial Y}\left[\frac{\mu}{S_c}\frac{\partial}{\partial Y}(\alpha_3+\alpha_4)\right].$$

This equation is free of reaction rate terms and therefore yields a general similarity between $\alpha_3 + \alpha_4$ and h_s when $S_c = L_e = P_R = 1$ and when the gas composition and enthalpy at the wall are constant. Furthermore, the $\alpha_3 + \alpha_4$ profile (and the $\alpha_1 + \alpha_2 = 1 - \alpha_3 - \alpha_4$ profile as well)

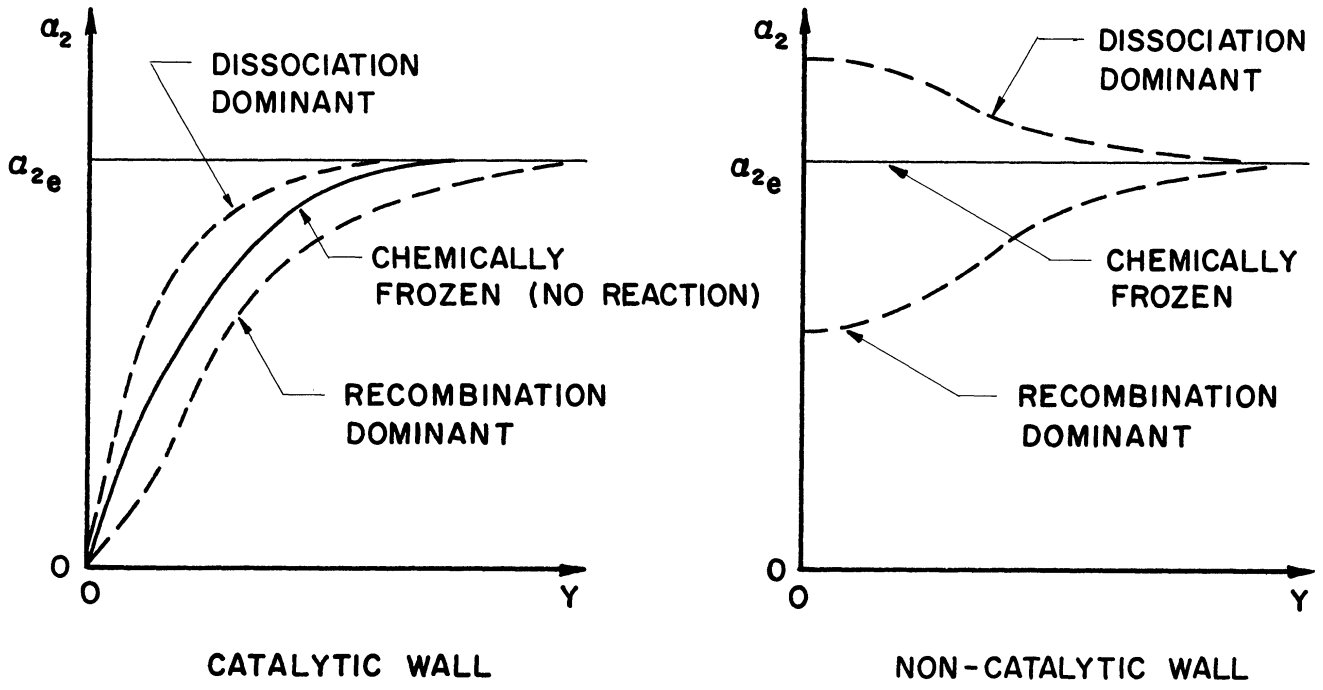

a) ATOMIC SPECIE PROFILE

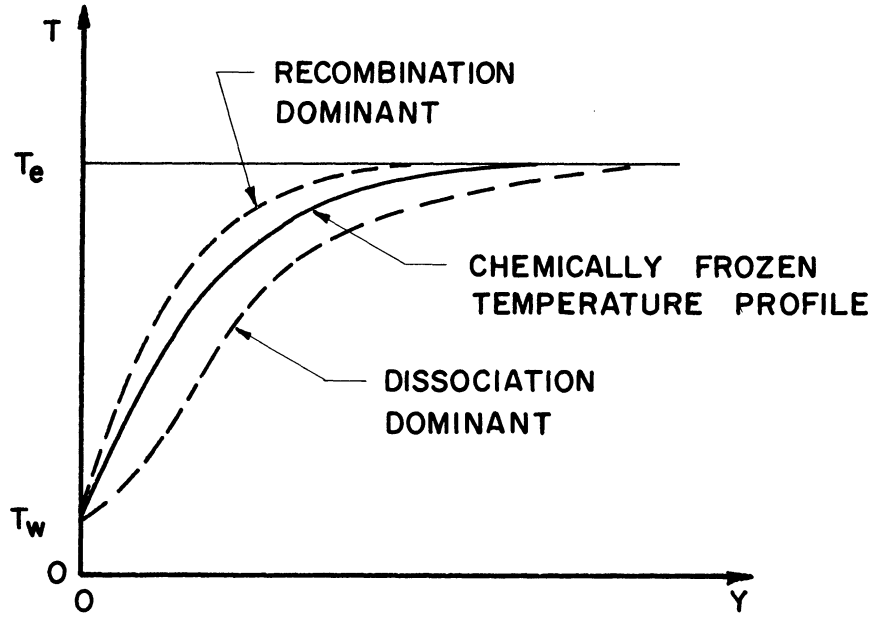

b) TEMPERATURE PROFILE

Figure 1. Illustration of the Reaction Rate Effect on the Boundary Layer Specie and Temperature Profiles Near Frozen Flow.

is similar to the velocity profile in the absence of a pressure gradient, regardless of the viscosity law, if the wall gas composition is constant.

Characteristic Non-Equilibrium Parameters and Hypersonic Environment

Previous investigations[6,25] have indicated the utility of dealing with reactions in flow problems in terms of the following characteristic parameter representing the ratio of a characteristic flow time to a characteristic reaction time:

$$\zeta = \frac{t_F}{t_R} \tag{2.81}$$

where t_F and t_R are defined according to the particular problem at hand. This parameter can be used to indicate qualitatively the reaction rate effect on composition changes relative to diffusion and convection effects. Two extremes of possible behavior are indicated by the definition of ζ: when ζ approaches zero, flow-induced composition changes are much faster than the reaction rate effect, whereas when ζ becomes very large, the reaction rate effect on the local flow composition completely predominates over diffusion and, or convection. Such extremes may occur for either gas or surface reaction rates and may be illustrated by means of the governing equations for both types of reactions.

Consider a typical i-th atomic specie conservation equation involving a net reaction rate term in steady flow:

$$\frac{d\alpha_i}{dt} = \vec{V} \cdot \nabla \alpha_i = -\frac{\nabla \cdot \rho_i \vec{V}_i}{\rho} + \frac{m_i K_i}{\rho} \tag{2.82}$$

in which $m_i K_i$ for dissociation-recombination can be expressed in the form

$$m_i K_i / \rho = 2 K_R' T^{\omega} \left(\frac{\rho}{R_0}\right)^2 g_i ,$$

where g_i is a dimensionless function of temperature and concentration that identically vanishes in classical thermodynamic equilibrium. Assuming that one can define an appropriate characteristic flow time t_F for convection-diffusion, and a reaction time

$$t_R^{-1} = 2 K_R' T_{REF.}^{\omega-2} (p_{REF}/R_o)^2$$

based on suitably chosen reference conditions, then Equation (2.82) may be written as

$$t_F\left(\vec{V}\cdot\nabla\alpha_i + \frac{\nabla\cdot\rho_i\vec{\mathcal{V}}_i}{\rho}\right) = \left(\frac{T}{T_{REF}}\right)^{\omega-2}\left(\frac{p}{p_{REF.}}\right)^2 \zeta\, g_i . \qquad (2.83)$$

When $\zeta \to 0$ with $g_i \neq 0$, the net reaction rate term becomes negligable and the flow composition is determined by the action of convection and diffusion alone; this is called a chemically frozen flow. On the other hand, when $\zeta \to \infty$, the function g_i must everywhere approach zero ($\alpha_i \to \alpha_{i_{EQ}}$) to maintain finite convection and diffusion terms on the left side of Equation (2.8 the flow approaches a thermodynamic equilibrium solution. The net reaction rate term, however, does not necessarily vanish at this extreme, since the product of ζ and g_i as $\zeta \to \infty$ and $\alpha_i - \alpha_{i_{EQ}} \to 0$ must equal a finite term on the left given by

$$\left[\left(\frac{T}{T_{REF}}\right)^{\omega-2}\left(\frac{p}{p_{REF.}}\right)^2 \zeta\, g_i\right]_{\substack{\zeta\to\infty \\ g_i\to 0}} = t_F\left[\vec{V}\cdot\nabla\alpha_{i_{EQ.}} + \left(\frac{\nabla\cdot\rho_i\vec{\mathcal{V}}_i}{\rho}\right)_{EQ.}\right]. \qquad (2.84)$$

The role of ζ is therefore an important one in understanding the qualitative features of the gas phase reaction rates; as ζ departs from zero, the reaction rates enter in proportionately to modify diffusion and convection effects, whereas when ζ is not large enough to be considered infinite, the

thermodynamic equilibrium composition is no longer a solution and the entire chemical specie conservation equation must be solved to accurately calculate the gas composition distribution.

Catalytic surface reactions on a flow boundary may also compete with diffusion and convection rates in determining the gas composition at the surface, and an analogous characteristic parameter to the above gas phase reaction case can be defined based on a characteristic surface reaction time. This has been discussed for the boundary layer by Rosner.[13] The role of the parameter can be shown quite generally, however, by considering an i-th atomic specie boundary condition at a surface (see Equation (2.6)) in the absence of overall mass transfer:

$$\rho_w \left(\alpha_i \vec{V}_i \cdot \vec{N}\right)_w = S_{ic} \tag{2.85}$$

where the net catalytic reaction rate S_{ic} per unit area is of the form

$$S_{ic} = \rho_w K_{ci} \left(\alpha_{i_{EQ.}} - \alpha_i\right). \tag{2.86}$$

If we define a characteristic diffusion time t_d based on an appropriate flow length L normal to the surface, and define a characteristic surface catalysis time

$$t_{R_c}^{-1} = K_{ci}/L ,$$

then Equation (2.85) can be used to express the amount of i-th specie diffused into the flow layer of depth L as

$$\frac{t_F}{L}\left(\alpha_i \vec{V}_i \cdot \vec{N}\right)_w = \zeta_c \left(\alpha_{i_{EQ.}} - \alpha_i\right)_w . \tag{2.87}$$

When $\zeta_c = t_D/t_{R_c}$ approaches zero, the net catalysis rate becomes very small and the composition at the surface is determined solely by diffusion (in this case, without any mass injection, the diffusion velocity vanishes at the surface). This extreme is appropriately called a non-catalytic wall. When ζ_c becomes very large, however, the maintenance of a finite diffusion on the left side of Equation (2.87) requires α_{i_W} to approach the equilibrium composition $\alpha_{i_{EQ_W}}$ corresponding to the wall temperature T_W; the surface reaction rate completely predominates over the diffusion (which, however, does not vanish in general) and the wall is said to be completely catalytic.

Characteristic Homogeneous Reaction Parameter for the Boundary Layer

The average flow and reaction times must be chosen such that the characteristic parameter ζ indicates the gross non-equilibrium effect of the boundary layer deceleration of the external flow. Consequently, ζ should be defined as the smallest value possible throughout the boundary layer to insure that a very large value of ζ would indeed indicate thermodynamic equilibrium everywhere in the boundary layer, and hence truly apply to the boundary layer as a whole. Now for a boundary layer, the characteristic diffusion time t_D is of the order $\delta^2/\mathscr{D}_{12_W}$; but since $\delta^2 \sim \mu_W X/\rho_W u_e$ and $\mathscr{D}_{12_W} = \mu_W/\rho_W Sc_W$, we can write this equally well as the characteristic convection time

$$t_F = \zeta\, t_R = \frac{Sc\, X}{u_e(x)} \quad . \tag{2.88}$$

Then if ζ is to be a minimum, the characteristic reaction time t_R should be defined in terms of reference conditions which yield a maximum value.

The reaction rates encountered in the dissociated boundary layer theory are of the form

$$2\rho K_R' T^{\omega-2} (\rho_e/R_0)^2 g_i ,$$

where g_i never exceeds unity so only the remaining factor contributes to order of magnitude changes in the reaction rate effect. Consequently, take

$$t_R^{-1} = 2K_R' \left(T_{REF.}^{\omega-1}\right)_{MIN.} (\rho_e/R_0)^2 \tag{2.89}$$

with the reference temperature $T_{REF.}$ chosen so as to minimize $T_{REF.}^{\omega-2}$ (clearly making the choice of $T_{REF.}$ dependent on whether ω is greater or less than 2). For $\omega < 2$, the maximum boundary layer temperature should be used, which for a highly cooled boundary layer is the outer edge temperature T_e. This gives exactly the parameter employed by Fay and Riddell, who used the Davidson recombination rate model $\omega = -3/2$. In the case $\omega > 2$, on the other hand, the minimum boundary layer temperature should be used (thus $T_{REF.} = T_W$ for the highly cooled situation).

For the important case of a cooled boundary layer, the proper boundary layer non-equilibrium parameter is

$$\zeta = \frac{2K_R' X S_c T_{REF.}^{\omega-2}}{u_e} \left(\frac{\rho_e}{R_0}\right)^2 \tag{2.90}$$

where

$$T_{REF.} = T_e \quad , \quad \omega < 2$$
$$= T_W \quad , \quad \omega > 2 \ .$$

This parameter will appear naturally in the course of actually solving the boundary layer equations in the presence of homogeneous reactions. Equation (2.90), evaluated at an axially-symmetric stagnation point for

various flight Mach Number- altitude conditions, is plotted in Figure 2 for several different values of ω. It is apparent from this graph that significant departures from equilibrium flow can occur at altitudes above 100,000 ft., depending on ω, and that the altitude at which non-equilibrium effects appear ($\zeta < 10^2$ for purposes of illustration) decreases noticeably as ω decreases. Clearly, the conclusions regarding boundary layer equilibrium depend on the recombination rate model employed. Also shown in Figure 2 is a plot of the Knudsen number of the gas behind the shock, based on nose radius,* defined as

$$K_N \equiv \frac{\text{mean free path}}{R}$$

When K_N approaches unity, we are in doubt concerning the assumption of continuum flow, so the presence of this curve in Figure 2 will indicate roughly whether or not the boundary layer non-equilibrium occurs in the continuum regime of flight. Because of the delay of non-continuum effects at higher altitudes due to hypersonic bow shock compression, it is seen from this figure that the boundary layer is nearly completely chemically frozen for $\omega < 2$ before any possible non-continuum effects occur; for $\omega > 2$, a noticeable degree of freezing has still occurred before K_N reaches the order of one. It appears that the analysis of chemical non-equilibrium can be confidently carried out with the usual continuum flow theory.

* Reference 27 shows that R (rather than boundary layer thickness) is a more satisfactory dimension to use in defining the regimes of high altitude hypersonic gas flows at the stagnation point.

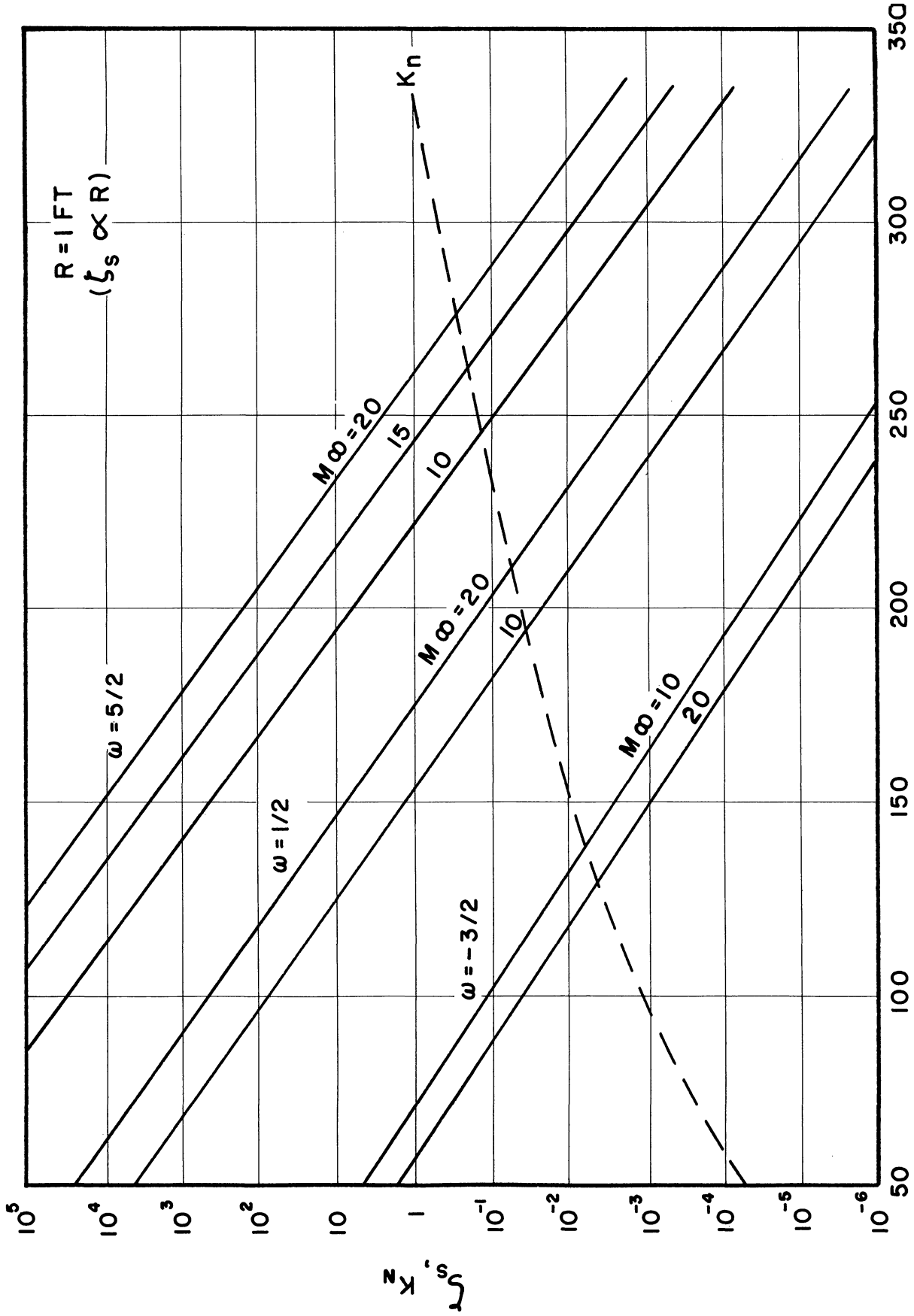

Figure 2. Stagnation Point Non-Equilibrium Parameter Versus Flight Altitute and Mach Number.

The parameter ζ will in general be a function of the distance along the body, because of the dependence on the external inviscid flow shown in Equation (2.90), and thus must be treated as a variable with respect to X. Therefore, the degree of gas phase chemical non-equilibrium in the boundary layer is expected to depend on X also. Only in the particular case of the stagnation point flow around a symmetrical body will ζ be independent of X; in this case $u_e/X = B_s$ and all the thermodynamic quantities are constants, so

$$\zeta = \frac{2 K_R' T_s^{\omega-2} S_c}{B_s} \left(\frac{\rho_s}{R_o}\right)^2. \tag{2.91}$$

On the other hand, ζ is not a constant for a uniform inviscid flow (constant p_e, T_e, u_e), such as occurs on a flat plate or cylinder, but rather is proportional to X;

$$\zeta_{PLATE, CYL.} = \frac{2 K_R' T_e^{\omega-2} S_c X}{u_e} \left(\frac{\rho_e}{R_o}\right)^2. \tag{2.92}$$

The inviscid flow over a hypersonic body such as a hemisphere-cylinder is of such a nature, however, that ζ may <u>not</u> be intermediate in value between those given by Equations (2.91) and (2.92). For example, Figure 3 shows the approximate inviscid flow pressure as a function of distance along a hemisphere-cylinder; the initial expansion follows the very rapid pressure drop predicted by the Newtonian theory, and this fairs into the pressure field due to the blunt nose effect (given by blast wave theory) about two body diameters downstream.[26] The subsequent die-off of the pressure shown is based upon neglect of the boundary layer-induced pressure gradient. The significant drop in pressure clearly will reduce the local

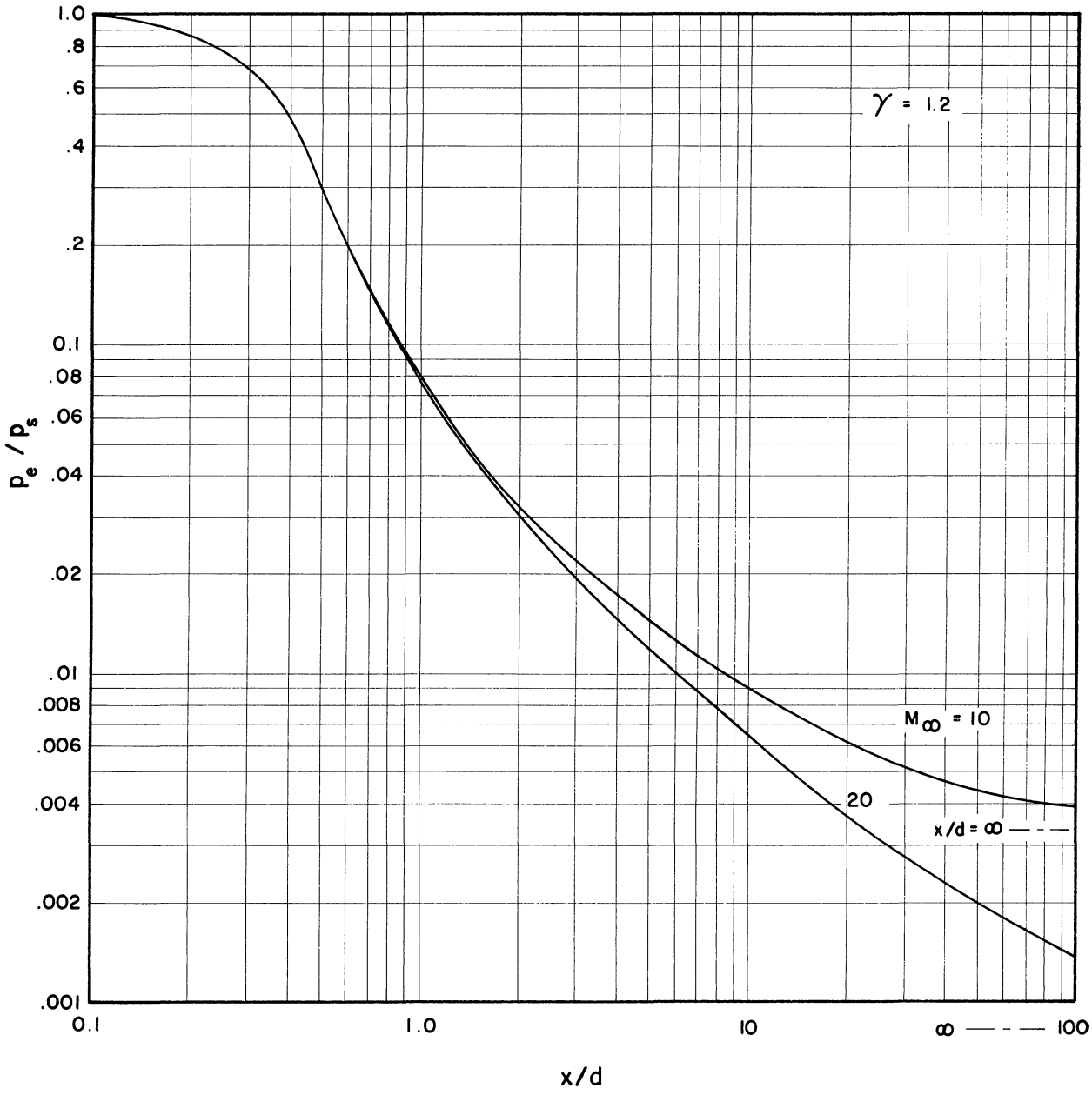

Figure 3. Inviscid Flow Pressure Distribution for a Hypersonic Hemisphere - Cylinder.

ζ by one or more orders of magnitude; to indicate the extent of this effect in this example, consider the ratio ζ/ζ_s given by

$$\frac{\zeta}{\zeta_s} = \left(\frac{p_e}{p_s}\right)^2 \left(\frac{T_e}{T_s}\right)^{\omega-2} \frac{B_s X}{u_e} \quad . \tag{2.93}$$

Assuming an isentropic equilibrium expansion around the body in terms of some effective specific heat ratio $\bar{\gamma}$ such that

$$T_e/T_s \simeq \left(p_e/p_s\right)^{\frac{\bar{\gamma}-1}{\bar{\gamma}}} ,$$

Equation (2.93) becomes

$$\frac{\zeta}{\zeta_s} = \left(\frac{p_e}{p_s}\right)^{2+\left(\frac{\bar{\gamma}-1}{\bar{\gamma}}\right)(\omega-2)} \frac{B_s X}{u_e} \quad . \tag{2.94}$$

For the pressure distribution shown in Figure 3, this ratio is plotted as a function of X for several values of ω (assuming $\bar{\gamma} = 1.2$) in Figure 4 to illustrate the typical variation which could be expected on a practical hypersonic body. The results clearly show a very significant reduction in ζ over the frontal part of the body, indicating the local boundary layer to be relatively further from equilibrium than at the stagnation point. Decreasing ω, however, tends to make ζ less sensitive to pressure variations. The possibility that a short hypersonic body may be covered by an entirely non-equilibrium boundary layer is suggested by this example. When the inviscid flow becomes uniform, ζ/ζ_s subsequently begins to rise proportionately to X. The chemical state of the boundary layer then tends back toward the stagnation point condition. For example,

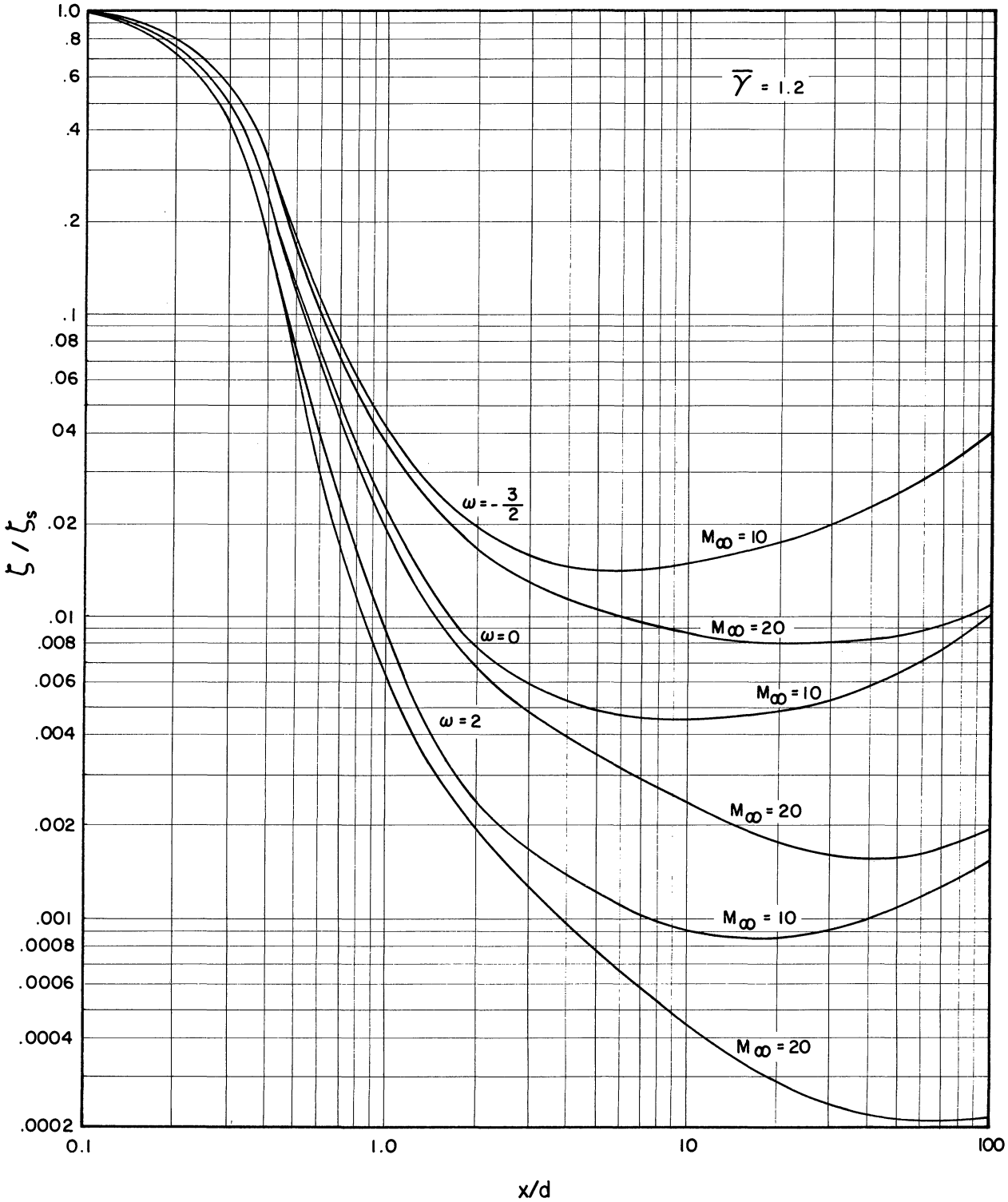

Figure 4. Variation of Boundary Layer Non-Equilibrium Parameter Along a Hemisphere-Cylinder.

if the inviscid flow becomes uniform when the local flow experiences only very small hypersonic disturbances, $u_e \approx u_\infty$ and $p_e \approx p_\infty$, Equation (2.94) estimates the X/d for which $\zeta/\zeta_s \simeq 1$ to be:

$$\left(\frac{X}{d}\right)_{\zeta/\zeta_s=1} \simeq \frac{u_\infty d}{B_s}\left(\frac{p_s}{p_\infty}\right)^{2+\left(\frac{\gamma-1}{\gamma}\right)(\omega-2)}, \qquad (2.95)$$

which is a very large number for hypersonic flow.

Surface Reaction Parameter

The proper reaction rate parameter ζ_c involves the behavior of the gas adjacent to the boundary surface. The appropriate flow time is that of the diffusive mass flux into the surface, given by

$$t_{F_c} = \delta^2/\mathcal{D}_{12_w} \sim \frac{Sc_w X}{u_e} \qquad (2.96)$$

in terms of the boundary layer thickness δ. The surface catalysis rates previously discussed are of the form

$$\rho_w K_c g_c ,$$

where g_c never exceeds unity. Since the significant flow length in this case is δ, the characteristic reaction time is

$$t_{R_c}^{-1} = K_c/\delta . \qquad (2.97)$$

Consequently, the surface catalysis parameter for the boundary layer is

$$\zeta_c \equiv \frac{t_{F_c}}{t_{R_c}} = Sc_w K_c \sqrt{\frac{\rho_w X}{\mu_w u_e}} \qquad (2.98)$$

in agreement with Reference 13. The axially-symmetric stagnation point value of ζ_c is plotted in Figure 5 as a function of altitude (the dependence on flight Mach Number is very small for $M_\infty \gg 1$), assuming $\rho\mu$ = constant and $T_W/T_e = .05$, for several different surface materials.* A

* Based on surface recombination data for atomic oxygen and nitrogen given in Reference 11.

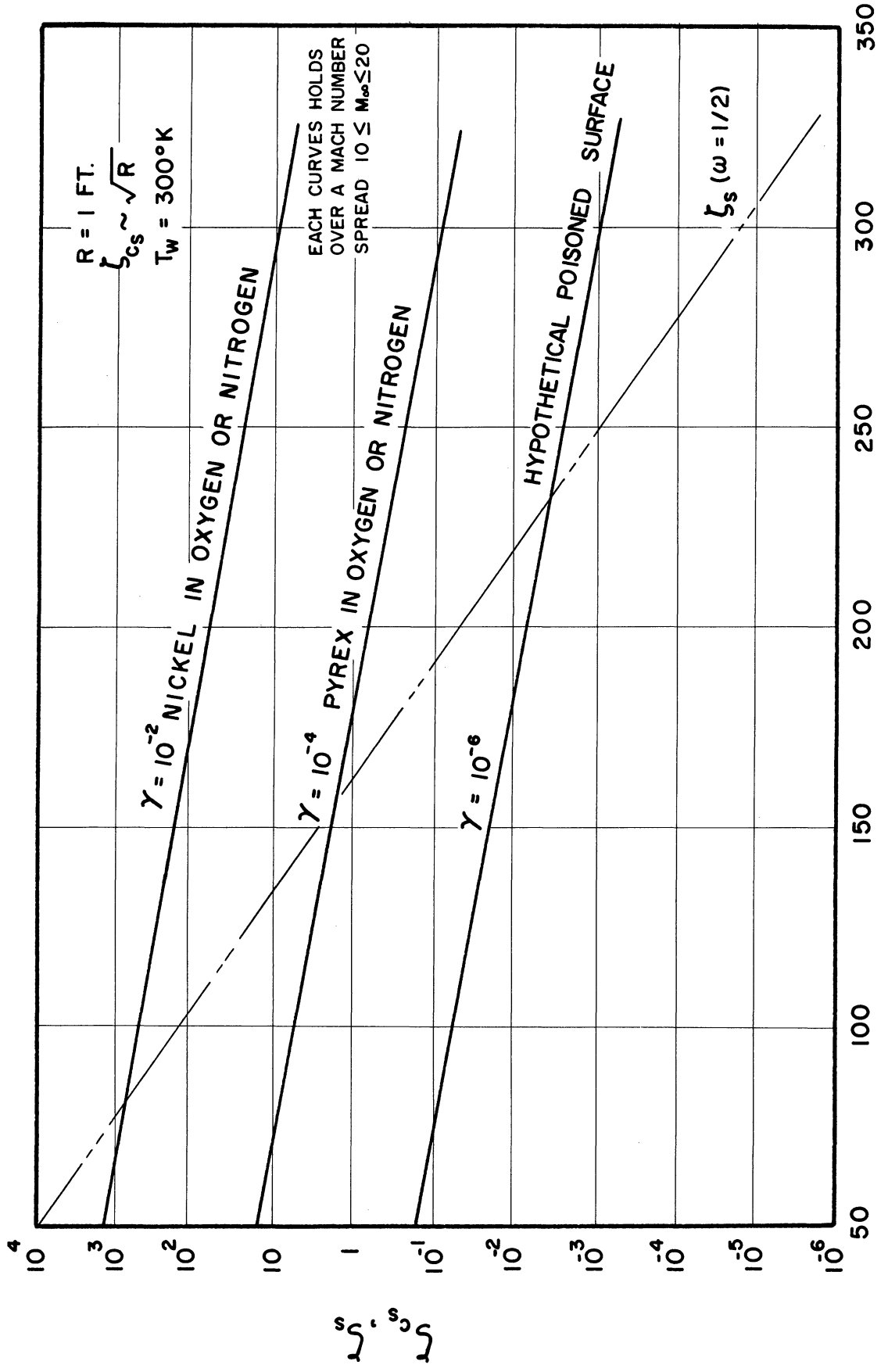

Figure 5. Stagnation Point Surface Catalysis Parameter Versus Flight Altitude and Mach Number.

significant non-catalytic effect is indicated at the higher altitudes with the use of non-metallic surfaces, such as the frequently employed plastic or glassy-like thermal protection coatings on missles. Figure 5 permits a rough assessment of the flight regimes in which significant catalytic inhibition can be expected with a given surface material or poisoning treatment. For the sake of comparison, the $\omega = 1/2$ case of the gas phase parameter ζ is also shown in the figure; examination of the curves suggests that non-catalytic surface effects for non-metallic walls are important when the boundary layer is out of equilibrium in the chemically frozen regime.

The dependence of ζ_c on the local inviscid flow indicated by Equation (2.98) causes it to vary along the body, changing the catalytic effect with X; ζ_c is a constant only in the stagnation point, for which

$$\zeta_{c_s} = \zeta_{c_w} K_c \sqrt{\rho_w / \mu_w B_s} \,. \tag{2.99}$$

Otherwise, ζ_c will vary in the following approximate manner with X (using $\rho_w \cong p_e (\bar{R}_w T_w)^{-1}$, with $\bar{R}_w$ constant, and assuming negligable wall temperature variations and an isentropic inviscid flow):

$$\frac{\zeta_c}{\zeta_{c_s}} = \frac{K_c}{K_{c_s}} \sqrt{\frac{B_s X}{u_e}} \left(\frac{p_e}{p_s} \right)^{1/2\bar{\gamma}} . \tag{2.100}$$

The ratio $K_c(X)/K_{c_s}$ will be unity except for some x-variation (such as a discontinuity) in the surface material. Equation (2.100) indicates for the hemisphere-cylinder example that the exapnsion over the frontal portion of the body produces a local surface reaction effect that is

more non-catalytic relative to the stagnation point for the same material. Far downstream, when the inviscid flow becomes uniform, ζ/ζ_{cs} will grow as $\sqrt{X}$ and may therefore reach and exceed unity for very long hypersonic bodies.

CHAPTER III

TRANSFORMATION TO THE SIMILARITY PLANE

Application of the Mangler-Stewartson-Blasius Transformation

There are several means of solving the boundary layer equations, such as the Kármán-Pohlhausen integral method and the Blasius series expansion method. Another fruitful approach is to deal with the equations in a new coordinate plane in which the three dimensional body effects and the majority of the compressibility effects have been eliminated by means of the combined Mangler-Stewartson transformation. Further, a functional form for the stream function is introduced, this form being that suited to an investigation of the possibilities for "similarity" (reduction of the governing equations in the new variables to a set of ordinary differential equations in a single coordinate). We will transform the boundary layer problem to a new ξ, η "similarity plane," and subsequently attack the chemically reacting boundary layer problem in this new set of variables.

First, a continuity-satisfying stream function ψ is defined as follows:

$$\frac{\partial \psi}{\partial x} = -\rho r_0^{\kappa} v \quad , \quad \frac{\partial \psi}{\partial y} = \rho r_0^{\kappa} u \quad . \tag{3.1}$$

Next we introduce the transformation

$$\xi = \int_0^x \rho_R \mu_R u_e r_0^{2\kappa} dx \tag{3.2}$$

$$\eta = \frac{\rho_e u_e r_0^{\kappa}}{\sqrt{2\xi}} \int_0^y \frac{\rho}{\rho_e} dy \tag{3.3}$$

and write the stream function in the form

$$\psi = \sqrt{2\xi}\, f(\xi, \eta) \quad . \tag{3.4}$$

As a consequence of these transformations, we get the following relations:

$$
\left.
\begin{aligned}
u(x,y) &= u_e \frac{df}{d\eta} \\
-v(x,y) &= \left(\sqrt{2\xi}/\rho\mu_0^*\right)\left[\frac{d\eta}{dx}\frac{df}{d\eta} + \frac{d\xi}{dx}\left(\frac{f}{2\xi} + \frac{df}{d\xi}\right)\right] \\
\rho\left(u\frac{d}{dx} + v\frac{d}{dy}\right) &= \rho\frac{u_e}{2\xi}\frac{d\xi}{dx}\left[2\xi\frac{df}{d\eta}\frac{d}{d\xi} - \left(f + 2\xi\frac{df}{d\xi}\right)\frac{d}{d\eta}\right] \\
\frac{d}{dy}\left(\mu\frac{d}{dy}\right) &= \rho\frac{u_e}{2\xi}\frac{d\xi}{dx}\frac{d}{d\eta}\left(\frac{\rho\mu}{\rho_R\mu_R}\frac{d}{d\eta}\right)
\end{aligned}
\right\} \qquad (3.5)
$$

and

$$
\left.
\begin{aligned}
\beta &= \frac{du_e/dx}{u_e/x} = x\frac{d\ln u_e}{dx} \\
\epsilon &= \frac{d\xi/dx}{\xi/x} = x\frac{d\ln\xi}{dx} .
\end{aligned}
\right\} \qquad (3.6)
$$

Now introduce the variables

$$\theta = \frac{T}{T_e}\,,\quad \beta = \frac{\alpha_2}{\alpha_{2e}}\,,\quad \chi = \frac{\alpha_4}{\alpha_{4e}}\,,\quad W = \frac{\alpha_3}{\alpha_{3e}}$$

$$C = \rho\mu/\rho_R\mu_R$$

$$\theta_{A_{2,4}} = T_{A_{2,4}}/T_e$$

$$\zeta_c = S_c\sqrt{\frac{\rho_w x}{\mu_w u_e}}\,K_c$$

$$\zeta = \frac{2K_R' T_e^{\omega-2} x}{u_e}\left(\frac{\rho_e}{R_0}\right)^2$$

$$C_p = \frac{\bar{c}_p}{\bar{c}_{pe}} = \frac{c_{p_1}}{c_{p_{1e}}}\left[\frac{1 + (c_{p_2}/c_{p_1} - 1)(\alpha_{2e}\beta + \alpha_{4e}\chi)}{1 + \alpha_e(c_{p_2}/c_{p_1} - 1)}\right]$$

and the following relations expressing equilibrium in the freestream (with consequent neglect of the freestream composition derivative terms in the

resulting equations):

$$\alpha_{2e}^2/(1+\alpha_e) = \frac{EXP(a)}{4p_e}(1-\alpha_e-\alpha_{3e})EXP(-\theta_{A_2})$$
$$\alpha_{4e}^2/(1+\alpha_e) = \frac{EXP(a)}{4p_e}\alpha_{3e}\,EXP(-\theta_{A_4}) \qquad (3.7)$$

where $\alpha_e = \alpha_{2_e} + \alpha_{4_e}$.

The application of these transformations to the boundary layer equations yield the following set of relations:

(1) First Atomic Specie

$$f\frac{\partial\beta}{\partial\eta}+\frac{\partial}{\partial\eta}\left(\frac{C}{S_c}\frac{\partial\beta}{\partial\eta}\right)=\frac{2\alpha_{2e}S\theta^{\omega-2}}{\epsilon S_c(1+\alpha_e)}\mathcal{Y}_2+2\xi\left(\frac{\partial f}{\partial\eta}\frac{\partial\beta}{\partial\xi}-\frac{\partial f}{\partial\xi}\frac{\partial\beta}{\partial\eta}\right) \qquad (3.8)$$

where

$$\mathcal{Y}_2=\frac{(1+\alpha_e)\beta^2}{1+\alpha_{2e}\beta+\alpha_{4e}\gamma}-\left(\frac{1-\alpha_{2e}\beta-\alpha_{4e}\gamma-\alpha_{3e}W}{1-\alpha_e-\alpha_{3e}}\right)EXP\left[-\frac{\theta_{A_2}(1-\theta)}{\theta}\right]. \qquad (3.9)$$

(2) Second Atomic Specie

$$f\frac{\partial\gamma}{\partial\eta}+\frac{\partial}{\partial\eta}\left(\frac{C}{S_c}\frac{\partial\gamma}{\partial\eta}\right)=\frac{2\alpha_{4e}S\theta^{\omega-2}}{\epsilon S_c(1+\alpha_e)}\mathcal{Y}_4+2\xi\left(\frac{\partial f}{\partial\eta}\frac{\partial\gamma}{\partial\xi}-\frac{\partial f}{\partial\xi}\frac{\partial\gamma}{\partial\eta}\right) \qquad (3.10)$$

where

$$\mathcal{Y}_4=\frac{(1+\alpha_e)\gamma^2}{1+\alpha_{2e}\beta+\alpha_{4e}\gamma}-W\,EXP\left[-\frac{\theta_{A_4}(1-\theta)}{\theta}\right]. \qquad (3.11)$$

(3) Second Molecular Specie

$$f\frac{dW}{d\eta}+\frac{d}{d\eta}\left(\frac{C}{S_c}\frac{dW}{d\eta}\right)=-\frac{\alpha_{4e}}{\alpha_{3e}}\frac{2\alpha_{4e}S\theta^{\omega-2}}{\epsilon S_c(1+\alpha_e)}\chi_4+2\xi\left(\frac{df}{d\eta}\frac{dW}{d\xi}-\frac{df}{d\xi}\frac{dW}{d\eta}\right). \tag{3.12}$$

(4) Momentum

$$f\frac{d^2f}{d\eta^2}+\frac{d}{d\eta}\left(C\frac{d^2f}{d\eta^2}\right)=\frac{2\beta}{\epsilon}\left[\left(\frac{df}{d\eta}\right)^2-\left(\frac{1+\alpha_{2e}\beta+\alpha_{4e}\chi}{1+\alpha_e}\right)\theta\right]+2\xi\left(\frac{df}{d\eta}\frac{d^2f}{d\eta d\xi}-\frac{df}{d\xi}\frac{d^2f}{d\eta^2}\right). \tag{3.13}$$

(5) Energy Equations

In terms of the variable $g \equiv h_s/h_{s_e}$, we have the stagnation enthalpy form

$$\begin{aligned} f\frac{dg}{d\eta}+\frac{d}{d\eta}\Bigg\{\frac{C}{P_R}\Bigg[\frac{dg}{d\eta}+(P_R-1)\frac{u_e^2}{2h_{s_e}}\frac{d}{d\eta}\left(\frac{df}{d\eta}\right)^2 \\ +(Le-1)\left[\alpha_{2e}\left(\frac{h_2-h_1}{h_{s_e}}\right)\frac{d\beta}{d\eta}+\alpha_{4e}\left(\frac{h_4-h_1}{h_{s_e}}\right)\frac{d\chi}{d\eta}\right]\Bigg\} \\ =2\xi\left(\frac{df}{d\eta}\frac{dg}{d\xi}-\frac{df}{d\xi}\frac{dg}{d\eta}\right). \end{aligned} \tag{3.14}$$

The constancy of h_{s_e} provides the following relationship (when the freestream composition derivatives are neglected):

$$\frac{dT_e/dx}{T_e/x}=-\frac{\beta u_e^2}{\bar{c}_{p_e}T_e}. \tag{3.15}$$

The temperature form can be written

$$C_p f \frac{\partial \theta}{\partial \eta} + \frac{\partial}{\partial \eta}\left(\frac{C}{P_R} C_p \frac{\partial \theta}{\partial \eta}\right) + \left(\frac{\kappa_{p_2} - \kappa_{p_1}}{\kappa_{p_e}}\right)\frac{C}{S_c}\left(\alpha_{2e}\frac{\partial \beta}{\partial \eta} + \alpha_{4e}\frac{\partial \chi}{\partial \eta}\right)\frac{\partial \theta}{\partial \eta}$$

$$+ \frac{u_e^2}{\kappa_{p_e} T_e}\left[C\left(\frac{\partial^2 f}{\partial \eta^2}\right)^2 + 2\frac{\beta}{\epsilon}\theta \frac{\partial f}{\partial \eta}\left(C_p - \frac{1+\alpha_{2e}\beta+\alpha_{4e}\chi}{1+\alpha_e}\right)\right]$$

$$= -\frac{2\alpha_{2e}\zeta\theta^{\omega-2}}{\epsilon S_c(1+\alpha_e)}\left[\frac{\alpha_{2e}(h_2-h_1)}{\kappa_{p_e}T_e}\right]\mathcal{Y}_2 \qquad (3.16)$$

$$- \frac{2\alpha_{4e}\zeta\theta^{\omega-2}}{\epsilon S_c(1+\alpha_e)}\left[\frac{\alpha_{4e}(h_4-h_1)}{\kappa_{p_e}T_e}\right]\mathcal{Y}_4$$

$$+ 2\xi C_p\left(\frac{\partial f}{\partial \eta}\frac{\partial \theta}{\partial \xi} - \frac{\partial f}{\partial \xi}\frac{\partial \theta}{\partial \eta}\right).$$

(6) Thermal Equation of State

$$\frac{\rho}{\rho_e} = \left(\frac{1+\alpha_{2e}\beta+\alpha_{4e}\chi}{1+\alpha_e}\right)\theta.$$

The outer boundary conditions at $\eta = \infty$ are $g = \theta = z = \chi = W = \partial f/\partial\eta = 1$. It is implied further that $\partial^2 f/\partial\eta^2 = \partial g/\partial\eta = \partial\theta/\partial\eta = \partial z/\partial\eta = \partial\chi/\partial\eta = \partial W/\partial\eta = 0$ as $\eta \to \infty$ and that the variations of α_{2_e}, α_{4_e} and α_{3_e} are negligable in the boundary layer equations.

At the inner boundary surface, the following conditions apply in the similarity plane (neglecting catalytic surface dissociation):

$$\left.\begin{aligned} f(0,\xi) &= \partial f/\partial\xi\,(0,\xi) = 0 \\ \theta(0,\xi) &= \theta_w \;;\; g(0,\xi) = g_w \end{aligned}\right\} \qquad (3.18)$$

$$\left.\begin{aligned} \frac{\partial \beta}{\partial \eta}(0,\xi) &= \frac{\mathcal{J}_c\ \beta(0,\xi)}{\sqrt{\epsilon\, C(0)/2}} \\ \frac{\partial \chi}{\partial \eta}(0,\xi) &= \left[\chi(0,\xi)/\beta(0,\xi)\right] \frac{\partial \beta}{\partial \eta}(0,\xi) \\ -\frac{\partial W}{\partial \eta}(0,\xi) &= \left[\frac{W(0,\xi) - W_{EQ.}(0,\xi)}{\beta(0,\xi)}\right] \frac{\partial \beta}{\partial \eta}(0,\xi) \,. \end{aligned}\right\} \tag{3.19}$$

The heat flux at the wall is

$$-\frac{\rho_R \dot{Q}_W}{C(0)\sqrt{\rho_R \mu_R \epsilon\, u_e/2x}} = h_{se}\left\{\frac{\partial g}{\partial \eta} + (Le-1)\left[\alpha_{2e}\left(\frac{h_2-h_1}{h_{se}}\right)\frac{\partial \beta}{\partial \eta} + \alpha_{4e}\left(\frac{h_4-h_1}{h_{se}}\right)\frac{\partial \chi}{\partial \eta}\right]\right\}_{\eta=0} \tag{3.20}$$

$$= \bar{c}_{Pe} T_e \left\{ C_p \frac{\partial \theta}{\partial \eta} + Le\left[\alpha_{2e}\left(\frac{h_2-h_1}{\bar{c}_{Pe} T_e}\right)\frac{\partial \beta}{\partial \eta} + \alpha_{4e}\left(\frac{h_4-h_1}{\bar{c}_{Pe} T}\right)\frac{\partial \chi}{\partial \eta}\right]\right\}_{\eta=0}. \tag{3.21}$$

This expression clearly illustrates that the recovery temperature on a surface in a dissociated gas flow, i.e., that on an adiabatic wall, is <u>not</u> in general defined by zero temperature gradient as in the ideal gas; indeed from Equation (3.21), we have

$$\left[\frac{\partial \theta}{\partial \eta}(0)\right]_{\dot{Q}_W=0} = -\frac{Le}{C_{pw}}\left[\alpha_{2e}\left(\frac{h_2-h_1}{\bar{c}_{Pe} T_e}\right)\frac{\partial \beta}{\partial \eta} + \alpha_{4e}\left(\frac{h_4-h_1}{\bar{c}_{Pe} T_e}\right)\right]_{\eta=0}. \tag{3.22}$$

The shear stress is

$$\frac{\tau_w}{C(0)\, u_e \sqrt{\rho_R \mu_R \epsilon\, u_e/2x}} = \frac{\partial^2 f}{\partial \eta^2}(0,\xi). \tag{3.23}$$

Exact Conditions for Similarity with Chemical Non-Equilibrium

The exact conditions which permit the neglect of all $\partial/\partial\xi$ of the dependent variables, reducing the governing equations to a set of ordinary differential equations in the single independent variable η, are twofold: first, the coefficients in the equations themselves must be independent of ξ (i.e., constants or functions of η only); second, the boundary conditions at both inner and outer boundaries must likewise be independent of ξ. If these conditions are met, it would be plausible to neglect the ξ dependence of all the dependent variables. The essential accomplishment of the Stewartson-Mangler-Blasius transformation in this case has been to completely absorb the direct effects of compressibility, axi-symmetry (three dimensionality) and inviscid flow variation along the body into coordinate stretching. The resulting equations in the stretched ξ, η plane describe the boundary layer effect relative to the freestream variations by a set of equations simpler than the original partial differential equations.

These exact conditions are met by a limited number of physical situations, since only certain particular combinations of inviscid flow-wall temperature variations will make the coefficients in the flow equations and boundary conditions constants or functions of η only. A number of these cases have received attention by various theoretical investigators. It is the purpose here to evaluate the exact similarity possibilities for a chemically reacting four component gas mixture boundary layer flow in the absence of overall surface mass transfer.

Similarity of the three species Equations (3.8), (3.10) and (3.12) requires:

$$\left.\begin{array}{l} f,\ \theta,\ z,\ \chi \text{ and } W \text{ all functions of } \eta\ , \\ C \text{ and } S_c \text{ constants or functions of } \eta\ , \\ \omega,\ \alpha_{2_e},\ \alpha_{4_e} \text{ and } \alpha_{3_e} \text{ constant}\ , \\ \epsilon \text{ constant}\ , \\ \zeta \text{ constant}\ . \end{array}\right\} \qquad (3.24)$$

The neglect of the inviscid flow composition gradients ($d\alpha_{i_e}/dX = 0$) is exact for either a symmetric body stagnation point or for a locally frozen flow at the edge of the boundary layer. Otherwise, it implies that the local composition is slowly-varying and $d\alpha_{i_e}/dX$ terms may be neglected. Such an assumption is consistent with the boundary layer approximation that streamwise reaction rate variations are small in comparison to variations across the boundary layer. The condition ϵ = constant implies ξ = constant$(X)^{\epsilon}$ and therefore the integral equation

$$X^{\epsilon} = \text{CONSTANT} \int_0^X \rho_R \mu_R u_e r_0^{2K} dX\ , \qquad (3.25)$$

which is satisfied, for example, by $\rho_R\mu_R$, u_e and r_0 all having the form constant$\cdot X^N$. The condition ζ = constant, which necessarily enters when a general real gas is considered, will be satisfied when

(a) $\zeta = 0$, corresponding to the case of a chemically frozen flow, or

(b) $\zeta = \infty$, corresponding to the thermodynamic equilibrium extreme, or

(c) u_e = constant$\cdot X$, p_e and T_e constant; this is met at the stagnation point of a symmetric body.

Examination will show that there are no other realistic $p_e(X)$, $u_e(X)$, and $T_e(X)$ variation combinations for which ζ will be a constant.

The condition for similarity of the momentum Equation (3.13) now becomes

$$\beta = \text{constant}, \quad \text{i.e., } u_e = \text{constant} \cdot X^{\beta}, \tag{3.26}$$

which is the well-known condition for inviscid subsonic flow on a wedge of semi-angle $\pi\beta/(1+\beta)$.

The temperature form of the energy equation, usually the necessary form when dealing with a reacting gas mixture, adds the following requirements:

$$P_R, \kappa_{P_i}, C_p \qquad \text{constants or functions of } \eta, \tag{3.27}$$

$$u_e^2/\bar{\kappa}_{P_e} T_e \qquad \text{constant}, \tag{3.28}$$

$$\alpha_{2e}\left(\frac{h_2 - h_1}{\bar{\kappa}_{P_e} T_e}\right), \; \alpha_{4e}\left(\frac{h_4 - h_1}{\bar{\kappa}_{P_e} T_e}\right) \qquad \text{constants or functions of } \eta. \tag{3.29}$$

The condition on the specific heats is clearly satisfied when c_{p_1} and c_{p_2} are taken as constants, or when the freestream and wall temperatures are constant. Condition (3.28) enters when the viscous dissipation of energy into heat is important; it is clearly satisfied when $u_e = 0$ (stagnation point), or when the external flow is independent of X (flat plate, cylinder or cone flow). Conditions (3.29) are satisfied either at a stagnation point or for a uniform inviscid flow (the latter, however, will not give similarity of the species or temperature equations except when $\zeta = 0$ or $\zeta \to \infty$).

The similarity of the total enthalpy form of the energy equation, which is of interest in some particular real gas flow problems, requires

$$g \text{ a function of } \eta, \tag{3.30}$$

$$u_e^2/2h_{s_e} \text{ constant}, \tag{3.31}$$

$$L_e \text{ constant or a function of } \eta. \tag{3.32}$$

The case $P_R = 1$ eliminates the necessity of condition (3.31), whereas the case $L_e = 1$ eliminates condition (3.32) as well as the similarity restrictions of the species equations. The ultimate usefulness of the total enthalpy equation depends on whether or not $g(0, \xi)$ is known (and this in general depends on the chemistry).

The inner surface boundary conditions (3.18) and (3.19) will give similarity if

$$\Theta_W,\ z_W,\ \chi_W,\ W_W \text{ and } W_{EQ}(o) \text{ are constant}, \tag{3.33}$$

$$\zeta_c = \text{constant}. \tag{3.34}$$

The condition on the catalytic parameter is obeyed when

(a) $\zeta_c = 0$, a completely non-catalytic wall, or

(b) $\zeta_c = \infty$, the opposite extreme of a completely catalytic wall, or

(c) $u_e = \text{constant} \cdot X$ and K_c, T_W and p_e are constant. This occurs only at the stagnation point with a given surface material.

Otherwise, one is left only with the case in which the surface material is distributed along X such that for a constant surface temperature,

$$K_c(X) = \text{CONSTANT}\sqrt{\frac{u_e}{\rho_e X}}\ . \tag{3.35}$$

A number of interesting real gas similarity cases can be formed by combinations of the foregoing similarity conditions involving the extremes of gas reaction effect. Both chemically frozen and thermodynamic equilibrium flows for the two extreme conditions of surface catalysis have similarity solutions for stagnation point and uniform inviscid flow (and for any

wedge flow if $P_R = 1$). However, the only similarity solution which includes <u>arbitrary</u> chemical reaction is obtained for the stagnation point flow of a symmetrical body, as pointed out by Fay and Riddell[6]. The formulation of this problem for the present four-specie air mixture representation is given below.

<u>Non-Equilibrium Stagnation Point Similarity Solution</u>

In the stagnation point flow on a symmetrical body ($X = 0$), we have the following values:

$$\left.\begin{aligned} &u_e = B_s X , \\ &r_o \simeq X , \\ &\epsilon_s = 2(1+K), \begin{cases} = 2, \text{ two-dimensional} \\ = 4, \text{ axially-symmetrical} \end{cases} \\ &\beta = 1 , \\ &\rho_R \mu_R = \text{constant} . \end{aligned}\right\} \qquad (3.36)$$

All other freestream quantities are independent of X, the viscous dissipation (of order X^2) drops out, and the non-equilibrium and catalysis parameters ζ and ζ_c assume constant values ζ_s and ζ_{c_s}, respectively. One therefore obtains the following exact similarity solution equations (denoting derivatives with respect to η by primes):

(1) Atomic Specie

$$f\beta' + \left(\frac{C}{S_c}\beta'\right)' = \frac{2\alpha_{2e}\zeta\theta^{\omega-2}}{S_c\epsilon(1+\alpha_e)}\mathcal{J}_2 \qquad (3.37)$$

where $\mathcal{J}_2$ and $\mathcal{J}_4$ are given by Equations (3.9) and (3.11), respectively.

(2) Second Atomic Specie

$$f\chi' + \left(\frac{C}{S_c}\chi'\right)' = \frac{2\alpha_{4e}\zeta\theta^{\omega-2}}{S_c\epsilon(1+\alpha_e)}\mathcal{J}_4 . \qquad (3.38)$$

(3) Second Molecular Specie

$$f W' + \left(\frac{C}{S_c} W'\right)' = - \frac{\alpha_{4e}}{\alpha_{3e}} \frac{2\alpha_{4e} \zeta \theta^{\omega-2}}{S_c \epsilon (1+\alpha_e)} \mathcal{J}_4 . \tag{3.39}$$

(4) Momentum

$$f f'' + (C f'')' = \frac{2}{\epsilon_s} \left[f'^2 - \left(\frac{1 + \alpha_{2e} \beta + \alpha_{4e} \chi}{1 + \alpha_e} \right) \theta \right]. \tag{3.40}$$

(5) Energy

$$\begin{aligned} C_p f \theta' + \left(\frac{C}{P_R} C_p \theta'\right)' + \frac{C}{S_c} \left(\frac{c_{p_2} - c_{p_1}}{\bar{c}_{pe}} \right) (\alpha_{2e} \beta' + \alpha_{4e} \chi') \theta' \\ = - \frac{2\alpha_{2e} \zeta_s \theta^{\omega-2}}{S_c \epsilon (1+\alpha_e)} \left[\frac{\alpha_{2e} (h_2 - h_1)}{\bar{c}_{pe} T_e} \right] \mathcal{J}_2 \\ - \frac{2\alpha_{4e} \zeta_s \theta^{\omega-2}}{S_c \epsilon (1+\alpha_e)} \left[\frac{\alpha_{4e} (h_4 - h_1)}{\bar{c}_{pe} T_e} \right] \mathcal{J}_4 \end{aligned} \tag{3.41}$$

where

$$C_p = \frac{c_{p_1}}{c_{p_{1e}}} \left[\frac{1 + (c_{p_2}/c_{p_1} - 1)(\alpha_{2e} \beta + \alpha_{4e} \chi)}{1 + \alpha_e (c_{p_2}/c_{p_1} - 1)} \right].$$

In the above equations,

$$C(\eta) = C(\theta, z, \chi, W),$$

$$S_c(\eta) = S_c(\theta, z, \chi, W),$$

$$P_R(\eta) = P_R(\theta, z, \chi, W),$$

$$h_{2,4} - h_1 = h_{2,4}(\theta)$$

are assumed known functions.

The corresponding boundary conditions are (cool wall):

$$
\left.
\begin{aligned}
f'(\infty) = g(\infty) = \chi(\infty) = W(\infty) = \theta(\infty) = 1 \\
f(0) = f'(0) = 0 \\
\theta(0) = \theta_w \\
g'(0) = \zeta_{c_s}\, g(0) \Big/ \sqrt{\epsilon_s\, C(0)/2} \\
\chi'(0) = \left[\chi(0)/g(0)\right] g'(0) \\
W'(0) = -\left[\frac{W(0) - W_{EQ.}(0)}{g(0)}\right] g'(0).
\end{aligned}
\right\} \qquad (3.42)
$$

Fay and Riddell solved these equations only for the two extremes $\zeta_{c_s} = 0$ ($z'(o) = 0$, non-catalytic wall) and $\zeta_{c_s} \to \infty$ ($z(o) = 0$, a completely catalytic wall surface).

Finally, the surface heat transfer is given by

$$
-\frac{P_R\, \dot{Q}_w / \bar{c}_{pe}\, T_e}{C(0)\sqrt{\rho_R/\mu_R\, \epsilon_s\, B_s/2}} = \left\{ \theta' + L_e \left[\frac{\alpha_{2e}(h_2 - h_1)}{\bar{c}_{pe}\, T_e}\, g' + \frac{\alpha_{4e}(h_4 - h_1)}{\bar{c}_{pe}\, T_e}\, \chi' \right] \right\}_{\eta = 0} \qquad (3.43)
$$

and the skin friction is

$$
\frac{\tau_w / u_e}{C(0)\sqrt{\rho_R/\mu_R\, \epsilon_s\, B_s/2}} = f''(0). \qquad (3.44)
$$

These equations govern the only possible exact similarity solution which includes arbitrary gas phase and surface reaction rates. They constitute a generalization of the problem formulated by Fay and Riddell in three respects: (a) the details of a four specie air mixture in the diffusion and reaction rate terms are more clearly brought out, (b) an arbitrary recombination rate temperature dependence is included, and (c) a general rate of catalytic wall recombination is allowed in the specie boundary conditions.

CHAPTER IV

CHEMICALLY FROZEN PERTURBATION ANALYSIS

The investigation of the deviations from chemical equilibrium in the laminar boundary layer is impeded by the lack of a similarity solution to the equations away from the stagnation point and by the need for computer solutions to study the influence of the various basic parameters even if one does have a set of similarity equations. Accordingly, an analysis of the problem is offered which overcomes these difficulties to some extent; the role of the dissociation-recombination rate in causing deviations from either extreme of chemical equilibrium is investigated by a chemical perturbation analysis. Many features of the non-equilibrium behavior are revealed in a fairly simple and straightforward manner by this method. In this chapter, the case of chemically frozen deviations are considered in detail for a highly cooled wall.

The chemical perturbation approach includes three particularly important features. First, it shows the influence of the basic chemical parameters involved in the gas phase reactions: activation energy, recombination rate constant, and recombination rate temperature dependence. Second, the theory accounts for the detailed behavior of the various species in dissociated air, as reflected in the previously given diffusion and reaction rate terms for a four component mixture. Third, the perturbation method provides differential equations for the dependent variable deviations that admit a wider range of exact and approximate conditions for which similarity-type of solutions can be made. Thus local non-equilibrium

in the boundary layer away from the stagnation point can be treated. The results of the analysis will be primarily aimed toward calculation of the heat transfer deviations, since this boundary layer parameter is potentially the most greatly affected by non-equilibrium for a highly cooled wall. Thermodynamic state profile deviations are also obtained as a result of the solutions.

The Frozen Perturbation Equations

Assumptions

Previous investigations by Adamson[7,25] and Broadwell[28] have indicated that deviations from the chemically frozen flow extreme may be treated in terms of a power series of the characteristic parameter ζ. For example, the first atomic specie behavior is of the form

$$\alpha_2(X,Y) = \alpha_{2_F}(X,Y) + \zeta \cdot \alpha_{2_I}(X,Y) + \zeta^2 \cdot \alpha_{2_{II}}(X,Y) + \ldots\ldots$$

where α_{2_F} is the chemically frozen atomic specie profile, and α_{2I}, α_{2II}, etc., are the first, second, etc., order deviations due to non-equilibrium. Similar expansions would apply to the other dependent variables. Substitution of such series into the governing boundary layer equations and subsequent equating of the net coefficient of each power of ζ equal to zero will produce a succession of equation sets for the zeroth, first, second, etc. order deviation functions. Each of these equation sets are then solved, subject to appropriate boundary conditions, for the desired quantities such as the wall gradients of temperature and species.

In order to retain, as simply as possible, only those features which appear to be of major importance to the influence of the gas phase

reaction rates on non-equilibrium, the following assumptions will be introduced at the start. (a) Assume $C = \rho\mu/\rho_R\mu_R = 1$, which is exact when $\mu \propto (1 + \alpha)T$. While the finer details of the effect of the viscosity law are certainly of interest, particularly in the presence of surface injection of gas species of noticeably different physical properties, inclusion of the exact $\rho\mu$ variation would demand digital computation to solve the resulting governing equations, and would add little to the understanding of the chemical non-equilibrium analysis. The assumption $C = 1$ eliminates a common coupling effect between the viscous transport terms in the momentum, specie and energy equations. (b) Assume L_e and P_R are constants. While these quantites do vary somewhat, it is consistent with the above assumption and the main objectives of the thesis to ignore the detailed dependence of these parameters on temperature and composition. (c) The specific heat c_{p_1} and c_{p_2} are assumed constant and the $c_{p_2}-c_{p_1}$ contribution to the h_2-h_1 and h_4-h_1 coefficients of the reaction rate terms in the energy equation, compared to that of the heats of formation, will be neglected. This seems a reasonable approximation when studying the main effects of the chemical non-equilibrium due to such reaction terms. Further, we shall neglect the remaining $c_{p_2}-c_{p_1}$ terms ($\mathcal{C}_p \equiv 1$) and consequently eliminate coupling between the energy and specie equations. Approximate calculations have shown that the specific heat perturbations contribute negligably to the temperature gradient deviation in comparison to the direct effect of the reaction rate; the exclusion of these terms (which otherwise greatly complicate the perturbation equations) does not alter the basic dissociation-recombination

chemistry effects that are the main object of inquiry. (d) We will neglect velocity profile perturbations due to non-equilibrium in comparison to those experienced by the composition and temperature profiles. Lees[4,14] has pointed out that the velocity profile solution has been found very insensitive to the pressure gradient term in the similarity plane momentum equation, and the specie and temperature profiles and their surface gradients are even less sensitive to the pressure gradient effect on the velocity profile for a highly cooled favorable pressure gradient boundary layer flow. Hence the pressure gradient term in the momentum equation is neglected by Lees. Similarly, it would seem that a satisfactory approximation for the purposes of studying non-equilibrium cooled boundary layers would be to ignore the pressure gradient term in the momentum equation and neglect all velocity perturbations due to chemical reaction, taking the velocity functions $f(\eta)$ and $f'(\eta)$ to be the known Blasius solutions. An important consequence of this is the linearization of the remaining specie and energy equations, since the velocity terms in these equations become known variable coefficients. (e) Finally, the effects of surface reaction shall be considered only for the two extremes of catalytic action, ignoring the intermediate surface reaction rate details but still accounting for the maximum possible differences due to surface recombination.

Characteristic Non-Equilibrium Parameter Expansion

The aforementioned perturbation of the boundary layer equations is carried out with the similarity plane (ξ, η) forms given in Chapter III. Together with the foregoing assumptions, then, we introduce into these equations the following expansions:

$$
\left.
\begin{aligned}
z &= z_F(\xi, \eta) + \zeta \cdot z_I(\xi, \eta) + \zeta^2 \cdot z_{II}(\xi, \eta) + \cdots\cdots \\
\chi &= \chi_F + \zeta \cdot \chi_I + \zeta^2 \cdot \chi_{II} + \cdots\cdot \\
W &= W_F + \zeta \cdot W_I + \zeta^2 \cdot W_{II} + \cdots\cdot \\
\theta &= \theta_F + \zeta \cdot \theta_I + \zeta^2 \cdot \theta_{II} + \cdots\cdot
\end{aligned}
\right\} \qquad (4.1)
$$

where the subscript "F" denotes the chemically frozen solution and where it is required that all the various deviation functions vanish at the outer "edge" ($\eta \to \infty$) of the boundary layer,

$$
\left.
\begin{aligned}
z_I(\infty) &= z_{II}(\infty) = \cdots\cdot = 0 \\
\chi_I(\infty) &= \chi_{II}(\infty) = \cdots\cdot = 0 \\
W_I(\infty) &= W_{II}(\infty) = \cdots\cdot = 0 \\
\theta_I(\infty) &= \theta_{II}(\infty) = \cdots\cdot = 0 \ .
\end{aligned}
\right\} \qquad (4.2)
$$

Corresponding to these perturbations, the net reaction rate functions $\mathcal{G}_2$ and $\mathcal{G}_4$ may be written as the following expansions:

$$
\left.
\begin{aligned}
\mathcal{G}_{2,4} &= \left(\mathcal{G}_{2,4}\right)_F + \left(\frac{\partial \mathcal{G}_{2,4}}{\partial \beta}\right)_F (\beta - \beta_F) + \left(\frac{\partial \mathcal{G}_{2,4}}{\partial \chi}\right)_F (\chi - \chi_F) \\
&\quad + \left(\frac{\partial \mathcal{G}_{2,4}}{\partial W}\right)_F (W - W_F) + \left(\frac{\partial \mathcal{G}_{2,4}}{\partial \theta}\right)_F (\theta - \theta_F) + \cdots\cdots \\
&= \left(\mathcal{G}_{2,4}\right)_F + \zeta \left[\left(\frac{\partial \mathcal{G}_{2,4}}{\partial \beta}\right)_F \beta_I + \left(\frac{\partial \mathcal{G}_{2,4}}{\partial \chi}\right)_F \chi_I \right. \\
&\quad \left. + \left(\frac{\partial \mathcal{G}_{2,4}}{\partial W}\right)_F W_I + \left(\frac{\partial \mathcal{G}_{2,4}}{\partial \theta}\right)_F \theta_I \right] + \cdots\cdots\cdot \ .
\end{aligned}
\right\} \qquad (4.3)
$$

The various derivatives in Equation (4.3) are given in Appendix D. Substitution of expansions (4.1) and (4.3) into the governing boundary layer equations, collecting terms and setting the net coefficient of each power of ζ equal to zero, will produce sets of equations governing the frozen, first order, second order, etc., deviation functions. Introducing the symbols

$$\left.\begin{aligned} q_{2,4} &= \frac{\alpha_{2,4_e}\, h f^{(0)}_{2,4}}{\bar{\rho}_e \bar{\mu}_e} \\ Q &= (d\zeta/dx)/(\zeta/x) \\ \mathbb{D}_{\beta_{2,4}} &= \left(\frac{d\mathcal{L}_{2,4}}{d\beta}\right)_F , \quad \mathbb{D}_{\chi_{2,4}} = \left(\frac{d\mathcal{L}_{2,4}}{d\chi}\right)_F \\ \mathbb{D}_{W_{2,4}} &= \left(\frac{d\mathcal{L}_{2,4}}{dW}\right)_F , \quad \mathbb{D}_{\theta_{2,4}} = \left(\frac{d\mathcal{L}_{2,4}}{d\theta}\right)_F , \end{aligned}\right\} \tag{4.4}$$

then the resulting perturbation equations for zeroth, first, and second order deviations, successively, are as follows:

(1) Zeroth Order (Chemically Frozen Flow)

$$S_c f \frac{d\beta_F}{d\eta} + \frac{d^2\beta_F}{d\eta^2} = 2 S_c f' \xi \frac{d\beta_F}{d\xi} \tag{4.5}$$

$$S_c f \frac{d\chi_F}{d\eta} + \frac{d^2\chi_F}{d\eta^2} = 2 S_c f' \xi \frac{d\chi_F}{d\eta} \tag{4.6}$$

$$S_c f \frac{dW_F}{d\eta} + \frac{d^2 W_F}{d\eta^2} = 2 S_c f' \xi \frac{dW_F}{d\eta} \tag{4.7}$$

$$f(\eta) f''(\eta) + f'''(\eta) = 0 \tag{4.8}$$

$$P_R f \frac{d\theta_F}{d\eta} + \frac{d^2\theta_F}{d\eta^2} + P_R\left(\frac{u_e^2}{\bar{r}_{Pe} T_e}\right)\left\{f''^2 + 2\frac{\beta}{\epsilon} f' \theta_F \left[\frac{\alpha_{2e}(1-\beta_F) + \alpha_{4e}(1-\chi_F)}{1+\alpha_e}\right]\right\} = 2 P_R f' \xi \frac{\partial \theta_F}{\partial \xi} \tag{4.9}$$

(2) First Order Frozen Deviations

$$S_c f \frac{d\beta_I}{d\eta} + \frac{d^2\beta_I}{d\eta^2} - \frac{2Q}{\epsilon} S_c f' \beta_I = \frac{2\alpha_{2e}}{\epsilon(1+\alpha_e)} \theta_F^{\omega-2} \mathcal{J}_{2F} + 2 S_c f' \xi \frac{\partial \beta_I}{\partial \xi} \tag{4.10}$$

$$S_c f \frac{d\chi_I}{d\eta} + \frac{d^2\chi_I}{d\eta^2} - \frac{2Q}{\epsilon} S_c f' \chi_I = \frac{2\alpha_{4e}}{\epsilon(1+\alpha_e)} \theta_F^{\omega-2} \mathcal{J}_{4F} + 2 S_c f' \xi \frac{\partial \chi_I}{\partial \xi} \tag{4.11}$$

$$S_c f \frac{dW_I}{d\eta} + \frac{d^2 W_I}{d\eta^2} - \frac{2Q}{\epsilon} S_c f' W_I = -\left(\frac{\alpha_{4e}}{\alpha_{2e}}\right) \frac{2\alpha_{4e}}{\epsilon(1+\alpha_e)} \theta_F^{\omega-2} \mathcal{J}_{4F} + 2 S_c f' \xi \frac{\partial W_I}{\partial \xi} \tag{4.12}$$

$$P_R f \frac{d\theta_I}{d\eta} + \frac{d^2\theta_I}{d\eta^2} - \frac{2Q}{\epsilon} P_R f' \theta_I + P_R\left(\frac{u_e^2}{\bar{r}_{Pe} T_e}\right) 2\frac{\beta}{\epsilon} f' \theta_F \left[\frac{\alpha_{2e}(1-\beta_F)}{1+\alpha_e}\left(\frac{\theta_I}{\theta_F} - \frac{\beta_I}{1-\beta_F}\right) + \frac{\alpha_{4e}(1-\chi_F)}{1+\alpha_e}\left(\frac{\theta_I}{\theta_F} - \frac{\chi_I}{1-\chi_F}\right)\right] = -\frac{2\alpha_{2e} L_e}{\epsilon(1+\alpha_e)} \theta_F^{\omega-2}\left(g_2 \mathcal{J}_{2F} + \frac{\alpha_{4e}}{\alpha_{2e}} g_4 \mathcal{J}_{4F}\right) + 2 P_R f' \xi \frac{\partial \theta_I}{\partial \xi} \tag{4.13}$$

(3) Second Order Frozen Deviations

$$S_c f \frac{\partial \beta_{II}}{\partial \eta} + \frac{\partial^2 \beta_{II}}{\partial \eta^2} - \frac{4Q}{\epsilon} S_c f' \beta_{II} = \frac{2\alpha_{2e} \theta_F^{\omega-2}}{\epsilon(1+\alpha_e)} \left[(\omega-2) \frac{\theta_I}{\theta_F} \mathcal{Y}_{2F} + \mathbb{D}_{\beta_2} \beta_I + \mathbb{D}_{\chi_2} \chi_I + \mathbb{D}_{W_2} W_I + \mathbb{D}_{\theta_2} \theta_I \right] + 2 S_c f' \xi \frac{\partial \beta_{II}}{\partial \xi} \tag{4.14}$$

$$S_c f \frac{\partial \chi_{II}}{\partial \eta} + \frac{\partial^2 \chi_{II}}{\partial \eta^2} - \frac{4Q}{\epsilon} S_c f' \chi_{II} = \frac{2\alpha_{4e} \theta_F^{\omega-2}}{\epsilon(1+\alpha_e)} \left[(\omega-2) \frac{\theta_I}{\theta_F} \mathcal{Y}_{4F} + \mathbb{D}_{\beta_4} \beta_I + \mathbb{D}_{\chi_4} \chi_I + \mathbb{D}_{W_4} W_I + \mathbb{D}_{\theta_4} \theta_I \right] + 2 S_c f' \xi \frac{\partial \chi_{II}}{\partial \xi} \tag{4.15}$$

$$S_c f \frac{\partial W_{II}}{\partial \eta} + \frac{\partial^2 W_{II}}{\partial \eta^2} - \frac{4Q}{\epsilon} S_c f' W_{II} = -\frac{\alpha_{4e}}{\alpha_{3e}} \frac{2\alpha_{4e} \theta_F^{\omega-2}}{\epsilon(1+\alpha_e)} \left[(\omega-2) \frac{\theta_I}{\theta_F} \mathcal{Y}_{4F} + \mathbb{D}_{\beta_4} \beta_I + \mathbb{D}_{\chi_4} \chi_I + \mathbb{D}_{W_4} W_I + \mathbb{D}_{\theta_4} \theta_I \right] + 2 S_c f' \xi \frac{\partial W_{II}}{\partial \xi} \tag{4.16}$$

$$P_R f \frac{\partial \theta_{II}}{\partial \eta} + \frac{\partial^2 \theta_{II}}{\partial \eta^2} - \frac{4Q}{\epsilon} P_R f' \theta_I + P_R \left(\frac{u_e^2}{\lambda_{Pe} T_e} \right) \frac{2\beta}{\epsilon} f' \theta_F \left\{ \frac{\alpha_{2e}(1-\beta_F)}{1+\alpha_e} \left[\frac{\theta_{II}}{\theta_F} - \left(\frac{\beta_I}{1-\beta_F} \right) \left(\frac{\theta_I}{\theta_F} + \frac{\beta_{II}}{\beta_I} \right) \right] + \frac{\alpha_{4e}(1-\chi_F)}{1+\alpha_e} \left[\frac{\theta_{II}}{\theta_F} - \left(\frac{\chi_I}{1-\chi_F} \right) \left(\frac{\theta_I}{\theta_F} + \frac{\chi_{II}}{\chi_I} \right) \right] \right\} = -\frac{2\alpha_{2e} \theta_F^{\omega-2} L_e}{\epsilon(1+\alpha_e)} \left[(\omega-2) \frac{\theta_I}{\theta_F} \left(g_2 \mathcal{Y}_{2F} + \frac{\alpha_{4e}}{\alpha_{2e}} g_4 \mathcal{Y}_{4F} \right) + \beta_I \left(g_2 \mathbb{D}_{\beta_2} + \frac{\alpha_{4e}}{\alpha_{2e}} g_4 \mathbb{D}_{\beta_4} \right) + \chi_I \left(g_2 \mathbb{D}_{\chi_2} + \frac{\alpha_{4e}}{\alpha_{2e}} g_4 \mathbb{D}_{\chi_4} \right) + W_I \left(g_2 \mathbb{D}_{W_2} + \frac{\alpha_{4e}}{\alpha_{2e}} g_4 \mathbb{D}_{W_4} \right) + \theta_I \left(g_2 \mathbb{D}_{\theta_2} + \frac{\alpha_{4e}}{\alpha_{2e}} g_4 \mathbb{D}_{\theta_4} \right) \right] + 2 P_R f' \xi \frac{\partial \theta_{II}}{\partial \xi} \tag{4.17}$$

The boundary conditions are as follows. At the outer edge of the boundary layer:

$$\left.\begin{aligned} f'(\infty) = z_F(\infty) = \chi_F(\infty) = W_F(\infty) = \Theta_F(\infty) = 1, \\ z_I(\infty) = \chi_I(\infty) = W_I(\infty) = \Theta_I(\infty) = 0, \\ z_{II}(\infty) = \chi_{II}(\infty) = W_{II}(\infty) = \Theta_{II}(\infty) = 0 . \end{aligned}\right\} \qquad (4.18)$$

At the body surface $\eta = 0$, on the other hand, we have the conditions:

$$\left.\begin{aligned} f(0) = f'(0) = 0 \\ \Theta_F(0) = \Theta_W \\ \Theta_I(0) = \Theta_{II}(0) = 0 \end{aligned}\right\} \qquad (4.19)$$

$$\left.\begin{aligned} \beta_F(0) = \beta_I(0) = \beta_{II}(0) = \chi_F(0) = \chi_I(0) = \chi_{II}(0) = 0, \\ W_F(0) = W_{EQ}(0), \quad W_I(0) = W_{II}(0) = 0 \text{ ; COOL CATALYTIC WALL} \end{aligned}\right\} \qquad (4.20)$$

$$\left.\begin{aligned} \frac{\partial \beta_F}{\partial n}(0) = \frac{\partial \beta_I}{\partial n}(0) = \frac{\partial \beta_{II}}{\partial n}(0) = \frac{\partial \chi_F}{\partial n}(0) = \frac{\partial \chi_I}{\partial n}(0) = \frac{\partial \chi_{II}}{\partial n}(0) \\ = \frac{\partial W_F}{\partial n}(0) = \frac{\partial W_I}{\partial n}(0) = \frac{\partial W_{II}}{\partial n}(0) \text{ ; NON-CATALYTIC WALL} \end{aligned}\right\} \qquad (4.21)$$

The surface skin friction, which remains unperturbed to the approximations used, is

$$\frac{\tau_w}{u_e \sqrt{\rho_R / \mu_R \epsilon u_e / 2x}} = f''(0). \qquad (4.22)$$

The surface heat transfer, however, shows the following non-equilibrium behavior in the neighborhood of the chemically frozen value, to second order deviations:

$$\frac{-P_R\left(\dot{Q}_w/\bar{c}_{p_e}T_e\right)}{\sqrt{\rho_R/\mu_R\,\epsilon\,u_e/2x}} = \underbrace{\left[\frac{\partial\theta_F}{\partial\eta} + L_e\left(g_2\frac{\partial\beta_F}{\partial\eta} + g_4\frac{\partial\chi_F}{\partial\eta}\right)\right]_{\eta=0}}_{Q_F} + \zeta\underbrace{\left[\frac{\partial\theta_I}{\partial\eta} + L_e\left(g_2\frac{\partial\beta_I}{\partial\eta} + g_4\frac{\partial\chi_I}{\partial\eta}\right)\right]}_{Q_I} + \zeta^2\underbrace{\left[\frac{\partial\theta_{II}}{\partial\eta} + L_e\left(g_2\frac{\partial\beta_{II}}{\partial\eta} + g_4\frac{\partial\chi_{II}}{\partial\eta}\right)\right]}_{Q_{II}} \tag{4.23}$$

Reduction to Ordinary Differential Equations

Each of the foregoing chemical perturbation equation sets can be examined by similarity arguments of the kind previously discussed in Chapter III. Because of the foregoing simplifying assumptions and the fact that the characteristic non-equilibrium parameter ζ does not appear explicitly in these equations, the exact and approximate similarity possibilities (reduction to sets of ordinary differential equations) are now somewhat greater. In general, an inspection indicates that neglect of ξ derivatives and the use of local constants for the ξ - dependent coefficients is justified when the following parameters are either constant or slowly-varying functions of X: the gas composition at the edge of the boundary layer, the parameters ϵ, β and $u_e^2/\bar{c}_{p_e}T_e$, the freestream and wall temperatures, and the non-equilibrium parameter derivative factor Q. The boundary conditions (4.18) through (4.21) (with the possible exception of the frozen temperature boundary condition θ_w) are all independent of ξ.

The similarity conditions are exactly satisfied for constant surface temperatures, regardless of the degree of surface cooling, in two cases. First, the symmetric stagnation point flow, for which $\beta = 1$,

$u_e = R_S X = 0, \epsilon = 2(K+1)$, and $Q = u_e^2/\bar{c}_{p_e} T_e = 0$. Second, a uniform inviscid flow (such as a flat plate or cylinder) for which u_e and $u_e^2/\bar{c}_{p_e} T_e$ are constants, $\beta = 0$, and $Q = \epsilon = 1$.

Approximate similarity can be obtained, however, over a wider range of local conditions. Regarding the specie equations, the freestream composition has already been assumed slowly-varying to be consistant with the chemically reacting boundary layer flow approximations. The frozen flow specie equations can be taken locally similar in view of the boundary conditions. The first and second order specie perturbation equations can likewise be approximated by ordinary differential equations if the reaction rate functions $(\mathcal{K}_{2,4})_F$ and their derivatives $\mathcal{D}_{\gamma_{2,4}}$, $\mathcal{D}_{\chi_{2,4}}$, $\mathcal{D}_{W_{2,4}}$ and $\mathcal{D}_{\theta_{2,4}}$ can be assumed functions of η only and if the parameter Q/ϵ is constant or a slowly-varying function of X. The former condition is met if the frozen specie and temperature profiles are approximately similar and $\Theta_{A_{2,4}}$ is constant or a slowly-varying function of X (since $\Theta_A \equiv T_A/T_e$, this in turn requires the freestream temperature to be constant or slowly-varying). These temperature conditions are taken up in the examination of the energy equations. Concerning the latter condition, Q/ϵ will be exactly constant when the parameters ζ and ξ vary with X as X^N. If such a form locally describes the variation of these quantities at various portions of the body, then as long as N itself varies slowly between these regions, Q/ϵ can be taken as a local constant at each X. The local value of the parameter Q can be obtained by differentiation of Equation (2.94):

$$Q = 1 - \beta + \left[2 + (\omega - 2)\left(\frac{\bar{\gamma} - 1}{\bar{\gamma}}\right)\right]\left(\frac{d\rho_e/dX}{\rho_e/X}\right). \qquad (4.24)$$

As an example of the typical variation of Q/ϵ on a hypersonic vehicle, the pressure distribution shown in Figure 3 has been used to calculate ϵ and Q; the resulting Q/ϵ distribution is plotted in Figure 6 as a function of distance along the hemisphere-cylinder. The results indicate that Q/ϵ is exactly constant at $X = 0$ (stagnation point, $Q = 0$), at $X/d \to \infty$ (uniform inviscid flow, $Q/\epsilon = +1$) and at $X/d \cong .7$ (in the neighborhood of the sonic point) with a minimum value around -2, depending on the value of ω. Otherwise, Q/ϵ appears to be everywhere a slowly-varying function of X with the possible exception of a region of approximately one body diameter in width on either side of the minimum point.

In addition to the foregoing conditions, the similarity of the energy equations imposes further requirements. The inner boundary conditions on the temperature deviations are independent of ξ, whereas the frozen temperature boundary condition $\theta_F(o) = \theta_W$ will give similarity when θ_W is constant or slowly-varying (further, θ_W itself has a very small effect on the frozen temperature profile, since we assume the wall to be highly cooled, $\theta_W \ll 1$). Concerning the coefficients in the equations, the approximate similarity of the temperature variable will depend on the factors T_e and $u_e^2/\bar{c}_{p_e} T_e$ being constant or slowly-varying functions of X. (The parameters q_2 and q_4 are local constants if T_e can be considered so). Now considering the inviscid flow as isentropic with some average $\bar{\gamma}$,

$$T_e \sim (p_e)^{\frac{\bar{\gamma}-1}{\bar{\gamma}}} ,$$

which indicates that even in the presence of significant pressure gradients (such as shown in Figure 3) the corresponding inviscid flow temperature

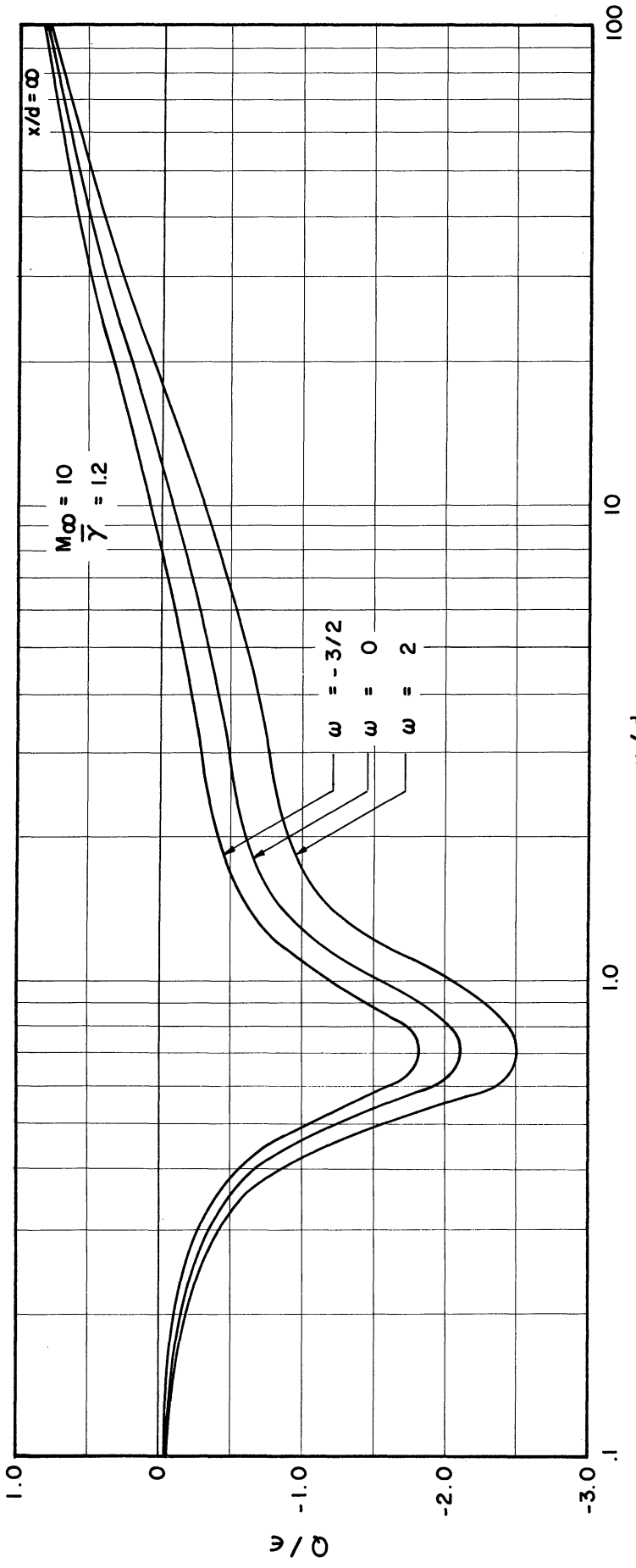

Figure 6. Variation of the Boundary Layer Non-Equilibrium Parameter Derivative Factor Q/ϵ along a Hemisphere-Cylinder.

variations should be much more gradual and can be taken as slowly-varying for the boundary layer theory. The kinetic energy/internal energy ratio $u_e^2/\bar{c}_{p_e}T_e$, using the fact that

$$1/2\ u_e^2 + c_{p_1}T_e(1 + q_2 + q_4) \cong h_{s_e} = \text{constant}, \qquad (4.25)$$

can be written as

$$\frac{u_e^2}{\bar{c}_{p_e}T_e} \simeq (1+q_2+q_4)\left[\frac{u_e^2/h_{se}}{1-\frac{1}{2}(u_e^2/h_{se})}\right]. \qquad (4.26)$$

This relation indicates two situations under which the $u_e^2/\bar{c}_{p_e}T_e$ term gives similarity of the energy equations. The first is the case in which u_e^2/h_{s_e} is very small(because of a low speed, high temperature inviscid flow) and can be neglected, regardless of the X-dependence. Such a situation would occur in the frontal region of a blunt-nosed hypersonic body where the flow originates from the strong parts of the bow shock and is at a very high temperature. The second case occurs when the magnitude of u_e^2/h_{s_e} is important but the X-dependence of the term is comparatively weak because $u_e(X)$ becomes a slowly-varying function. For many hypersonic flows of interest, it appears that in the regions where $u_e^2/\bar{c}_{p_e}T_e$ varies significantly with X it is small enough to neglect, whereas when its size builds up to a significant effect, the X-variation has noticeably weakened ($\beta \to 0$). We shall therefore make the approximation that the $u_e^2/\bar{c}_{p_e}T_e$ term can be taken as a local constant in the energy equation while neglecting the $\partial\theta/\partial\xi$ terms at each X. When including this local term in the energy equation for a cooled boundary layer flow, we shall further neglect the $\beta/\epsilon(1-z)\theta_F f'$ and $\beta/\epsilon(1-X)\theta_F f'$ terms in the frozen energy equation (compared to f''^2) and the perturbations of these terms in the first and second

order energy equations, since they enter in proportionally to $\beta/\epsilon \cdot \left(u_e^2/\bar{c}_{p_e} T_e\right)$ and are therefore negligable when $u_e^2/\bar{c}_{p_e} T_e$ is of significant size (accepting the above approximation that this latter occurs only when β becomes very small).

Accepting the approximations (and limitations) in the foregoing similarity arguments for a cooled non-equilibrium laminar boundary layer, the zeroth, first and second order specie and temperature profile deviations are governed by the following sets of ordinary linear differential equations (denoting $d/d\eta$ by a prime):

(1) Zeroth Order

$$S_c f \beta_F' + \beta_F'' = 0 \tag{4.27}$$

$$S_c f \chi_F' + \chi_F'' = 0 \tag{4.28}$$

$$S_c f W_F' + W_F'' = 0 \tag{4.29}$$

$$P_r f \theta_F' + \theta_F'' + P_r \left(\frac{u_e^2}{\bar{c}_{p_e} T_e}\right) f''^2 = 0 \tag{4.30}$$

where f, f' and f'' are the known Blasius functions, i.e., solutions to the equation

$$f f'' + f''' = 0$$

with $f'(\infty) = 1$ and $f(o) = f'(o) = 0$.

(2) First Order Deviations

$$S_c f \beta_I' + \beta_I'' - \frac{2\xi}{\epsilon} S_c f' \beta_I = \frac{2\alpha_{2e} \theta_F^{\omega-2}}{\epsilon(1+\alpha_e)} \mathcal{L}_{2F} \tag{4.31}$$

$$S_c f \chi_I' + \chi_I'' - \frac{2\xi}{\epsilon} S_c f' \chi_I = \frac{2\alpha_{4e} \theta_F^{\omega-2}}{\epsilon(1+\alpha_e)} \mathcal{L}_{4F} \tag{4.32}$$

$$S_c f W_I' + W_I'' - \frac{2Q}{\epsilon} S_c f' W_I = -\left(\frac{\alpha_{4e}}{\alpha_{3e}}\right) \frac{2\alpha_{4e}\theta_F^{\omega-2}}{\epsilon(1+\alpha_e)} \mathcal{Y}_{4F} \tag{4.33}$$

$$P_R f \theta_I' + \theta_I'' - \frac{2Q}{\epsilon} P_R f' \theta_I = -\frac{2\alpha_{2e} L_e \theta_F^{\omega-2}}{\epsilon(1+\alpha_e)} \left(q_2 \mathcal{Y}_{2F} + \frac{\alpha_{4e}}{\alpha_{2e}} q_4 \mathcal{Y}_{4F} \right) \tag{4.34}$$

(3) Second Order Deviations

$$S_c f \beta_{II}' + \beta_{II}'' - \frac{4Q}{\epsilon} S_c f' \beta_{II} = \frac{2\alpha_{2e}\theta_F^{\omega-2}}{\epsilon(1+\alpha_e)} \left[(\omega-2)\frac{\theta_I}{\theta_F} \mathcal{Y}_{2F} + \beta_I \mathbb{F}_{\beta_2} + \chi_I \mathbb{F}_{\chi_2} + W_I \mathbb{F}_{W_2} + \theta_I \mathbb{F}_{\theta_2} \right] \tag{4.35}$$

$$S_c f \chi_{II}' + \chi_{II}'' - \frac{4Q}{\epsilon} S_c f' \chi_{II} = \frac{2\alpha_{4e}\theta_F^{\omega-2}}{\epsilon(1+\alpha_e)} \left[(\omega-2)\frac{\theta_I}{\theta_F} \mathcal{Y}_{4F} + \beta_I \mathbb{F}_{\beta_4} + \chi_I \mathbb{F}_{\chi_4} + W_I \mathbb{F}_{W_4} + \theta_I \mathbb{F}_{\theta_4} \right] \tag{4.36}$$

$$S_c f W_{II}' + W_{II}'' - \frac{4Q}{\epsilon} S_c f' W_{II} = -\left(\frac{\alpha_{4e}}{\alpha_{3e}}\right) \frac{2\alpha_{4e}\theta_F^{\omega-2}}{\epsilon(1+\alpha_e)} \left[(\omega-2)\frac{\theta_I}{\theta_F} \mathcal{Y}_{4F} + \beta_I \mathbb{F}_{\beta_4} + \chi_I \mathbb{F}_{\chi_4} + W_I \mathbb{F}_{W_4} + \theta_I \mathbb{F}_{\theta_4} \right] \tag{4.37}$$

$$P_R f \theta_{II}' + \theta_{II}'' - \frac{4Q}{\epsilon} P_R f' \theta_{II} = -\frac{2\alpha_{2e} L_e \theta_F^{\omega-2}}{\epsilon(1+\alpha_e)} \left[(\omega-2)\frac{\theta_I}{\theta_F} \left(q_2 \mathcal{Y}_{2F} + \frac{\alpha_{4e}}{\alpha_{2e}} q_4 \mathcal{Y}_{4F} \right) + \beta_I \left(q_2 \mathbb{F}_{\beta_2} + \frac{\alpha_{4e}}{\alpha_{2e}} q_4 \mathbb{F}_{\beta_4} \right) + \chi_I \left(q_2 \mathbb{F}_{\chi_2} + \frac{\alpha_{4e}}{\alpha_{2e}} q_4 \mathbb{F}_{\chi_4} \right) + W_I \left(q_2 \mathbb{F}_{W_2} + \frac{\alpha_{4e}}{\alpha_{2e}} q_4 \mathbb{F}_{W_4} \right) + \theta_I \left(q_2 \mathbb{F}_{\theta_2} + \frac{\alpha_{4e}}{\alpha_{2e}} q_4 \mathbb{F}_{\theta_4} \right) \right] \tag{4.38}$$

The boundary conditions (4.18) through (4.21) still apply; the shear stress is given by Equation (4.22), and the heat transfer is given by Equation (4.23) when the partial derivatives are made total derivatives with respect to η.

Solution to the Frozen Perturbation Equations

Chemically Frozen (Zeroth Order) Solutions

This group of equations and boundary conditions can be solved easily in terms of known integrals of the Blasius velocity functions. We shall consider each of the equations in turn.

The atomic specie Equation (4.27), viewed as a first order equation in z_F', can be integrated by means of the integration factor $\mathrm{EXP}(S_c \int_0^\eta f d\eta)$ and subsequently integrated again to obtain the general solution:

$$\beta_F(\eta) = \beta_F(0) + \beta_F'(0) \int_0^\eta \mathrm{EXP}\left(-S_c \int_0^\eta f\, d\eta\right) d\eta . \qquad (4.39)$$

The integral has been given, for example, by Goldstein[29] for a slightly different scale factor in η and f which can easily be adjusted to the present case; in particular, reference 30 gives the approximation

$$\int_0^\infty \mathrm{EXP}\left(-S_c \int_0^\eta f\, d\eta\right) d\eta \simeq \left(.47\, S_c^{1/3}\right)^{-1} . \qquad (4.40)$$

Applying the boundary conditions $z_F(\infty) = 1$ and either $z_F(0) = 0$ (catalytic wall) or $z_F'(0) = 0$ (non-catalytic wall) to Equation (4.39) gives the following two solutions:

$$\left[\beta_F(\eta)\right]_{CAT.} = .47\, S_c^{1/3} \int_0^\eta \mathrm{EXP}\left(-S_c \int_0^\eta f\, d\eta\right) d\eta \qquad (4.41)$$

with $z_F'(o)]_{CAT.} = .47\ S_c^{1/3}$, and

$$[z_F(\eta)]_{NON-CAT.} = 1. \qquad (4.42)$$

The frozen second atomic specie Equation (4.28), when compared to Equation (4.27), shows that the variables χ_F and z_F are linearly related. In view of the boundary conditions on z_F and χ_F being the same for either wall catalysis condition, then*

$$\chi_F = z_F . \qquad (4.43)$$

In the catalytic case, the atomic specie concentrations are zero on the surface, whereas in the non-catalytic case, the build-up of atoms in the absence of surface reaction gives a uniform steady state concentration distribution.

The total atomic specie profile becomes

$$\frac{\alpha_F}{\alpha_{F_e}} = \frac{\alpha_{2e}\beta_F + \alpha_{4e}\chi_F}{\alpha_e} = \beta_F . \qquad (4.44)$$

Using the tabulated values of the integral in Equation (4.41), this solution is plotted versus η for various Schmidt numbers in Figure 7. Also shown for comparison is the total atomic specie profile obtained by Fay and Riddell[6] for $L_e = 1.4$ ($S_c = .5$). The discrepancy in the catalytic wall profiles, including a 44% greater wall slope than found by Fay and Riddell, is the result of the $\rho\mu/\rho_R\mu_R \equiv C = 1$ assumption in the present theory. (Application of an approximate method for correcting $C = 1$ boundary layer calculations to account for variable $\rho\mu$ affects, described in Appendix F, brings the present theory value of $z_F'(o)_{CAT.}$ down to within a few percent of the Fay and Riddell value). It is interesting to note from Figure 7

* It can be shown that this result is also obtained if the quasi-two component diffusion flux term is used instead of Fick's law.

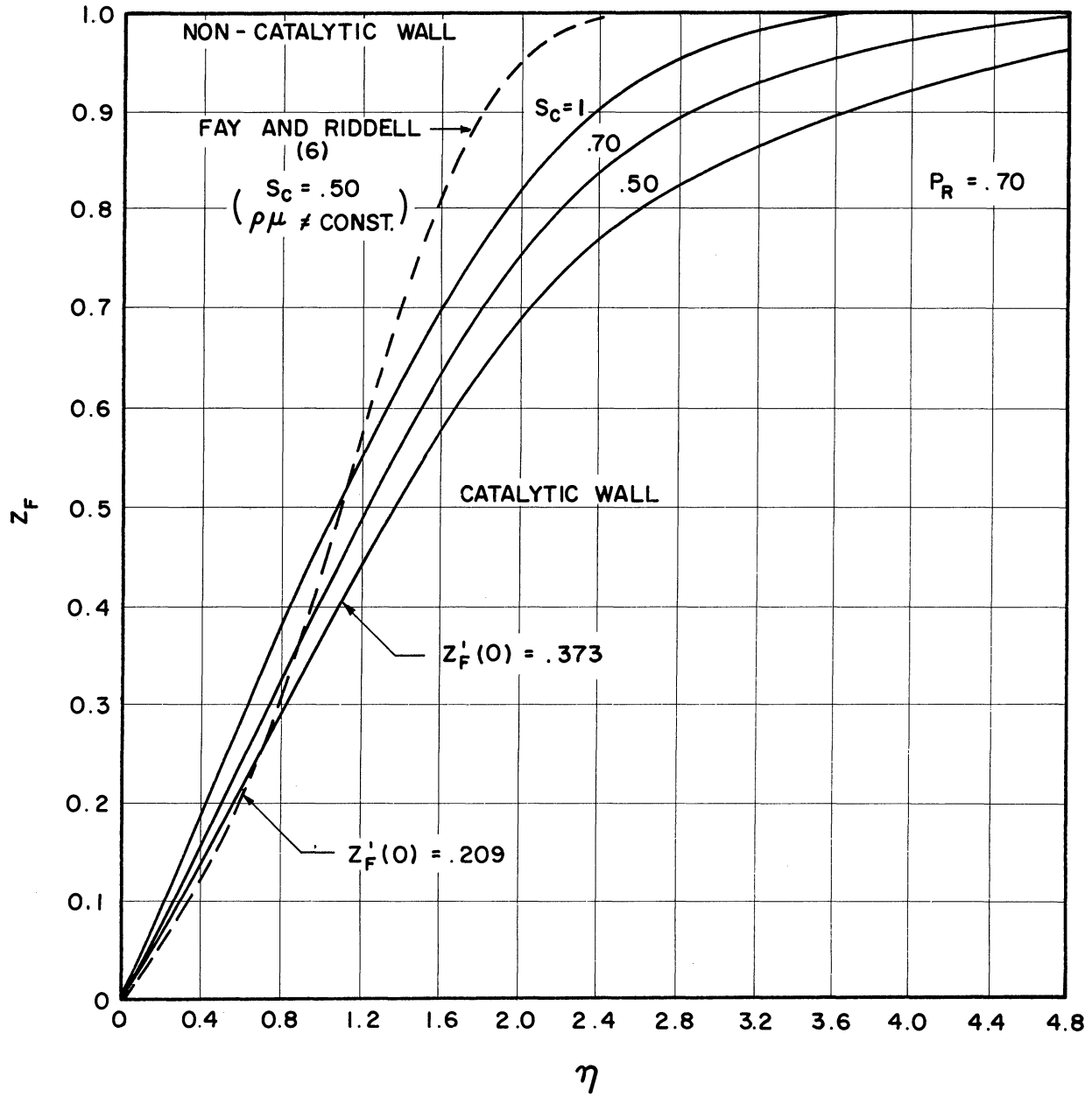

Figure 7. Atomic Specie Distribution in the Chemically Frozen Laminar Boundary Layer.

that the C = 1 assumption approximately doubles the boundary layer thickness.

The second molecular specie Equation (4.29) integrates in the same way; applying the boundary conditions $W_F(\infty) = 1$ and either $W_F(o) = W_{EQ}(o)$ or $W_F'(o) = 0$, we have

$$W_F(\eta) = W_{EQ}(0) + [1 - W_{EQ}(0)]\, g_F(\eta) , \qquad (4.45)$$

which can be used for either catalysis extreme since $z_F = 1$ (non-catalytic solution) gives the correct answer when inserted into the equation. This result shows that when $W_{EQ}(o) = 1$ (i.e., $\alpha z_{EQ}(o) = \alpha z_e$), the catalytic wall solution coincides with that for the non-catalytic case and there is no steady state diffusion of molecular nitrogen. Such a conclusion is, of course, based on the use of the Fick law diffusion.* Some typical $W_F(\eta)$ profiles are shown in Figure 8; when $W_{EQ}(o) > 1$, the catalytic wall provides an excess of molecular nitrogen at the wall over that in the freestream.

The energy Equation (4.30) is a second order non-homogeneous differential equation that can be treated as a first order non-homogeneous equation for $\theta_F'(\eta)$ and therefore integrated to yield the following result:

$$\theta_F(\eta) = \theta_W + \theta_F'(0)\int_0^\eta \exp\left(-P_R\int_0^\eta f\, d\eta\right) - \left(\frac{u_e^2}{2\bar{h}_e T_e}\right) 2P_R \int_0^\eta \left[(f'')^{P_R}\left[\int_0^\eta (f'')^{2-P_R}\, d\eta\right] d\eta\right] . \qquad (4.46)$$

(θ_{F_P})

The integral θ_{F_P} constitutes the non-homogeneous particular integral of the energy equation contributed by the dissipation term and is a tabulated function.(29) Applying the boundary conditions $\theta_F(\infty) = 1$ and $\theta_F(o) = \theta_W$,

---

* If the quasi-two component diffusion flux term were to have been used instead in Equation (4.37), it would be found that the solution (4.45) is again obtained provided one takes $W_{EQ}(o) = (1 - \alpha_e)^{-1}$

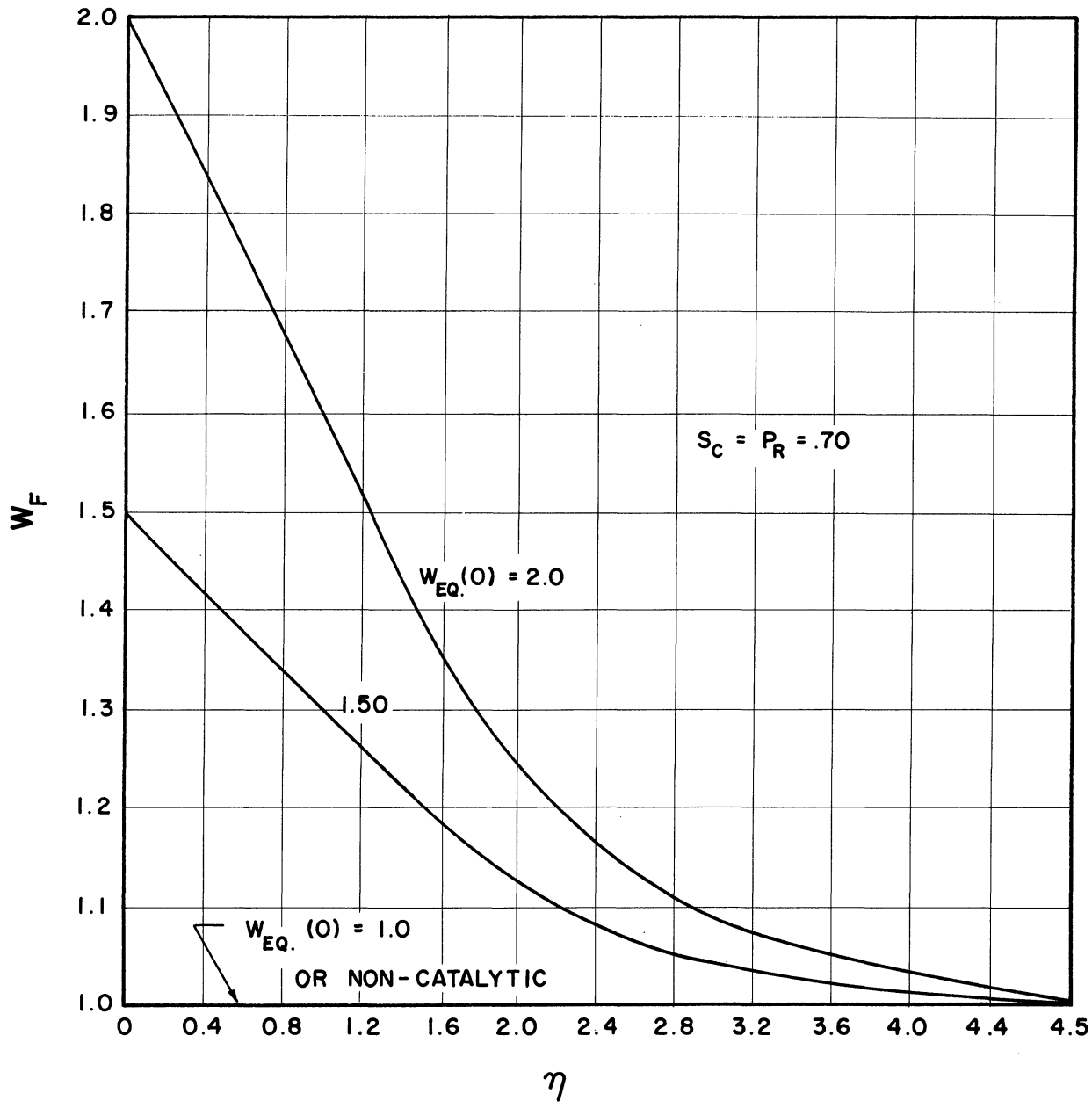

Figure 8. Molecular Nitrogen Distribution in the Chemically Frozen Laminar Boundary Layer.

the following solution is obtained:

$$\theta_F(\eta) = \underbrace{\theta_w + .47(P_R)^{1/3}(1-\theta_w)\int_0^\eta EXP\left(-P_R\int_0^\eta f\,d\eta\right)d\eta}_{\theta_{F_c}} + \left(\frac{u_e^2}{2\bar{c}_{p_e}T_e}\right)\underbrace{\left[.47(P_R)^{1/3}\theta_{F_p}(\infty)\cdot\int_0^\eta EXP\left(-P_R\int_0^\eta f\,d\eta\right)d\eta - \theta_{F_p}(\eta)\right]}_{\theta_{F_p}} \tag{4.47}$$

with

$$\theta_F'(0) = .47P_R^{1/3}\left[1-\theta_w+\left(\frac{u_e^2}{2\bar{c}_{p_e}T_e}\right)\theta_{F_p}(\infty)\right] \tag{4.48}$$

where

$$\theta_{F_p}(\infty) \simeq \sqrt{P_R}\,.$$

This solution is plotted in Figure 9 for $P_R = .70$, $\theta_w = .05$, and several values of the $u_e^2/\bar{c}_{p_e}T_e$ parameter. The viscous dissipation causes a bulge in the temperature profile (and consequent increase in the wall gradient) which would be increasingly prominent for larger θ_w values. However, for highly cooled walls and $u_e^2/\bar{c}_{p_e}T_e \leq 2$, the viscous dissipation heating does not appear to drastically distort the profile, and will therefore be found to have a very minor effect on the dissociation rate in the non-equilibrium perturbation analysis. Also shown in Figure 9 is the stagnation point catalytic wall temperature profile computed by Fay and Riddell using variable $\rho\mu$ and specific heat data. A comparison indicates the error in the present theory due to the combined assumptions of $C = 1$ and equal constant molecular and atomic specie specific heats; the present theory gives a 24% higher wall temperature gradient in this example due to these

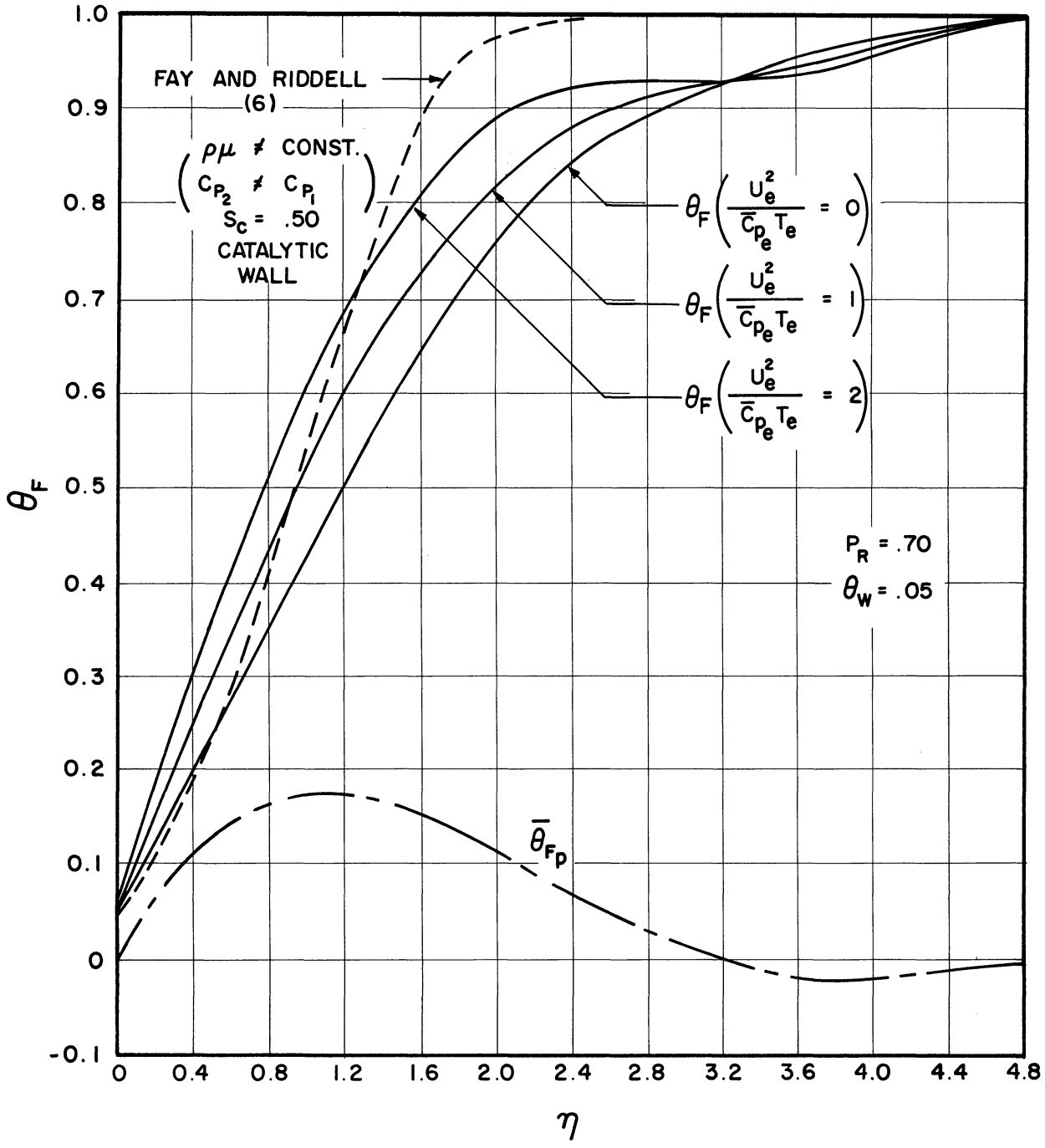

Figure 9. Temperature Distribution in the Chemically Frozen Laminar Boundary Layer.

two assumptions. However, the general temperature profile shape for a cooled wall is not notably different and proves quite accurate for use in the perturbation theory.

The chemically frozen temperature solution (4.47) is independent of the gas composition, since an energy equation coupling term involving the atomic species and proportional to the difference between the atomic and molecular specific heats has been neglected. However, if we return to the general energy Equation (3.16) and again apply the previously discussed similarity approximations without the assumption $c_{p_2} = c_{p_1}$, the following chemically frozen flow energy equation is obtained:

$$\left[P_R f + (L_e+1)\frac{\mathcal{C}_{p_F}'}{\mathcal{C}_{p_F}}\right]\theta_F' + \theta_F'' + P_R\left(\frac{u_e^2}{\bar{c}_{p_e} T_e}\right)\frac{f''^2}{\mathcal{C}_{p_F}} = 0 \qquad (4.49)$$

where

$$\mathcal{C}_{p_F} = \frac{1 + \alpha_e(c_{p_2}/c_{p_1} - 1)\beta_F}{1 + \alpha_e(c_{p_2}/c_{p_1} - 1)}, \qquad (4.50)$$

and where c_{p_2} and c_{p_1} are assumed constant. Since the frozen atomic specie profile z_F is known, Equation (4.49) can be solved to show the effect of the specific heat inequality on the frozen temperature profile (particularly the wall gradient). For the non-catalytic surface ($z_F = \mathcal{C}_{p_F} = 1$), we see immediately that $c_{p_2} - c_{p_1}$ has absolutely no effect on the equation; solution (4.47) is exact in this case. In the opposite extreme of a completely catalytic surface, however, the effect is present. Viewed as a first order equation for θ_F' and subject to the boundary conditions $\theta_F(\infty) = 1$ and $\theta_F(o) = \theta_W$, Equation (4.49) in this case can be integrated

twice to obtain the solution. In the case of negligable dissipation, for example, we have

$$\theta_F(\eta) = \theta_w + (1-\theta_w)\frac{\int_0^{\eta} EXP\left(-P_R\int_0^{\eta} f\,d\eta\right)\left[\rho/\rho(0)\right]^{-(1+Le)}\,d\eta}{\int_0^{\infty} EXP\left(-P_R\int_0^{\eta} f\,d\eta\right)\left[\rho/\rho(0)\right]^{-(1+Le)}\,d\eta} \qquad (4.51)$$

with

$$\theta_F'(0) = (1-\theta_w)\Big/\int_0^{\eta} EXP\left(-P_R\int_0^{\eta} f\,d\eta\right)\left[\rho/\rho(0)\right]^{-(1+Le)}\,d\eta\,, \qquad (4.52)$$

and where $\rho/\rho(o) = 1 + (c_{p_2}/c_{p_1} - 1)\alpha_e z_F$ for a catalytic wall. Since $(c_{p_2}/c_{p_1} - 1)\alpha_e z_F$ varies from zero at the wall to a value of .2 at the edge of the boundary layer (for $\alpha_e = .50$, $c_{p_2}/c_{p_1} = 1.4$), we can make the approximation

$$\left[\rho/\rho(0)\right]^{-(1+Le)} \simeq 1-(1+Le)\alpha_e(c_{p_2}/c_{p_1}-1)\beta_F$$

to simplify the calculations. In particular, Equation (4.52) simplifies tc

$$\theta_F'(0) \simeq \frac{.47\,P_R^{1/3}(1-\theta_w)}{1-.47\,P_R^{1/3}(1+Le)\alpha_e(c_{p_2}/c_{p_2}-1)\int_0^{\infty}\beta_F EXP\left(-P_R\int_0^{\eta} f\,d\eta\right)d\eta}\,, \qquad (4.53)$$

which clearly shows that the effect of $c_{p_2} > c_{p_1}$ is to increase the catalytic wall temperature gradient and raise the entire temperature profile above the non-catalytic wall solution. Direct evaluation of the integral in Equation (4.53) shows that

$$\int_0^{\infty}\beta_F EXP\left(-P_R\int_0^{\eta} f\,d\eta\right)d\eta \simeq .47\,S_c^{1/3}\times 1.49\,(.47\,P_R)^{-2/3}. \qquad (4.54)$$

For the example $S_c = .50$, $P_R = .70$, $\alpha_e = .50$ and $c_{p_2}/c_{p_1} = 1.4$, we have

$$\theta'(0)/\left[\theta'(0)\right]_{c_{p_2}=c_{p_1}} \simeq 1.305\,,$$

which is a 31% increase over the $c_{p_2} = c_{p_1}$ (or non-catalytic) value, a significant alteration in the temperature gradient.

The frozen heat transfer function (4.23), computed from the foregoing specie and temperature ($c_{p_2} = c_{p_1}$) solutions, is as follows:

$$Q_F = \theta_F'(0) + Le\,(g_2 + g_4)\,f_F''(0). \tag{4.55}$$

For the catalytic wall case, we therefore have

$$\left[Q_F\right]_{CAT.} = .47\,P_R^{1/3}\left[1 - \theta_W + (g_2+g_4)Le^{2/3} + \sqrt{P_R}\left(\frac{u_e^2}{2\bar{c}_{p_e}T_e}\right)\right] \tag{4.56}$$

which has, for example, been given by Lees[4]. In the case of $c_{p_2} \neq c_{p_1}$, on the other hand, the original heat flux expression (3.21) would give

$$\left[Q_F\right]_{\substack{CAT. \\ c_{p_2}\neq c_{p_1}}} = Q_{p_F}(0)\,\theta_F'(0) + Le\,(g_2+g_4)\,f_F''(0). \tag{4.57}$$

Using solutions (4.53) and (4.54), this becomes (for negligable dissipation)

$$\left[Q_F\right]_{\substack{CAT. \\ c_{p_2}\neq c_{p_1}}} \simeq .47\,P_R^{1/3}\left\{\frac{(1-\theta_W)\left[1+\alpha_e\left(c_{p_2}/c_{p_1}-\right)\right]^{-1}}{1-.47\times1.49\left(\frac{.47}{Le}\right)^{1/3}(1+Le)\alpha_e\left(c_{p_2}/c_{p_1}-1\right)} + (g_2+g_4)Le^{2/3}\right\}. \tag{4.58}$$

Hence the $c_{p_2} \neq c_{p_1}$ effect on heat transfer will be less pronounced than that on the temperature gradient $\theta_F'(0)$ alone, because of the factor $Q_{p_F}(0)$. For the previously cited example ($\alpha_e = .50$, $S_c = .5$, $P_R = .7$, $c_{p_2}/c_{p_1} = 1.4$), we have

$$\frac{Q_F\big]_{\substack{\text{CONDUCTION} \\ c_{p_2}\neq c_{p_1}}}}{Q_F\big]_{\substack{\text{CONDUCTION} \\ c_{p_2}= c_{p_1}}}} = \frac{Q_{p_F}(0)\left[\theta_F'(0)\right]_{c_{p_2}\neq c_{p_1}}}{\left[\theta_F'(0)\right]_{c_{p_2}= c_{p_1}}} \simeq 1.09.$$

The unequal specific heat effect in this example increases the temperature gradient by 31%, whereas the increase in heat transfer is 9% or only one third as much. The $c_{p_2} = c_{p_1}$ approximation for computing heat transfer may be acceptable for many practical purposes. On a non-catalytic wall ($z_F' = 0$), there is complete inhibition of surface atom recombination, and only the heat conduction mode remains:

$$\left[Q_F\right]_{NON\text{-}CAT.} = .47\, P_R^{1/3}\left[1 - \theta_W + \sqrt{P_R}\left(\frac{u_e^2}{2\mathcal{H}_{Fe}T_e}\right)\right], \tag{4.59}$$

which is exact whether c_{p_1} and c_{p_2} are equal or not. Using the foregoing functions Q_F, the local heat transfer variation for a particular frozen flow problem can be calculated by the use of the X-dependent term on the left side of Equation (4.23), as demonstrated in detail by Lees[4] for example.

The foregoing frozen boundary layer solutions can now be used to rewrite the reaction rate functions appearing in the first order deviation equations. The functions $(\mathcal{H}_{2,4})_F$ given by Equations (3.9) and (3.11), for example, can be written in the following forms:

$$\mathcal{H}_{2F} = \left(\frac{1+\alpha_e}{1+\alpha_e\beta_F}\right)\left\{\beta_F^2 - (1-C_1)\left(\frac{1-\alpha_e^2\beta_F^2}{1-\alpha_e^2}\right)EXP\left[-\frac{\theta_{A2}}{\theta_{Fc}}(1-\theta_{Fc})\cdot C_2\right]\right\} \tag{4.60}$$

$$\mathcal{H}_{4F} = \left(\frac{1+\alpha_e}{1+\alpha_e\beta_F}\right)\left\{\beta_F^2 - (1+C_3)\left(\frac{1-\alpha_e^2\beta_F^2}{1-\alpha_e^2}\right)EXP\left[-\frac{\theta_{A4}}{\theta_{Fc}}(1-\theta_{Fc})\cdot C_2\right]\right\} \tag{4.61}$$

where

$$C_1 = \frac{\alpha_{3e}(1-\alpha_e)(1-\beta_F)}{(1-\alpha_e-\alpha_{3e})(1-\alpha_e\beta_F)}\left[W_{EQ.}(0) - (1-\alpha_e)^{-1}\right] \tag{4.62}$$

$$C_2 = \left[1 - \left(\frac{u_e^2}{2\bar{h}_{Pe}T_e}\right)\left(\frac{\bar{\theta}_{Fp}}{1-\theta_{Fc}}\right)\right]\left[1 + \left(\frac{u_e^2}{2\bar{h}_{Pe}T_e}\right)\cdot\frac{\bar{\theta}_{Fp}}{\theta_{Fc}}\right] \tag{4.63}$$

$$C_3 = \frac{(1-\alpha_e)(1-\beta_F)}{1-\alpha_e\beta_F}\left[W_{EQ}(0) - (1-\alpha_e)^{-1}\right]. \tag{4.64}$$

Now for a highly cooled wall, the recombination rate (z_F^2 term) dominates these reaction rate terms completely over the inner half of the boundary layer ($\eta < 2$); the exponential dissociation term contributes significantly to the $\mathcal{Y}$ function only in the outer ($\eta > 2$) region. This situation allows some convenient simplifications to be made in Equations (4.60) and (4.61). First, the factor $(1 - \alpha_e^2 z_F^2)/(1 - \alpha_e^2)$ will be taken as unity; it is exactly so for a non-catalytic wall, whereas for the catalytic wall the major error resulting from this assumption occurs when the exponential term which the factor multiplies is extremely small (when the dissociation exponential becomes of significant size for $\eta > 2$, the subject factor approaches unity). Second, the specie factors C_1 and C_3 will be neglected. Again, this is exact for a non-catalytic wall. For the catalytic wall case, these factors become comparable to unity only in the inner part of the boundary layer where the exponential term they multiply becomes vanishingly small. The error incurred by the neglect of these factors in the pertubation analysis has been found to be extremely small. In passing, it is interesting to note that the use of the quasi-two component diffusion scheme for α_3 $\left(W_{EQ}(o) = (1-\alpha_e)^{-1}\right)$ causes C_1 and C_3 to be exactly zero everywhere. Third, the factor C_2, which is a correction to the dissociation rate for the viscous dissipation heating distortion of the frozen temperature

profile, will be assumed unity for a highly cooled wall. The main distortion (largest value of $C_2 > 1$) occurs in the inner part of the boundary layer; calculations have verified that the effect of $C_2 > 1$ on the dissociation exponential is extremely small in the perturbation analysis.

The recombination rate temperature dependence function $\theta_F^{\omega-2}$ will also be affected by the dissipation; using $\theta_F = \theta_{F_c} + \left(\frac{u_e^2}{2\bar{c}_{p_e} T_e}\right) \bar{\theta}_{F_P}$, we have

$$\theta_F^{\omega-2} = \theta_{F_c}^{\omega-2} \left[1 + \left(\frac{u_e^2}{2 \bar{c}_{p_e} T_e} \right) \frac{\bar{\theta}_{F_P}}{\theta_{F_c}} \right]^{\omega-2} . \tag{4.65}$$

The effect of dissipation on this recombination rate temperature dependence term is by far the most prominent way in which dissipation can influence the highly cooled wall non-equilibrium perturbations (the degree of the effect depending on the values of ω, $u_e^2/\bar{c}_{p_e} T_e$ and θ_W). The complete expression (4.65) will be retained in the subsequent theory in order to assess the significance of the dissipation in the non-equilibrium behavior where $\omega \neq 2$.

The foregoing approximations simplify the reaction rate functions used in the perturbation analysis to the following:

$$R_2 \equiv \theta_F^{\omega-2} \mathcal{Y}_{2F} \simeq \theta_F^{\omega-2} \left(\frac{1+\alpha_e}{1+\alpha_e \beta_F} \right) \left\{ \beta_F^2 - EXP\left[-\frac{\theta_{A_2}}{\theta_{F_c}} (1 - \theta_{F_c}) \right] \right\} \tag{4.66}$$

$$R_4 \equiv \theta_F^{\omega-2} \mathcal{Y}_{4F} \simeq \theta_F^{\omega-2} \left(\frac{1+\alpha_e}{1+\alpha_e \beta_F} \right) \left\{ \beta_F^2 - EXP\left[-\frac{\theta_{A_4}}{\theta_{F_c}} (1 - \theta_{F_c}) \right] \right\} \tag{4.67}$$

where θ_{F_c} is the $u_e^2/\bar{c}_{p_e} T_e = 0$ temperature profile. The function $\mathcal{Y}_2$ is plotted versus η for various values of the activation energy parameter θ_{A_2} in Figure 10 (catalytic wall) and Figure 11 (non-catalytic wall). The parameter θ_{A_2} is seen to noticeably influence these functions only in the outer part of a cooled boundary layer, this effect being more prominent in the catalytic wall case.

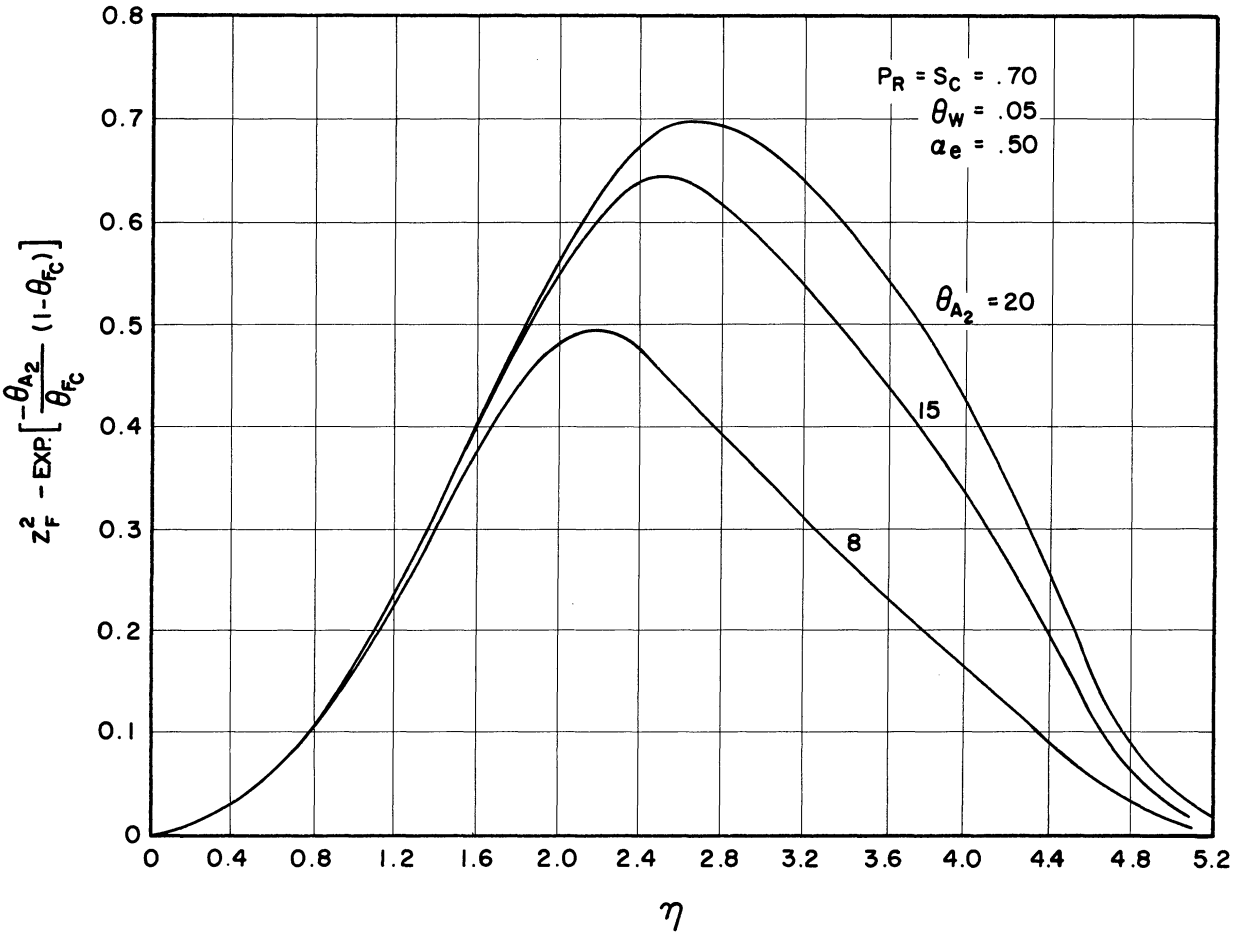

Figure 10. First Order Reaction Rate Distribution in a Catalytic Wall Boundary Layer.

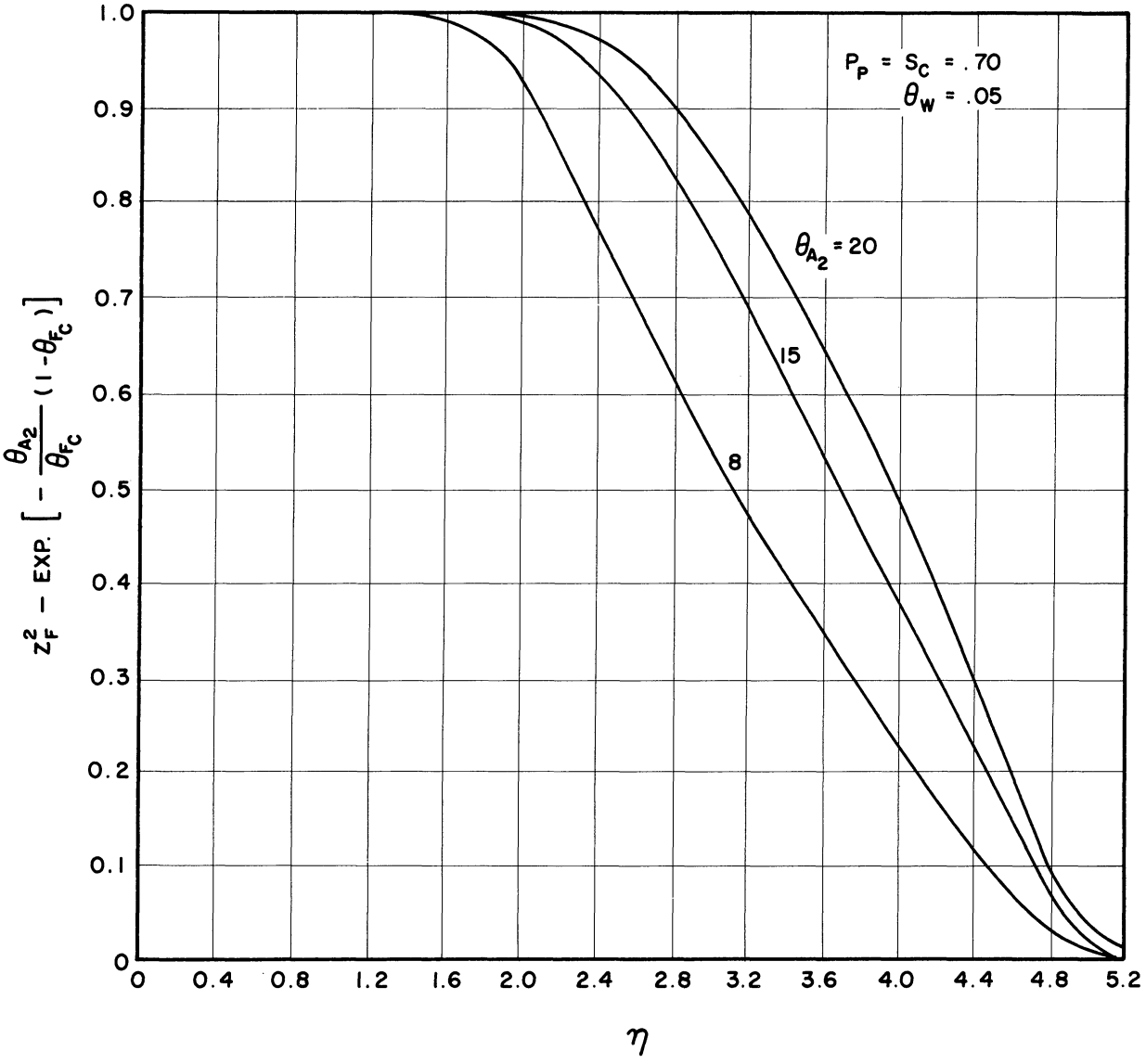

Figure 11. First Order Reaction Rate Distribution in a Non-Catalytic Wall Boundary Layer.

First Order Deviations

The governing linear non-homogeneous differential equations can be solved by standard methods once a homogeneous solution (complementary integral) is found. The form of the variable coefficients in these equations, however, generally prevents a closed form solution and requires that a numerical integration procedure be used.

(1) First Atomic Specie (Oxygen)

The complementary integral of Equation (4.31), a solution to the associated homogeneous differential equation

$$S_c f \beta_{I_c}' + \beta_{I_c}'' - \frac{2Q}{\epsilon} S_c f' \beta_{I_c} = 0 , \tag{4.68}$$

is of the form $z_{I_c} = A \cdot z_{c1}(\eta) + B \cdot z_{c2}(\eta)$, where A and B are arbitrary constants and z_{c1}, z_{c2} are two linearly independent functions, each of which is determined by a numerical integration of Equation (4.68) by Milnes Method (30) for arbitrary non-zero values of Q/ϵ.* This method requires four values of z_{c1} and z_{c2} near the wall with which to start the numerical procedure; these are provided by a series solution for z_{I_c} in the neighborhood of the wall ($\eta \ll 1$). Since in this region the Blasius velocity profile behaves as $f = \alpha'\eta^2/2 - \beta'\eta^5 + \cdots$ ($\alpha' = .47$, $\beta' = .0018$), direct substitution into Equation (4.68) produces the following series solution for z_{I_c} ($\eta \ll 1$):

$$\beta_{I_c} = A\underbrace{\left[1 + \frac{\alpha' S_c \, Q/\epsilon}{3}\eta^3 + \cdots\right]}_{\beta_{c1}} + B\underbrace{\eta\left[1 + \frac{\alpha' S_c}{6}\left(\frac{Q}{\epsilon} - \frac{1}{4}\right)\eta^3 + \cdots\right]}_{\beta_{c2}} . \tag{4.69}$$

* In the two particular cases $Q = 0$ and $Q/\epsilon = -1/2$, analytical solutions to equation 4.68 can be obtained; see Appendix E.

This solution provides the desired starting values of z_{c_1} and z_{c_2} for the numerical integration, the typical results of which are shown in Figures 12 (z_{c_1}) and 13 (z_{c_2}) for various values of Q/ϵ and $S_c = .70$.

With these complementary integrals known, a standard method yields the following complete solution to the full non-homogeneous differential Equation (4.31) (see, for example, Page 3, Chapter 1 of Reference 31):

$$\beta_I = \left\{ \frac{\beta_I(0)}{A} + [A\beta_I'(0) - B\beta_I(0)] I_{\beta_1} + \frac{2\alpha_{2e}}{\epsilon(1+\alpha_e)} I_{\beta_2} \right\} \cdot \beta_{I_c}(\eta) \tag{4.70}$$

where

$$I_{\beta_1} = \int_0^\eta \frac{EXP\left(-S_c \int_0^\eta f\, d\eta\right)}{\beta_{I_c}^2} d\eta \tag{4.71}$$

$$I_{\beta_2} = \int_0^\eta \frac{EXP\left(-S_c \int_0^\eta f\, d\eta\right)}{\beta_{I_c}^2} \left[\int_0^\eta \beta_{I_c} R_2\, EXP\left(S_c \int_0^\eta f\, d\eta\right) d\eta \right] d\eta , \tag{4.72}$$

with the reaction rate function R_2 given by Equation (4.66). Application of the boundary conditions $z_I(\infty) = 0$ and either $z_I(0) = 0$ or $z_I'(0) = 0$ requires that $B \equiv 0$ in either case in order that solution (4.70) be free of arbitrary constants. As a result, the catalytic and non-catalytic wall solutions are:

$$\left[\beta_I(\eta)\right]_{CAT} = -\frac{2\alpha_{2e}}{\epsilon(1+\alpha_e)} \beta_{c_1}(\eta) \left[\frac{\hat{I}_{\beta_1}(\eta)}{\hat{I}_{\beta_1}(\infty)} \cdot \hat{I}_{\beta_2}(\infty) - \hat{I}_{\beta_2}(\eta) \right]_{CAT.} \tag{4.73}$$

with

$$\left[\beta_I'(0)\right]_{CAT} = -\frac{2\alpha_{2e}}{\epsilon(1+\alpha_e)} \left[\frac{\hat{I}_{\beta_2}(\infty)}{\hat{I}_{\beta_1}(\infty)} \right]_{CAT} , \tag{4.74}$$

$$\left[\beta_I(\eta)\right]_{NON-CAT.} = -\frac{2\alpha_{2e}}{\epsilon(1+\alpha_e)} \beta_{c_1}(\eta) \left[\hat{I}_{\beta_2}(\infty) - \hat{I}_{\beta_2}(\eta) \right]_{NON-CAT.} \tag{4.75}$$

with

$$\left[\beta_I(0)\right]_{NON-CAT.} = -\frac{2\alpha_{2e}}{\epsilon(1+\alpha_e)} \left[\hat{I}_{\beta_2}(\infty) \right]_{NON-CAT.} , \tag{4.76}$$

where $\hat{I}_{z_1}$ and $\hat{I}_{z_2}$ are the integrals I_{z_1}, I_{z_2}, respectively, in which z_{I_c} is replaced by z_{c_1}. The imposed boundary conditions therefore require the use of only the z_{c_1} part of the complementary integral, z_{c_1} having the properties $z_{c_1}(o) = 1$, $z'_{c_1}(o) = 0$. The corresponding behavior of the integrals at the wall is seen to be $\hat{I}_{z_1}(o) = \hat{I}_{z_2}(o) = \hat{I}'_{z_2}(o) = 0$ and $\hat{I}'_{z_1}(o) = 1$. Using the z_{c_1} solutions (Figure 12), evaluation of the integrals $\hat{I}_{z_1}$ and $\hat{I}_{z_2}$ for desired combinations of the parameters Q/ϵ, ω and θ_{A_2} completes the solution. Since $\mathcal{Y}_{z_F}$ is positive throughout the boundary layer (recombination dominating dissociation), as shown in Figures 10 and 11, the integral $\hat{I}_{z_2}$ is positive (and $\hat{I}_{z_1}$ will also be positive) as long as z_{c_1} is positive (which it always is in the neighborhood of the wall). Therefore, z_I and z'_I are negative for small η and recombination-dominated non-equilibrium deviation tends to reduce both the atom concentration in the vicinity of a non-catalytic wall and the atomic diffusion flux at a completely catalytic wall, agreeing with previous qualitative predictions given in Chapter II (See Figure 1).

Equations (4.73) and (4.75), when multiplied by the parameter ζ, give the non-dimensional first order atomic oxygen perturbations. Typical deviation profiles throughout the boundary layer will be shown later for the total atomic specie. Regarding the maximum deviation quantities at the wall, the first order specie gradient perturbation at a catalytic surface is

$$\left[\zeta\, \beta_I'(0)\right]_{CAT.} = -\frac{2\alpha_{2e}\zeta}{\epsilon(1+\alpha_e)}\left[\frac{\hat{I}_{\beta_2}(\infty)}{\hat{I}_{\beta_1}(\infty)}\right]_{CAT.} . \tag{4.77}$$

On the other hand, the first order specie concentration perturbation at a non-catalytic wall surface is

$$\left[\zeta\, \beta_I(0)\right]_{NON\text{-}CAT.} = -\frac{2\alpha_{2e}\zeta}{\epsilon(1+\alpha_e)}\left[\hat{I}_{\beta_2}(\infty)\right]_{NON\text{-}CAT.} . \tag{4.78}$$

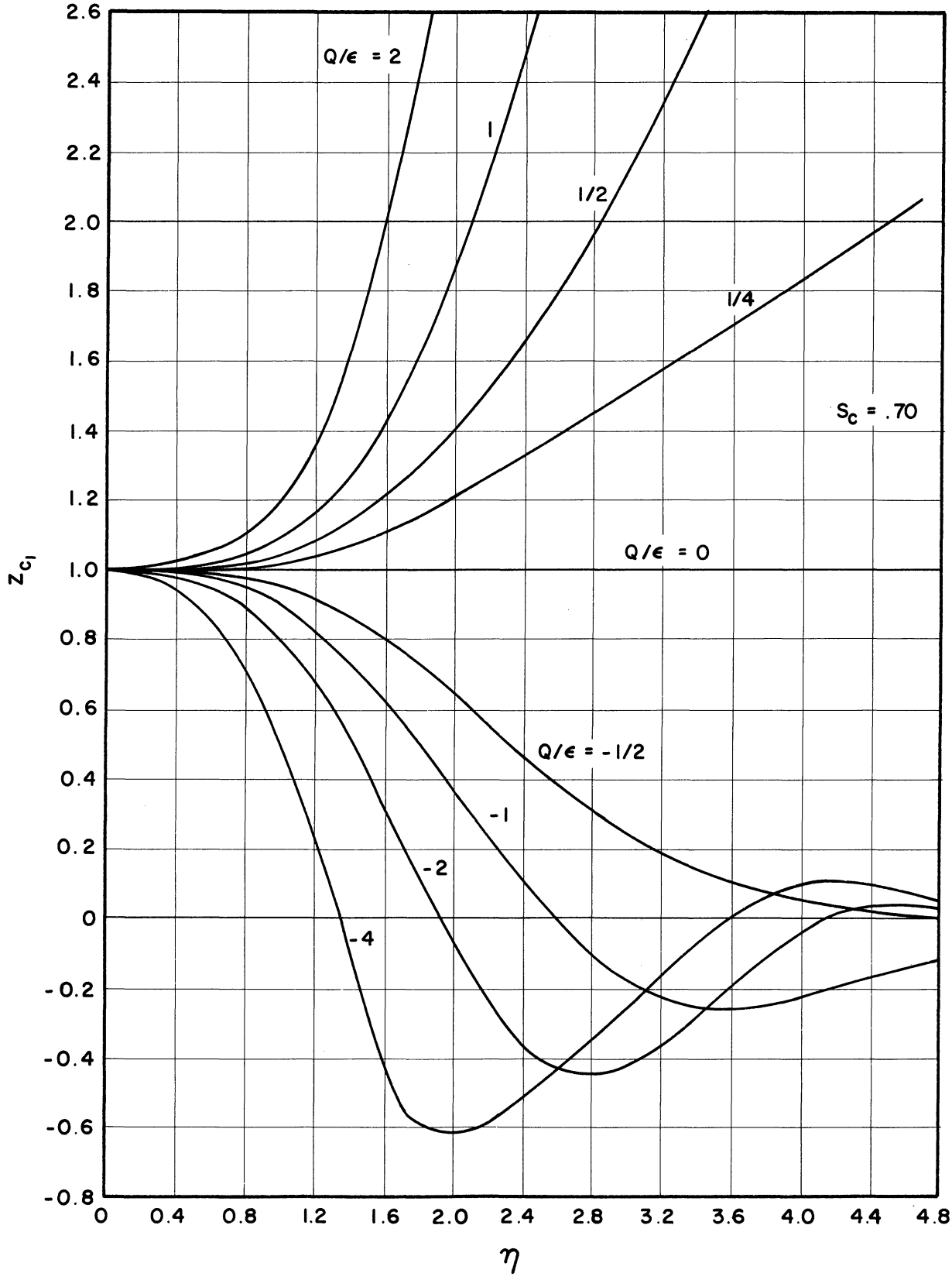

Figure 12. First Order Complementary Integral Function z_{c_1}.

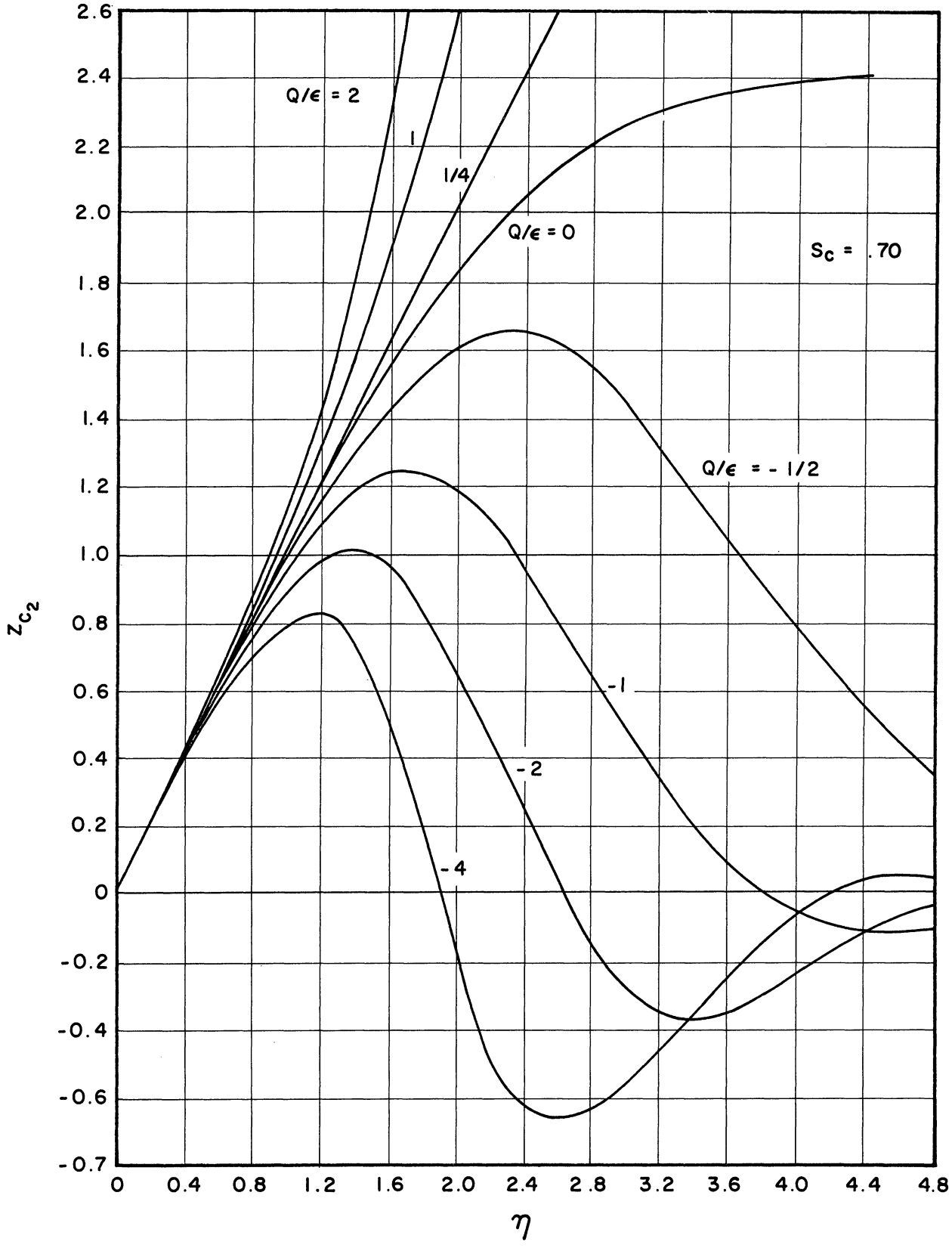

Figure 13. First Order Complementary Integral Function z_{c_2}.

The surface values of the perturbations involve only the total values of $\hat{I}_{z_1}$ and $\hat{I}_{z_2}$ across the entire boundary layer, $\hat{I}_{z_1}(\infty)$ and $\hat{I}_{z_2}(\infty)$. The calculated values of the deviations $z_I'(o)]_{CAT.}$ and $z_I(o)]_{NON-CAT.}$, referred to the value for a stagnation point flow with a Davidson recombination rate ($Q = 0$, $\omega = -3/2$), are shown in Figure 14 (catalytic wall) and Figure 15 (non-catalytic wall) for various values of Q/ϵ and the recombination parameter ω. It is seen from this data that the first order solutions are very sensitive to negative values of the non-equilibrium parameter derivative factor Q/ϵ, being several orders of magnitude larger than the stagnation point value when $Q/\epsilon \leq -2$, and about 50% of the stagnation value when $Q/\epsilon = +1$ with the same recombination rate law. The recombination parameter ω also has a noticeable effect on these results, more so for a non-catalytic wall than for a catalytic one; an increase in ω significantly reduces the non-equilibrium perturbation for a given Q/ϵ. This occurs because ω enters the reaction rate integral as $\theta_F^{\omega-2}$ and for a cooled wall ($\theta_W \ll 1$), $\theta_F^{\omega-2}$ will decrease if ω is increased, particularly at small values of θ_F in the neighborhood of the wall. A comparison of the two Figures, in view of the difference in the values of $\hat{I}_{z_2}$ (∞; $Q = 0$, $\omega = -3/2$), shows that the non-catalytic wall atom concentration perturbation is over 100 times greater than the catalytic wall atom concentration gradient deviation. This is due to the absence of any surface reaction "restraint" on the gas composition in the neighborhood of the wall in the latter case. For a given value of ζ, the non-catalytic wall boundary layer will experience a much larger deviation from chemically frozen flow due to gas phase chemical reaction.

The calculated effect of the freestream dissociation level (α_e) on the catalytic wall atomic specie gradient deviation is shown in Figure 16;

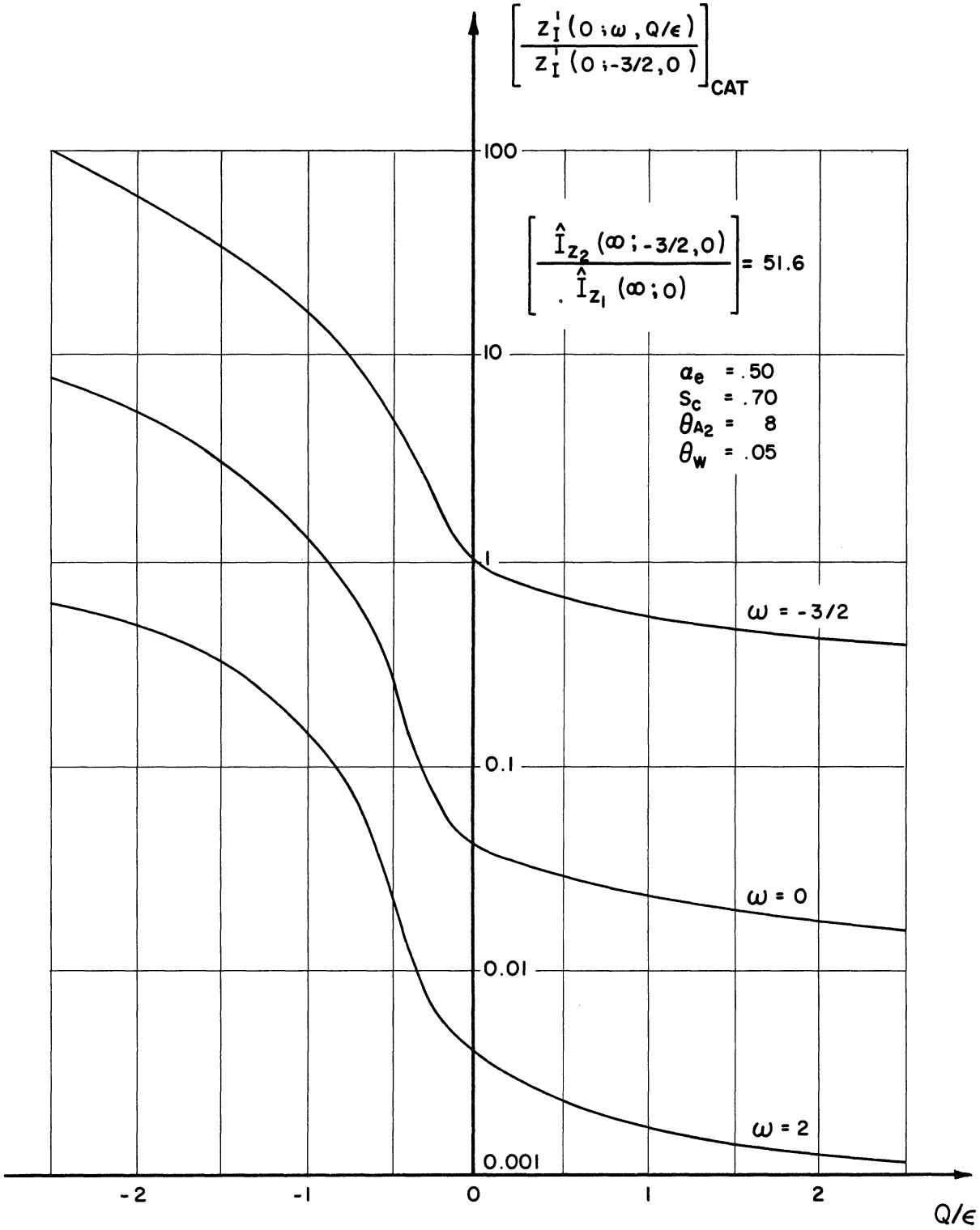

Figure 14. First Order Catalytic Wall Atomic Specie Gradient Deviation versus Q/ϵ and ω.

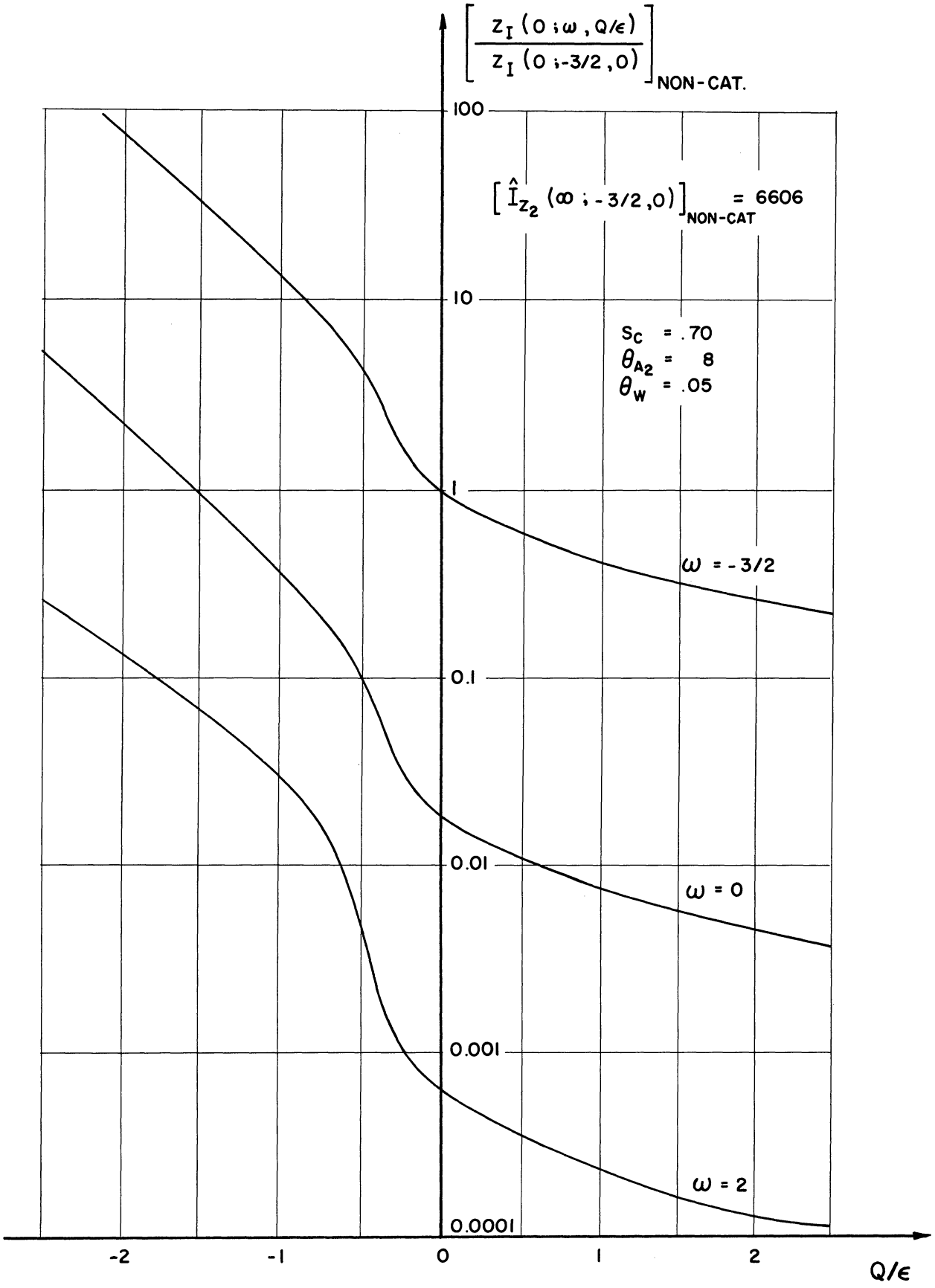

Figure 15. First Order Non-Catalytic Wall Atom Concentration Deviation versus Q/ϵ and ω.

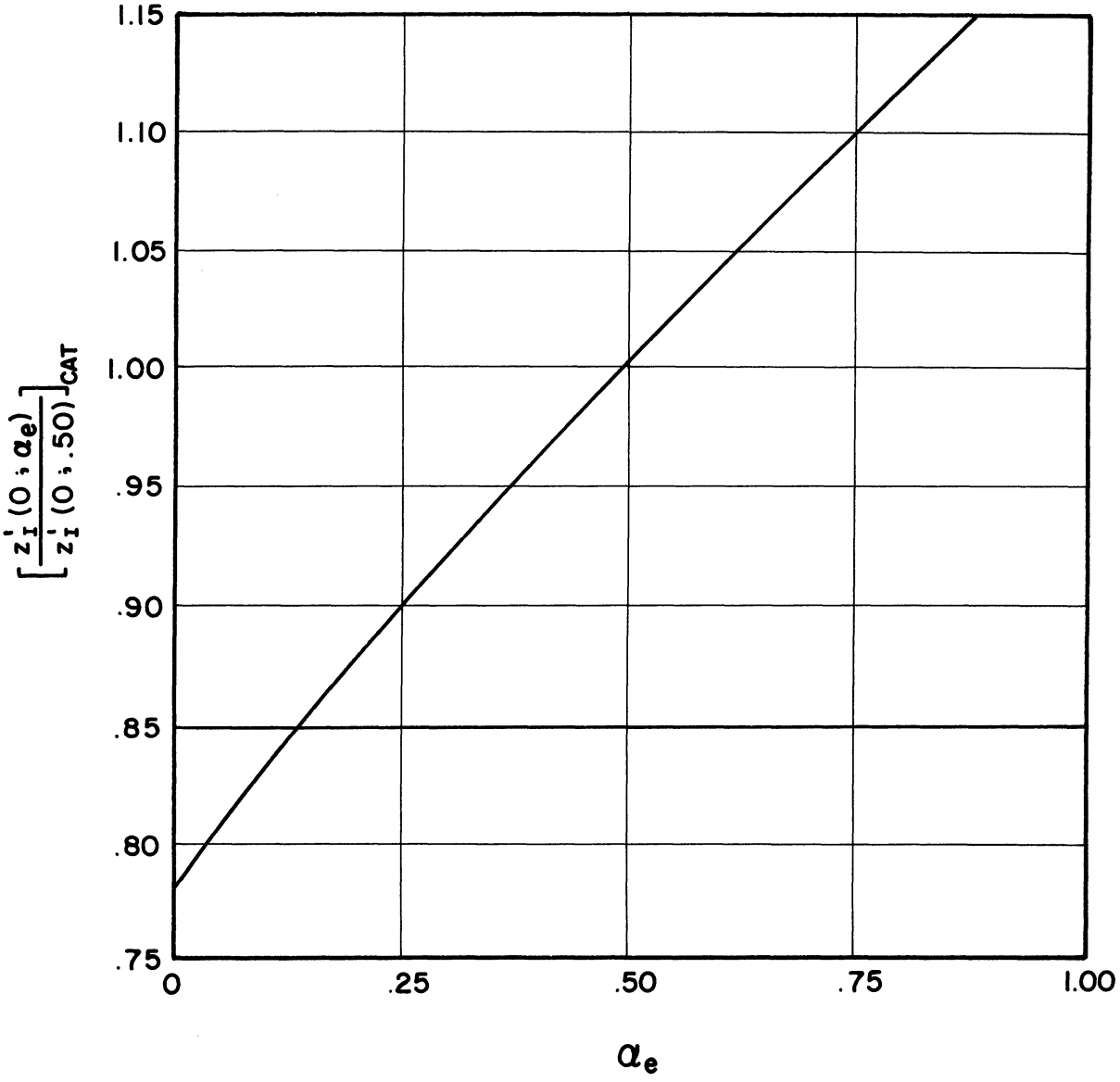

Figure 16. Freestream Dissociation Level Effect on the Catalytic Wall Deviations.

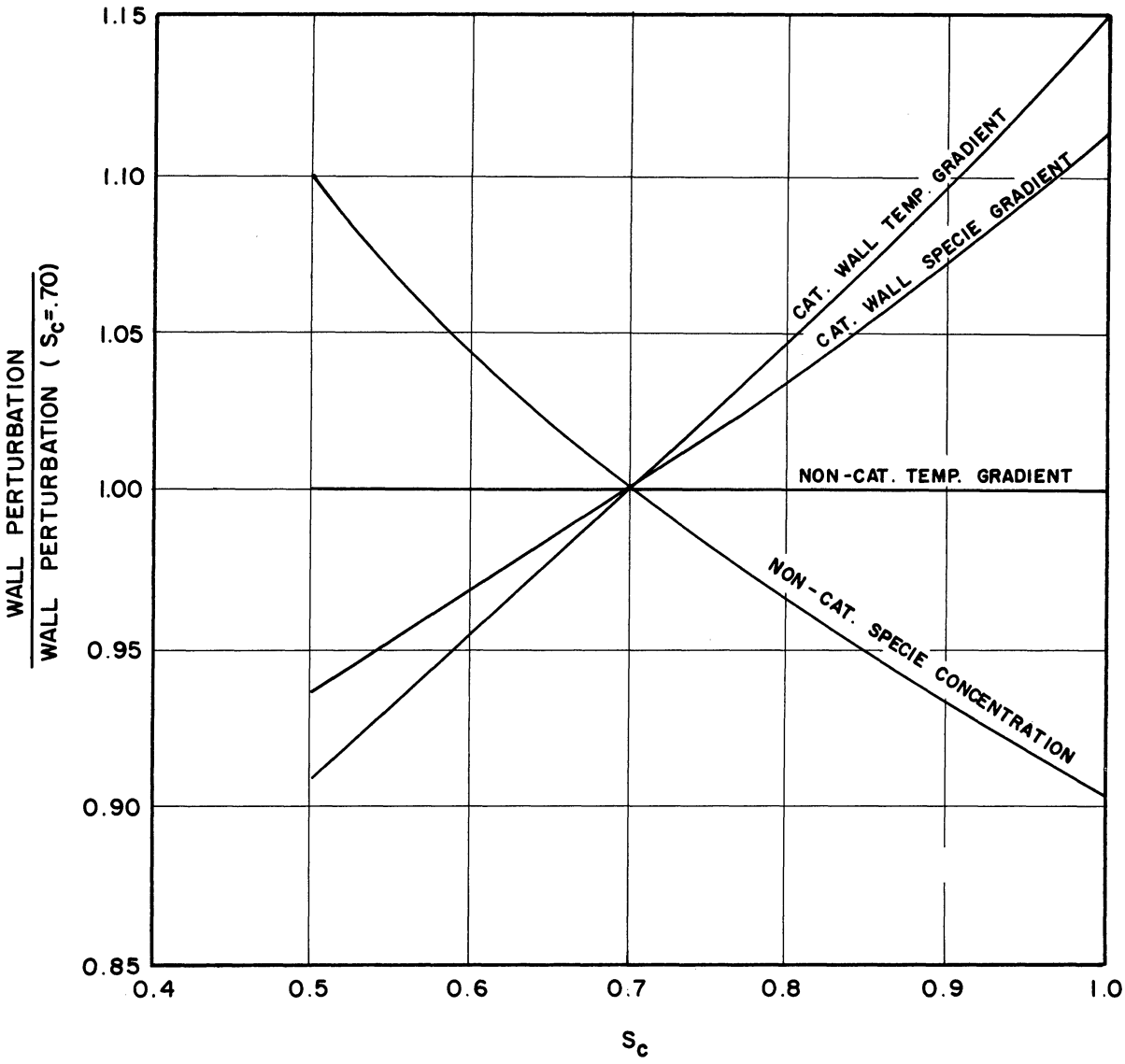

Figure 17. Schmidt Number Effect on the First Order Perturbations.

this curve applies equally well to the catalytic wall temperature gradient solution. The effect of Schmidt number on the first order deviations is shown in Figure 17. Although this effect is a minor one in the perturbation analysis, it is interesting to note that it's direction is reversed when the wall surface is changed from catalytic to non-catalytic because of the change in the recombination rate term z_F^2 in the reaction rate function.

The integral $\hat{I}_{z_2}(\infty)$ has also been evaluated for all the previously indicated combinations of Q/ϵ and ω as a function of θ_{A_2} over a range from 8 to 20 (a range that includes the θ_{A_4} values as well) for the highly cooled wall example $\theta_W = .05$; the effect on the perturbation solutions is shown in Figure 18. It is clear from this Figure that the integral is not very sensitive to θ_{A_2} for $\theta_{A_2} \geq 5$; doubling the value from 8 to 16, for example, increases $\hat{I}_{z_2}(\infty)$ by less than five percent. This slight increase is to be expected from the exponential manner in which θ_{A_2} enters the integrand for a cooled wall (See Equation (4.66)). The dissociation rate which contains this term exhibits a very rapid rise in the outer portion of the boundary layer primarily because of the influence of the cooled wall temperature function θ_F. This behavior is not changed very much, as far as it contributes to the overall reaction function R_2, when θ_{A_2} is changed by a factor of two or less. The sensitivity of $\hat{I}_{z_2}(\infty)$ to this activation energy parameter will be much greater when the wall is not highly cooled; the calculations have indicated that Figure 18 is applicable for $\theta_W \leq .20$. The assumption of a highly cooled wall is progressively worse for higher θ_W values and θ_{A_2} will exert an increasingly more prominent effect on the perturbation solutions.

The recombination rate temperature dependence term $\theta_F^{\omega-2}$ in the integrand of $\hat{I}_{z_2}$ causes the latter to be very sensitive to the value of θ_W

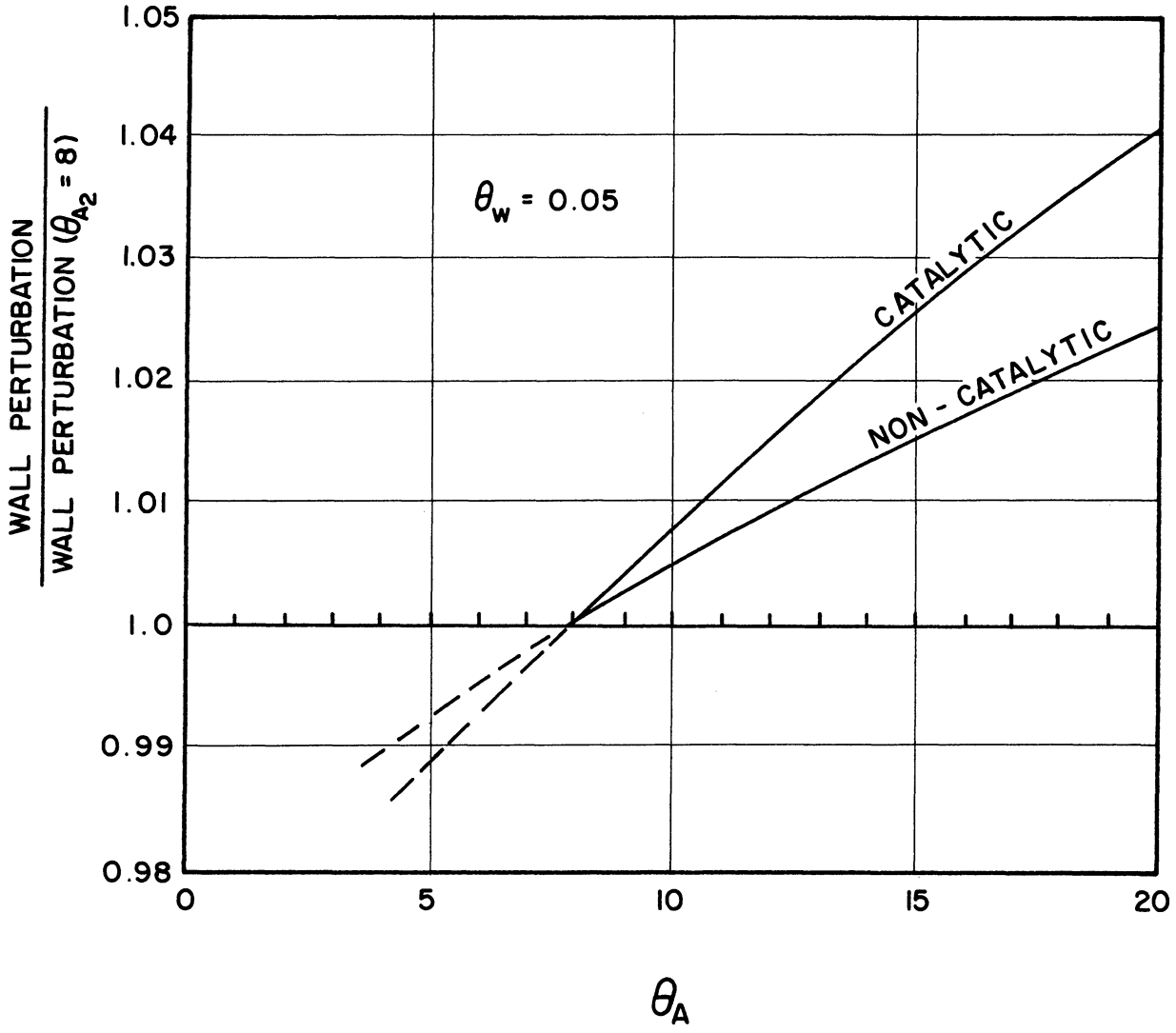

Figure 18. The Effect of Activation Energy Parameter on the First Order Perturbations.

when it is small compared to one and when ω departs significantly from a value of two. The calculated effect of the Θ_W variable for a highly cooled wall was found to be representable by the following formula:

$$\frac{\text{Wall Perturbation } (\omega, \Theta_{W_1})}{\text{Wall Perturbation } (\omega, \Theta_{W_2})} \simeq \frac{\Theta_{W_1}}{\Theta_{W_2}}^{\omega-2} \tag{4.79}$$

for both catalytic and non-catalytic surfaces. For a highly cooled wall with $\omega < 2$, this equation predicts a significant correction due to small changes in Θ_W. For example, a 20% correction from $\Theta_{W_2} = .05$ to $\Theta_{W_1} = .04$ would increase the first order atomic specie and temperature deviations by a factor of 2.20 or 120%.

The viscous dissipation also enters the recombination temperature dependence term (Equation 4.65) and has been evaluated as a function of the parameter $u_e^2/\tilde{c}_{p_e}T_e$. The results, which clearly depend on the recombination rate exponent ω and to a far lesser extent on the wall temperature ratio Θ_W, are shown in Figure 19. The effect of increasing $u_e^2/\tilde{c}_{p_e}T_e$ is to reduce the size of the first order perturbations when $\omega < 2$, this reduction being slightly greater for smaller values of Θ_W. When $u_e^2/\tilde{c}_{p_e}T_e > 1$, the dissipation effect on the recombination term becomes significant to the accurate calculation of local non-equilibrium specie and temperature deviations in the highly cooled boundary layer. The catalytic wall deviations are approximately one third as sensitive to the dissipation correction shown in Figure 19 for the non-catalytic wall case, due to the smaller recombination rate specie term in the neighborhood of a catalytic wall (compare Figures 10 and 11).

(2) Second Atomic Specie (Nitrogen)

Equation (4.32) is similar to the first atomic specie Equation (4.31); since the boundary conditions on χ_I are exactly the same as for z_I,

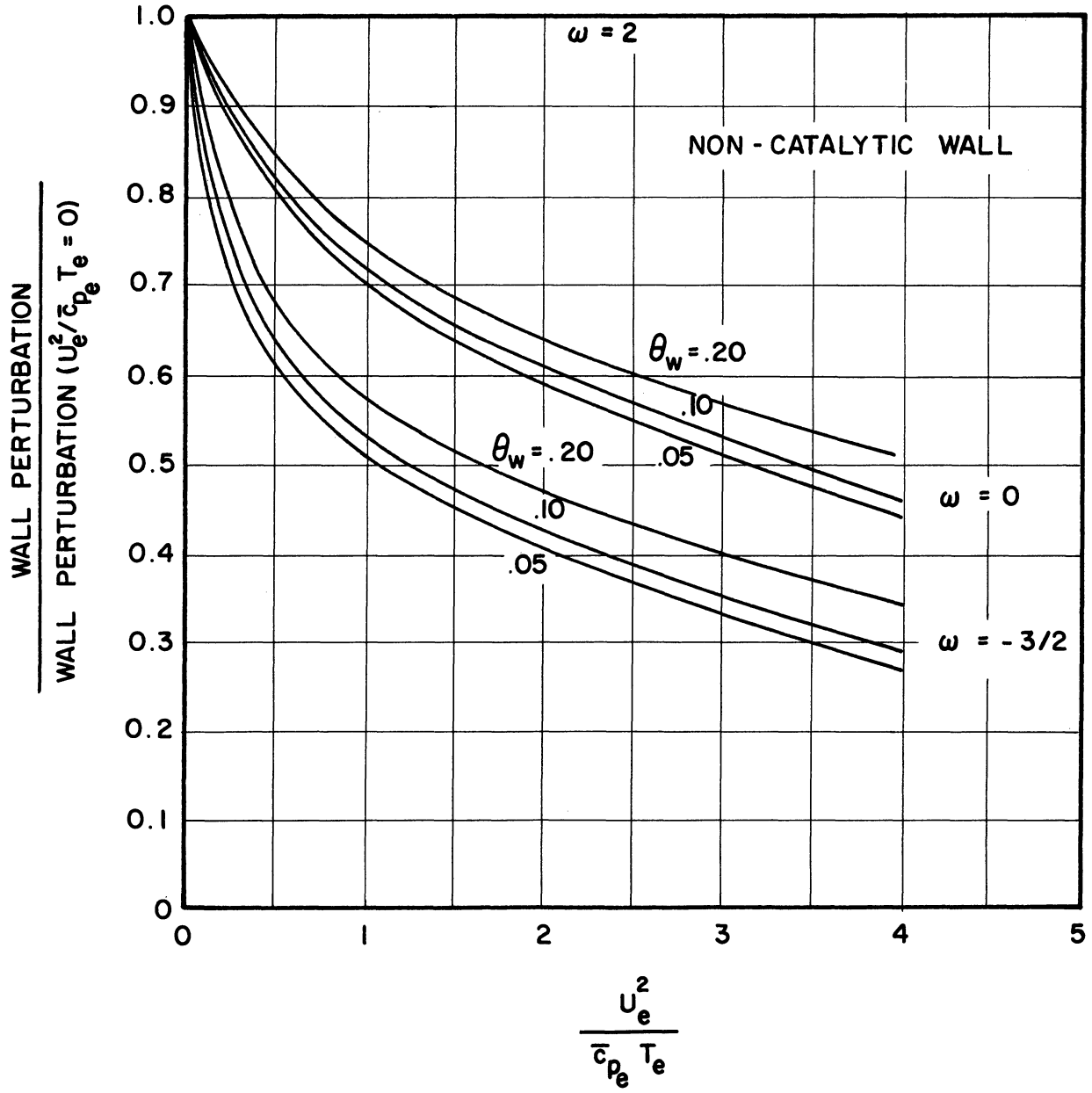

Figure 19. The Effect of Viscous Dissipation on the First Order Perturbations.

the two solutions will be analogous. The complementary integrals are exactly equal ($\chi_{I_c} = z_{I_c}$), and the non-homogeneous reaction rate term for χ_I is $\mathcal{Y}_{4F}$ instead of $\mathcal{Y}_{2F}$. Consequently, the χ_I solution is given by Equations (4.73-4.76) by merely replacing α_{2_e} by α_{4_e} and $\hat{I}_{z_2}$ by $\hat{I}_{z_4}$, where $\hat{I}_{z_4}$ is the integral given by Equation (4.72) with θ_{A_2} replaced by θ_{A_4}, i.e., $\hat{I}_{z_4} = \hat{I}_{z_2}(\theta_{A_4})$. The value of θ_{A_4} ranges from 16 to 18 (roughly twice θ_{A_2}). The insensitivity of the $\hat{I}_{z_2}$ integral to large changes in this activation energy parameter for highly cooled walls indicates that the approximation $\hat{I}_{z_4} \simeq \hat{I}_{z_2}$, based on a common average value of θ_A, would be acceptable. This gives a very simple solution for χ_I, namely a direct proportionality between the two atomic specie deviations:

$$\chi_I \simeq \frac{\alpha_{4e}}{\alpha_{2e}} \cdot \beta_I \quad . \tag{4.80}$$

(3) Total Atomic Specie

The total atomic specie deviation is

$$\left(\frac{\alpha}{\alpha_e}\right)_I = \zeta\left(\frac{\alpha_{2e}}{\alpha_e}\beta_I + \frac{\alpha_{4e}}{\alpha_e}\chi_I\right) \simeq \frac{\alpha_{2e}}{\alpha_{4e}}\left(1 + \frac{\alpha_{4e}^2}{\alpha_{2e}^2}\right)\zeta\,\beta_I \,, \tag{4.81}$$

with z_I given by Equations (4.73-4.76). Some representative profiles, $(\alpha/\alpha_e)_I$ versus η, are shown in Figures 20 (catalytic wall) and 21 (non-catalytic wall) for a value of $\zeta = 10^{-4}$. These curves illustrate the typical distribution of the non-equilibrium atomic specie deviation throughout the boundary layer and clearly exhibit the previously discussed sensitivity to the parameters ω and Q/ϵ. Also shown in Figure 21 is the corresponding profile obtained in Reference 6, which is seen to be in qualitative agreement with the present theory. The difference between the two results, as will be

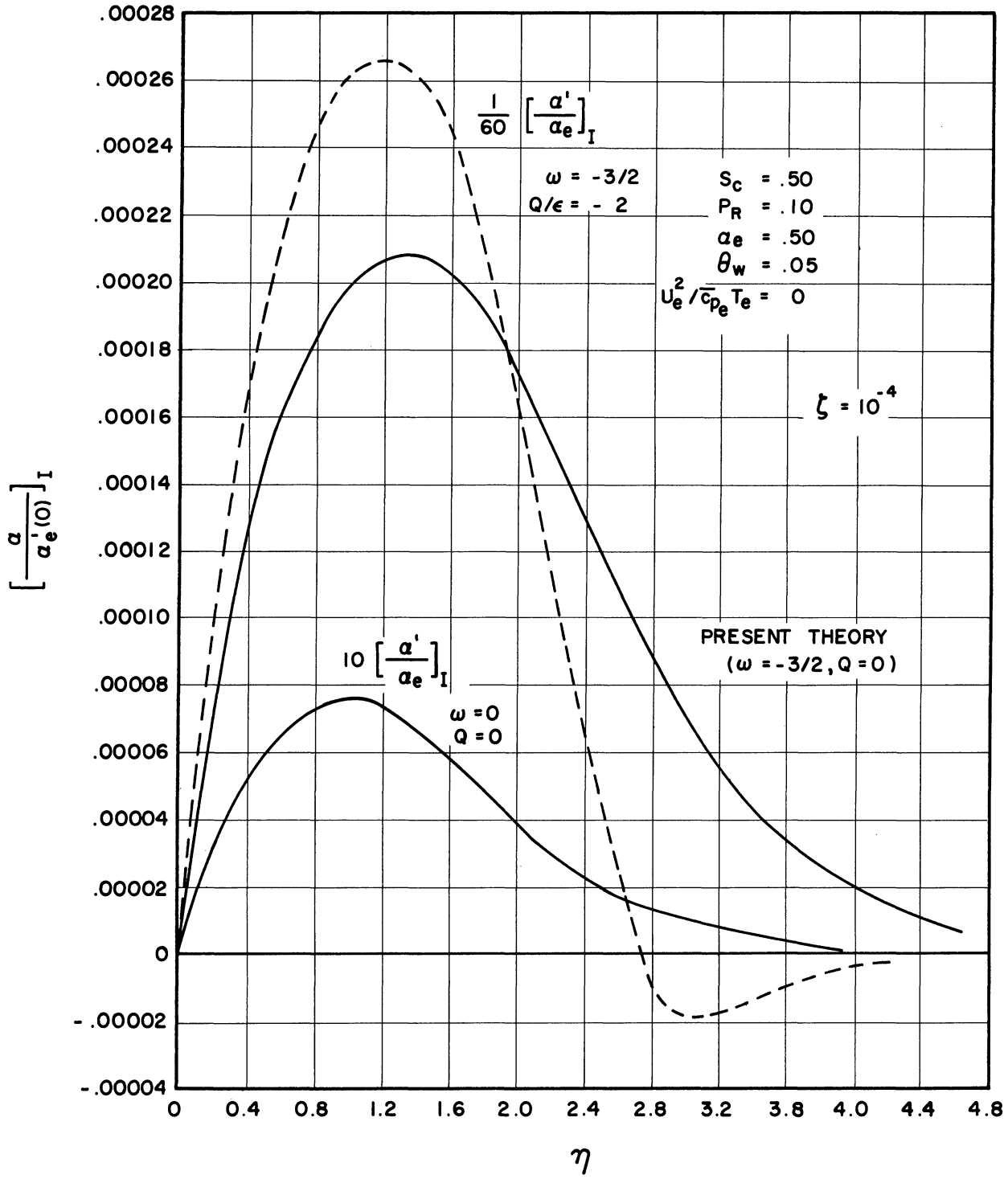

Figure 20. First Order Atomic Specie Deviation Distribution in a Catalytic Wall Boundary Layer.

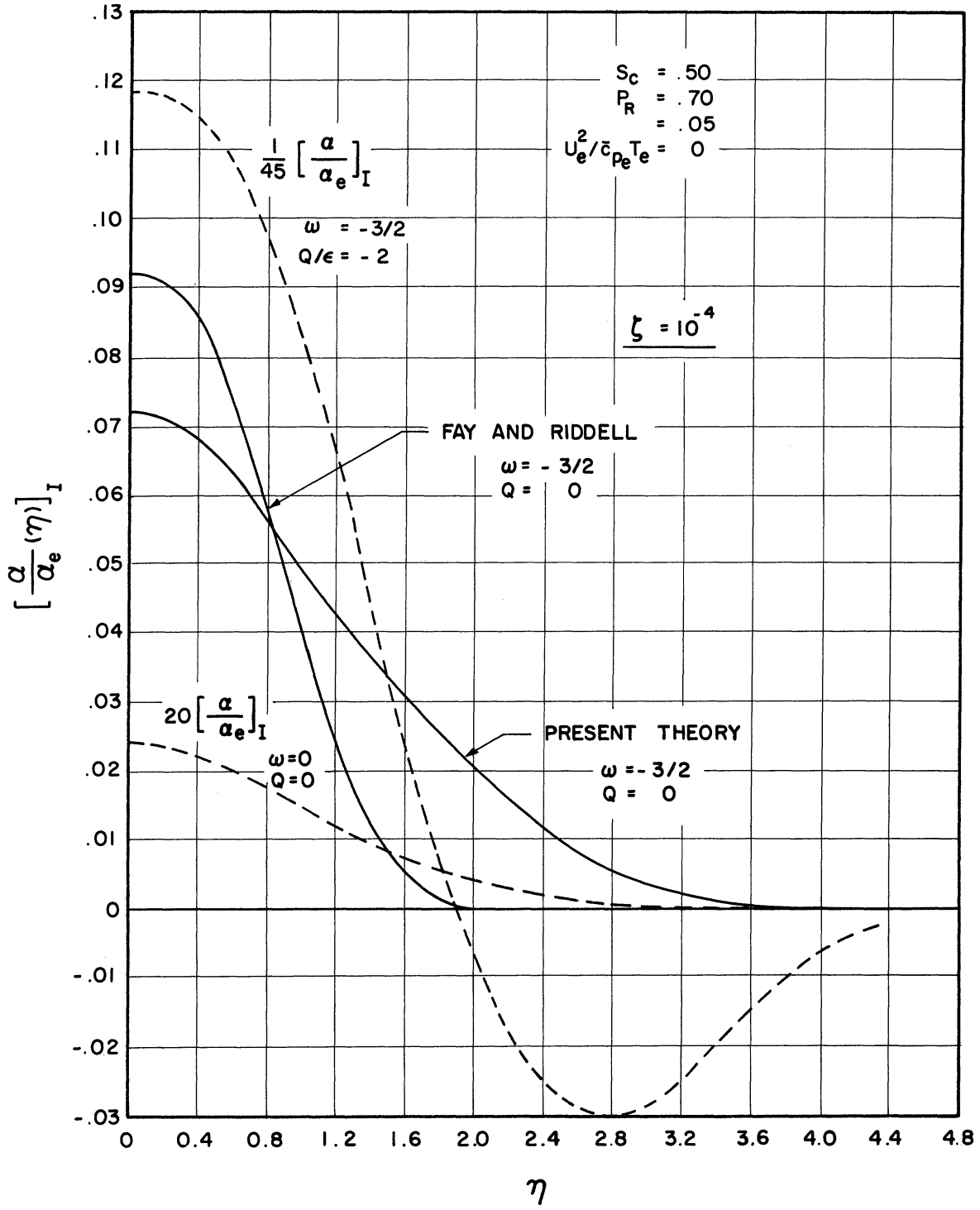

Figure 21. First Order Atomic Specie Deviation Distribution in a Non-Catalytic Wall Boundary Layer.

subsequently discussed, is primarily due to the use of a larger value for the total atomic specie reaction rate in Reference 6. A comparison of Figures 21 and 22 shows that the catalytic wall specie profiles for $\zeta = 10^{-4}$ would barely be discernable on the scale of Figure 22; the non-catalytic wall perturbations are much larger for the same value of ζ.

The first order total atomic specie gradient and concentration deviations at a catalytic or non-catalytic wall, respectively, are

$$\left[\left(\frac{\alpha'}{\alpha_e}(0)\right)_I\right]_{CAT.} = -\frac{2\alpha_{2e}^2\zeta}{\epsilon(1+\alpha_e)\alpha_e}\left(1+\frac{\alpha_{4e}^2}{\alpha_{2e}^2}\right)\left[\frac{\hat{I}_{\beta_2}(\infty)}{\hat{I}_{\beta_1}(\infty)}\right]_{CAT.} \tag{4.82}$$

and

$$\left[\left(\frac{\alpha}{\alpha_e}(0)\right)_I\right]_{NON-CAT.} = -\frac{2\alpha_{2e}^2\zeta}{\epsilon(1+\alpha_e)\alpha_e}\left(1+\frac{\alpha_{4e}^2}{\alpha_{2e}^2}\right)\left[\hat{I}_{\beta_2}(\infty)\right]_{NON-CAT.} \tag{4.83}$$

These are plotted versus ζ in Figure 22 for several example combinations of the parameters ω and Q/ϵ (for the first order deviations, the curves are necessarily straight lines, the curvature being introduced by the second and higher order perturbation terms). The slopes of the lines are drastically increased when either ω or Q/ϵ is increased negatively. Also shown for comparison is the $Q = 0$, $\omega = -3/2$ solution of Fay and Riddell, corrected from $\theta_W = .04$ (which they used) to $\theta_W = .05$ by means of Equation (4.79). Their result varies linearly with ζ for very small ζ and therefore independently confirms the assumed non-equilibrium perturbation expansion in the present analysis. Furthermore, the Fay and Riddell curve develops a negative curvature when $\zeta > 2 \times 10^{-5}$; with further increase in ζ, the wall deviations are progressively less than predicted by the linear first order theory. This indicates that the second order perturbations are opposite in sign to those given by the first order theory and constitute increasingly larger subtractive

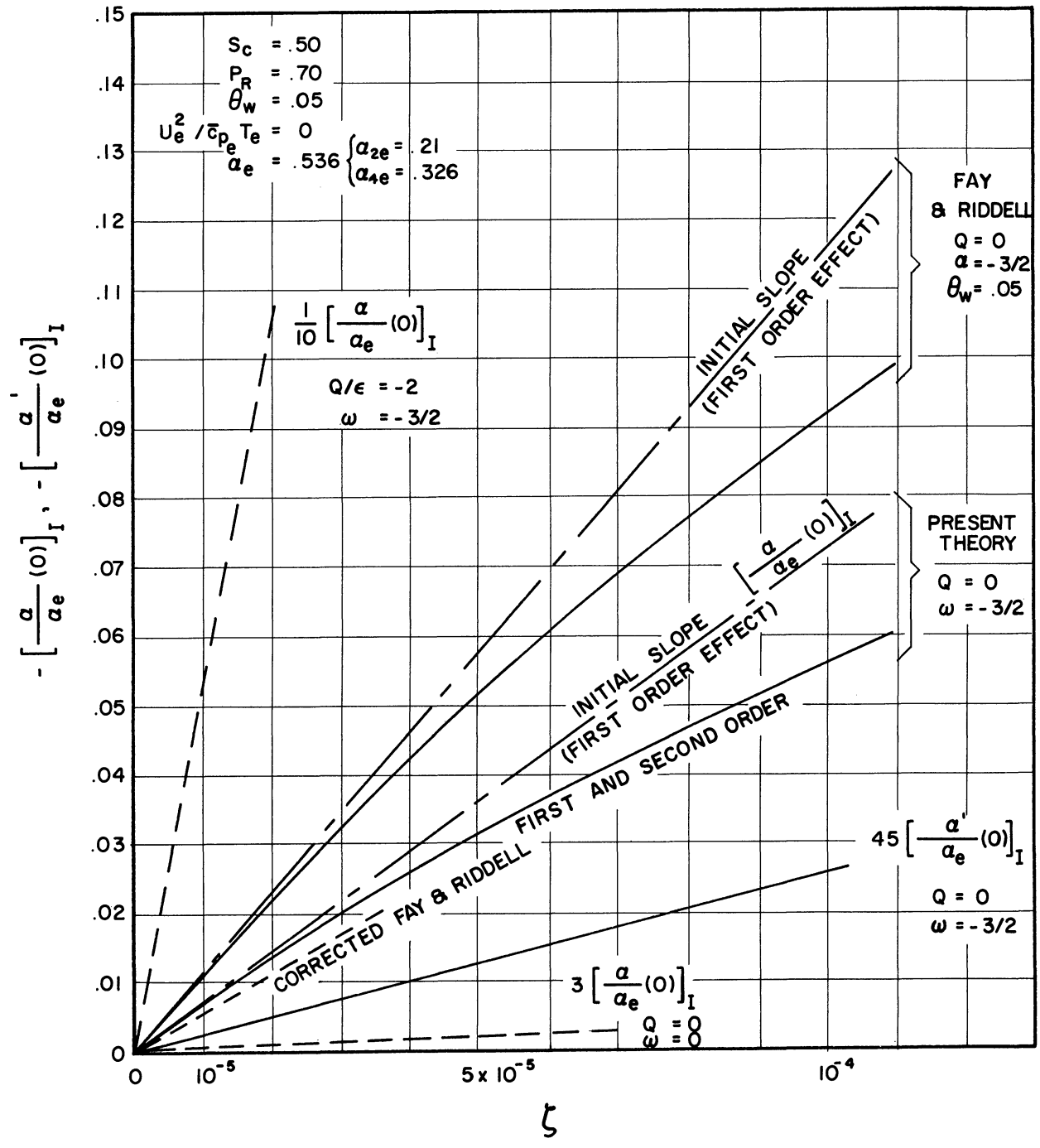

Figure 22. Total Atomic Specie Deviations Versus the Non-Equilibrium Parameter ζ.

corrections as ζ increases.

On the scale of Figure 22, the catalytic wall total atomic specie gradient deviations are extremely small when $\zeta \leq 10^{-4}$, again illustrating the negligible size of catalytic wall perturbations in comparison to those on a non-catalytic wall at the same values of ζ, Q/ϵ and ω. Of course, the non-catalytic wall deviation for $Q/\epsilon \geq 0$ and $\omega \geq -3/2$ is itself a small absolute number; for the stagnation point example ($Q = 0$, $\omega = -3/2$), the effect of non-equilibrium at $\zeta = 5 \times 10^{-5}$ decreases the chemically frozen wall atom concentration by 4% according to the present theory. When Q/ϵ is negative, however, this local perturbation would be much larger (for the same value of ζ) because of the greater initial slope of the deviation curve shown in Figure 22. The small size of these deviations is an expected consequence (and limitation) of a perturbation type of solution; nevertheless, analysis of these small increments reveals the important basic mechanisms (and the significant physical parameters therein) which govern the non-equilibrium behavior in the chemically frozen regime.

A comparison of the value of $[\alpha/\alpha_e(o)]_I$ with that found by Fay and Riddell in the stagnation point example (Figure 22) shows the latter to be 72.7% greater at $\zeta = 10^{-5}$. Analysis has shown that this discrepancy is almost entirely due to the difference between the reaction rates used in the two respective theories. The total atomic specie reaction rate used by Fay and Riddell, as previously pointed out in Chapter II, was a binary form based on the total atomic specie concentration variable α (the first term in Equation (2.58)), thereby neglecting a subtractive correction due to the individual atomic specie behavior which is important in the presence of a significant amount of atomic nitrogen at the edge of the boundary layer. In

the present comparative example, where $\alpha_{4e} = .326$ and $\alpha_{2e} = .210$, calculations indicate that the neglect of this second reaction rate term by Fay and Riddell leads to too large a total atomic specie reaction rate (and non-catalytic wall concentration perturbation) by approximately the factor $2\alpha_{2e}\alpha_{4e}/\alpha_e^2 = .47$. When the Fay and Riddell value at $\zeta = 10^{-5}$ is reduced by 47%, a much better agreement with the present theory occurs. The corrected Fay and Riddell curve in this case drops slightly below the present theory. However, some difference between the two theories would be expected because the former theory includes a variable $\rho\mu$ expression in the digital computations (whereas $\rho\mu$ has been assumed constant in the present theory). However, provided we take $\rho_R\mu_R = \rho_W\mu_W$ (as Fay and Riddell did), the effect of variable $\rho\mu$ on the perturbations is small in comparison with the effect of the reaction rate difference between the present theory and Fay and Riddell's work. This particular example clearly brings out the importance of accounting for individual atomic specie behavior in formulating the reaction rates for a non-equilibrium theory of a multicomponent gas mixture. In the foregoing example, for instance, the application of a more accurate reaction rate expression predicts roughly one-half the initial rate of non-equilibrium deviation from frozen flow found in Reference 6 for the same flow conditions. Consequently, it appears that the chemically frozen regime at the stagnation point persists to larger values of ζ than shown in Reference 6.

(4) Second Molecular Specie

A direct comparison of Equations (4.33) and (4.32), since W_I and χ_I share the same boundary conditions, gives the following solution:

$$W_I = -\frac{\alpha_{4e}}{\alpha_{3e}}\chi_I \simeq -\frac{\alpha_{4e}^2}{\alpha_{2e}\alpha_{3e}}\beta_I \,. \qquad (4.84)$$

This agrees with the previous statement (Chapter II) that α_3 and α_4 must be linearly related regardless of the gas phase reaction rates. The negative sign in Equation (4.84) means that non-equilibrium perturbation from frozen flow increases the molecular nitrogen whenever the atomic nitrogen is decreased in the boundary layer.

(5) Energy Equation

Equation (4.34) is quite similar to the species equations. The associated homogeneous equation for Θ_I is the same as that for z_I if S_c is replaced by P_R; hence the complementary integral Θ_{I_c} of Equation (4.34) can be written

$$\Theta_{I_c} = \beta_{I_c}(P_R).$$

Furthermore, the inner boundary condition on Θ_I, $\Theta_I(o) = 0$, is analogous to the catalytic wall specie solution, so that the full solution to Equation (4.34) is similar in form to Equations (4.73) and (4.74):

$$\Theta_I = \frac{2\alpha_{2e} L_e}{\epsilon(1+\alpha_e)} \beta_{c_1}(P_R) \left\{ g_2 \left[\frac{\hat{I}_{\theta_1}(n)}{\hat{I}_{\theta_1}(\infty)} \hat{I}_{\theta_2}(\infty) - \hat{I}_{\theta_2}(n) \right] + \frac{\alpha_{4e}}{\alpha_{2e}} g_4 \left[\frac{\hat{I}_{\theta_1}(n)}{\hat{I}_{\theta_1}(\infty)} \hat{I}_{\theta_4}(\infty) - \hat{I}_{\theta_4}(n) \right] \right\} \tag{4.85}$$

with

$$\Theta_I'(0) = \frac{2\alpha_{2e} L_e}{\epsilon(1+\alpha_e)} \left[\frac{g_2 \hat{I}_{\theta_2}(\infty) + \frac{\alpha_{4e}}{\alpha_{2e}} g_4 \hat{I}_{\theta_4}(\infty)}{\hat{I}_{\theta_1}(\infty)} \right] \tag{4.86}$$

and where $\hat{I}_{\theta_1} = \hat{I}_{z_1}(P_R)$ and

$$\hat{I}_{\theta_{2,4}} = \int_0^\eta \frac{EXP(-P_R\int_0^\eta f\,d\eta)}{\beta_{c_1}^2(\eta;P_R)}\left[\int_0^\eta \beta_{c_1}(\eta;P_R)\,R_{2,4}\,EXP(P_R\int_0^\eta f\,d\eta)\,d\eta\right]d\eta \quad . \tag{4.87}$$

The integrals $\hat{I}_{\theta_{2,4}}$ and $\hat{I}_{z_{2,4}}$ (also $\hat{I}_{\theta_1}$ and $\hat{I}_{z_1}$) are actually equal when $S_c = P_R(L_e = 1)$. Recombination - dominated non-equilibrium perturbation, since the $\hat{I}_\theta$ integrals are positive, increases the wall temperature gradient near frozen flow. The typical temperature perturbation profiles (θ_I versus η) have the same general shape as the catalytic wall atomic specie profiles shown in Figure 20.

The first order temperature gradient deviations at the wall are given by the product of ζ and Equation (4.86) and involve only the total values of the temperature integrals across the entire boundary layer, $\hat{I}_{\theta_{2,4}}(\infty)$. These integrals exhibit the same insensitivity to the activation energy parameter for highly cooled walls as found for the corresponding specie integrals (Figure 18), so that the assumption $\hat{I}_{\theta_2} = \hat{I}_{\theta_4}$ is a good approximation; hence

$$\zeta\,\theta_I'(0) \simeq \frac{2\alpha_{2e}Le\,\zeta}{\epsilon(1+\alpha_e)}\left(g_2 + \frac{\alpha_{4e}}{\alpha_{2e}}g_2\right)\frac{\hat{I}_{\theta_2}(\infty)}{\hat{I}_{\theta_1}(\infty)} \quad . \tag{4.88}$$

The calculated values of $[\theta_I'(o)]_{NON\text{-}CAT.}$, referred to the value for $Q = 0$ and $\omega = -3/2$, are shown in Figure 23 (the values of $[\theta_I'(o)]_{CAT.}$ are nearly the same as the values of $[z_I'(o)]_{CAT}$ shown in Figure 14 except for a small Schmidt number correction given in Figure 17). The results in Figure 23 show, like the previous atomic specie solutions, the following features:

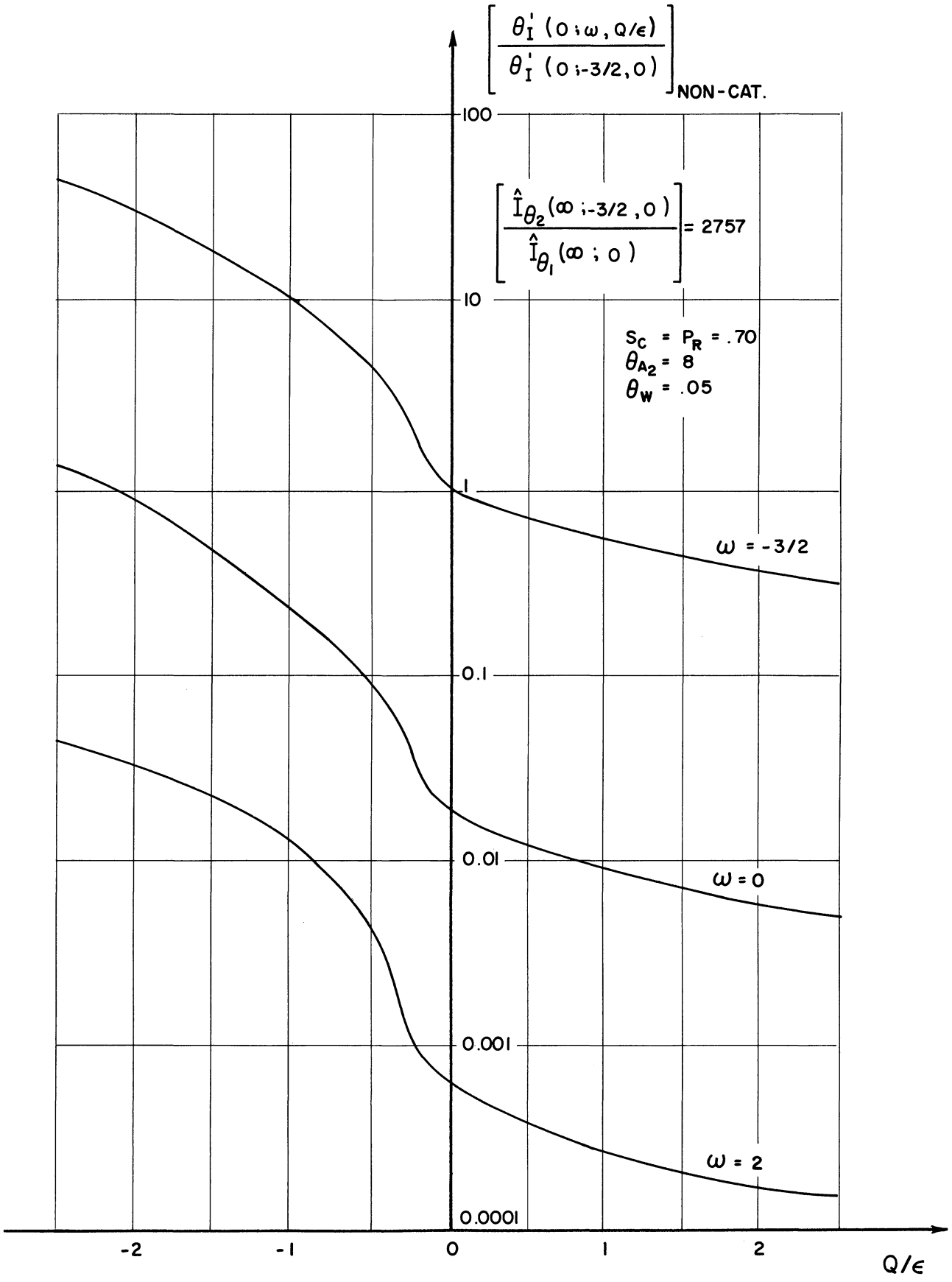

Figure 23. First Order Non-Catalytic Wall Temperature Gradient Deviation versus Q/ϵ and ω.

(a) A profound sensitivity to the parameters Q/ϵ and ω of nearly the same extent as the atomic specie solutions. The non-catalytic temperature gradient perturbation is slightly less sensitive to Q/ϵ in comparison to $[z\ (o)]_{NON-CAT.}$ for $Q/\epsilon < -1$. (b) The non-catalytic wall temperature gradient perturbation is over 50 times greater than that on a catalytic wall for the same ζ and flow conditions. While this is one-half of the difference between non-catalytic and catalytic wall effects exhibited by the atomic specie deviations, one still can conclude that the catalytic wall non-equilibrium effects are vanishingly small when $\zeta < 10^{-4}$ in comparison to the corresponding non-catalytic behavior. (c) Figure 19 can also be used to correct the temperature gradient perturbation solutions for the dissipation effect on the recombination rate temperature term. Equation (4.79) is likewise applicable for corrections to different highly cooled wall temperature values.

Equation (4.88) is plotted versus ζ in Figure 24 for several combinations of the parameters Q/ϵ and ω; the slopes of the lines, as in the corresponding atomic specie case (Figure 22), increase notably when either Q/ϵ or ω is decreased. Also shown in this figure are the results of Fay and Riddell,[6] corrected to $\Theta_W = .05$. Their temperature data also exhibits the expected linearity with ζ for small ζ and indicates that the second order effect, as in the atomic specie deviations, begins at about $\zeta = 2 \times 10^{-5}$ and subsequently constitutes a subtractive correction to the first order theory. The temperature gradient deviations are approximately the same size as (but opposite in sign to) the corresponding wall atomic specie deviations; at $\zeta = 5 \times 10^{-5}$, the non-equilibrium effect

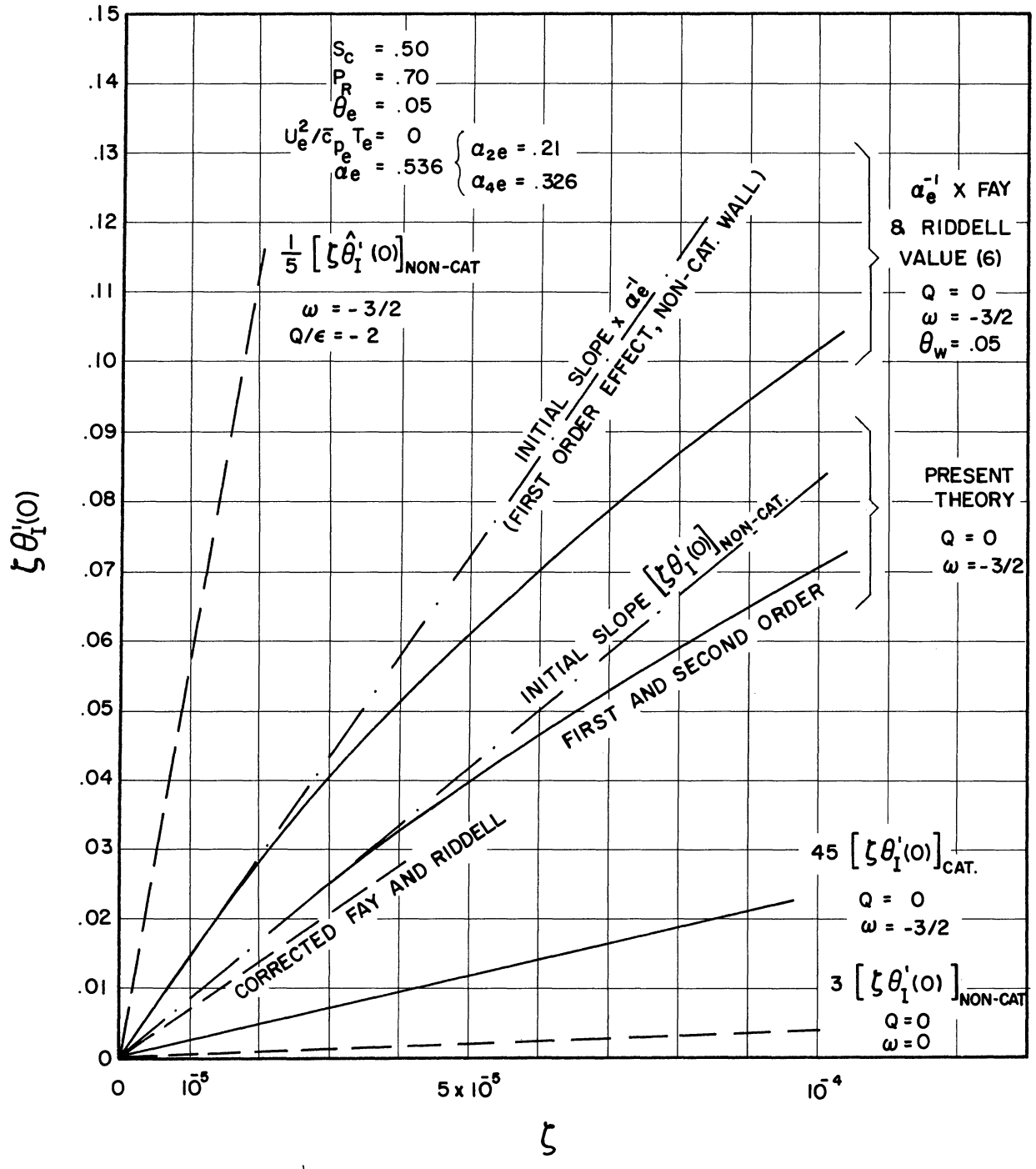

Figure 24. Wall Temperature Gradient Deviations Versus the Non-Equilibrium Parameter ζ.

increases the wall temperature gradient over the chemically frozen value by 4%.

The disagreement with Fay and Riddell's results in the stagnation flow example shown in Figure 24 is again primarily due to the larger total atomic specie reaction rate used in Reference 6. Furthermore, when this rate term is applied to the energy equation, Fay and Riddell do not correctly average the atomic specie reaction rate terms over the corresponding heats of formation (see Equation (A-10), page 40 , Reference 6). These authors assume that

$$\sum_{ATOMS} h_{f_i}^{(o)} \left(\frac{m_i K_i}{\rho}\right) \simeq \sum_{ATOMS} \alpha_{ie} h_{f_i}^{(o)} \times \sum_{ATOMS} \frac{m_i K_i}{\rho}$$

$$= \alpha_e \left[h_{f_2}^{(o)} \frac{m_2 K_2}{\rho} + h_{f_4}^{(o)} \frac{m_4 K_4}{\rho} \right] \qquad (4.89)$$

$$- \left[h_{f_4}^{(o)} - h_{f_2}^{(o)} \right] \left[\alpha_{2e} \frac{m_4 K_4}{\rho} - \alpha_{4e} \frac{m_2 K_2}{\rho} \right]$$

for the four component mixture used in this thesis. Now in this case, the first bracket alone is the correct representation of the summation on the left side of Equation (4.89). Thus, Fay and Riddell err in this energy equation term by using too small a value (i.e., $\alpha_e < 1$). The second term is negligable in comparison to the first and therefore does not contribute significantly to the error. This is the reason that α_e^{-1} times the Fay and Riddell result is shown in Figure 24; the difference between this and the present theory is now reconcilable on the basis of the difference in reaction rates themselves. Reduction of the Fay and Riddell results in Figure 24 by approximately 47% (the previously estimated error in

their rate for the comparative flow example) produces very good agreement with the present theory, considering the difference in the $\rho\mu$ laws used. It is worth noting that the two errors in Reference 6 mentioned above (the average heat of formation coefficient of the energy equation reaction term is too low by a factor α_e and the reaction rate itself is about 47% too high) tend to cancel to a great extent; this means that the temperature non-equilibrium behavior is actually more accurate than the corresponding specie deviation solutions (which contain only the reaction rate overestimate). Again, however, we must stress the necessity to carefully and accurately formulate both specie and energy reaction terms when dealing with a multicomponent mixture if the physical effects of dissociation-recombination in the boundary layer are to be clearly understood.

The specific heat effect, particularly the inequality of atomic and molecular specie specific heats, is very small in the non-equilibrium temperature gradient perturbations, as indicated by the excellent agreement between the present theory (which assumes $c_{p_1} = c_{p_1} = \text{constant}$) and the Fay and Riddell results (in which variable and unequal specific heat data are included in the digital computations). This might be expected for a non-catalytic wall on the basis of the complete absence of the specific heat inequality effect found in the chemically frozen case. Furthermore, it is confirmed by purely theoretical reasoning. The retention of the $c_{p_2} - c_{p_1}$ terms in the original energy equation can be shown to add the following additional term on the left side of the first perturbation energy Equation (4.34) when c_{p_1} and c_{p_2} are constant:

$$(Le+1)\left\{\frac{C_{P_F}'}{C_{P_F}}\theta_I' + \left[\frac{C_{P_I}'}{C_{P_F}} - \frac{C_{P_I}}{C_{P_F}}\left(\frac{C_{P_F}'}{C_{P_F}}\right)\right]\theta_F'\right\} \tag{4.90}$$

where

$$C_{P_F} = \frac{1+(c_{p_2}/c_{p_1}-1)(\alpha_{2e}\beta_F + \alpha_{4e}\chi_F)}{1+\alpha_e(c_{p_2}/c_{p_1}-1)} \tag{4.91}$$

$$C_{P_I} = \frac{(c_{p_2}/c_{p_1}-1)(\alpha_{2e}\beta_I + \alpha_{4e}\chi_I)}{1+\alpha_e(c_{p_2}/c_{p_1}-1)} \,. \tag{4.92}$$

When $\alpha_e(c_{p_2}/c_{p_1} - 1)$ is very small compared to one, of course, this term is obviously negligable. However, for the flow examples considered in Figures 22 and 24, this parameter is about .20, which is not very small compared to unity; hence, a further examination of Equation (4.90) is necessary. For a non-catalytic wall ($z_F' = C_{p_F}' = 0$, $z_F = C_{p_F} = 1$), Equation (4.90) reduces to

$$\frac{(Le+1)\alpha_{2e}\left(1+\frac{\alpha_{4e}^2}{\alpha_{2e}^2}\right)(c_{p_2}/c_{p_1}-1)\beta_I'(0)}{1+\alpha_e(c_{p_2}/c_{p_1}-1)} \,, \tag{4.93}$$

which is extremely small in comparison to the non-catalytic value of the reaction rate term on the right side of the energy Equation (4.34), particularily in the neighborhood of the wall where $z_I' \approx 0$. Hence, the $c_{p_2} - c_{p_1}$ effect on the temperature gradient perturbation should be very small. On the other hand, in the catalytic wall case, the entire term (4.90) remains and is comparable in size to the corresponding catalytic value of the reaction rate term on the right side of Equation (4.34).

However, because the catalytic wall temperature deviations are in themselves so extremely small (approximately 1/50 of the corresponding non-catalytic wall deviations), the specific heat effect would hardly be noticeable even if it changed the $\theta_I'(o)$ solution by 100%. Based on the effect of $c_{p_2} - c_{p_1}$ on the frozen flow catalytic wall temperature gradient, a 30% effect would seem nearer the actual value. It appears that inclusion of the specific heat effect is a refinement which adds negligably to the accuracy of the present perturbation analysis and constitutes an improvement, mainly in the catalytic wall case, which is expediently handled only by digital computation.

(6) Heat Transfer

The first order wall heat flux perturbation, defined in Equation (4.23) (for equal specific heats) as

$$\mathcal{S} Q_I = \mathcal{S}\{\theta_I'(0) + Le[g_2 \beta_I'(0) + g_4 \chi_I'(0)]\},$$

can now be written by means of the above atomic specie and temperature gradient deviation solutions in the following forms for highly cooled catalytic and non-catalytic walls, respectively:

$$\left.\begin{aligned}\left[\mathcal{S} Q_I\right]_{CAT.} &= \frac{2\alpha_{2e} Le\, \mathcal{S}}{\epsilon(1+\alpha_e)}\left(g_2 + \frac{\alpha_{4e}}{\alpha_{2e}} g_4\right)\left[\theta_I'(0) - \beta_I'(0)\right]_{CAT.} \\ &= \frac{2\alpha_{2e} Le\, \mathcal{S}}{\epsilon(1+\alpha_e)}\left(g_2 + \frac{\alpha_{4e}}{\alpha_{2e}} g_4\right)\left[\frac{\hat{I}_{\theta_2}(\infty)}{\hat{I}_{\theta_1}(\infty)} - \frac{\hat{I}_{\beta_2}(\infty)}{\hat{I}_{\beta_1}(\infty)}\right]_{CAT}\end{aligned}\right\} \qquad (4.94)$$

$$\left.\begin{aligned}\left[\mathcal{S} Q_I\right]_{NON\text{-}CAT.} &= \frac{2\alpha_{2e} Le\, \mathcal{S}}{\epsilon(1+\alpha_e)}\left(g_2 + \frac{\alpha_{4e}}{\alpha_{2e}} g_4\right)\left[\theta_I'(0)\right]_{NON\text{-}CAT.} \\ &= \frac{2\alpha_{2e} Le\, \mathcal{S}}{\epsilon(1+\alpha_e)}\left(g_2 + \frac{\alpha_{4e}}{\alpha_{2e}} g_4\right)\left[\frac{\hat{I}_{\theta_2}(\infty)}{\hat{I}_{\theta_1}(\infty)}\right]_{NON\text{-}CAT.}\end{aligned}\right\} \qquad (4.95)$$

The catalytic wall heat transfer perturbation, being the difference between atomic specie and temperature gradient deviations which are nearly equal in

the Lewis number range $.8 \leq L_e \leq 1.4$, is immediately seen to be a very small increment. In fact, when $L_e \equiv 1$ ($\hat{I}_{\theta_2} = \hat{I}_{z_2}$ and $\hat{I}_{z_2} = \hat{I}_{z_1}$ since $S_c = P_R$ in this case), the perturbation vanishes. This, of course, agrees with the known fact that the increase in heat conduction is just balanced by the decrease in the diffusive heat flux when all the atoms are recombined on the wall and the Lewis number is unity. When $S_c < .70$ ($L_e > 1$ for $P_R = .70$), which is the normal case for air, a very small decrease in heat transfer due to non-equilibrium perturbation from frozen flow exists since $[\theta_I'(o)]_{CAT.}$ is slightly less than $[z_I'(o)]_{CAT.}$ because of the slightly different complimentary integral function z_{c_1} present in the integrands of the reaction rate integrals (see Figure 17). This decrement in heat transfer is extremely small in comparison to either the catalytic heat conduction or heat diffusion perturbation (which are in themselves very small). The non-catalytic wall heat transfer perturbation consists entirely of heat conduction in the absence of any surface recombination; therefore, Figure 24 also represents the heat transfer perturbation for this case when equal specific heats is assumed. The various "correction" curves (Figure 16-19) and wall temperature correction formula (4.79) can be applied directly to Equation (4.95) for various local flow situations. Figure 23 can be used to assess the effects of the local non-equilibrium parameter derivative factor Q/ε and possible changes in recombination rate law on the non-equilibrium heat transfer perturbation.

In addition to a very small indirect effect on the temperature gradient perturbation, the unequal specific heat term also can alter the conduction heat transfer as a result of a small perturbation in

the specific heat coefficient of the temperature gradient. If one includes this specific heat term in the wall heat flux expression (assuming c_{p_1} and c_{p_2} are unequal constants), the heat conduction part of the perturbation ζQ_I assumes the following form:

$$\left[\zeta Q_I\right]_{\substack{\text{CONDUCTION} \\ c_{p_1} \neq c_{p_2}}} = \zeta\left[\mathcal{C}_{p_I}(0)\,\theta_F'(0) + \theta_I'(0)\right] \tag{4.96}$$

with

$$\mathcal{C}_{p_I}(0) = \frac{\alpha_e\left(c_{p_2}/c_{p_1} - 1\right)\left[\frac{\alpha}{\alpha_e}(0)\right]_I}{1 + \alpha_e\left(c_{p_2}/c_{p_1} - 1\right)}$$

The specific heat perturbation therefore adds a separate increment to the heat conduction, $\mathcal{C}_{p_I}(0)\,\theta_F'(0)$, in addition to modifying $\theta_I'(0)$ itself. This increment vanishes for a catalytic wall ($\alpha_{I_W} \equiv 0$) but constitutes a subtractive correction to the equal specific heat non-catalytic wall heat transfer that is proportional to the chemically frozen wall temperature gradient, the difference in specific heats, and the wall total atomic specie concentration deviation. For the $Q = 0$, $\omega = -3/2$ stagnation point flow shown in Figures 22 and 24, for example, Equation (4.96) predicts the following ratio for a non-catalytic wall:

$$\left[Q_I\right]_{\text{CONDUCTION}} \Big/ \left[Q_I\right]_{\substack{\text{CONDUCTION} \\ c_{p_1} = c_{p_2}}} = .87$$

for $c_{p_2}/c_{p_1} = 1.4$. This is a 13% reduction in wall heat transfer perturbation due to unequal specific heats. Since the specific heat effect on $\theta_I'(0)$ is negligable, a direct and simple account of the specific heat inequality in the non-catalytic heat transfer can be taken by merely subtracting from $\left[\theta_I'(0)\right]_{c_{p_1} = c_{p_2}}$ the first term in Equation (4.96), which is proportional to known values of the frozen and perturbation solutions.

Second Order Deviations

The second order frozen deviations are analyzed in the same way as the first order solutions. However, the presence of much more complicated non-homogeneous reaction terms in the second order specie and energy equations makes the numerical task of evaluating the particular integrals which arise very laborious, although still possible to do on a desk calculator. The form of the second order deviation solutions will be given to indicate the nature of this increased complexity, and to show that the second order perturbations are inherently negative with respect to the foregoing first order deviations.

(1) First Atomic Specie

The second order atomic specie Equation (4.35) is of the same form as the first order specie Equation (4.31), the only difference between them being that twice the value of Q/ϵ appears in the second order equation. Therefore, the second order complementary integral is obtained directly from the first order case by using $2 \cdot Q/\epsilon$ instead of Q/ϵ in the latter:

$$z_{II_c}(\eta; S_c, Q/\epsilon) = z_{I_c}(\eta; S_c, 2 \cdot Q/\epsilon) \quad .$$

Since the boundary conditions on z_I and z_{II} are the same, the complete solution to Equation (4.35) is formally identical to that for z_I when $z_{1_c}(Q/\epsilon)$ is replaced by $z_{1_c}(2 \cdot Q/\epsilon)$ and when the first order reaction rate function on the right side of Equation (4.31) is replaced by the second order reaction rate function on the right side of Equation (4.35). The following solution results:

$$\left[\beta_{II}(\eta)\right]_{CAT.} = -\frac{2\alpha_{2e}}{\epsilon(1+\alpha_e)} \beta_{c_1}(\eta; 2\frac{Q}{\epsilon}) \left[\frac{\Delta\hat{z}_1(\eta)}{\Delta\hat{z}_1(\infty)} \cdot \Delta z_2(\infty) - \Delta z_2(\eta)\right]_{CAT.} \qquad (4.97)$$

with

$$\left[\beta_{II}'(0)\right]_{CAT.} = -\frac{2\alpha_{2e}}{\epsilon(1+\alpha_e)}\left[\frac{\Delta\hat{\beta}_2(\infty)}{\Delta\hat{\beta}_1(\infty)}\right]_{CAT.}, \tag{4.98}$$

$$\left[\beta_{II}(\eta)\right]_{NON-CAT.} = -\frac{2\alpha_{2e}}{\epsilon(1+\alpha_e)}\beta_{c_1}(\eta;\tfrac{2\varphi}{\epsilon})\left[\Delta\hat{\beta}_2(\infty) - \Delta\hat{\beta}_2(\eta)\right]_{NON-CAT} \tag{4.99}$$

with

$$\left[\beta_{II}(0)\right]_{NON-CAT.} = -\frac{2\alpha_{2e}}{\epsilon(1+\alpha_e)}\left[\Delta\hat{\beta}_2(\infty)\right]_{NON-CAT.}, \tag{4.100}$$

where

$$\Delta\hat{\beta}_1 = \int_0^{\eta} \frac{EXP\left(-S_c\int_0^{\eta} f\,d\eta\right)}{\beta_{1c}^2(\eta;\,2\frac{\varphi}{\epsilon})}\,d\eta \tag{4.101}$$

$$\Delta\hat{\beta}_2 = \int_0^{\eta} \frac{EXP\left(-S_c\int_0^{\eta} f\,d\eta\right)}{\beta_{1c}^2(\eta;\,2\frac{\varphi}{\epsilon})}\left[\int_0^{\eta}\beta_{1c}(\eta;\,2\frac{\varphi}{\epsilon})\cdot\mathcal{R}_2\,EXP\left(S_c\int_0^{\eta} f\,d\eta\right)d\eta\right]d\eta \tag{4.102}$$

and

$$\mathcal{R}_2 = \theta_F^{\omega-2}\left\{\mathcal{D}_{\beta_2}\beta_I + \mathcal{D}_{\chi_2}\chi_I + \mathcal{D}_{W_2}W_I + \theta_I\left[(\omega-2)\frac{\chi_{2F}}{\theta_F} + \mathcal{D}_{\theta_2}\right]\right\}. \tag{4.103}$$

The values of the reaction rate derivative functions $\mathcal{D}_{\beta_2}$, $\mathcal{D}_{\chi_2}$, $\mathcal{D}_{W_2}$ and $\mathcal{D}_{\theta_2}$ are given in Appendix D. When these relations are used in conjunction with the first order solutions (4.80) and (4.84), the second order reaction function $\mathcal{R}_2$ appearing in the integrand of $\Delta\hat{\beta}_2$ can be expressed as follows:

$$\mathcal{R}_2\,\theta_F^{2-\omega} = \beta_I\left\{2\left(\frac{1+\alpha_e}{1+\alpha_e\beta_F}\right)\beta_F\right.$$

$$\left. - \left(\frac{\alpha_{2e}}{1+\alpha_e\beta_F}\right)\left[\left(1+\frac{\alpha_{4e}^2}{\alpha_{2e}^2}\right)\left(\frac{1+\alpha_e}{1+\alpha_e\beta_F}\right)\beta_F^2 - \left(1+2\frac{\alpha_{4e}^2}{\alpha_{2e}^2}\right)\left(\frac{1+\alpha_e\beta_F}{1-\alpha_e-\alpha_{3e}}\right)EXP\left[-\frac{\theta_{A_2}}{\theta_F}(1-\theta_F)\right]\right]\right\} \tag{4.104}$$

$$+ \frac{\theta_I}{\theta_F}\left\{(\omega-2)\chi_{2F} - C_1\frac{\theta_{A_2}}{\theta_F}\left(\frac{1-\alpha_e\beta_F}{1-\alpha_e}\right)EXP\left[-\frac{\theta_{A_2}}{\theta_F}(1-\theta_F)\right]\right\}.$$

It is apparent from this expression that the computation of the second order solutions involves a great deal more labor than the preceeding first order solutions. Since z_{c_1} is always positive near the wall, the second order specie deviation will be negative when $\hat{\mathcal{I}}_{z_2}(\infty)$ is positive (i.e., when the integrand of $\hat{\mathcal{I}}_{z_2}$, involving the second order reaction rate functions, is predominantly positive throughout the boundary layer). The function $\mathcal{R}_2$ determines the sign of $\hat{\mathcal{I}}_{z_2}$ and hence of the second order specie deviation function z_{II}. Now the coefficient of z_I in $\mathcal{R}_2$, for $\omega < 2$ and a highly cooled wall, was found to always be predominantly positive throughout the boundary layer, whereas the coefficient of θ_I is a negative value. Since the previous first order results have shown z_I to be negative and θ_I positive, the second order reaction function $\mathcal{R}_2$ (and the second order integral $\hat{\mathcal{I}}_{z_2}$) is therefore a negative function throughout the boundary layer. Thus, the second order specie deviation function is opposite in sign to the first order deviation and acts as a subtractive correction to the overestimate of the chemically frozen deviations predicted by the first order theory. On physical grounds, this would be expected from the fact that the second order deviations are proportional to the products of frozen reaction rate function derivatives and the first order deviations; since these derivatives have a sign which is opposite to that of the first order deviation functions in the highly cooled boundary layer, the second order deviations tend to "drive" the solution back toward frozen equilibrium.

(2) Second Atomic Specie

The solution to Equation (4.36), in which χ_{II} is subject to the same boundary conditions as imposed on the first atomic specie function

z_{II}, is completely analogous to the foregoing solution for z_{II}; the complementary integrals are the same and χ_{II} is given by Equations (4.97) through (4.103) when α_{2_e} is replaced by α_{4_e} and the integral $\mathcal{I}_{z_2}$ is replaced by $\mathcal{I}_{z_4}$, where $\mathcal{I}_{z_4}$ is obtained from $\mathcal{I}_{z_2}$ by replacing θ_{A_2} by θ_{A_4} and the reaction function $\mathcal{R}_2$ by

$$\mathcal{R}_4 = \theta_F^{\omega-2}\left\{\mathcal{D}_{z_4}\beta_I + \mathcal{D}_{\chi_4}\chi_I + \mathcal{D}_{w_4}w_I + \theta_I\left[(\omega-2)\frac{\mathcal{I}_{4F}}{\theta_F} + \mathcal{D}_{\theta_4}\right]\right\}. \qquad (4.105)$$

The function $\mathcal{R}_4$ can be rewritten, with the aid of the values of $\mathcal{D}_{z_4}$, $\mathcal{D}_{\chi_4}$, $\mathcal{D}_{w_4}$ and $\mathcal{D}_{\theta_4}$ given in Appendix B and the first order solutions (4.79) and (4.83), in the following form:

$$\mathcal{R}_4\theta_F^{2-\omega} = \beta_I\left\{2\frac{\alpha_{4e}}{\alpha_{2e}}\left(\frac{1+\alpha_e}{1+\alpha_e\beta_F}\right)\beta_F\right.$$

$$\left.-\left(\frac{\alpha_{2e}}{1+\alpha_e\beta_F}\right)\left[\left(1+\frac{\alpha_{4e}^2}{\alpha_{2e}^2}\right)\left(\frac{1+\alpha_e}{1+\alpha_e\beta_F}\right)\beta_F^2 - \frac{\alpha_{4e}^2}{\alpha_{2e}^2}\left(\frac{1+\alpha_e\beta_F}{1-\alpha_e-\alpha_{3e}}\right)EXP\left[-\frac{\theta_{A_4}}{\theta_F}(1-\theta_F)\right]\right]\right\} \qquad (4.106)$$

$$+\frac{\theta_I}{\theta_F}\left\{(\omega-2)\mathcal{I}_{4F} - \left(\frac{1-\alpha_e\beta_F}{1-\alpha_e}\right)\frac{\theta_{A_4}}{\theta_F}C_3\,EXP\left[-\frac{\theta_{A_4}}{\theta_F}(1-\theta_F)\right]\right\}.$$

The predominant sign of $\mathcal{R}_4$, like $\mathcal{R}_2$, is found to be negative for $\omega < 2$ and a highly cooled wall; accordingly, χ_{II} is positive in the neighborhood of the wall (whereas χ_I is negative).

(3) Total Atomic Specie

The second order total atomic specie deviation is given by

$$\left(\frac{\alpha}{\alpha_e}\right)_{II} = \zeta^2\left(\frac{\alpha_{2e}}{\alpha_e}\beta_{II} + \frac{\alpha_{4e}}{\alpha_e}\chi_{II}\right).$$

As a single illustrative example of the typical second order effect, the integrals $\vec{\mathcal{I}}_{g_2}(\infty)$ and $\vec{\mathcal{I}}_{g_4}(\infty)$ have been evaluated for the non-catalytic wall (which exhibits the greatest non-equilibrium deviation) with $Q = 0$ and $\omega = 3/2$ (stagnation point flow with the Davidson recombination rate law). The increased complexity of the second order reaction rate terms makes the pursuit of as comprehensive a parametric study as the first order case unfeasible in this thesis (although it would be expected, based on an inspection of the above second order solution integrals, that the second perturbation exhibits at least as much if not more sensitivity to the parameters Q/ϵ and ω as the first order perturbations and about the same sensitivity to the parameters S_c, Θ_A, Θ_W and $u_e^2/\overline{c}_{p_e} T_e$). This specific calculation has confirmed the insensitivity of the results to the Θ_A parameter and further has shown that it is an accurate approximation to take $\vec{\mathcal{I}}_{g_2} = \vec{\mathcal{I}}_{g_4}$ for a highly cooled wall. The second perturbation of the total atomic specie concentration at the wall, given by

$$\left(\frac{\alpha}{\alpha_e}(0)\right)_I = \frac{2\alpha_{2e}^2 \mathcal{J}^2}{\epsilon(1+\alpha_e)\alpha_e}\left(1+\frac{\alpha_{4e}^2}{\alpha_{2e}^2}\right)\frac{\vec{\mathcal{I}}_{2g}(\infty)}{\vec{\mathcal{I}}_{1g}(\infty)} \quad , \qquad (4.107)$$

is shown for this example in Figure 23. The difference between this result and the second order effect shown by the Fay and Riddell calculation reflects the reaction rate discrepancy previously discussed for the first order theory. At $\zeta = 10^{-4}$, the second order effect in this example constitutes a 20% subtractive correction to the value predicted by the first order linear variation.

(4) Second Molecular Specie

The W_{II} solution, as far as heat transfer is concerned, is actually needed only if the third perturbation were to be computed (to evaluate the non-homogeneous reaction rate terms). However, it is readily obtained in terms of the χ_{II} solution by inspection of Equations (4.36) and (4.37) and the respective boundary conditions:

$$W_{II} = - \frac{\alpha_{4e}}{\alpha_{3e}} \chi_{II} \quad . \tag{4.108}$$

(5) Energy Equation

Just like the first order case, the complementary integral of Equation (4.38) is found from that of the specie Equation (4.35) by replacing S_c by P_R in the latter:

$$\theta_{II_c} = z_{II_c}(P_R) \quad . \tag{4.109}$$

The full solution to Equation (4.38), in view of the $\theta_{II}(o) = 0$ inner boundary condition, is similar in form to the catalytic wall second order atomic specie deviation function solution:

$$\theta_{II}(\eta) = \frac{2\alpha_{2e} L_e}{\epsilon(1+\alpha_e)} g_{c_1}(\eta; \tfrac{2Q}{\epsilon}, P_R) \left\{ g_2 \left[\frac{\Delta\vec{\theta}_1(\eta)}{\Delta\vec{\theta}_1(\infty)} \Delta\vec{\theta}_2(\infty) - \Delta\vec{\theta}_2(\eta) \right] + \frac{\alpha_{4e}}{\alpha_{2e}} g_4 \left[\frac{\Delta\vec{\theta}_1(\eta)}{\Delta\vec{\theta}_1(\infty)} \Delta\vec{\theta}_4(\infty) - \Delta\vec{\theta}_4(\eta) \right] \right\} \tag{4.110}$$

with

$$\theta_{II}'(0) = \frac{2\alpha_{2e} L_e}{\epsilon(1+\alpha_e)} \left[\frac{g_2 \Delta\vec{\theta}_2(\infty) + \frac{\alpha_{4e}}{\alpha_{2e}} g_4 \Delta\vec{\theta}_4}{\Delta\vec{\theta}_1(\infty)} \right] \tag{4.111}$$

and where $\hat{\theta}_1 = \hat{g}_1(P_R)$ and

$$\hat{\theta}_{2,4} = \int_0^\eta \frac{EXP(-P_R \int_0^\eta f\,d\eta)}{g_{c_1}^2(\eta; 2\frac{Q}{\epsilon}, P_R)} \left[\int_0^\eta g_{c_1}(\eta; 2\frac{Q}{\epsilon}, P_R) R_{2,4} EXP(P_R \int_0^\eta f\,d\eta)\, d\eta \right] d\eta \quad (4.112)$$

Using the same arguments employed for the specie integrals, $\hat{g}_{2,4}$ and $\hat{\theta}_{2,4}$ are found to be predominantly negative in the highly cooled boundary layer. Consequently, θ_{II} and $\theta'_{II}(o)$ are negative and therefore opposite in sign to the first order temperature perturbations.

The integrals $\hat{\theta}_2(\infty)$ and $\hat{\theta}_4(\infty)$ have been evaluated for the $Q = 0$, $\omega = -3/2$ non-catalytic wall case ($\theta_W = .05$) and found to be very nearly equal, again verifying the insensitivity of the non-equilibrium deviations to the activation energy parameter for a highly cooled wall. The equal specific heat non-catalytic wall second order temperature gradient perturbation (ζ^2 times Equation (4.111)) for this special case is shown in Figure 25. The present second order deviations are smaller than those predicted by Fay and Riddell in accord with the discrepancies between the two theories noted in the first order case.

Further Discussion of Results

Application of First Order Theory to the Calculation of Local Non-Equilibrium Deviations in the Laminar Boundary Layer

The foregoing analysis has shown the first order non-equilibrium deviations from chemically frozen flow to be proportional to the product of the characteristic non-equilibrium parameter ζ and an integral of the first order reaction rate function across the boundary layer. These integrals were found to be extremely sensitive to the recombination rate law exponent ω and the non-equilibrium parameter derivative function $Q = \frac{d\zeta/dX}{\zeta/X}$. However,

ζ also depends on ω and the local inviscid flow and the sensitivity of ζ times the deviation integrals to ω and the local inviscid flow is different than that of the integrals alone. This net behavior of the atomic specie and temperature deviations must be taken into account when applying the theory to a calculation of local atomic specie concentration and heat transfer deviations in a highly cooled hypersonic boundary layer. Since the theory has shown that a non-catalytic wall exhibits a far greater non-equilibrium behavior in the chemically frozen regime than a catalytic wall, the present discussion will be confined to the former case.

Consider the ratio of the first order deviations for any two values of the recombination rate parameter, ω_1 and ω_2 (non-catalytic wall):

$$\frac{[\zeta\, g_I(0)]_{\omega_1}}{[\zeta\, g_I(0)]_{\omega_2}} = \frac{\zeta(\omega_1)}{\zeta(\omega_2)} \cdot \frac{\hat{I}_{g_2}(\infty;\omega_1)}{\hat{I}_{g_2}(\infty;\omega_2)} \tag{4.113}$$

for the atom concentration and

$$\frac{[\zeta\, \theta_I'(0)]_{\omega_1}}{[\zeta\, \theta_I'(0)]_{\omega_2}} = \frac{\zeta(\omega_1)}{\zeta(\omega_2)} \cdot \frac{\hat{I}_{\theta_2}(\infty;\omega_1)}{\hat{I}_{\theta_2}(\infty;\omega_2)} \tag{4.114}$$

for the temperature gradient. The dependence of $\hat{I}_{g_2}$ and $\hat{I}_{\theta_2}$ on ω is given in Figures 15 and 23, respectively, and the definition of ζ (Equation (2.90)) provides

$$\frac{\zeta(\omega_1)}{\zeta(\omega_2)} = \left(\frac{T_e}{300\,^\circ K}\right)^{\omega_1-\omega_2}, \tag{4.115}$$

all other conditions remaining the same. As an example of the effect of a change in the recombination rate temperature dependence, the ratios (4.113) and (4.114) have been evaluated as a function of ω_1 for $\omega_2 = -3/2$ and

several freestream temperatures at the stagnation point ($Q = 0$). The results, which are approximately the same for both Equation (4.113) and (4.114), are given in Table II. These data show that the net deviations still remain sensitive to the parameter ω, but the trend of the effect is opposite to that on the deviation integrals alone because the factor exerts the dominant influence and causes the deviations to increase with increasing ω. The heat transfer add surface composition deviations are equally affected by ω for the non-catalytic case. Both of these deviations are greater when the freestream temperature is increased, as indicated by Equation (4.115). These results suggest that local non-equilibrium deviations calculated on the basis of a recombination rate temperature dependence exponent significantly greater than -3/2 could be larger than those calculated on the basis of $\omega = -3/2$.

TABLE II

EFFECT OF RECOMBINATION RATE LAW ON THE FIRST ORDER HEAT TRANSFER DEVIATIONS FROM FROZEN FLOW

($\theta_W = .05$, $u_e^2/c_{p_e}T_e = 0$)

		$[\zeta\theta_I'(o)]_{\omega_1}/[\zeta\theta_I'(o)]_{\omega=-3/2}$	
ω_1	$I_{\theta_2}(\infty,\omega)/I_{\theta_2}(\infty,-3/2)$	$T_e = 3000°K$	$T_e = 6000°K$
-3/2	1	1	1
0	1.85×10^{-2}	.585	1.624
2	6.51×10^{-4}	2.06	23.3

The non-catalytic wall heat transfer (equal specific heat value), for example, would increase by a factor of 23 for $T_e = 6000°K$ if ω were to be changed from -3/2 to 2.

The parameter Q/ϵ also has a pronounced effect on the deviation integrals and it is a sensitive function of the local inviscid flow (Figure 6). The products $\zeta \cdot z_I(o)$ and $\zeta \cdot \theta_I'(o)$ exhibit a different variation with the local inviscid flow than predicted by the effect of Q/ϵ on $z_I(o)$ and $\theta_I'(o)$, however, since ζ also may vary along a hypersonic body (such as shown in Figure 4). As an illustration of this, consider the following ratios which represent the local wall atom concentration and temperature gradient deviations expressed as a fraction of the corresponding stagnation point values:

$$\frac{\zeta\, \beta_I(o)}{[\zeta\, \beta_I(o)]_{Q=0}} \quad \text{and} \quad \frac{\zeta\, \theta_I'(o)}{[\zeta\, \theta_I'(o)]_{Q=0}} .$$

These are plotted versus the distance along a hypersonic hemisphere-cylinder at $M_\infty = 10$ in Figure 25 for $\omega = -3/2$, based on the inviscid flow data shown in Figures 4 and 6 and the Q/ϵ dependence of the deviation functions given by Figures 15 and 23. This example is intended to illustrate two facts: (a) the local non-equilibrium frozen flow deviations for a given recombination rate law can change significantly over the length of a blunt-nosed hypersonic body, and (b) the non-equilibrium state of the stagnation point is a good indicator of the local non-equilibrium behavior on such a body only in the immediate neighborhood of the stagnation point ($X/d \leq .25$) and at a point approximately one body diameter downstream of the stagnation point. Figure 25 shows that in the nose region $X/d > .25$, particularly in the neighborhood of the sonic point ($X/d \simeq .60 - .70$), the boundary layer may noticeably "unfreeze" relative to the stagnation point. Accordingly, the heat transfer perturbation becomes roughly three times greater than the stagnation value. Further downstream, the flow subsequently tends

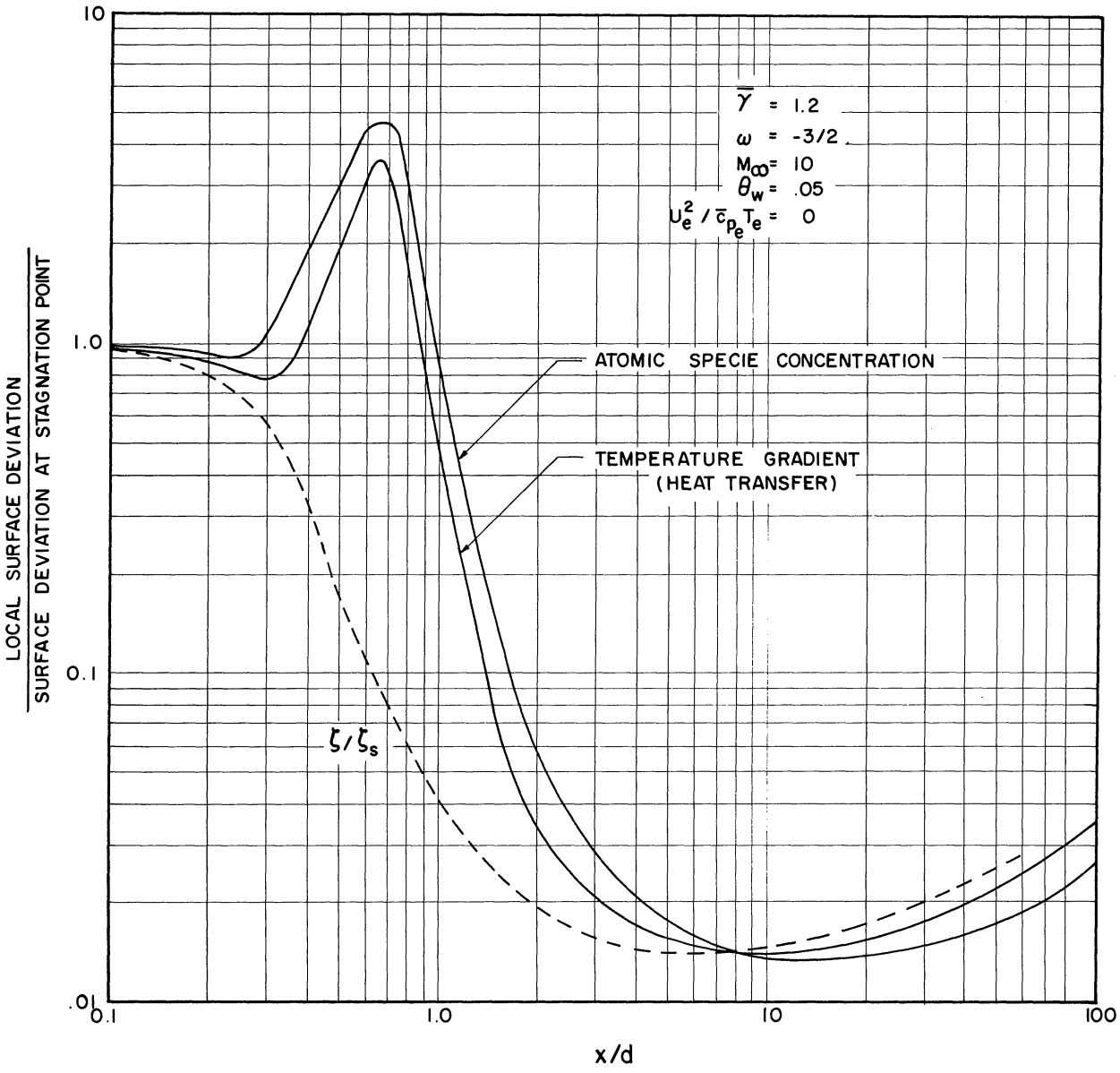

Figure 25. Local First Order Composition and Heat Transfer Deviations from Chemically Frozen Flow Along a Hypersonic Hemisphere-Cylinder.

to rapidly "freeze" relative to the stagnation point, dropping the local heat transfer perturbation to as much as 1/100 of the stagnation value in the region X/d ≃ 10. Finally, at very large X/d, the local boundary layer deviations begin to gradually increase, tending to approach and exceed the stagnation pont point value. If the body were extremely long, the boundary layer would continue to unfreeze and eventually approach a state of thermodynamic equilibrium regardless of the stagnation point situation. This trend toward thermodynamic equilibrium at X/d → ∞ is further accelerated by the increased pressures associated with the boundary layer-inviscid flow interreaction that undoubtedly occur in this region.

The Error in the Use of Fick' Law

The perturbation analysis is based on governing equations in which the mass diffusion terms for each of the four component species have been assumed to obey Fick's law. While it has been found that the assumption of equal physical properties (except atomic specie heats of formation) between the two molecular species and between the two atomic species leads exactly to Fick's law for each atomic specie diffusion flux, the molecular diffusion fluxes do not obey this law under these conditions. The error in assuming Fick law diffusion for the α_3 specie consequently feeds into the non-equilibrium analysis in two ways. First, it causes a direct error in both the frozen and the non-equilibrium perturbation molecular nitrogen solutions. The largest error occurs for the catalytic wall case. Second, it has an indirect effect on the atomic specie and temperature perturbation, since α_3 enters the reaction rate as part of a term multiplying the dissociation rate exponential. We can show, however, that this second effect is negligible in the perturbation.

analysis (this is done below). Then the error in α_3 can be considered separately from the atomic specie and temperature solution if a particular interest in a more accurate molecular specie profile arises.

The exact multicomponent mixture diffusion expression (Appendix A), when applied to the present approximate four specie mixture, gives the following expression for the α_3 diffusion flux term ($\mathscr{D}_{13} \neq \mathscr{D}_{12}$):

$$\rho \alpha_3 \vec{V}_3 = -\rho \mathscr{D}_{12} \left\{ \nabla \alpha_3 - \left(1 - \frac{\mathscr{D}_{13}}{\mathscr{D}_{12}}\right) \left[\frac{\alpha_3 \nabla \alpha + (1-\alpha) \nabla \alpha_3}{1 + \left(2 \frac{\mathscr{D}_{13}}{\mathscr{D}_{12}} - 1\right) \alpha} \right] \right\}. \tag{4.116}$$

This in turn yields the following boundary layer specie conservation equation:

$$\rho \left(u \frac{\partial \alpha_3}{\partial x} + v \frac{\partial \alpha_3}{\partial y} \right) = \frac{\partial}{\partial y} \left\{ \frac{\mu}{Sc} \frac{\partial \alpha_3}{\partial y} \left[1 - \frac{\left(1 - \frac{\mathscr{D}_{13}}{\mathscr{D}_{12}}\right)(1-\alpha)}{1 + \left(2 \frac{\mathscr{D}_{13}}{\mathscr{D}_{12}} - 1\right) \alpha} \right] \right\}$$
$$- \frac{\partial}{\partial y} \left\{ \frac{\mu}{Sc} \frac{\partial \alpha}{\partial y} \left[\frac{\left(1 - \frac{\mathscr{D}_{13}}{\mathscr{D}_{12}}\right) \alpha_3}{1 + \left(2 \frac{\mathscr{D}_{13}}{\mathscr{D}_{12}} - 1\right) \alpha} \right] \right\} + 2 \rho K_R' T^{\omega - 2} \left(\frac{p_e}{R_e} \right)^2 g_4. \tag{4.117}$$

This equation reduces to Equation (2.66) only when $\mathscr{D}_{13}/\mathscr{D}_{12} = 1$ or when α_3 and α are constant. Comparison with Equation (2.65) shows that α_3 and α_4 are linearly related, independent of chemical reaction, only when either of these two special conditions hold. The boundary conditions are fixed independently of the diffusion law for either a catalytic or non-catalytic wall. Consequently, the error due to the use of Fick law diffusion for α_3 distorts the slope $\alpha_3'(0)$ at a catalytic wall but distorts only the non-equilibrium wall perturbations of α_3 at a non-catalytic wall, since the chemically frozen solution $\alpha_{3_F} = \alpha_{3_e}$ prevails in the latter case for any form of the diffusion law. The non-Fick diffusion effect would therefore appear to be of most interest in the former case. Equation (4.117) can be transformed to the similarity plane form (as in Chapter 3) and subjected to the similarity approximations and perturbation analysis to evaluate the

non-Fick effect on the chemically frozen catalytic wall α_3 profile and the first, second, etc., order non-equilibrium deviation profiles. Since the prime interest of the present work lies in the atomic specie and temperature variables, a detailed investigation of such a solution is not considered here.

The effect of the error in α_3, which is greatest in the vicinity of the wall, can be neglected as far as the atomic specie and temperature non-equilibrium perturbations are concerned because of the following considerations: (a) In general, α_3 enters these perturbation solutions as a term in the coefficient of the exponential dissociation part of the reaction rate integrals. As we have previously seen, errors in this coefficient in the inner part of the boundary layer have an extremely small effect on the perturbation solutions for a highly cooled wall (the dissociation term contributes significantly to the integral only for $\eta > 2$, where the error in α_3 becomes small). (b) Furthermore, in the first perturbation case, the α_3 term enters as the chemically frozen value; since the non-catalytic wall solution for α_{3_F} is exact, there is no error in the first perturbations in this case. A slight effect on the dissociation term coefficient for a catalytic wall would be present because the non-Fick diffusion alters the slope of the $\alpha_3(\eta)$ profile. However, it would be a negligable effect because of the extremely small size of the dissociation exponential. The error in the molecular specie profile, as it affects the other perturbations, might be more prominent when the wall is not highly cooled.

CHAPTER V

DEVIATIONS FROM THERMODYNAMIC EQUILIBRIUM

Some Features of Non-Equilibrium Couette Flow

The relative simplicity of the governing equations and the qualitative similarity to a boundary layer flow makes the Couette flow problem a valuable theoretical research tool, and as such it has proven particularly useful in obtaining a better qualitative understanding of various hypersonic real gas effects [15, 28, 32, 33]. We wish to consider deviations from dissociation-recombination equilibrium in such a Couette flow with the sole object of indicating the general features of the non-equilibrium behavior which may serve as a guide in a subsequent appraisal of the same problem in the laminar boundary layer.

Couette Flow Equations

The Couette flow constitutes the motion of a gas between two parallel infinite planes spaced a distance δ apart, the upper plane moving at a velocity U with respect to the stationary lower plane. The equations describing this problem are obtained from the previously given boundary layer equations by setting the derivatives in the X direction and the normal flow velocity equal to zero, so that only gradients in the normal direction Y remain. If we assume a Fick law diffusion in a four component air mixture, then, we obtain the following governing equations:

$$\frac{d}{dy}\left(\rho \mathscr{D}_{12} \frac{d\alpha_2}{dy}\right) = -m_2 K_2 \tag{5.1}$$

$$\frac{d}{dy}\left(\rho \mathscr{D}_{12} \frac{d\alpha_4}{dy}\right) = -m_4 K_4 \tag{5.2}$$

$$\frac{d}{dY}\left(\rho \mathcal{D}_{12}\,\frac{d\alpha_3}{dY}\right) = \mathcal{M}_4 \mathcal{K}_4 \tag{5.3}$$

where

$$\mathcal{M}_2 \mathcal{K}_2 = -2\rho K_R' T^{\omega-2}\left(\frac{p}{R_0}\right)^2\left[\frac{\alpha_2^2}{1+\alpha} - (1-\alpha-\alpha_3)\frac{EXP(a - T_{A2}/T)}{4p}\right] \tag{5.4}$$

$$\mathcal{M}_4 \mathcal{K}_4 = -2\rho K_R' T^{\omega-2}\left(\frac{p}{R_0}\right)^2\left[\frac{\alpha_4^2}{1+\alpha} - \alpha_3\,\frac{EXP(a - T_{A4}/T)}{4p}\right] \tag{5.5}$$

$$\frac{d\tau}{dY} = \frac{d}{dY}\left(\mu \frac{du}{dY}\right) = 0 \tag{5.6}$$

$$p = \text{CONSTANT} = \rho \frac{R_0}{M_1}(1+\alpha)T \tag{5.7}$$

$$\frac{d}{dY}\left\{\frac{\mu}{P_R}\left[\bar{C}_p \frac{dT}{dY} + L_e\left[(h_2 - h_1)\frac{d\alpha_2}{dY} + (h_4 - h_1)\frac{d\alpha_4}{dY}\right] + P_R \frac{d(u^2/2)}{dY}\right)\right\} = 0 \tag{5.8}$$

The boundary conditions to be imposed are analogous to those for a boundary layer problem. At the moving plane Y = δ, u = U and T = T_e, and we shall prescribe the gas composition to be known, and equal to the equilibrium composition for the given values of p and T_e:

$$\alpha_i(\delta) = \alpha_{ie}$$

where

$$\alpha_{2e}^2/(1+\alpha_e) = (1-\alpha_e-\alpha_{3e})\,\frac{EXP(a - T_{A2}/T_e)}{4p} \tag{5.9}$$

$$\alpha_{4e}^2/(1+\alpha_e) = \frac{\alpha_{3e}\ EXP(a - T_{A4}/T_e)}{4p} \tag{5.10}$$

$$\alpha_{3e} \simeq .79 - \alpha_{4e}. \tag{5.11}$$

At the stationary inner boundary, u = 0, T(o) = T_W and

$$\alpha_2(0) = \alpha_{2EQ.}(0) \simeq 0, \quad \alpha_4(0) = \alpha_{4EQ.}(0) \simeq 0, \quad \alpha_3(0) = \alpha_{3EQ.}(0)$$

for a catalytic wall or

$$\frac{d\alpha_2}{dy}(0) = \frac{d\alpha_4}{dy}(0) = \frac{d\alpha_3}{dy}(0) = 0$$

for a non-catalytic wall. The gas heat flux at the stationary wall is given by

$$-\frac{P_R \dot{Q}_W}{\mu_W} = \left\{ \bar{C}_p \frac{dT}{dy} + L_e\left[(h_2 - h_1)\frac{d\alpha_2}{dy} + (h_4 - h_1)\frac{d\alpha_4}{dy}\right]\right\}_{y=0}. \tag{5.12}$$

It is convenient to simplify the problem, retaining only those physical features of major importance to the non-equilibrium chemistry, by the introduction of the following assumptions:

$$\rho/\mu = \rho_W/\mu_W = \text{CONSTANT}$$
$$S_c \equiv \mu/\rho \mathcal{D}_{12} = \text{CONSTANT}, \quad P_R = \text{CONSTANT}$$
$$\bar{C}_p, \ h_2 - h_1, \ h_4 - h_1 \quad \text{CONSTANT}.$$

Further, introduce the following new variables:

$$\beta \equiv \frac{\alpha_2}{\alpha_{2e}}, \quad \gamma \equiv \frac{\alpha_4}{\alpha_{4e}}, \quad W \equiv \frac{\alpha_3}{\alpha_{3e}}, \quad \theta \equiv \frac{T}{T_e},$$

$$\bar{u} \equiv \frac{u}{U} \;,\quad \theta_{A_{2,4}} \equiv \frac{T_{A_{2,4}}}{T_e} \;,\quad \beta_{2,4} \equiv \left(\frac{h_{2,4} - h_1}{\bar{c}_p T_e}\right)\alpha_{2,4e} \;,$$

$$\zeta \equiv \frac{2 k_R' S_c T_e^{\omega-2} \delta^2 \rho_e}{\mu_e}\left(\frac{p}{R_0}\right)^2 .$$

Finally, introduce the following coordinate transformation:

$$\eta = \int_0^{y/\delta} \frac{\rho}{\rho_e}\, d\left(\frac{y}{\delta}\right) . \tag{5.13}$$

Applying these transformations to the foregoing Couette flow equations, using relations (5.9) and (5.10) to simplify the reaction rate terms, we get the following simplified forms of the governing equations (denoting derivatives with respect to η by primes):

$$\beta'' = \frac{\alpha_{2e}\zeta\theta^{\omega-2}}{1+\alpha_e}\mathcal{Y}_2 \tag{5.14}$$

$$\chi'' = \frac{\alpha_{4e}\zeta\theta^{\omega-2}}{1+\alpha_e}\mathcal{Y}_4 \tag{5.15}$$

$$W'' = -\left(\frac{\alpha_{4e}}{\alpha_{3e}}\right)\frac{\alpha_{4e}\zeta\theta^{\omega-2}}{1+\alpha_e}\mathcal{Y}_4 \tag{5.16}$$

where

$$\mathcal{Y}_2 = \frac{(1+\alpha_e)\beta^2}{1+\alpha_{2e}\beta+\alpha_{4e}\chi} - \left(\frac{1-\alpha_{2e}\beta-\alpha_{4e}\chi-\alpha_{3e}W}{1-\alpha_e-\alpha_{3e}}\right)EXP\left[-\frac{\theta_{A_2}}{\theta}(1-\theta)\right] \tag{5.17}$$

$$\mathcal{Y}_4 = \frac{(1+\alpha_e)\chi^2}{1+\alpha_{2e}\beta+\alpha_{4e}\chi} - W\,EXP\left[-\frac{\theta_{A_4}}{\theta}(1-\theta)\right] . \tag{5.18}$$

$$\bar{u}'' = 0 \tag{5.19}$$

$$\left[\theta + Le\left(q_2 \beta + q_4 \chi\right)\right]'' = -Pr\left(\frac{v^2}{\bar{c}_p T_e}\right)\left(\bar{u}'\right)^2 . \tag{5.20}$$

The corresponding boundary conditions now read:

$$\eta = \eta_d = \int_0^1 \frac{\rho}{\rho_e} d\left(\frac{y}{\delta}\right) : \quad \beta = \chi = W = \theta = \bar{u} = 1$$

$$\eta = 0 : \quad \bar{u} = 0, \quad \theta = \theta_w ; \quad \beta(0) = \chi(0) = 0,$$

$$W(0) = W_{EQ.}(0), \text{ CATALYTIC WALL};$$

$$\beta'(0) = \chi'(0) = W'(0) = 0, \text{ NON-CATALYTIC WALL}.$$

Regardless of chemical reaction, the momentum Equation (5.19) and the energy Equation (5.20) (using the boundary conditions) can be integrated twice to give the following results:

$$\bar{u} = \eta/\eta_d \tag{5.21}$$

$$\theta - \theta_w = (1-\theta_w)\frac{\eta}{\eta_d} + (1-\frac{\eta}{\eta_d})\frac{\eta}{\eta_d} Pr\left(\frac{v^2}{2\bar{c}_p T_e}\right) + Le\left\{q_2\left\langle[1-\beta(0)]\frac{\eta}{\eta_d} - [\beta-\beta(0)]\right\rangle + q_4\left\langle[1-\chi(0)]\frac{\eta}{\eta_d} - [\chi-\chi(0)]\right\rangle\right\}. \tag{5.22}$$

The latter provides a relation between temperature and the mixture composition that holds for an arbitrary degree of non-equilibrium. The heat transfer can therefore be written entirely in terms of the composition

variables as follows:

$$-\frac{\eta_d P_R \delta \dot{Q}_W}{\bar{\rho}_r T_e / M_e} = 1 - \theta_W + P_R\left(\frac{U^2}{2\bar{c}_p T_e}\right) + L_e\left\{q_{B_2}[1-g(0)] + q_A[1-\chi(0)]\right\}. \quad (5.23)$$

This equation indicates that the Couette Flow heat flux to a cool catalytic inner surface (z(o) and X(o) zero) is invariant to chemical reaction in the gas. The non-catalytic case is not, however, since z(o) and X(o) must in general be obtained from a solution of the reaction rate-influenced atomic specie equations. Non-equilibrium effects on heat transfer would therefore be expected to be of most interest in conjunction with the non-catalytic wall case.

The Thermodynamic Equilibrium State

This extreme of dissociation-recombination behavior arises, as previously pointed out, when ζ becomes very large and the corresponding factors in the reaction rate terms in the species equations vanish. Referring to Equations (5.19) and (5.20) for example, we see that as $\zeta \to \infty$, the net reaction functions $\mathcal{G}_2$ and $\mathcal{G}_4$ must approach zero to maintain finite diffusion on the left sides. $\mathcal{G}_{2,4} = 0$ provide the classical thermodynamic equilibrium relations from which the specie concentrations are calculated as functions of pressure and temperature, as follows:*

$$\frac{\beta_{EQ.}^2}{1 + \alpha_{2e}\beta_{EQ.} + \alpha_{4e}\gamma_{EQ.}} = \left(\frac{1 - \alpha_{2e}\beta_{EQ.} - \alpha_{4e}\gamma_{EQ.} - \alpha_{3e}W_{EQ.}}{1 - \alpha_e - \alpha_{3e}}\right) EXP\left[-\frac{\theta_{A_2}}{\theta_{EQ.}}(1-\theta_{EQ.})\right] \quad (5.24)$$

* This discussion of equilibrium relations between the species and temperature applies equally well to a boundary layer flow problem.

$$\frac{\chi_{EQ.}^2}{1+\alpha_{2e}\beta_{EQ.}+\alpha_{4e}\chi_{EQ.}} = W_{EQ.}\ EXP\left[-\frac{\theta_{Af}}{\theta_{EQ.}}(1-\theta_{EQ.})\right] . \tag{5.25}$$

The thermodynamic equilibrium composition solution is completed by the following relationship between α_3, α_2 and α_4 (i.e., between W_{EQ}, z_{EQ} and χ_{EQ}) in the assumed absence of NO formation:

$$\alpha_{3EQ.} \simeq .79 - \alpha_{4EQ.}$$

or

$$W_{EQ.} = .79/\alpha_{3e} - (\alpha_{4e}/\alpha_{3e})\chi_{EQ.} \tag{5.26}$$

The derivation of this relation is given in Appendix G. This result is based on the absence of diffusion; any deviation from exact thermodynamic equilibrium must therefore introduce deviations from Equation (5.26) due to the actual diffusion processes which occur in the gas. Equations (5.24), (5.25) and (5.26) provide three relations with which to calculate the three unknown equilibrium specie concentration functions as a function of the temperature distribution. Consequently, the thermodynamic equilibrium energy equation can be expressed entirely in terms of the temperature; the Couette flow temperature profile (5.39) for equilibrium can be found from Equation (5.22) when $z(\Theta_{EQ})$ and $\chi(\Theta_{EQ})$ are substituted.

Once the equilibrium temperature is known, one could calculate from the specie equations the actual value of the reaction rate functions for a large but non-infinite ζ. For example, from Equation (5.14),

$$\mathcal{J}_2 = \frac{\beta_{EQ.}''(1+\alpha_e)}{\alpha_{2e}\zeta\,\theta_{EQ.}^{\omega-2}} = \frac{\left(\theta_{EQ.}''\frac{d\beta_{EQ.}}{d\theta_{EQ.}} + \theta_{EQ.}''\frac{d^2\beta_{EQ.}}{d\theta_{EQ.}^2}\right)(1+\alpha_e)}{\alpha_{2e}\zeta\,\theta_{EQ.}^{\omega-2}} . \tag{5.27}$$

Also, the equilibrium temperature profile permits one to return to

Equations (5.24-5.26) and calculate the chemical specie concentration profiles in the flow. This equilibrium composition is determined solely by the temperature distribution and consequently there is no provision for actually applying separate specie boundary conditions such as would be required in the presence of arbitrary surface catalysis. The exact equilibrium concentration profiles therefore cannot be influenced by the wasll chemistry (this is consistent with the above neglect of diffusion currents in calculating the specie-temperature relationships, since the wall-gas specie boundary conditions in general are concerned with a matching of the gas diffusion rate with the surface reaction rate). Only in the extreme case of a completely catalytic wall (where $\alpha_i(o) = \alpha_{i_{EQ.}}(T_W)$) will the equilibrium solution in the gas be strictly compatible with the surface chemistry. The equilibrium diffusion current $z'_{EQ.} = \frac{dz_{EQ.}}{d\theta_{EQ.}} \times \theta'_{EQ.}$ in the gas approaching a non-catalytic wall will not agree with the zero diffusion requirement right at the surface unless the wall is so highly cooled that $\frac{dz_{EQ.}}{d\theta_{EQ.}}(o) \to 0$. Consequently, an infinitesimally thin gas layer may exist, adjacent to the wall, across which the specie concentration gradient adjusts from $z'_{EQ.}(o)$ to zero, and outside of which the flow is everywhere in exact thermodynamic equilibrium at $\zeta \to \infty$. This behavior leads one to expect that this sublayer will spread outward and assume a finite thickness when the flow departs from thermodynamic equilibrium.

Small Deviations from Thermodynamic Equilibrium

Any deviation from the thermodynamic equilibrium solution must involve just those features that have been neglected in the equilibrium calculations. A study of the prominent physical features of near-equilibrium Couette flow will be made by considering small deviations from the

equilibrium solution as follows:

$$\begin{aligned} \zeta &= \zeta_{EQ.} + Z, \quad \chi = \chi_{EQ.} + X, \\ w &= w_{EQ.} + W, \quad \theta = \theta_{EQ.} + \Theta, \end{aligned} \tag{5.28}$$

accompanied by corresponding expansions in the reaction rate functions (noting that $\mathcal{G}_{2,4} \equiv 0$ at equilibrium),

$$\mathcal{G}_{2,4} = \mathcal{D}_{\zeta_{2,4}} Z + \mathcal{D}_{\chi_{2,4}} X + \mathcal{D}_{w_{2,4}} W + \mathcal{D}_{\theta_{2,4}} \Theta \tag{5.29}$$

where

$$\left.\begin{aligned} \mathcal{D}_{\zeta_{2,4}} &= \left(\frac{d\mathcal{G}_{2,4}}{d\zeta}\right)_{EQ.}, \quad \mathcal{D}_{\chi_{2,4}} = \left(\frac{d\mathcal{G}_{2,4}}{d\chi}\right)_{EQ.}, \\ \mathcal{D}_{w_{2,4}} &= \left(\frac{d\mathcal{G}_{2,4}}{dw}\right)_{EQ.}, \quad \mathcal{D}_{\theta_{2,4}} = \left(\frac{d\mathcal{G}_{2,4}}{d\theta}\right)_{EQ.}. \end{aligned}\right\} \tag{5.30}$$

Substitution of these expansions into the Couette flow equations and retention only of first order deviation terms produces the following differential equations:

$$Z'' = \frac{\alpha_{2e}\, \zeta\, \theta_{EQ.}^{\omega-2}}{1+\alpha_e}\left(\mathcal{D}_{\zeta_2} Z + \mathcal{D}_{\chi_2} X + \mathcal{D}_{w_2} W + \mathcal{D}_{\theta_2} \Theta\right) - \zeta_{EQ.}'' \tag{5.31}$$

$$X'' = \frac{\alpha_{4e}\, \zeta\, \theta_{EQ.}^{\omega-2}}{1+\alpha_e}\left(\mathcal{D}_{\zeta_4} Z + \mathcal{D}_{\chi_4} X + \mathcal{D}_{w_4} W + \mathcal{D}_{\theta_4} \Theta\right) - \chi_{EQ.}'' \tag{5.32}$$

$$W'' = -\left(\frac{\alpha_{4e}}{\alpha_{3e}}\right)\frac{\alpha_{4e}\, \zeta\, \theta_{EQ.}^{\omega-2}}{1+\alpha_e}\left(\mathcal{D}_{\zeta_4} Z + \mathcal{D}_{\chi_4} X + \mathcal{D}_{w_4} W + \mathcal{D}_{\theta_4} \Theta\right) - w_{EQ.}'' \tag{5.33}$$

$$\Theta = L_e\, \mathcal{G}_2\left[\left(1 - \frac{n}{n_d}\right) Z(0) - Z\right] + L_e\, \mathcal{G}_4\left[\left(1 - \frac{n}{n_d}\right) X(0) - X\right]. \tag{5.34}$$

The following boundary conditions, taking into account those which prevail on the equilibrium solution, must be imposed on the deviation functions:

$$Z(\eta_d) = X(\eta_d) = W(\eta_d) = \Theta(\eta_d) = 0 \tag{5.35}$$

$$\left.\begin{aligned} &\Theta'(0) = 0 \;;\; Z(0) = X(0) = W(0) = 0 \text{ (CATALYTIC WALL)}; \\ &Z'(0) = -\beta_{EQ}'(0),\; X'(0) = -\chi_{EQ}'(0),\; W'(0) = W_{EQ}'(0) \text{ (NON-CATALYTIC WALL)}. \end{aligned}\right\} \tag{5.36}$$

Since $W_{EQ}' = -\frac{\alpha_{4e}}{\alpha_{3e}} \chi_{EQ}'$ and $W_{EQ}'' = -\frac{\alpha_{4e}}{\alpha_{3e}} \chi_{EQ}''$ from Equation (5.26), a comparison of Equations (5.32), (5.33) in view of the boundary conditions shows that

$$W = -\frac{\alpha_{4e}}{\alpha_{3e}} X . \tag{5.37}$$

The molecular nitrogen deviation is hence proportional to the negative of the atomic nitrogen specie deviation.

This set of second order, linear, non-homogeneous differential equations, constitutes a formidable mathematical problem because of the variable reaction rate derivative coefficients and the coupling between the variables Z and X. The general procedure for solving these equations would be to obtain two uncoupled fourth order equations for Z and X, respectively, by solving Equations (5.31-5.34) simultaneously; each of these equations would then be attacked by some suitable method, if possible. However, it is found that this general problem becomes so complicated that the original purpose of considering the Couette flow would be defeated. Some further simplifications of the equations, with respect to both the coefficients and coupling between the variables, must be made if any

physical insight into the near-equilibrium behavior is to be gained. Therefore, in the spirit of pointing out some of the prime qualitative features, some simplifying approximations shall be used.

Approximate Solution

The similarity of the boundary conditions and the proportionality between the atomic species previously found in the chemically frozen regime suggest the assumption $\mathcal{X} \propto Z$. This seems to be a reasonable simplifying approximation for the purpose of evaluating the main qualitative features of the near-equilibrium behavior. Therefore, we shall assume

$$\mathcal{X} \simeq \text{CONSTANT} \cdot Z = A Z \,, \tag{5.38}$$

where the value of the constant A is chosen so as to be consistent with the boundary conditions. Now Equation (5.38) is compatible with the outer boundary conditions $Z(\eta_1)=\mathcal{X}(\eta_1)=0$ and the catalytic inner wall boundary conditions $Z(0)=\mathcal{X}(0)=0$ for any value of A. However, the inner non-catalytic wall condition necessarily determines A to be

$$A = \frac{\mathcal{X}'(0)}{Z'(0)} = \frac{\chi_{EQ}'(0)}{\beta_{EQ}'(0)} \,. \tag{5.39}$$

Assumption (5.38) completely eliminates the coupling between the two atomic specie Equations (5.31) and (5.32) in view of Equations (5.33) and (5.34) . Consequently, we must solve the following single second order non-homogeneous differential equation for $Z(\eta)$ subject to boundary conditions (5.35-5.36):

$$Z'' - \left(\frac{\alpha_{2e}}{1+\alpha_e}\theta_{EQ}^{\omega-2}\mathcal{K}_1\right)\beta Z = \left(\frac{\alpha_{2e}}{1+\alpha_e}\theta_{EQ}^{\omega-2}\mathcal{K}_2\right)\left(1-\frac{\eta}{\eta_1}\right)\beta Z(0) - \beta_{EQ}'' \tag{5.40}$$

where

$$\tilde{F}_1(\eta) = \mathbb{E}_{g_2} - Le\, g_2 \mathbb{E}_{\theta_2} + A\left(\mathbb{E}_{\chi_2} - \frac{\alpha_{4e}}{\alpha_{3e}} \mathbb{E}_{W_4} - Le\, g_4 \mathbb{E}_{\theta_2}\right) \tag{5.41}$$

$$\tilde{F}_2(\eta) = Le\,(g_2 + g_4 A)\, \mathbb{E}_{\theta_2} \,. \tag{5.42}$$

Unfortunately, $\tilde{F}_1$ and $\tilde{F}_2$ vary quite noticeably across the channel; the exact solution to Equation (5.40) would therefore require lengthy and cumbersome numerical integration. To avoid such an unfeasible numerical complexity and bring out the essential physical features of the problem, we shall now introduce two additional simplifying assumptions.

(a) Assume that certain average constant values of the coefficients $\tilde{F}_1$ and $\tilde{F}_2$, $\bar{F}_1$ and $\bar{F}_2$ respectively, can be used in Equation (5.40). While such an assumption will certainly lead to sizable errors in the magnitude of the solutions, it seems a reasonable one when the main objective is a purely qualitative appraisal of the near-equilibrium behavior.

(b) Assume that the equilibrium specie profile $z_{EQ_o}(\eta)$ is a cubic in η $\left(z^{IV}_{EQ_o}(\eta) \equiv 0\right)$. This is a good description of the $z_{EQ_o}(\eta)$ behavior near the wall and can satisfy the $z_{EQ_o}(\eta_d) = 1$ condition and simplify the particular non-homogeneous integral of Equation (5.40). Taking the derivatives $z'_{EQ_o}(o)$ and $z''_{EQ_o}(o)$ to be known, the following cubic profile satisfies the conditions $z_{EQ_o}(\eta_d) = 1$ and $z_{EQ_o}(o) = 0$:

$$\beta_{EQ}(\eta) = \beta'_{EQ}(0)\cdot\eta\left(1 - \frac{\eta^2}{\eta_d^2}\right) + \beta''_{EQ}(0)\,\eta^2\left(1 - \frac{\eta}{\eta_d}\right) + \left(\frac{\eta}{\eta_d}\right)^2 \tag{5.43}$$

with

$$\beta'''_{EQ} = \text{CONSTANT} = \frac{6}{\eta_d^3}\left[1 - \beta'_{EQ}(0)\cdot\eta_d - \frac{\beta''_{EQ}(0)\cdot\eta_d^2}{2}\right]. \tag{5.44}$$

The introduction of these two assumptions into Equation (5.40) yields the following differential equation with constant coefficients for Z :

$$Z'' - \zeta \mathcal{F}_1^* Z = \zeta \mathcal{F}_2^* (1 - \frac{\eta}{\eta_d}) Z(0) - \beta_{EQ}'' \qquad (5.45)$$

where

$$\mathcal{F}_{1,2}^* = \left(\frac{\alpha_{2e}}{1+\alpha_{1e}}\right) \cdot \mathcal{F}_{1,2} \ .$$

The exact values of the reaction rate derivatives $\mathcal{D}_{\beta_2}$, $\mathcal{D}_{\theta_2}$, etc., are given in Appendix H as functions of the equilibrium specie and temperature variables. Inspection of these formulae shows that for a highly cooled wall, the two derivatives $\mathcal{D}_{\beta_2}$ and $\mathcal{D}_{\theta_2}$ determine the predominate sign of the functions $\mathcal{F}_1$ and $\mathcal{F}_2$ above. Since $\mathcal{D}_{\beta_2} \geq 0$ and $\mathcal{D}_{\theta_2} < 0$, the signs of $\mathcal{F}_1$ and $\mathcal{F}_2$ across the channel will be predominately positive and negative, respectively; hence $\mathcal{F}_1^* > 0$ and $\mathcal{F}_2^* < 0$.

Equation (5.45) can be directly solved in closed form. The complementary integral of the associated homogeneous equation is ($\mathcal{F}_1^* > 0$)

$$Z_c = C_1 \, EXP\left(\sqrt{\mathcal{F}_1^* \zeta}\, \eta\right) + C_2 \, EXP\left(-\sqrt{\mathcal{F}_1^* \zeta}\, \eta\right).$$

A particular integral of the non-homogeneous equation, when $z_{EQ.}^{IV}(\eta) = 0$, is seen to be

$$Z_p = -\left(\frac{\mathcal{F}_2^*}{\mathcal{F}_1^*}\right)\left(1 - \frac{\eta}{\eta_d}\right) Z(0) + \frac{\beta_{EQ}''}{\zeta \mathcal{F}_1^*} \ .$$

The complete solution $Z = Z_c + Z_p$ involves two unknown arbitrary constants C_1 and C_2 which are determined from the boundary conditions on Z. The following solutions are obtained:

$$\left[Z(\eta)\right]_{CAT} = -\frac{\beta_{EQ}''(0)}{\zeta \mathcal{F}_1^*}\left\{\frac{SINH\left[\sqrt{\zeta \mathcal{F}_1^*}(\eta_d - \eta)\right] + \frac{\beta_{EQ}''(\eta_d)}{\beta_{EQ}''(0)} SINH\left(\sqrt{\zeta \mathcal{F}_1^*}\, \eta\right)}{SINH\left(\sqrt{\zeta \mathcal{F}_1^*}\, \eta_d\right)}\right\} + \beta_{EQ.}''(\eta_d) / \zeta \mathcal{F}_1^* \qquad (5.46)$$

where

$$\left[Z'(0)\right]_{CAT} = \frac{\beta_{EQ.}'''}{\zeta\phi_{i}^{*}} + \frac{\beta_{EQ.}''(0)}{\sqrt{\zeta\phi_{i}^{*}}}\left[\frac{\cosh\left(\sqrt{\zeta\phi_{i}^{*}}\,\eta_d\right) - \dfrac{\beta_{EQ.}''(\eta_d)}{\beta_{EQ.}''(0)}}{\sinh\left(\sqrt{\zeta\phi_{i}^{*}}\,\eta_d\right)}\right] \tag{5.47}$$

$$= \frac{\beta_{EQ}''(0)}{\sqrt{\zeta\phi_{i}^{*}}} \qquad @ \quad \zeta \gg 1$$

and

$$\begin{aligned}\left[Z(\eta)\right]_{NON\text{-}CAT} = Z(0)\Bigg[&\left(1+\frac{\phi_2^{*}}{\phi_i^{*}}\right)\cosh\left(\sqrt{\zeta\phi_i^{*}}\,\eta\right) - \frac{\left(\phi_2^{*}/\phi_i^{*}\right)\sinh\left(\sqrt{\zeta\phi_i^{*}}\,\eta\right)}{\eta_d\sqrt{\zeta\phi_i^{*}}} - \frac{\phi_2^{*}}{\phi_i^{*}}\left(1-\frac{\eta}{\eta_d}\right)\Bigg] \\ &- \left[\beta_{EQ}'(0) + \frac{\beta_{EQ.}'''}{\zeta\phi_i^{*}}\right]\frac{\sinh\left(\sqrt{\zeta\phi_i^{*}}\,\eta\right)}{\sqrt{\zeta\phi_i^{*}}} \\ &- \frac{\beta_{EQ.}''(0)}{\zeta\phi_i^{*}}\left[\cosh\left(\sqrt{\zeta\phi_i^{*}}\,\eta\right) - \frac{\beta_{EQ}''(\eta)}{\beta_{EQ.}''(0)}\right]\end{aligned} \tag{5.48}$$

where

$$\begin{aligned}\left[Z(0)\right]_{NON\text{-}CAT.} = &\frac{\beta_{EQ.}''(0)}{\zeta\phi_i^{*}}\left[\frac{\cosh\left(\sqrt{\zeta\phi_i^{*}}\,\eta_d\right) + \dfrac{\beta_{EQ.}'''}{\beta_{EQ.}''(0)\sqrt{\zeta\phi_i^{*}}} - \dfrac{\beta_{EQ.}''(\eta_d)}{\beta_{EQ.}''(0)}}{\left(1+\dfrac{\phi_2^{*}}{\phi_i^{*}}\right)\cosh\left(\sqrt{\zeta\phi_i^{*}}\,\eta_d\right) - \dfrac{\left(\phi_2^{*}/\phi_i^{*}\right)\sinh\left(\sqrt{\zeta\phi_i^{*}}\,\eta_d\right)}{\eta_d\sqrt{\zeta\phi_i^{*}}}}\right] \\ &+ \frac{\beta_{EQ}'(0)}{\sqrt{\zeta\phi_i^{*}}}\left[\frac{\sinh\left(\sqrt{\zeta\phi_i^{*}}\,\eta_d\right)}{\left(1+\dfrac{\phi_2^{*}}{\phi_i^{*}}\right)\cosh\left(\sqrt{\zeta\phi_i^{*}}\,\eta_d\right) - \dfrac{\left(\phi_2^{*}/\phi_i^{*}\right)\sinh\left(\sqrt{\zeta\phi_i^{*}}\,\eta_d\right)}{\eta_d\sqrt{\zeta\phi_i^{*}}}}\right]\end{aligned} \tag{5.49}$$

$$= \frac{\beta_{EQ.}'(0)}{\left(1+\dfrac{\phi_2^{*}}{\phi_i^{*}}\right)\sqrt{\zeta\phi_i^{*}}} \qquad @ \quad \zeta \gg 1.$$

The remaining specie and temperature deviations may now be computed with $Z(\eta)$ known.

Properties of the Approximate Solution

(a) The specie deviations $[Z'(o)]_{CAT.}$ and $[Z(o)]_{NON-CAT.}$ vanish for $\zeta \to \infty$, behaving as $1/\sqrt{\zeta}$ for $\zeta \gg 1$. The non-catalytic wall specie gradient does not necessarily vanish, however, since $z'_{EQ.}(o)$ in the gas may be zero.

(b) Solutions (5.46-5.49) show that the near-equilibrium behavior depends directly on the various derivatives of the equilibrium atomic specie profile at the wall. The catalytic wall specie deviation is proportional to the second derivative $z''_{EQ.}(o)$, whereas the non-catalytic wall deviation is proportional to $z'_{EQ.}(o)$ for large ζ. For a given value of ζ, these deviations become vanishingly small whenever the wall is highly cooled enough to cause the equilibrium specie derivatives (as well as the concentration itself) to approach zero. Furthermore, the sign of the deviations depends on the equilibrium specie-temperature relations at the wall. We have

$$\beta'_{EQ}(o) = \frac{d\beta_{EQ.}}{d\theta_{EQ.}}(o) \cdot \theta'_{EQ}(o) \tag{5.50}$$

$$\beta''_{EQ}(o) = \frac{d^2\beta_{EQ.}}{d\theta^2_{EQ.}}(o) \cdot \theta'^2_{EQ.}(o) + \frac{d\beta_{EQ.}}{d\theta_{EQ.}}(o)\, \theta''_{EQ}(o), \tag{5.51}$$

where $dz_{EQ.}/d\theta_{EQ.}$ is always positive (the equilibrium dissociation level always increases with a temperature rise) and $d^2z_{EQ.}/d\theta^2_{EQ.}$ is positive up to approximately 50% dissociation and hence positive at a cool wall. Therefore, $z'_{EQ.}(o)$ and $z''_{EQ.}(o)$ will have the same sign on a cool wall ($\theta'_{EQ.}(o) > 0$) only when $\theta''_{EQ.}(o)$ is positive or a very small negative number. From Equation (5.22), the equilibrium temperature derivatives are found to be

$$\theta'_{EQ.}(0) = \frac{1 - \theta_W + P_R(U^2/2\bar{c}_p T_e) + Le(g_2 + A g_4)}{\eta_d \left[1 + Le \frac{d\beta_{EQ.}}{d\theta_{EQ.}}(0) \cdot (g_2 + A g_4)\right]} \tag{5.52}$$

$$\theta''_{EQ.}(0) = \frac{-P_R(U^2/2\bar{c}_p T_e \eta_d) - Le\left[g_2 \frac{d^2\beta_{EQ.}}{d\theta_{EQ.}^2}(0) + g_4 \frac{d^2\chi_{EQ.}}{d\theta_{EQ.}^2}(0)\right]\theta'^2_{EQ.}(0)}{1 + Le \frac{d\beta_{EQ.}}{d\theta_{EQ.}}(0) \cdot (g_2 + A g_4)} . \tag{5.53}$$

Substitution of these values into Equation (5.51) gives:

$$\beta''_{EQ.}(0) = - \frac{P_R (U^2/2\bar{c}_p T_e \eta_d) \frac{d\beta_{EQ.}}{d\theta_{EQ.}}(0)}{1 + Le \frac{d\beta_{EQ.}}{d\theta_{EQ.}}(0) \cdot (g_2 + A g_4)} \tag{5.54}$$
$$+ \frac{\theta'^2_{EQ.}(0)\left\{\left[1 - Le\, g_2 \frac{d\beta_{EQ.}}{d\theta_{EQ.}}(0)\right]\frac{d^2\beta_{EQ.}}{d\theta_{EQ.}^2}(0) - Le\, g_4 \frac{d\beta_{EQ.}}{d\theta_{EQ.}}(0) \frac{d^2\chi_{EQ.}}{d\theta_{EQ.}^2}(0)\right\}}{1 + Le \frac{d\beta_{EQ.}}{d\theta_{EQ.}}(0) \cdot (g_2 + A g_4)} .$$

If a linear equilibrium specie-temperature relationship is assumed* ($dz_{EQ.}/d\theta_{EQ.}$ = constant, $d^2z_{EQ.}/d\theta^2_{EQ.} = 0$), Equation (5.54) shows that $z''_{EQ.}(0)$ is entirely due to a negative viscous dissipation term. The catalytic wall atomic specie gradient perturbation from equilibrium is therefore negative and opposite in sign to the non-catalytic wall perturbation (the latter, being proportional to $z'_{EQ.}(0)$, is always positive). However, this result conflicts with the catalytic wall diffusion increase found in Reference 6. Alternatively, when a significant non-linearity in the $z_{EQ.}(\theta_{EQ.})$ relation is allowed (which is a much more realistic assumption), the positive second term in Equation (5.54) can

---

* Such an assumption is made in Reference 28, for example.

predominate for highly cooled walls when $\frac{dz_{EQ.}}{d\theta_{EQ.}}$ is small. The catalytic wall atomic specie gradient in this case is positive like the non-catalytic wall result. This state of affairs is in qualitative agreement with known results for the laminar boundary layer. The present analysis therefore furnishes the following important conclusion: the near-thermodynamic equilibrium behavior in a highly cooled Couette flow will be a reliable qualitative analogue of such behavior in the laminar boundary layer only when a non-linear $z_{EQ.}(\theta_{EQ.})$ relationship is accounted for in the former problem. Furthermore, it is the catalytic wall case which is sensitive to this non-linear effect; the non-catalytic wall deviations from equilibrium are proportional to $z'_{EQ.}(o) \propto dz_{EQ.}/d\theta_{EQ.}(o)$ and therefore not affected by the assumption $z''_{EQ.} = 0$.

(c) The typical distribution of the atomic specie deviation Z across the channel as a function of ζ, computed from Equations (5.46) and (5.48), is shown in Figure 26. The magnitude of the perturbations shown is, of course, not accurate because of the approximations used in the solutions. However, an interesting qualitative feature of the non-catalytic solution is shown, namely that the adjustment between the gas and reaction-free surface occurs within a kind of sublayer in the channel whose thickness decreases as ζ increases. Since the slope $[Z'(o)]_{NON-CAT.} = - z'_{EQ.}(o)$ is fixed while the specie deviation Z(o) decreases as $1/\sqrt{\zeta}$, the sublayer thickness

$$\frac{Z(o)}{Z'(o)} \propto \frac{1}{\sqrt{\zeta}}$$

ultimately approaches zero when $\zeta \to \infty$. A similar result has been found by Broadwell (28) and Hirschfelder (9).

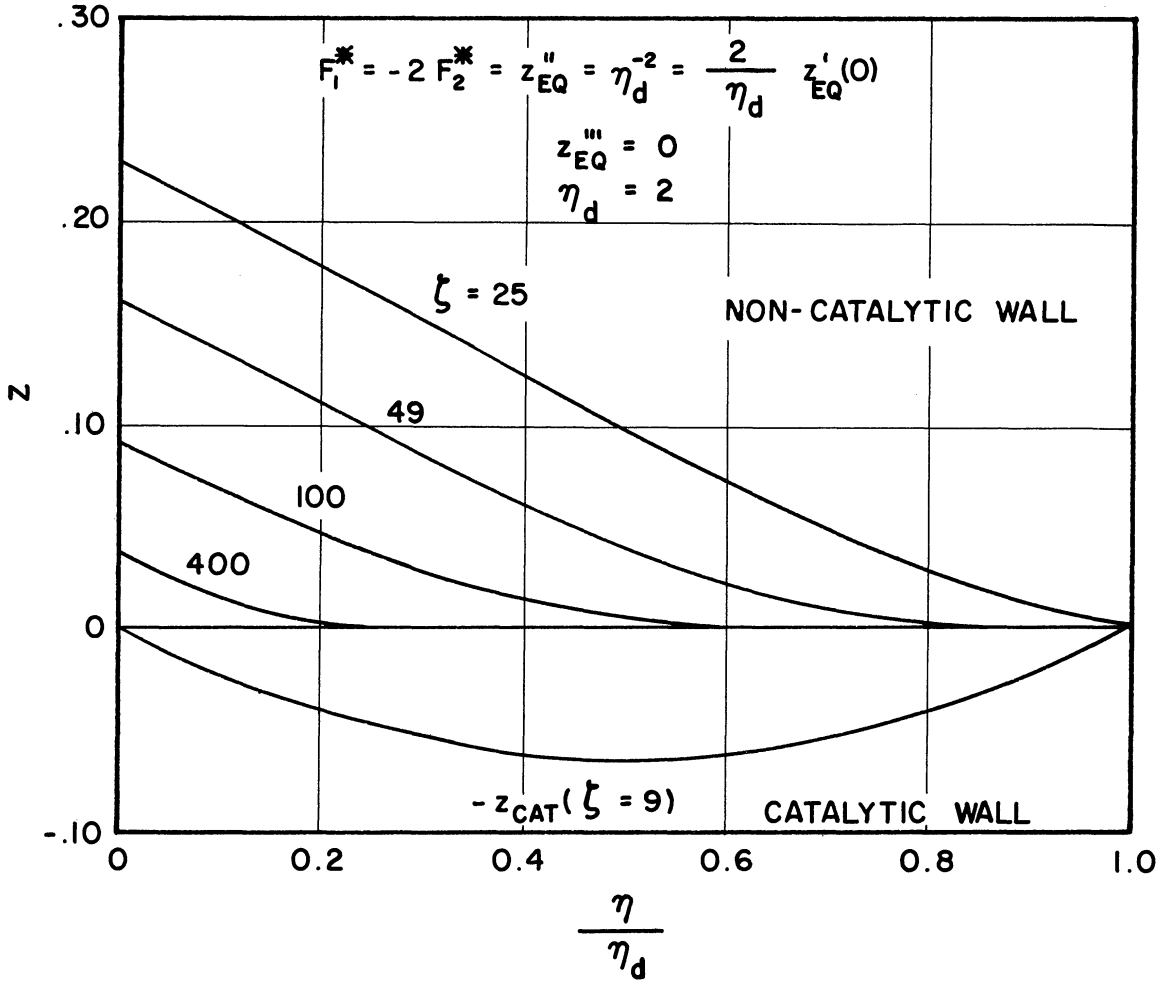

Figure 26. Atomic Specie Deviation Profiles in a Couette Flow Near Thermodynamic Equilibrium.

(d) The temperature perturbation in the gas is given entirely in term of the atomic specie solution:

$$\theta' = Le(\beta_2 + A\beta_4)\left[\left(1 - \frac{n}{n_d}\right)Z(0) - Z\right], \tag{5.55}$$

$$\theta'(0) = -Le(\beta_2 + A\beta_4)\left[\frac{Z(0)}{n_d} + Z'(0)\right]. \tag{5.56}$$

The catalytic wall temperature deviation is always opposite in sign to the atomic specie deviation. The corresponding temperature gradient deviation for $\zeta \gg 1$, substituting relation (5.47) into Equation (5.56), becomes

$$\left[\theta'(0)\right]_{CAT} = -\frac{Le(\beta_2 + A\beta_4)\beta''_{EQ.}(0)}{\sqrt{\beta_{i}^{*}}}, \tag{5.57}$$

which vanishes for $\zeta \to \infty$. The catalytic wall heat conduction will decrease due to thermodynamic equilibrium deviation whenever $z''_{EQ.}(o)$ is positive, which in turn is true whenever the $z_{EQ.}(\theta_{EQ.})$ relation is highly non-linear in the presence of a cooled wall. On the other hand, the non-catalytic wall temperature gradient perturbation, from Equation (5.49), becomes

$$\left[\theta'(0)\right]_{NON-CAT.} = -Le(\beta_2 + A\beta_4)\beta'_{EQ}(0)\left[\frac{1}{n_d\left(1 + \frac{\beta_2^{*}}{\beta_1^{*}}\right)\sqrt{\beta_{i}^{*}}} - 1\right] \tag{5.58}$$

for $\zeta \gg 1$. This equation predicts that the heat conduction perturbation in the gas does not vanish as $\zeta \to \infty$ because of the inner boundary condition $Z'(o) = -z'_{EQ.}(o)$ required by the absence of surface reaction. However, the region adjacent to the wall in which the non-vanishing temperature perturbation exists will shrink to zero as $\zeta \to \infty$, leaving a temperature gradient jump right at the wall. When the wall is highly cooled enough to give $z'_{EQ.}(o) \to 0$ as well as $z_{EQ.}(o) = 0$, the heat conduction deviation becomes

vanishingly small even when ζ does not approach infinity. Otherwise, Equation (5.58) shows that the non-catalytic wall heat conduction initially increases due to highly cooled wall non-equilibrium deviation at large values of ζ. As ζ decreases, the sign of this deviation will ultimately change and the heat conduction will then decrease with further departure from equilibrium.

(e) The heat transfer deviation on a catalytic wall is exactly zero; that on a non-catalytic wall is given by Equation (5.23):

$$-\left(\frac{\mu_d P_R \delta \dot{Q}_w}{\lambda_p T_e / \mu_e}\right)_I \equiv Q_I = -L_e(\beta_2 + A\beta_4) Z(0)$$

and is always opposite in sign to the atomic specie deviation at the wall. For large ζ, the use of solution (5.49) gives

$$[Q_I]_{NON-CAT} = \frac{-L_e(\beta_2 + A\beta_4)\beta_{EQ.}'(0)}{\left(1 + \frac{\sigma_2^*}{\sigma_i^*}\right)\sqrt{\beta \sigma_i^*}} \,. \tag{5.59}$$

The sum of the wall heat conduction and diffusion perturbations in the gas vanishes as $\zeta \to \infty$. Furthermore, we see that the heat transfer calculation is not affected by the non-linearity of the $z_{EQ.}(\theta_{EQ.})$ relation as far as sign is concerned; Equations (5.50) and (5.52) show that $z'_{EQ.}(o)$ is always positive on a cooled wall and the heat transfer therefore decreases as a result of departure from thermodynamic equilibrium in the Couette flow.

The above general features should be useful as a guide in analyzing the highly cooled laminar boundary layer near equilibrium and in any future detailed numerical solutions (accounting for the variable coefficients) which may be of interest. The recombination rate temperature dependence term $\theta_{EQ.}^{\omega-2}$

would have a powerful effect on the results. Here we have found it to enter as $(\theta_{EQ.}^{\omega-2})_{AV.}^{-1/2}$; one would expect a decrease in ω to reduce the size of the deviations on a highly cooled wall for a given value of ζ.

Laminar Boundary Layer Flow

A small perturbation analysis of the boundary layer equations can be carried out near the thermodynamic equilibrium extreme in the same manner as Couette flow problem. The thermodynamic equilibrium solution ($\zeta \to \infty$) remains qualitatively the same, with the notable exception that the energy equation is a second order differential equation in the temperature variable (including effects of convection) instead of an algebraic relationship between the temperature and the concentration variables. The equilibrium specie-temperature relationships,* when inserted into the boundary layer energy equation, provide an equation from which the thermodynamic equilibrium boundary layer temperature distribution is determined. For this purpose, the following enthalpy form is used since it is free from explicit reaction rate terms (the temperature distribution can subsequently be calculated from the relation $h = \Sigma \alpha_i h_i$):

$$f\frac{\partial g_{EQ.}}{\partial \eta} + \frac{\partial}{\partial \eta}\left\{\frac{C}{P_R}\frac{\partial g_{EQ.}}{\partial \eta}\left\langle 1+(L_e-1)\left[\alpha_{2e}\left(\frac{h_2-h_1}{h_{se}}\right)\frac{d\beta_{EQ.}}{dg_{EQ.}} + \alpha_{4e}\left(\frac{h_4-h_1}{h_{se}}\right)\frac{d\chi_{EQ.}}{dg_{EQ.}}\right]\right\rangle + C\left(\frac{P_R-1}{P_R}\right)\left(\frac{u_e^2}{2h_{se}}\right)\frac{\partial}{\partial \eta}\left(\frac{\partial f}{\partial \eta}\right)^2\right\} = 2\xi\left(\frac{\partial f}{\partial \eta}\frac{\partial g_{EQ.}}{\partial \xi} - \frac{\partial f}{\partial \xi}\frac{\partial g_{EQ.}}{\partial \eta}\right) \tag{5.60}$$

where

$$g_{EQ.} = \frac{h_{EQ.}}{h_{se}} + \left(\frac{u_e^2}{2h_{se}}\right)\left(\frac{\partial f}{\partial \eta}\right)^2 \tag{5.61}$$

and $d\beta_{EQ}/dg_{EQ.} = (d\beta_{EQ.}/d\theta_{EQ.})/(dg_{EQ.}/d\theta_{EQ.})$, etc.

---

* For equilibrium, these relations can also be viewed as giving z_{EQ}, χ_{EQ} and w_{EQ} as functions of enthalpy as well as θ_{EQ}, since the equilibrium temperature and enthalpy are directly related.

For example, the assumption of similarity (neglect of ξ derivatives) and $P_R = L_e = C = 1$ permits Equation (5.60) to be integrated to the following solution:*

$$g_{EQ.} = g_{EQ.}(0) + .47\, P_R^{1/3}\left[1 - g_{EQ.}(0)\right]\int_0^{\eta} EXP\left(-P_R\int_0^{\eta} f\, d\eta\right) d\eta \qquad (5.62)$$

from which the equilibrium temperature distribution can be calculated through Equation (5.61) by using

$$h_{EQ.} = \int_0^{T_{EQ.}} c_{p_1}\, dT + \alpha_{2_{EQ.}}\int_0^{T_{EQ.}} (c_{p_2} - c_{p_1})\, dT + \alpha_{2_{EQ.}}\, h_2^{(0)} + \alpha_{4_{EQ.}}\, h_4^{(0)}. \qquad (5.63)$$

The equilibrium heat transfer in general would be found from Equation (3.20) using the relations $\partial z/\partial\eta = \left(\frac{dz_{EQ.}}{dg_{EQ.}}\right)\partial g/\partial\eta$, etc. to express the composition in terms of the stagnation enthalpy variable.

Deviations From Thermodynamic Equilibrium

The behavior of the boundary layer equations near equilibrium can be investigated by assuming expansions of the dependent variables as in Equations (5.28-5.30). While it has been found that deviations from the opposite chemically frozen extreme can be taken in the form of a series of ascending positive powers of ζ for small ζ ($Z = z_I \cdot \zeta + z_{II}\zeta^2 + \cdots$, for example), an analogous attempt to assume at the start that the thermodynamic equilibrium deviations are a series of negative powers of ζ for large ζ fails. (The resulting equations governing the deviation variables turn out to be algebraic and consequently incapable of satisfying the required surface boundary conditions). Substituting expansions (5.28) and (5.29) into the boundary layer equations, using the simplifying assumptions that were invoked

---

* A numerical solution to Equation (5.60) for P_R, $L_e \neq 1$ has been given at the stagnation point in reference 6.

for the chemically frozen perturbation analysis,* and retaining only first order terms in the deviation functions, we find that the deviations are governed by the following second order, linear, non-homogeneous differential equations:

$$S_c f \frac{dZ}{d\eta} + \frac{d^2 Z}{d\eta^2} = \frac{2\alpha_{2e} S \theta_{EQ}^{\omega-2}}{\epsilon(1+\alpha_e)}\left(E_{\beta_2} Z + E_{\chi_2} X + E_{W_2} W + E_{\theta_2}\theta\right) + 2 S_c f' \xi \frac{dZ}{d\xi} - \left(S_c f' \frac{d\beta_{EQ}}{d\eta} + \frac{d^2\beta_{EQ}}{d\eta^2} - 2 f' S_c \xi \frac{d\beta_{EQ}}{d\xi}\right) \tag{5.64}$$

$$S_c f \frac{dX}{d\eta} + \frac{d^2 X}{d\eta^2} = \frac{2\alpha_{4e} S \theta_{EQ}^{\omega-2}}{\epsilon(1+\alpha_e)}\left(E_{\beta_4} Z + E_{\chi_4} X + E_{W_4} W + E_{\theta_4}\theta\right) + 2 S_c f' \xi \frac{dX}{d\xi} - \left(S_c f' \frac{d\chi_{EQ}}{d\eta} + \frac{d^2\chi_{EQ}}{d\eta^2} - 2 f' S_c \xi \frac{d\chi_{EQ}}{d\xi}\right) \tag{5.65}$$

$$S_c f \frac{dW}{d\eta} + \frac{d^2 W}{d\eta^2} = -\left(\frac{\alpha_{4e}}{\alpha_{3e}}\right)\frac{2\alpha_{4e} S \theta_{EQ}^{\omega-2}}{\epsilon(1+\alpha_e)}\left(E_{\beta_4} Z + E_{\chi_4} X + E_{W_4} W + E_{\theta_4} W\right) + 2 S_c f' \xi \frac{dW}{d\xi} - \left(S_c f' \frac{dW_{EQ}}{d\eta} + \frac{d^2 W_{EQ}}{d\eta^2} - 2 f' S_c \xi \frac{dW_{EQ}}{d\xi}\right) \tag{5.66}$$

$$P_R f \frac{d\theta}{d\eta} + \frac{d^2\theta}{d\eta^2} + 2 P_R \left(\frac{u_e^2}{c_{p_e} T_e}\right)\frac{e}{\epsilon} f' \theta_{EQ}\left[\frac{\alpha_{2e}(1+\beta_{EQ})}{1+\alpha_e}\left(\frac{\theta}{\theta_{EQ}} - \frac{Z}{1+\beta_{EQ}}\right) + \frac{\alpha_{4e}(1-\chi_{EQ})}{1+\alpha_e}\left(\frac{\theta}{\theta_{EQ}} - \frac{X}{1-\chi_{EQ}}\right)\right] = -\frac{2\alpha_{2e} L_e S \theta_{EQ}^{\omega-2}}{\epsilon(1+\alpha_e)}\left\{q_2\left[E_{\beta_2} Z + E_{\chi_2} X + E_{W_2} W + E_{\theta_2}\theta\right] + \frac{\alpha_{4e}}{\alpha_{2e}} q_4\left[E_{\beta_4} Z + E_{\chi_4} X + E_{W_4} W + E_{\theta_4}\theta\right]\right\} + 2 P_R f' \xi \frac{d\theta}{d\xi} - \left(P_R f \frac{d\theta_{EQ}}{d\eta} + \frac{d^2\theta_{EQ}}{d\eta^2} - 2 P_R f' \xi \frac{d\theta_{EQ}}{d\xi}\right). \tag{5.67}$$

The heat transfer deviation is given by

$$-\left(\frac{P_R}{c_{p_e} T_e}\sqrt{\frac{2X}{\rho_R \mu_R \epsilon u_e}}\,\dot{Q}_W\right)_I \equiv Q_I = \left[\frac{d\theta}{d\eta} + L_e\left(q_2 \frac{dZ}{d\eta} + q_4 \frac{dX}{d\eta}\right)\right]_{\eta=0}. \tag{5.68}$$

---

* $\rho\mu$ = constant, P_R and S_c constants, $C_{p_1} = C_{p_2}$ = constant, and velocity profile perturbations negligible.

The attending boundary conditions to be satisfied at the edge of the boundary layer ($\eta \to \infty$) are

$$Z(\infty) = X(\infty) = W(\infty) = \theta'(\infty) = 0 \; ;$$

those applicable to the inner surface are given by Equations (5.35) and (5.36). An inspection of Equations (5.65) and (5.66), in view of the boundary conditions, leads to the following solution for W :

$$W = - \frac{q_{4e}}{\alpha_{3e}} \cdot X \; , \tag{5.69}$$

the same result found in the chemically frozen deviation regime.

Before attempting any detailed solution of the above equations, some general characteristics of the problem are worth noting in advance. First, it is seen that the reaction rate derivative coefficients and the $\theta_{EQ.}^{\omega-2}$ term vary throughout the boundary layer, complicating the mathematics in the same way as encountered in the Couette flow problem. Second, the coupling between Z , X and θ demands a simultaneous solution of the above equations to obtain higher order uncoupled differential equations for each variable. In the boundary layer case, since the energy equation is a second order differential equation, the resulting order of these individual equations for Z , X and θ will be sixth (instead of fourth order in the Couette flow problem, where the energy equation was an algebraic relation). In this respect, the boundary layer problem is much more complicated than the Couette flow. This feature of coupling between the variables did not arise in the chemically frozen perturbation analysis because the first order reaction rate terms were non-homogeneous functions $\mathcal{Y}_{3,4}$ evaluated at the frozen flow solution that (contrary to the present thermodynamic equilibrium

analysis) do not vanish. Consequently, the thermodynamic equilibrium perturbation analysis is far more complicated mathematically than the frozen perturbation analysis. Third, the presence of the convection terms in the boundary layer equations adds a further complication in the form of the variable velocity function coefficients that is absent in the Couette flow problem.

The foregoing considerations suggest that the treatment of the general thermodynamic equilibrium deviation problem poses even more formidable a mathematical task than the foregoing Couette flow analysis. A detailed analysis of the present problem which includes all of the above complicating features would demand digital computation. Accordingly, some simplifying assumptions must be introduced in order to obtain any physical insight as to the behavior of the laminar boundary layer near thermodynamic equilibrium. Several of these approximations are similar to those used in the above Couette flow analysis. (a) Assume that the equilibrium solution is locally similar ($\partial z_{EQ.}/\partial\xi = \partial\chi_{EQ.}/\partial\xi = \partial\theta_{EQ.}/\partial\xi \simeq 0$). This is a satisfactory assumption provided the freestream temperature is slowly-varying along the body and the wall is highly cooled. (b) Neglect the $\beta \cdot (U_e^2/c_{p_e}T_e)$ terms in the temperature deviation equations, according to the arguments given for the frozen deviation case. (c) Assume $L_e = 1$. This assumption, which causes the total enthalpy distribution and heat transfer on a catalytic wall to be invariant to gas reaction, permits a simple integration of the energy equation and greatly facilitates the present objective of a qualitative appraisal of specie and temperature deviations. Furthermore, this assumption does not significantly alter the individual specie and temperature behavior from that at $L_e \neq 1$ when

L_e is near unity, and has little effect on the non-catalytic wall heat transfer. (d) Assume that the deviation functions depend on ξ only through the local non-equilibrium parameter $\zeta(x)$ for a slowly-varying freestream, i.e.,

$$\frac{\partial}{\partial \xi} = \frac{d\zeta}{d\xi} \frac{\partial}{\partial \zeta} .$$

Then the $\partial/\partial\xi$ terms in the deviation equations assume the form

$$\frac{Q}{\epsilon} \cdot \zeta \frac{\partial (\text{DEVIATION})}{\partial \zeta}$$

where $Q/\epsilon \equiv (\partial\zeta/\partial\xi)/(\zeta/\xi)$. Now the Couette flow results have indicated that for $\zeta \gg 1$, the near-equilibrium behavior (at least in the vicinity of the wall) depends on ζ as

$$\text{DEVIATION} \propto \frac{1}{\sqrt{\zeta}}$$

so that

$$(Q/\epsilon) \cdot \zeta \frac{\partial(\text{DEVIATION})}{\partial \zeta} \propto \frac{Q/\epsilon}{\sqrt{\zeta}} .$$

Therefore when $Q/\epsilon \sim O(1)$ and $\zeta \gg 1$, we can ignore the ξ dependence of the deviations in comparison with the η dependence across the boundary layer. (e) The first and second atomic specie deviations will be assumed to be proportional:

$$\mathcal{X} = A\mathcal{Z} = \frac{\chi'_{EQ.}(0)}{\beta'_{EQ.}(0)} \mathcal{Z} . \qquad (5.70)$$

This assumption uncouples the two atomic specie deviation Equations (5.64) and (5.65).

An immediate consequence of the foregoing assumptions is the integration of the perturbation energy equation, avoiding the need to use Equation (5.67). When $L_e = 1$ and the velocity profile deviation is neglected, the total enthalpy perturbation

$$\left(\frac{h_{se}}{c_{p_1} T_e}\right)(g - g_{EQ.}) \equiv \mathcal{T} = \mathcal{O} + g_2 Z + g_4 \mathcal{I} \tag{5.71}$$

for $C_{p_1} = C_{p_2}$ = constant is governed (from Equation (3.14)) by the following equation:

$$f P_R \mathcal{T}' + \mathcal{T}'' = 0 \ . \tag{5.72}$$

Equation (5.72) can be integrated twice with the outer boundary conditions $\mathcal{O}(\infty) = Z(\infty) = \mathcal{I}(\infty) = \mathcal{T}(\infty) = 0$ to give

$$\mathcal{T}(\eta) = \mathcal{T}(0)\left[1 - .47 P_R^{1/3} \int_0^\eta EXP\left(-P_R \int_0^\eta f\, d\eta\right) d\eta\right] \tag{5.73}$$

where

$$\mathcal{T}(0) = g_2 Z(0) + g_4 \mathcal{I}(0) = (g_2 + A g_4) Z(0) \tag{5.74}$$

$$\mathcal{T}'(0) = -.47 P_R^{1/3}\, \mathcal{T}(0). \tag{5.75}$$

For a catalytic wall, $\mathcal{T}(o) = 0$ and we get the well-known result $\mathcal{O} + q_2 Z + q_4 \mathcal{I} = 0$ for a Fick diffusion law with $L_e = 1$. On the other hand, a non-catalytic wall leaves $\mathcal{T}(o)$ to be determined as a parameter in the equations and $\mathcal{T}'(o)$ is given by Equation (5.75). By means of this solution for $\mathcal{T}$, we can express the temperature deviation in terms of the atomic specie deviation. Since $\mathcal{I}$, W and $\mathcal{O}$ are now expressed in terms of the single unknown $Z(\eta)$, we have to solve the following linear ordinary non-homogeneous second order differential equation (substituting the aforementioned approximations into Equation (5.64)):

$$S_c f Z' + Z'' - J F_1(\eta) \cdot Z = J F_2(\eta) \mathcal{T} - S_c f \beta'_{EQ.} - \beta''_{EQ.} \tag{5.76}$$

where

$$F_1(\eta) = \frac{2\alpha_{2e}}{\epsilon(1+\alpha_e)} \theta_{EQ.}^{\omega-2} \left[\mathbb{E}_{g_2} - g_2 \mathbb{E}_{\theta_2} + A\left(\mathbb{E}_{\chi_2} - \frac{\gamma_{4e}}{\gamma_{3e}} \mathbb{E}_{W_2} - g_4 \mathbb{E}_{\theta_2}\right)\right] \tag{5.77}$$

and

$$\mathcal{F}_2(\eta) = \frac{2\alpha_{2e}\,\theta_{EQ.}^{\omega-2}}{\epsilon(1+\alpha_e)}\,\mathcal{D}_{\theta_2} \tag{5.78}$$

are predominately positive and negative, respectively, throughout a highly cooled laminar boundary layer.

Approximate Solution

The variable and cumbersome coefficients $\mathcal{F}_1$ and $\mathcal{F}_2$ would demand a lengthy numerical integration of Equation (5.76) if an exact solution for were desired. However, we shall sacrifice a certain quantitative error in the solution, as was done in the Couette flow case, by assuming average constant values $\mathcal{F}_1^*$ and $\mathcal{F}_2^*(<0)$ for these functions. This approximation should still preserve the qualitative features of the near-equilibrium behavior. Furthermore, it has been found during the course of a study of the solutions to Equation (5.76) that the convection terms $S_c f Z'$ and $S_c' f z_{EQ}'$ exert a very small affect on the behavior of $Z(\eta)$ over the inner part of the boundary layer for either wall catalysis extreme when $\zeta \gg 1$. These two terms can be neglected in the present approximate analysis. Finally, the functions $\mathcal{T}(\eta)$ and $z_{EQ}(\eta)$ will be approximated by the following approximate expansions near a cooled wall:

$$\begin{aligned} \mathcal{T}(\eta) &\simeq \mathcal{T}(0)\cdot(1-.47\,Pr^{1/3}\eta) \\ \beta_{EQ.}(\eta) &\simeq \beta_{EQ.}'(0)\cdot\eta + \tfrac{1}{2}\beta_{EQ.}''(0)\cdot\eta^2 \end{aligned} \tag{5.79}$$

These two approximations are adequate for the present objective of describing the non-equilibrium behavior only in the vicinity of the wall. They enable a simple particular solution of Equation (5.76) to be obtained.

Utilizing the foregoing approximations, the complementary solution to the associated homogeneous equation

$$S_c f Z_c' + Z_c'' - \zeta\, Z_c = 0 \tag{5.80}$$

is

$$Z_c = C_1 \exp(\sqrt{\zeta\mathcal{F}_1^*}\,\eta) + C_2 \exp(-\sqrt{\zeta\mathcal{F}_1^*}\,\eta), \tag{5.81}$$

and a particular non-homogeneous integral to Equation (5.76) is

$$Z_p \simeq -\frac{\mathcal{F}_2^*}{\mathcal{F}_1^*}\,\mathcal{F}(0)\left(1-.47\,P_R^{1/3}\eta\right)+\frac{\beta_{EQ.}''(0)}{\zeta\mathcal{F}_1^*}\,. \tag{5.82}$$

The complete solution $Z = Z_c + Z_p$ involves the two arbitrary constants C_1, C_2 which are chosen so as to satisfy the boundary conditions $Z(\infty) = 0$ and either $Z(o) = \mathcal{F}(o) = 0$ (catalytic wall) or $Z'(o) = -z'_{EQ.}(o)$ (non-catalytic wall). Since the present theory is really valid only for the inner part of the boundary layer, however, the $Z(\infty) = 0$ condition shall be applied at an effective "infinity" $\eta = \bar{\eta}$ for which the approximate $\mathcal{F}(\eta)$ function in Equation (5.79) vanishes:

$$\bar{\eta} = \left(.47\,P_R^{1/3}\right)^{-1}.$$

The results for the wall deviations* when $\zeta \gg 1$ are as follows:

$$\left[Z'(0)\right]_{CAT.} = \frac{\beta_{EQ.}''(0)}{2\sqrt{\zeta\mathcal{F}_1^*}} \tag{5.83}$$

$$\left[Z(0)\right]_{NON\text{-}CAT.} = \frac{\beta_{EQ.}'(0)}{\left[1+(g_2+A g_4)\frac{\mathcal{F}_2^*}{\mathcal{F}_1^*}\right]\sqrt{\zeta\mathcal{F}_1^*}}\,. \tag{5.84}$$

These are essentially the same results that were found in the Couette flow case, which is not too surprising when we note that convective effects play a fairly weak role in the above development for $\zeta \gg 1$. The deviations (5.83) and (5.84) exhibit the same general properties that were discussed for the Couette flow; both vanish as $1/\sqrt{\zeta\,\mathcal{F}_1^*}$ when $\zeta \to \infty$ and the catalytic wall case demands a consideration of the non-linearity in $z_{EQ.}(\theta_{EQ.})$ in order to determine the sign of $z''_{EQ.}(o)$. We have

---

* In view of the various approximations introduced, we shall confine further discussion to deviations in the immediate vicinity of the wall.

$$\beta_{EQ.}'(0) = \frac{d\beta_{EQ.}}{d\theta_{EQ.}}\,\theta_{EQ.}'(0)$$

$$\beta_{EQ.}''(0) = \frac{d^2\beta_{EQ.}}{d\theta_{EQ.}^2}\,\theta_{EQ.}'^2(0) + \frac{d\beta_{EQ.}}{d\theta_{EQ.}}\,\theta_{EQ.}''(0).$$

Using the approximate equilibrium energy equation solution (5.62) and Equation (5.63), we have the equilibrium temperature derivatives($C_{p_2} = C_{p_1}$) as

$$\theta_{EQ.}'(0) = \left(\frac{h_{se}}{C_p T_e}\right)\left[\frac{.47\, P_R^{1/3}(1-g_w)}{1+\frac{d\beta_{EQ.}}{d\theta_{EQ.}}(0)\cdot(g_2+A\,g_4)}\right] \tag{5.85}$$

$$\theta_{EQ.}''(0) = \frac{-(u_e^2/C_p T_e)f''^2(0) - \theta_{EQ}'^2(0)\left[g_2\frac{d^2\beta_{EQ.}}{d\theta_{EQ.}^2}(0) + g_4\frac{d^2\chi_{EQ.}}{d\theta_{EQ.}^2}(0)\right]}{1+\frac{d\beta_{EQ.}}{d\theta_{EQ.}}(0)\cdot(g_2+A\,g_4)}. \tag{5.86}$$

$z_{EQ.}'(o)$ is always positive; $z_{EQ.}''(o)$ on the other hand becomes

$$\beta_{EQ.}''(0) = \frac{-\frac{d\beta_{EQ.}}{d\theta_{EQ.}}(0)\left(\frac{u_e^2}{C_p T_e}\right)f''^2(0) + \theta_{EQ.}'^2(0)\left\{\frac{d^2\beta_{EQ.}}{d\theta_{EQ.}^2}(0)\left[1-g_2\frac{d\beta_{EQ.}}{d\theta_{EQ.}}(0)\right] - g_4\frac{d\beta_{EQ.}}{d\theta_{EQ.}}(0)\frac{d^2\chi_{EQ.}}{d\theta_{EQ.}^2}(0)\right\}}{1+\frac{d\beta_{EQ.}}{d\theta_{EQ.}}(0)\cdot(g_2+A\,g_4)}. \tag{5.87}$$

The viscous dissipation tends to decrease $\theta_{EQ.}''(o)$ and the catalytic wall specie gradient deviation, whereas a significant non-linearity in $z_{EQ.}(\theta_{EQ.})$ will make $\theta_{EQ.}''(o)$ and $[Z'(o)]_{CAT.}$ positive on a highly cooled wall ($z_{EQ.}'(o)$ small). The non-catalytic specie deviation is not sensitive to this non-linear effect; $Z(o)$ approaches zero as $\zeta \to \infty$ with a constant derivative $Z'(o) = -z_{EQ.}'(o)$ at the wall. This behavior, as previously pointed out,

means that the non-catalytic deviations due to a departure from thermodynamic equilibrium are largest at the wall and decay outward over a "sublayer" thickness $Z(o)/z'_{EQ_o}(o) \propto 1/\sqrt{\bar{\rho}_1^* \zeta}$.

The temperature gradient perturbation is related directly to the specie variables by Equation (5.75):

$$\mathcal{T}'(0) = \Theta'(0) + (\beta_2 + A\beta_4) Z'(0) = -.47 P_R^{1/3} (\beta_2 + A\beta_4) \cdot Z(0).$$

Therefore,

$$\left[\Theta'(0)\right]_{CAT} = -(\beta_2 + A\beta_4)\left[Z'(0)\right]_{CAT.} = -\frac{(\beta_2 + A\beta_4)\beta_{EQ}''(0)}{\sqrt{\zeta \bar{\rho}_1^*}} \qquad (5.88)$$

and

$$\left[\Theta'(0)\right]_{NON-CAT} = -(\beta_2 + A\beta_4)\beta_{EQ}'(0)\left\{\frac{.47 P_R^{1/3}}{\left[1 + (\beta_2 + A\beta_4)\frac{\bar{\rho}_2^*}{\bar{\rho}_1^*}\right]\sqrt{\zeta \bar{\rho}_1^*}} - 1\right\}. \qquad (5.89)$$

The catalytic wall gradient will decrease with a departure from thermodynamic equilibrium when $z''_{EQ_o}(o)$ is positive (very highly cooled wall). The non-catalytic wall perturbation, however, does not vanish at $\zeta \to \infty$ because of the $Z'(o) = - z'_{EQ_o}(o)$ boundary condition. As the boundary layer departs from equilibrium, the non-catalytic wall temperature gradient will decrease; the temperature deviation correspondingly grows within a sublayer adjacent to the wall whose thickness spreads as $1/\sqrt{\zeta \bar{\rho}_1^*}$. The deviation profile behavior near the wall implied by these simple results is shown qualitatively in Figure 27. This Figure illustrates the sublayer behavior on a non-catalytic wall and the change in the sign of the catalytic wall perturbations when the wall is not highly cooled enough to give $z''_{EQ_o}(o) > 0$ (Equation 5.87). As $\zeta \to \infty$, the non-catalytic specie and temperature perturbations vanish at $\eta > 0$, leaving only a discontinuity in $Z'(o)$ and $\Theta'(o)$ at the wall that is

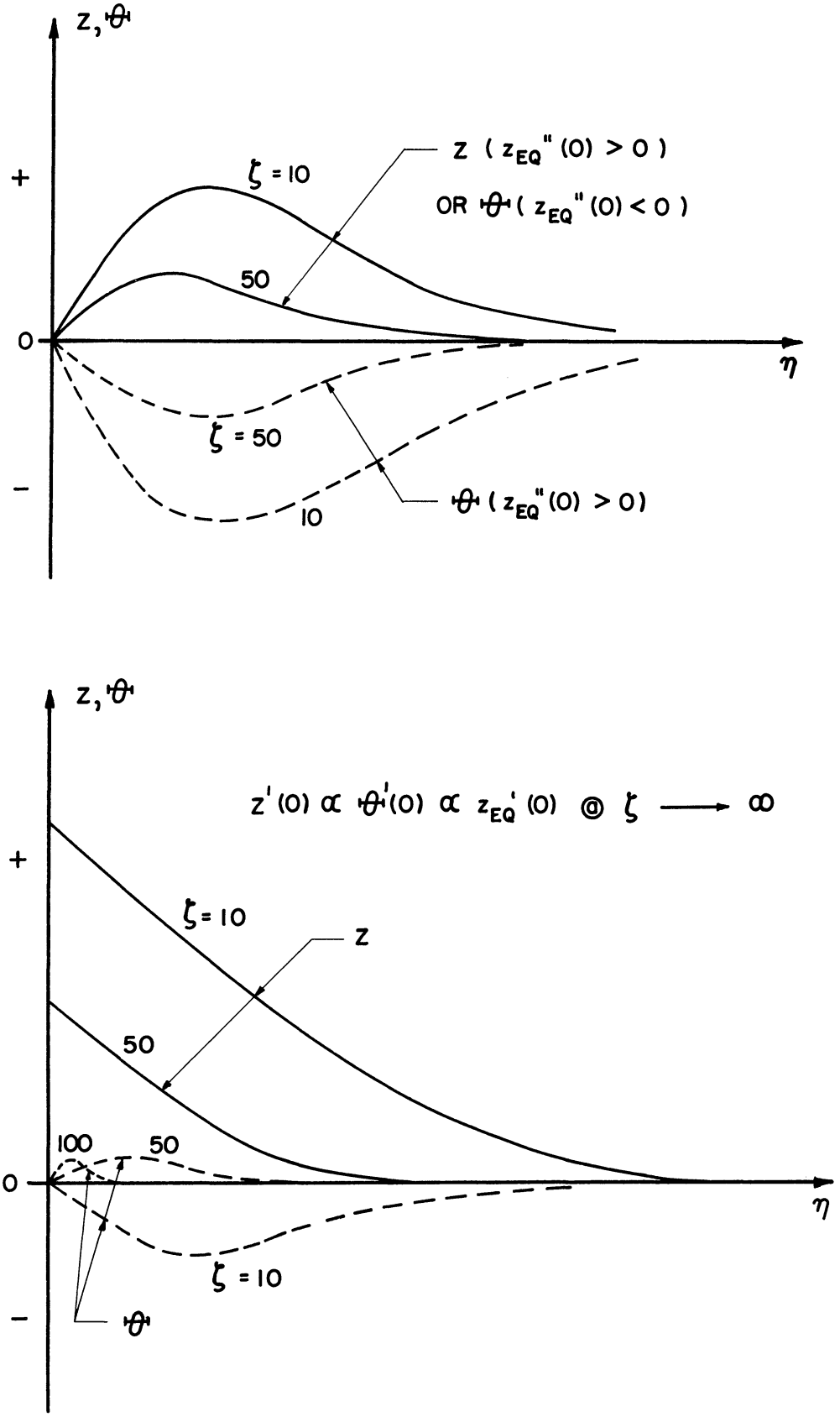

Figure 27. Illustration of Thermodynamic Equilibrium Deviations in the Highly Cooled Laminar Boundary Layer.

proportional to the equilibrium diffusion velocity $z'_{EQ}(o)$. For a very highly cooled wall, such a discontinuity is extremely small.

The heat transfer perturbation is given by Equation (5.68):

$$Q_I = \Theta'(0) + Le(g_2 + A g_4) Z'(0).$$

The catalytic wall value is exactly zero for $L_e = 1$. Using the previously found values for $\Theta'(o)$ and $Z'(o)$ (computed for $L_e = 1$) as estimates, the above equation shows that

$$\left[Q_I\right]_{\substack{CAT. \\ Le \neq 1}} \simeq (Le-1)(g_2 + A g_4) \frac{\beta_{EQ.}''(0)}{2\sqrt{\beta F_1^*}} . \qquad (5.90)$$

This predicts that the catalytic wall heat transfer for $L_e > 1$ will increase due to non-equilibrium when $z''_{EQ}(o) > 0$. This agrees with the result of Fay and Riddell.[6] The non-catalytic heat transfer perturbation, on the other hand, becomes

$$\left[Q_I\right]_{NON-CAT.} = - \frac{.47 P_R^{1/3} (g_2 + A g_4) \beta_{EQ.}'(0)}{\left[1 + \left(\frac{F_2^*}{F_1^*}\right)(g_2 + A g_4)\right] \sqrt{\beta F_1^*}} . \qquad (5.91)$$

While the non-catalytic temperature and specie gradient perturbations have been shown non-vanishing in general for $\zeta \to \infty$, the net heat transfer deviation does vanish at the thermodynamic equilibrium extreme. The above heat transfer deviations vary with ζ as $1/\sqrt{\zeta}$ according to the present highly simplified analysis. This prediction is confirmed by an analysis of the near-equilibrium heat transfer behavior given in Reference 6, which shows a $1/\sqrt{\zeta}$ dependence on ζ when $\zeta \gg 1$. This agreement lends some confidence as to the value of a simplified qualitative approach in assessing the main physical features of departures from thermodynamic equilibrium.

Further Discussion of Results

The foregoing results provide some qualitative understanding of the near-equilibrium behavior in the boundary layer and would no doubt also be valuable as a guide in interpreting more exact and detailed solutions. No attempt has been made at an exhaustive discussion of the results in view of the admitted error in the magnitude of the predictions. However, the simplified analysis does provide three major conclusions of some importance: (a) The non-linearity of the equilibrium atomic specie-temperature relation must be taken into account even in a simple theory if accurate catalytic wall non-equilibrium behavior is to be obtained. When the wall is not highly cooled and, or viscous dissipation is important, the catalytic wall heat transfer may decrease with a departure from thermodynamic equilibrium in spite of a non-linear effect. The non-catalytic wall is not sensitive to this non-linearity, however. (b) The catalytic wall diffusion, heat conduction and heat transfer deviations vanish as $1/\sqrt{\zeta}$ for $\zeta \to \infty$. The surface reaction requirement $z(o) = z_{EQ}(o)$ is completely compatible with the equilibrium concentration distribution near the wall in this case. When the wall is reaction-free, however, the equilibrium concentration gradient $z'_{EQ}(o)$ in the gas (computed solely on the basis of the equilibrium temperature distribution) does not strictly agree with the zero diffusion requirement $z'(o) = 0$ right at the surface. Consequently, there is actually a state of non-equilibrium in the gas within an extremely thin layer adjacent to the wall when $\zeta \to \infty$. We have found that the non-catalytic wall specie and temperature gradient perturbations do not vanish at $\zeta \to \infty$ but remain proportional to the change of z' required across the sublayer (namely $- z'_{EQ}(o)$). The temperature and specie concentration deviations themselves do become vanishingly small within this sublayer,

however. When the boundary deviates from thermodynamic equilibrium because of a decrease in ζ, the sublayer thickness grows as $1/\sqrt{\zeta}$ and the non-equilibrium perturbations grow in size and spread out laterally from wall into the flow (driven, so to speak, by the specie gradient jump existing at the wall when the remaining portion of the flow is at equilibrium). The total energy flux across the thin sublayer must be constant and therefore cannot show any discontinuous behavior across it; the non-equilibrium heat transfer perturbation therefore vanishes as $1/\sqrt{\zeta}$ when $\zeta \to \infty$ even though the individual temperature and atomic specie wall gradients do not. (c) The favorable agreement between the approximate Couette flow and laminar boundary layer analysis indicates that the former is a dependable qualitative model of the dissociation-recombination non-equilibrium behavior in the latter problem.

CHAPTER VI

CONCLUSION

Summary

There are two primary objectives connected with the present study: (a) a description of the basic theoretical features which are involved in the formulation of a chemically reacting gas mixture flow problem, particularly those which are important in the study of dissociation-recombination non-equilibrium, and (b) a detailed study of the non-equilibrium effects in a highly cooled dissociated laminar boundary layer as they affect deviations in composition, temperature and heat transfer from either a chemically frozen or thermodynamic equilibrium flow extreme. Objective (a) has lead to the consideration of a four component representation of an air mixture with the attending formulation of multicomponent gas mixture diffusion and reaction rates. It has also required that we consider the effect of possible surface-catalyzed recombination reactions entering the problem through the composition variable boundary conditions. Finally, objective (a) lead to the definition and interpretation of the basic characteristic reaction time - flow time ratios which naturally appear in such flow problems. These parameters have been used to establish the hypersonic flight regimes in which gaseous non-equilibrium and non-catalytic surface effects become important (Figures 2 and 6), and also to illustrate the fact that the non-equilibrium state of the boundary can vary widely over the length of a typical blunt-nosed hypersonic body (Figure 4). Objective (b) has been concerned with the effect of the various significant aerodynamic and

chemical parameters (such as recombination rate temperature dependence, activation energy of the atomic species, the extremes of the surface catalysis effect, and the dependence on the local non-equilibrium parameter) on the non-equilibrium deviations. The governing equations were cast into the well-known "similarity plane" form by means of the Stewartson-Mangler-Blasius transformation. The similarity limitations for an arbitrary degree of non-equilibrium, plus the desire to study the initial trends from the two chemical behavior extremes without the use of digital computation, led to the development of a chemical perturbation analysis which is applicable over a fairly wide range of local flow conditions at the edge of the boundary layer. The introduction of suitable approximations for the highly cooled wall case enables the equations governing the deviations from both chemically frozen and thermodynamic equilibrium extremes to be reduced to sets of linear ordinary differential equations which can be solved by standard methods. The effect of the aforementioned significant parameters on the composition, temperature and heat transfer deviations was given in detail for the chemically frozen regime, whereas a qualitative analysis was given of the near-thermodynamic equilibrium behavior because the latter case is so much more cumbersome from a numerical standpoint. However, in both cases, the important physical mechanisms "driving" the non-equilibrium behavior have been clearly displayed.

General Conclusions

The detailed results of the investigation summarized above can be used to infer a number of rather general conclusions about the important theoretical elements required for any non-equilibrium theory and the actual

behavior of the non-equilibrium deviations encountered in a highly cooled laminar boundary layer (with surface mass transfer absent).

(a) Variable $\rho\mu$ and unequal specific heat data, which can be feasibly included only when a digital computation is utilized in solving the governing equations, appear to have a minor effect on the non-equilibrium deviations. These variables do play a role of some significance in the chemically frozen and thermodynamic equilibrium flow extremes for the case of a catalytic wall: the variable $\rho\mu$ tends to reduce the wall composition and temperature gradients by roughly 50%, whereas the unequal specific heat effect acts in the opposite direction in tending to increase the wall temperature gradient proportionally to $(c_{p_2}-c_{p_1})\,\alpha_e$. The heat transfer is affected much less than the temperature gradient by the specific heat inequality.

(b) The results of the present theory, when compared to other solutions for a particular case,[6] have already brought out the importance of accounting for individual specie behavior in formulating reaction rates in the gas when the detailed non-equilibrium behavior is to be studied. The use of an equivalent binary system of lumped atomic and molecular species can overestimate the initial rate of deviation from frozen flow by as much as 50% when a significant amount of atomic nitrogen exists in the flow. Care must also be taken when the individual rates are averaged over the respective heats of formation in the reaction rate heat source term which occurs in the temperature form of the energy equation.

(c) The use of Fick's diffusion law for each specie in a multicomponent air mixture is a satisfactory approximation, at least as far as the atomic specie and temperature behavior is concerned, for a cooled

boundary layer flow when there is no ablation, etc. of species with radically different properties into the main flow. Some error in the detailed molecular specie profiles will result from this assumption, however.

(d) It is important to account for the catalytic state of the wall surface when appraising non-equilibrium effects (particularly concerning heat transfer). The results of the present investigation have shown that the non-equilibrium deviations from the two chemical behavior extremes are much greater for a completely non-catalytic wall than for a completely catalytic one. The state of the wall catalysis is governed by a characteristic reaction time-flow time ratio that involves the surface temperature and material, as well as the diffusion and convection flow properties. For glassy-like wall, the non-catalytic condition appears a definite possibility in the hypersonic flight regimes for which significant non-equilibrium effects may occur ($M_\infty > 10$, altitudes above 100,000 ft.).

(e) The non-equilibrium state of the boundary layer can vary notably over the length of a hypersonic blunt-nosed body; the stagnation point situation is generally not an accurate indicator of the non-equilibrium behavior downstream along the body. Particularly in the neighborhood of the sonic region, the deviations from frozen flow appear to be as much as three times larger than those at the stagnation point. This variation of effect generally excludes the possibility of a local similarity solution to the full boundary layer equations except in the two chemcial behavior extremes. The use of a perturbation type of analysis, which sacrifices a consideration of non-equilibrium effects over the full range of ζ, gains however a wider

range of local application under varying freestream pressure and temperature.

(f) The non-equilibrium behavior on a highly cooled wall is sensitive to the value of the recombination rate temperature exponent ω, because of the dependence of the characteristic parameter ζ on ω and also because of the effect of the value of ω on the recombination rate in the governing equations. This effect is small only when ω is very near a value of two (and vanishes when $\omega \equiv 2$). The results of the frozen perturbation analysis will be of use in assessing the effect of any change in the recombination rate on the non-equilibrium behavior (Table II).

(g) The non-equilibrium behavior, insofar as can be deduced from the chemically frozen and thermodynamic equilibrium perturbation analyses, is very insensitive to large changes in the activation energy when the wall is highly cooled ($\theta_w \leq .20$). The difference between atomic oxygen and nitrogen activation energies therefore causes a very small difference between the non-equilibrium behavior of these two species; the deviations can be considered essentially proportional to each other. When the wall is not cooled, however, this conclusion is reversed; the activation energy may then play a very prominent role in the non-equilibrium behavior.

Chemically Frozen Deviations

Several conclusions specifically related to the frozen perturbation analysis are worth listing.

(a) The deviations in composition, temperature and heat transfer from the corresponding chemically frozen solutions behave as a series of

ascending powers of ζ, the initial deviation being linear in ζ and the second order terms being proportional to ζ^2 (these constitute subtractive corrections to the first order results). The coefficients of ζ, ζ^2, etc. are determined from a solution of the boundary layer equations governing each coefficient function. The analysis of the deviations becomes increasingly complex for the second and higher order effects.

(b) The frozen deviations, in addition to the dependence on ζ described in (a), also depend significantly on the local streamwise derivative of this factor, i.e., the parameter $Q/\epsilon \propto \frac{d\zeta/dX}{\zeta/X}$. When Q/ϵ is negative, the deviations increase rapidly with a decrease in Q/ϵ and can become 100 times the $Q = 0$ result (stagnation point) when $Q/\epsilon = -2$ (for a given value of ζ), for example. Positive Q/ϵ reduces the deviations to a much lesser extent (relative to $Q = 0$). This parameter Q/ϵ arises from the perturbation analysis of the governing boundary layer equations.

(c) The qualitative effects of non-equilibrium on the composition and temperature distribution in the boundary layer were found to be as follows: As ζ is increased, the catalytic wall diffusion current (atomic specie wall gradient) and non-catalytic wall atom concentration both decrease, the heat conduction in both catalysis extremes increases, the non-catalytic wall heat transfer (pure conduction) increases, and the catalytic wall heat transfer decreases very slightly for $L_e > 1$ (the decrease in diffusion of heat to the wall being slightly greater than the increase in heat conduction). While the catalytic wall deviations are always much smaller than those for the non-catalytic case at the same value of ζ when the Lewis number is of the order of one, both cases were found to exhibit about the

same insensitivity to the activation energy parameter for a highly cooled wall.

Thermodynamic Equilibrium Perturbation

The mathematics associated with this opposite extreme of the non-equilibrium effect "spectrum" and the complexity of the variable coefficients in the governing differential equations for the perturbations resulted in a much less detailed analysis of the problem than given in the chemically frozen regime. However, the main physical features behind the departure of composition and temperature distributions from exact equilibrium as ζ decreases were displayed and indicated several important conclusions.

(a) A series method of solution, in terms of ascending negative powers of ζ, is not a feasible method of attack. An approximate study of the general small deviations from equilibrium indicated that, at least near the wall, the deviations in heat transfer, catalytic atomic diffusion, catalytic heat conduction (temperature gradient) and non-catalytic wall atom concentration all vary as $1/\sqrt{\zeta}$ when $\zeta \gg 1$. The non-catalytic specie and temperature gradients do not vanish at $\zeta \to \infty$, however; they remain proportional to the equilibrium wall diffusion flux (which is extremely small for a very highly cooled wall).

(b) The catalytic wall non-equilibrium deviations depend significantly on the non-linearity of the equilibrium specie-temperature relationship, while the non-catalytic wall results do not. If the wall is not highly cooled, it has been found that this non-linear effect may cause the heat transfer deviation to be opposite in sign to that for the highly cooled situation (in the latter case, the heat transfer increases due to a

deviation from thermodynamic equilibrium for $L_e > 1$). This result should be useful as a guide in any future study of non-equilibrium flow over slightly cooled or "hot" surfaces.

(c) Like the frozen deviations, the thermodynamic equilibrium deviations are affected by changes in the recombination rate parameter ω. The results of the qualitative analysis, however, seem to indicate that this effect may be somewhat different in both magnitude and direction from that found in the chemically frozen perturbation analysis. Unlike the frozen case, however, the thermodynamic extreme does not appear to be sensitive to the non-equilibrium derivative factor Q/ϵ when $\zeta \gg 1$.

Limitations

By way of a conclusion to the present chapter, it is desirable to emphasize that the major conclusions listed above depend on several key assumptions made in the present theory. When conditions are not in agreement with these assumptions, many of the present results may be changed. In addition to the neglect of variable fluid properties, mass transfer (ablation, coolant injection, etc.), radiation, thermal diffusion, and electromagnetic body forces, there were three particularly important assumptions made in the course of formulating the governing equations for the non-equilibrium perturbations. (a) Slowly-varying freestream properties. The freestream temperature and velocity variations with X were assumed gradual enough to permit local similarity approximations to the behavior of the chemically frozen, thermodynamic equilibrium, and the non-equilibrium composition and temperature throughout the boundary layer. Such an assumption appears to be fairly reasonable provided there are no

shock waves or flame fronts impinging on the boundary layer, nor any abrupt changes in the body shape. (b) Neglect of any Nitric Oxide that may possibly be in the flow. Arguments based on rather sparse data tend to indicate that the small amounts of this constituent present in the air at the edge of the boundary are not significant to the calculation of non-equilibrium effects. However, should future improvements in the knowledge about the NO rates indicate that it may play a more important role, the present perturbation method can be repeated for a five component mixture including the NO recombination-dissociation chemistry.

(c) Assumption of a highly cooled wall. This is by far the most critical assumption, since many subsequent simplifications and conclusions are either directly or indirectly based on this condition (such as the neglect of velocity profile perturbations because of the insensitivity of the boundary layer momentum equation to the pressure gradient term, the predominance of recombination over dissociation in the reaction rate terms for the inner half of the boundary layer, the minor role generally played by viscous dissipation in the non-equilibrium behavior, and the neglect of surface-catalyzed dissociation reactions). When the wall is not highly cooled, it is expected that the effects of the recombination rate parameter α and the activation energy found in the present analysis may be somewhat reversed, the latter parameter playing a very prominant role in the non-equilibrium behavior. A non-equilibrium perturbation approach may still be a valuable tool in the "hot wall" problem, but it most certainly would demand a "fresh start" by a reappraisal of the proper theoretical approximations in the governing equations.

APPENDIX A

MULTICOMPONENT MIXTURE TRANSPORT COEFFICIENTS

Viscosity Coefficient

Reference 17 gives the following mixture value in terms of the individual component viscosities:

$$\mu = \sum_i \frac{\mu_i}{1 + \frac{n}{n_i} \sum_{j \neq i} \frac{n_j}{n} Q_{ij}}$$

where (A.1)

$$Q_{ij} = \frac{\sqrt{2}}{4} \frac{\left[1 + \sqrt{\mu_i/\mu_j}\,(M_j/M_i)^{1/4}\right]^2}{\sqrt{1 + M_i/M_j}} \,.$$

Diffusion Coefficient

Reference 16 gives the following expression for the N-component mixture diffusion coefficient:

$$D_{ij} = \frac{(-1)^{i+j} \tilde{F}^{ji} - \tilde{F}^{ii}}{n_j |\tilde{F}_{ij}|} \tag{A.2}$$

where

$$\tilde{F}_{ij} = (1 - \delta_{ij}) \left(\frac{n_i}{\rho \mathcal{D}_{ij}} + \frac{n_j}{\rho m_i} \sum_{k \neq i} \frac{n_k}{\mathcal{D}_{ik}} \right) \tag{A.3}$$

and where

$$|\tilde{F}_{ij}| = \begin{vmatrix} \tilde{F}_{11} & \tilde{F}_{12} & \cdots & \tilde{F}_{1N} \\ \tilde{F}_{21} & \tilde{F}_{22} & \cdots & \tilde{F}_{2N} \\ \vdots & \vdots & & \vdots \\ \tilde{F}_{N1} & \tilde{F}_{N2} & \cdots & \tilde{F}_{NN} \end{vmatrix}$$

and

$$\mathcal{F}^{ij} = \begin{vmatrix} \tilde{F}_{11} & \tilde{F}_{12} & \cdots & \tilde{F}_{1,j-1} & \tilde{F}_{1,j+1} & \cdots & \tilde{F}_{1N} \\ \tilde{F}_{21} & \tilde{F}_{22} & \cdots & \tilde{F}_{2,j-1} & \tilde{F}_{2,j+1} & \cdots & \tilde{F}_{2N} \\ \vdots & \vdots & & & & & \\ \tilde{F}_{i-1,1} & \tilde{F}_{i-1,2} & \cdots & \tilde{F}_{i-1,j-1} & \tilde{F}_{i-1,j+1} & \cdots & \tilde{F}_{i-1,N} \\ \tilde{F}_{i+1,1} & \tilde{F}_{i+1,2} & \cdots & \tilde{F}_{i+1,j-1} & \tilde{F}_{i+1,j+1} & \cdots & \tilde{F}_{i+1,N} \\ \vdots & \vdots & & \vdots & \vdots & & \vdots \\ \tilde{F}_{N,1} & \tilde{F}_{N,2} & \cdots & \tilde{F}_{N,j-1} & \tilde{F}_{N,j+1} & \cdots & \tilde{F}_{N,N} \end{vmatrix} \qquad \text{(A.4)}$$

and where by definition of binary diffusion,

$$\mathcal{D}_{ij} = \mathcal{D}_{ji} .$$

In the particular case of a three-component mixture, the above reduces to the simpler formula

$$D_{ij}/\mathcal{D}_{ij} = 1 + \frac{(m_k/m_j)\mathcal{D}_{ik} - \mathcal{D}_{ij}}{\mathcal{D}_{ij} + (m_i/m_k)\mathcal{D}_{jk} + (m_j/m_k)\mathcal{D}_{ik}} , \qquad \text{(A.5)}$$

with indices cyclically permuted; clearly this gives $D_{ij} = \mathcal{D}_{ij}$ only when $m_k = 0$ in general.

APPENDIX B

DIFFUSION COEFFICIENT RATIO ESTIMATES

Kinetic theory[16] yields the following expression for the binary diffusion coefficient between two gases:

$$\mathcal{D}_{ij} = \frac{\text{CONSTANT}}{\Omega_{ij}} \sqrt{\frac{T}{M}\left(\frac{m_i + m_j}{m_i m_j}\right)} \qquad \text{(B.1)}$$

where Ω_{ij} is a collision integral proportional to the mutal collision cross-section of the gas particles. When $i = j$, $\mathcal{D}_{ii}$ has the physical significance of a "self-diffusion" coefficient describing the kinetic motion of particular particles amongst other particular particles, such as isotopes of equal mass but different nuclei.

Consider a three component O_2, O, N_2 mixture (denoted by species 1, 2 and 3, respectively) with the approximations $m_1 = m_3 = 2m_2$; then

$$\frac{\mathcal{D}_{23}}{\mathcal{D}_{12}} = \frac{\Omega_{12}}{\Omega_{23}} \sqrt{\left(\frac{m_2 + m_3}{m_1 + m_2}\right)\frac{m_1}{m_3}} = \frac{\Omega_{12}}{\Omega_{23}} \qquad \text{(B.2)}$$

$$\frac{\mathcal{D}_{13}}{\mathcal{D}_{12}} = \frac{\Omega_{12}}{\Omega_{13}} \sqrt{\left(\frac{m_1 + m_3}{m_1 + m_2}\right)\frac{m_2}{m_3}} = \sqrt{\frac{2}{3}}\,\frac{\Omega_{12}}{\Omega_{13}} \,. \qquad \text{(B.3)}$$

Now take $\Omega_{ij} \sim (d_i/2 + d_i/2)^2$, where d_i is the i-th specie particle diameter. Then, for purposes of a rough estimate, take $d_1 = d_3 = 2d_2$ and hence obtain

$$\frac{\Omega_{12}}{\Omega_{23}} \simeq 1 \,, \quad \frac{\Omega_{12}}{\Omega_{13}} \simeq \left(\frac{3}{4}\right)^2 = .563 \,. \qquad \text{(B.4)}$$

Consequently we have from Equations (B.2) and (B.3) the estimates

$$\mathcal{D}_{23}/\mathcal{D}_{12} = 1 \tag{B.5}$$

$$\mathcal{D}_{13}/\mathcal{D}_{12} = \sqrt{\tfrac{2}{3}} \times .563 = .460 \approx \tfrac{1}{2} \; . \tag{B.6}$$

APPENDIX C

CATALYTIC SURFACE REACTIONS

The catalytic production rate for a j-th gaseous specie has been shown[10,11,12] to be proportional to the kinetic mass flux $\rho\sqrt{R_o T/2\pi M_j}$ of the specie upon the wall, and is approximately given by the expression

$$S_{j_C} = \gamma_j \rho_w \sqrt{\frac{R_o T_w}{2\pi M_j}} \left(\alpha_{j_{EQ.}} - \alpha_j\right)_w , \qquad (C.1)$$

where γ_j is a "catalytic efficiency factor" accounting for the fact that not all collisions with the wall result in a catalytic reaction effect. A general discussion of the definition of γ_j for a multicomponent mixture has been given by Rosner.[12] It is often convenient to rewrite Equation (C.1) in terms of a surface reaction parameter K_{c_j} as

$$S_{j_C} = \rho_w K_{c_j} \left(\alpha_{j_{EQ.}} - \alpha_j\right)_w . \qquad (C.2)$$

The results of various investigations into surface catalysis can be given either in terms of a catalytic efficiency or in terms of the parameter K_c. Different surfaces exhibit varying recombination efficiencies and some may have their catalytic nature altered by suitable coatings or deposits. For example, the experimental studies of Marsden and Linnett[24] show that for atomic oxygen recombination in the 300 - 700°K wall temperature range, roughly 100 times more heat is released on a platinum surface than on a glassy one. Further data on the catalytic recombination of oxygen and nitrogen atoms may be found in a summary given in a paper by Goulard.[11] Some of the possible surface recombination mechanisms, for example, would be (a) two gas phase atoms colliding in a close enough proximity of the

the surface to allow a surface atom to act as a third body in transmitting the heat of recombination to the surface material, (b) two separate gas atoms are absorbed in the surface structure and retain sufficient mobility to subsequently meet and recombine within this structure, and (c) possible gas phase atom collision with a layer of absorbed but immobile atoms and subsequent recombination. The results of Marsden and Linnett indicate that (b) and (c) are the probable mechanisms for glass and platinum surfaces, respectively. The concept of surface "poisoning" in inhibiting catalytic atom recombination appears in regard to these latter two mechanisms, wherein the poisoner uses up all available absorption sites on the surface. Also, the physical nature of the surface, as well as the material, may decidely influence recombination.

Equation (C.2) can be written for each specie of the four specie air mixture in this paper as follows:

$$\left.\begin{aligned} S_{2_c} &= -\rho_w K_{c_2} (\alpha_2 - \alpha_{2_{EQ.}})_w \\ S_{4_c} &= -\rho_w K_{c_4} (\alpha_4 - \alpha_{4_{EQ.}})_w \\ S_{3_c} &= -\rho_w K_{c_3} (\alpha_3 - \alpha_{3_{EQ.}})_w \ , \end{aligned}\right\} \qquad (C.3)$$

and $S_{1_c} = -(S_{2_c} + S_{4_c} + S_{3_c})$ since $\sum_j S_{j_c} = 0$. In view of the assumed equality of physical properties between the atomic species 2 and 4 (and between 1 and 3), we shall take $K_{c_2} \simeq K_{c_4}$ and $K_{c_1} \simeq K_{c_3}$ since K_{c_j} refers to an activation energy - independent recombination process. Then as a direct result of the $\sum_j S_{j_c} = 0$ requirement, one gets

$$K_{c_3} = -K_{c_2}$$

and we can write the following approximate net catalytic production rates for the subject mixture:

$$\left.\begin{aligned} S_{2_c} &\simeq -\rho_w K_{c_2} (\alpha_2 - \alpha_{2_{EQ.}})_w \\ S_{4_c} &\simeq -\rho_w K_{c_2} (\alpha_4 - \alpha_{4_{EQ.}})_w \\ S_{3_c} &\simeq +\rho K_{c_2} (\alpha_3 - \alpha_{3_{EQ.}})_w \ . \end{aligned}\right\} \qquad (C.4)$$

APPENDIX D

REACTION RATE DERIVATIVES AT FROZEN FLOW

The derivatives of the reaction rate functions $\mathcal{G}_2$ and $\mathcal{G}_4$ (defined by Equation (3.9) and (3.11)) with respect to the specie and temperature variables, evaluated at the chemically frozen flow, are found to be the following:

$$\mathcal{D}_{\beta_2} = 2\left(\frac{1+\alpha_e}{1+\alpha_e\beta_F}\right)\beta_F - \left(\frac{\alpha_{2e}}{1+\alpha_e\beta_F}\right)\left\{\left(\frac{1+\alpha_e}{1+\alpha_e\beta_F}\right)\beta_F^2 - \left(\frac{1+\alpha_e\beta_F}{1-\alpha_e-\alpha_{3e}}\right)EXP\left[-\frac{\theta_{A2}}{\theta_F}(1-\theta_F)\right]\right\} \tag{D.1}$$

$$\mathcal{D}_{\chi_2} = -\frac{\alpha_{4e}}{1+\alpha_e\beta_F}\left\{\left(\frac{1+\alpha_e}{1+\alpha_e\beta_F}\right)\beta_F^2 - \left(\frac{1+\alpha_e\beta_F}{1-\alpha_e-\alpha_{3e}}\right)EXP\left[-\frac{\theta_{A2}}{\theta_F}(1-\theta_F)\right]\right\} \tag{D.2}$$

$$\mathcal{D}_{W_2} = \left(\frac{\alpha_{3e}}{1-\alpha_e-\alpha_{3e}}\right)EXP\left[-\frac{\theta_{A2}}{\theta_F}(1-\theta_F)\right] \tag{D.3}$$

$$\mathcal{D}_{\theta_2} = -\frac{\theta_{A2}}{\theta_F^2}\left(\frac{1-\alpha_e\beta_F-\alpha_{3e}W_F}{1-\alpha_e-\alpha_{3e}}\right)EXP\left[-\frac{\theta_{A2}}{\theta_F}(1-\theta_F)\right] \tag{D.4}$$

$$\mathcal{D}_{\beta_4} = -\frac{\alpha_{2e}(1+\alpha_e)\beta_F^2}{(1+\alpha_e\beta_F)^2} \tag{D.5}$$

$$\mathcal{D}_{\chi_4} = 2\left(\frac{1+\alpha_e}{1+\alpha_e\beta_F}\right)\beta_F - \frac{\alpha_{4e}(1+\alpha_e)\beta_F^2}{(1+\alpha_e\beta_F)^2} \tag{D.6}$$

$$\mathcal{D}_{W_4} = -EXP\left[-\frac{\theta_{A4}}{\theta_F}(1-\theta_F)\right] \tag{D.7}$$

$$\mathcal{D}_{\theta_4} = -\frac{\theta_{A4}}{\theta_F^2}W_F\,EXP\left[-\frac{\theta_{A4}}{\theta_F}(1-\theta_F)\right]. \tag{D.8}$$

The frozen flow solution $z_F = \chi_F$ has been used in the above relations.

APPENDIX E

ANALYTICAL COMPLEMENTARY INTEGRAL SOLUTIONS

Equation (4.68) in the text admits analytical solutions for two special values of the non-equilibrium derivative parameter.

$Q = 0$

This corresponds to stagnation point conditions; Equation (4.68) is in this case

$$S_c f \beta_{I_c}' + \beta_{I_c}'' = 0 , \tag{E.1}$$

which integrates directly to the following solution:

$$\beta_{I_c} = \beta_{I_c}(0) + \beta_{I_c}'(0) \int_0^\eta EXP\left(-S_c \int_0^\eta f\, d\eta\right) d\eta . \tag{E.2}$$

Since $z_{I_c} = A \cdot z_1(\eta) + B \cdot z_2(\eta)$, where $A = z_{I_c}(o)$ and $B = z_{I_c}'(o)$ (Equation 4.69), we see that in this case

$$\beta_1 = 1 , \quad \beta_2 = \int_0^\eta EXP\left(-S_c \int_0^\eta f\, d\eta\right) d\eta .$$

$Q/\epsilon = -1/2$

This corresponds to a slightly favorable pressure gradient flow such as might occur slightly downstream from a hypersonic blunt body stagnation point. In this case, Equation (4.68) can be written

$$\left(\beta_{I_c}' + S_c f \beta_{I_c}\right)' = 0 , \tag{E.3}$$

which integrates to the solution

$$\beta_{I_c} = EXP\left(-S_c \int_0^\eta f\, d\eta\right)\left[\beta_{I_c}(0) + \beta_{I_c}'(0) \int_0^\eta EXP\left(-S_c \int_0^\eta f\, d\eta\right) d\eta\right]. \tag{E.4}$$

Hence,

$$\left[\beta_{1,2}\right]_{Q/\epsilon = -\frac{1}{2}} = EXP\left(-S_c \int_0^\eta f\, d\eta\right) \cdot \left[\beta_{1,2}\right]_{Q=0} .$$

APPENDIX F

APPROXIMATE CORRECTION METHOD FOR VARIABLE $\rho\mu$ EFFECT

Probstein (34) has outlined an approximate method of accounting for the effect of variable $\rho\mu$ on wall temperature, enthalpy and specie gradient solutions calculated on the basis of $\rho\mu/\rho_W\mu_W = C = 1$. This method, developed for equilibrium flow, should be also applicable to catalytic wall frozen flow situations as well, since the $\rho\mu$ variation across the boundary layer is about the same in either case. Probstein's approach is simply to replace the integrated effect of the variable $\rho\mu$ across the boundary layer by some average constant value of $C = C_{AV.} < 1$* such that

$$(\text{WALL GRADIENT})_{C\neq 1} \simeq (\text{WALL GRADIENT})_{C=1.} \times C_{AV.} \quad .$$

Reference (34) outlines an iterative scheme, based on the original similarity plane form of the energy equation with variable C, by which the appropriate value of $C_{AV.}$ can be calculated with the use of the best known viscosity versus enthalpy data. The similarity between the specie and enthalpy energy equations for a highly cooled laminar boundary layer flow with negligible dissipation makes this method applicable to the correction of diffusion gradients as well as enthalpy and temperature gradients at the wall. Probstein's approximate method, when applied as a correction to enthalpy gradients calculated on the basis of $C = 1$, gives fairly good agreement with exact variable $\rho\mu$ solutions computed by several investigators.

The value of $C_{AV.}$ given by Probstein is not very sensitive to the wall temperature ratio as long as the wall is highly cooled ($\theta_W \ll 1$).

* For a highly cooled wall, C varies from 1 at the wall to a value of the order .1-.2 at the edge of the boundary layer, when the variable molecular weight is accounted for.

Hence we can use his results to estimate the variable $\rho\mu$ effect on the present frozen flow catalytic specie and temperature gradients with confidence. For $g_W = .032$ ($C_e = .18$), Reference (34) indicates that

$$C_{AV.} \simeq .55.$$

When this is applied to the present stagnation value $[z_F'(o)]_{\substack{CAT. \\ C=1}} = .373$, we get

$$[z_F'(o)]_{\substack{CAT. \\ C<1}} \simeq .205,$$

as compared to

$$[z_F'(o)]_{FAY\ AND\ RIDDELL} = .209\ ,$$

which is a satisfactory agreement considering the slight difference in velocity profiles used in the two theories. A similar agreement between the catalytic wall temperature gradients is obtained when such a viscosity law correction is applied to the present theory (proper allowance being made for the specific heat inequality effect noted in the text of Chapter IV).

In the non-catalytic wall case, the frozen temperature gradient is much less sensitive to the variable $\rho\mu$ effect since there is no molecular weight variation across the boundary layer. The foregoing correction is much too drastic; indeed the C = 1 result of the present theory checks very well with Fay and Riddell (there being no specific heat inequality effect in the non-catalytic case):

$$\theta_F'(o)]_{\substack{NON\text{-}CAT. \\ C=1}} = .417\ ,$$

$$\theta_F'(o)]_{FAY\ AND\ RIDDELL} = .415$$

for the stagnation point.

The above results would seem to indicate that the non-equilibrium deviations would not be significatnly affected by variable $\rho\mu$ for the non-catalytic wall case. The effect would be more noticeable for the catalytic wall and would appear (on the basis of the above examples) to further reduce the already extremely small heat conduction and diffusion perturbations that occur in this case. Unfortunately, the mathematical complexity of the non-equilibrium boundary layer perturbation equations makes the application of Probstein's approach to estimate $C \neq 1$ effects in the perturbation solutions quite complicated in comparison to the frozen solution.

APPENDIX G

DERIVATION OF EQUILIBRIUM RELATION BETWEEN MOLECULAR AND ATOMIC SPECIES

Consider the four component air mixture (NO neglected) in which $m_1 = m_2 = 2m_2 = 2m_4$. The mole fractions of each specie are then related to the corresponding mass fractions as follows:

$$\left.\begin{aligned} \frac{N_1}{N} &= \frac{\alpha_1}{2-(\alpha_1+\alpha_3)}\,, \quad \frac{N_2}{N} = \frac{2\alpha_2}{2-(\alpha_1+\alpha_3)}\,, \\ \frac{N_3}{N} &= \frac{\alpha_3}{2-(\alpha_1+\alpha_3)}\,, \quad \frac{N_4}{N} = \frac{2\alpha_4}{2-(\alpha_1+\alpha_3)}\,. \end{aligned}\right\} \tag{G.1}$$

Now in the classical thermodynamic equilibrium (no diffusion) steady state, the number of moles of oxygen and nitrogen atoms is conserved regardless of reaction in the gas. This requirement can be stated as:

$$\left.\begin{aligned} 2\left(\frac{N_1}{N}\right)_{EQ.} + \left(\frac{N_2}{N}\right) &= 2 \times .21 \times \left(\frac{\text{INITIAL MOLES OF UNDISSOCIATED AIR}}{N}\right) \\ 2\left(\frac{N_3}{N}\right) + \left(\frac{N_4}{N}\right) &= 2 \times .79 \times \left(\frac{\text{INITIAL MOLES OF UNDISSOCIATED AIR}}{N}\right). \end{aligned}\right\} \tag{G.2}$$

Division of these two statements produces the equation

$$\frac{2(N_1/N)_{EQ.} + (N_2/N)_{EQ.}}{2(N_3/N)_{EQ.} + (N_4/N)_{EQ.}} = \frac{.21}{.79}\,. \tag{G.3}$$

Using the fact $\sum_i N_i/N = 1$ to eliminate N_1/N and substituting relations (G.1), Equation (G.3) yields the following result after some algebraic manipulation:

$$(\alpha_3)_{EQ.} = .79 - (\alpha_4)_{EQ.}\,. \tag{G.4}$$

This result is valid when the Nitric oxide is negligible and $m_1 = 2m_2 = \cdots$ etc. are good approximations.

APPENDIX H

REACTION RATE DERIVATIVES AT THERMODYNAMIC EQUILIBRIUM

The various derivatives of the reaction rate functions $\mathcal{G}_2$ and $\mathcal{G}_4$ (Equations (3.9) and (3.11)) with respect to the specie and temperature variables, evaluated at thermodynamic equilibrium conditions, are as follows:

$$\mathcal{D}_{\beta_2} = \frac{2(1+\alpha_e)\beta_{EQ.}}{1+\alpha_{2e}\beta_{EQ.}+\alpha_{4e}\chi_{EQ.}} + \frac{\alpha_{2e}(2\alpha_{2e}\beta_{EQ.}+2\alpha_{4e}\chi_{EQ.}+\alpha_{3e}W_{EQ.})}{(1-\alpha_e-\alpha_{3e})(1+\alpha_{2e}\beta_{EQ.}+\alpha_{4e}\chi_{EQ.})} EXP\left[-\frac{\theta_{A2}}{\theta_{EQ.}}(1-\theta_{EQ.})\right] \quad (H.1)$$

$$\mathcal{D}_{\chi_2} = \frac{\alpha_{4e}(2\alpha_{2e}\beta_{EQ.}+2\alpha_{4e}\chi_{EQ.}+\alpha_{3e}W_{EQ.})}{(1-\alpha_e-\alpha_{3e})(1+\alpha_{2e}\beta_{EQ.}+\alpha_{4e}\chi_{EQ.})} EXP\left[-\frac{\theta_{A2}}{\theta_{EQ.}}(1-\theta_{EQ.})\right] \quad (H.2)$$

$$\mathcal{D}_{W_2} = \frac{\alpha_{3e}}{1-\alpha_e-\alpha_{3e}} EXP\left[-\frac{\theta_{A2}}{\theta_{EQ.}}(1-\theta_{EQ.})\right] \quad (H.3)$$

$$\mathcal{D}_{\theta_2} = -\frac{\theta_{A2}}{\theta_{EQ.}^2}\left(\frac{1-\alpha_{2e}\beta_{EQ.}-\alpha_{4e}\chi_{EQ.}-\alpha_{3e}W_{EQ.}}{1-\alpha_e-\alpha_{3e}}\right) EXP\left[-\frac{\theta_{A2}}{\theta_{EQ.}}(1-\theta_{EQ.})\right] \quad (H.4)$$

$$\mathcal{D}_{\beta_4} = -\frac{\alpha_{2e}W_{EQ.} EXP\left[-\frac{\theta_{A4}}{\theta_{EQ.}}(1-\theta_{EQ.})\right]}{1+\alpha_{2e}\beta_{EQ.}+\alpha_{4e}\chi_{EQ.}} \quad (H.5)$$

$$\mathcal{D}_{\chi_4} = \frac{2(1+\alpha_e)\chi_{EQ.}}{1+\alpha_{2e}\beta_{EQ.}+\alpha_{4e}\chi_{EQ.}} - \frac{\alpha_{4e}W_{EQ.} EXP\left[-\frac{\theta_{A4}}{\theta_{EQ.}}(1-\theta_{EQ.})\right]}{1+\alpha_{2e}\beta_{EQ.}+\alpha_{4e}\chi_{EQ.}} \quad (H.6)$$

$$\mathcal{D}_{W_4} = -EXP\left[-\frac{\theta_{A4}}{\theta_{EQ.}}(1-\theta_{EQ.})\right] \quad (H.7)$$

$$\mathcal{D}_{\theta_4} = -\frac{\theta_{A4}}{\theta_{EQ.}} W_{EQ.} EXP\left[-\frac{\theta_{A4}}{\theta_{EQ.}}(1-\theta_{EQ.})\right]. \quad (H.8)$$

The equilibrium relations (5.24) and (5.26) have been used in writing the above relations.

BIBLIOGRAPHY

1. Rosner, D. "Recent Advances in Convective Heat Transfer with Dissociation and Atom Recombination," Jet Propulsion, July 1958.

2. Griffith, W. "Recent Advances in Real Gas Effects in Hypersonic Flow," Jet Propulsion, March 1958.

3. Adams, M. "Recent Advances in Ablation," Journal of American Rocket Society, September 1959.

4. Lees, L. "Laminar Heat Transfer over Blunt-Nosed Bodies at Hypersonic Flight Speeds," Jet Propulsion, 26, 1956.

5. Kemp, N., Rose, P. and Detra, R. Laminar Heat Transfer Around Blunt Bodies in Dissociated Air, AVCO Research Report 15, May 1958.

6. Fay, J. and Riddell, F. Theory of Stagnation Point Heat Transfer in Dissociated Air, AVCO Research Report 1, April 1957.

7. Adamson, T., Nicholls, J. and Sherman, P. A Study of the Hypersonic Laminar Boundary Layer with Dissociation, University of Michigan Engineering Research Institute Report 1, Project 2606-6-T, May 1957.

8. Adamson, T., Nicholls, J. and Sherman, P. A Study of the Hypersonic Laminar Boundary Layer with Dissociation, University of Michigan Engineering Research Institute Final Report, Project 2606-6-F, September 1957.

9. Hirschfelder, J. "Heat Transfer in Chemically Reacting Mixtures," Journal of Chemical Physics, 26, No. 2, 1957.

10. Scala, S. Hypersonic Stagnation Point Heat Transfer to Surfaces Having Finite Catalytic Efficiency, G. E. MOSD Report R-58SD-236, January 1958.

11. Goulard, R. "On Catalytic Recombination Rates in Hypersonic Stagnation Heat Transfer," Jet Propulsion, November 1958.

12. Rosner, D. "Boundary Conditions for the Flow of a Multi-Component Gas," Jet Propulsion, August, 1958.

13. Rosner, D. "Chemically Frozen Boundary Layers with Catalytic Surface Reaction," Journal of the Aero. Sci., August 1959.

14. Lees, L. Convective Heat Transfer with Mass Addition and Chemical Reaction, Third Comb. and Prop. Symp., NATO-AGARD, March 1958.

15. Knuth, E. Compressible Couette Flow with Diffusion of a Reactive Gas from a Decomposing Wall, 1958 Heat Transfer and Fluid Mechanics Institute, University of California, June 1958.

16. Hirshfelder, J., Curtiss, C. and Bird, R. Molecular Theory of Gases and Liquids, Wiley, New York, 1954.

17. Bromley, L. and Wilke, C. "Viscosity Behavior of Gases," Industrial and Engineering Chemistry, July, 1951.

18. Hansen, C. "Note on the Prandtl Number for Dissociated Air," Journal of the Aero. Sci., August 1952.

19. Sutton, G. and Scala, S. "Energy Transfer at a Chemically Reacting or Slip Interface," Journal of American Rocket Society, February 1959.

20. Penner, S. Chemical Reactions in Flow Systems, AGARDO Graph 7, Butterworths, London, 1953.

21. Logan, J. Relaxation Phenomena in Hypersonic Aerodynamics, I.A.S. 25th Annual Meeting, Preprint 728, January 1958.

22. Mason, R. and Squires, K. The Kinetics of the Dissociation of Nitric Oxide, Lockheed MSD Report 48381, III, January 1959.

23. Davidson, N. Rates of Selected Reactions Involving Nitrogen and Oxygen, AVCO Research Report 32, June 1958.

24. Marsden, D. and Linnett, J. The Kinetics of the Recombination of Oxygen Atoms at a Glass Surface, Proc. Royal Soc., A, No. 1199, 234, March 1956.

25. Marble, F. and Adamson, T. "Ignition and Combustion in a Laminar Mixing Zone," Jet Propulsion, 24, No. 2, 1954.

26. Adams, M. and Probstein, R. "On the Validity of Continuum Theory for Satellite and Hypersonic Flight Problems at High Altitudes," Jet Propulsion, February 1958.

27. Lees, L. and Kubota, T. "Inviscid Hypersonic Flow Over Blunt-Nosed Slender Bodies," Journal of Aero. Sci., March 1957.

28. Broadwell, J. A Simple Model of the Non-Equilibrium Dissociation of a Gas in Couette and Boundary Layer Flow, Douglas Aircraft Co. Rep. SM-22888, August 1957.

29. Goldstein, S. (ed.). Modern Developments in Fluid Dynamics, Clarendon Press, Oxford, 1938.

30. Nelson, A. Folley, K. and Coral, M. Differential Equations, Heath, New York, 1952.

31. Rainville, E. Intermediate Differential Equations, Wiley, New York, 1943.

32. Liepmann, H. and Bleviss, Z. The Effects of Dissociation and Ionization on Compressible Couette Flow, Douglas Aircraft Co. Report SM -19831, May 1956.

33. Bleviss, Z. The Effects of Combined Electric and Magnetic Fields in Hypersonic Ionized Couette Flow, Douglas Aircraft Co. Report SM-23314, 1958.

34. Probstein, R. "Methods of Calculating the Equilibrium Heat Transfer Rate at Hypersonic Speeds," Jet Propulsion, June 1956.